11β-hydroxysteroid dehydrogenase type 1: A new therapeutic target post-myocardial infarction?

Sara Jane McSweeney

PhD

The University of Edinburgh

2010

Declaration

I hereby declare that all work described in this thesis was performed entirely by myself, except for the procedures stated in the acknowledgements. The work contains no material that has been accepted for the award of any other degree or diploma in any university or tertiary institution and to the best of my knowledge contains no material published or written by any other person, except where stated in the text.

Sara Jane McSweeney

Acknowledgements

It is a pleasure to thank those who have made this thesis possible. Firstly, I would like to thank my primary supervisor, Gillian Gray, whose scientific guidance, support and encouragement has enabled me to pursue my aspiration to complete a PhD. Likewise, I thank my secondary supervisors, Paddy Hadoke and Brian Walker, whose great experience and scientific knowledge has been invaluable. I also extend my gratitude to my fellow students and colleagues in lab E3.17, in the Endocrinology department and in the BRF for their practical help and advice, and for making my PhD experience not only productive, but a fun one.

I would like to acknowledge the help of Susan Harvey and Bob Morris (Medical Reseach Council/Centre for Inflammation Research Histology service) who conducted some of the histology staining and David Brownstein who conducted the histological analysis which aided in the characterisation of the basal cardiac phenotype of the 11HSD1$^{-/-}$ mice. During my PhD I had the pleasure of supervising Hiba Khaled (a Masters student) and Hector Scott (an Honours student) in their laboratory work and I thank them for their assistance with some of the histology and immunohistochemistry work.

Lastly, and very importantly, I am forever indebted to my parents, Mervyn and Julie, my siblings, Katie, Alicia and Christian, and my partner, Dave. Without their support, encouragement and understanding this thesis would not have been possible.

Abstract

Glucocorticoids can reduce infarct size when given immediately after myocardial infarction (MI) but are detrimental when administration is continued into the post-infarct healing phase. A number of experimental studies have shown that reduction of infarct expansion by enhancing blood supply to the infarct border reduces remodelling and improves heart function post-MI. Previous experiments from this laboratory have shown that mice unable to locally regenerate corticosterone due to deficiency in 11β-hydroxysteroid dehydrogenase type 1 (11HSD1) have an enhanced angiogenic response during myocardial infarct healing that is associated with improved cardiac function. We hypothesized that the enhanced angiogenic response in 11HSD1 knock out ($^{-/-}$) mice would be preceded by augmented inflammation. Moreover this would be associated with improved cardiac function.

This thesis aimed firstly to establish that murine cardiac phenotype was not influenced by 11HSD1 deficiency. 11HSD1$^{-/-}$ and C57Bl6 control mice had comparable cardiac structure and function. 11HSD1 expression was localised to fibroblasts and vascular smooth muscle cells in the myocardium.

The second aim of this thesis was to characterise the healing response after MI in 11HSD1$^{-/-}$ mice compared to C57Bl6 mice. Neutrophil infiltration peaked 2 days after MI and was significantly enhanced in the 11HSD1$^{-/-}$ mice relative to C57Bl6 mice, despite comparable infarct size in both groups. This was followed by increased macrophage accumulation in the infarct border. Furthermore, in the 11HSD1$^{-/-}$ mice a greater proportion of macrophages were of the alternatively activated phenotype. Left ventricular expression of pro-angiogenic IL-8, but not VEGF, was increased. Cellular proliferation and vessel density at 7 days were greater in 11HSD1$^{-/-}$ compared to C57Bl6 hearts. This was associated with improved cardiac function 7 days post-MI.

The third aim of this thesis was to determine whether the enhancement in vessel density and cardiac function was maintained beyond the initial wound healing phase. 11HSD1$^{-/-}$ mice retained the increased vessel density compared to C57Bl6 mice and these vessels were smooth muscle coated suggesting vessel maturation. This was associated with sustained improvement in cardiac function and modification of the scar characteristics.

The final aim of this thesis was to establish whether the effect of the knock out could be recapitulated by administration of a small molecule inhibitor of 11HSD1 after MI. Oral administration of the 11HSD1 inhibitor had no effect on inflammation, angiogenesis and heart function as determined at 7 days post-MI relative to vehicle treated animals.

In conclusion, the data confirm the enhancement in vessel density and cardiac function in 11HSD1$^{-/-}$ mice and demonstrate that this was preceded by enhanced inflammation. This was not due to an underlying cardiac phenotype or modification of the infarct size. Increased infiltration of alternatively activated macrophages may have been the source of pro-angiogenic factor, IL-8, which was also increased at the time of angiogenesis. Importantly the enhanced vessel density was retained 4 weeks after MI, these vessels were mature suggesting longevity and the improvement in cardiac function was retained. While pharmacological inhibition did not recapitulate the effect of the knock out this may have been due to route of administration. The data provides compelling evidence that further development and use of small molecule inhibitors of 11HSD1 may be of benefit post-MI.

Presentations

Oral

'Sustained enhancement of cardiac function follows increased recruitment of pro-angiogenic macrophages to the healing infarcts of 11β-hydroxsteroid dehydrogenase type 1 knock out mice' at the American Heart Association Scientific Sessions; Orlando, November 2009.

'11HSD1: A New Therapeutic Target Post Myocardial Infarction' at the Centre for Cardiovascular Science Symposium Day; Edinburgh June 2009.

'Improved heart function follows enhancement of the inflammatory and angiogenic response in the healing myocardial infarct of 11HSD1 knock out mice' Heart Failure Congress 2009 European Society of Cardiology and International Society for Heart Research; Nice, May 2009.

'Research Degrees in the Sciences' at the University of Edinburgh Postgraduate Open Day; March 2009

'A student's perspective' invited to present a students perspective of postgraduate study in the Queen's Medical Research Institute at the Institute annual open day for prospective PhD students, 2008.

'Deficiency of 11HSD1 augments the inflammatory response during myocardial infarct healing' at the British Society for Cardiovascular Research meeting; Manchester June 2008.

Poster

‘11HSD1 deficiency augments the inflammatory and angiogenic response after myocardial infarction and is associated with improved heart function’ at the Scottish Cardiovascular Forum; Inverness, January 2009; and at the Scottish Society for Experimental Medicine; Edinburgh November 2008;

‘Temporal characterisation of inflammatory cell infiltration and cardiac function post myocardial infarction in the mouse’ at the official launch of the Integrative Mammalian Biology Capacity Initiative, Glasgow April 2008; and at the Scottish Cardiovascular Forum; Edinburgh, February 2008.

Abbreviations

Abbreviation	Term
-/-	knock out
6PG	6- phosphogluconate
11HSD	11β-hydroxysteroid dehydrogenase
αSMA	α-smooth muscle actin
ACE	angiotensin converting enzyme
ACTH	adrenocorticotrophic hormone
Ang	angiopoietin
ANOVA	analysis of variance
APN	aminopeptidase-N
bFGF	basic fibroblast growth factor
BMDC	bone marrow-derived cells
BOOST	Bone Marrow transfer to enhance ST-elevation infarct regeneration
BrdU	bromodeoxyuridine
BSA	bovine serum albumin
C	complement cascade
CBG	corticosteroid-binding globulin
CP	crossing point
CPM	counts per minute

CRF	corticotrophin-releasing factor
CVD	cardiovascular disease
DAB	3, 3'-diaminobenzidine
DEPC	diethylpyrocarbonate
ECM	extracellular matrix
EF	ejection fraction
eNOS	endothelial nitric oxide synthase
EPC	endothelial progenitor cell
EPHESUS	Eplerenone Post-acute myocardial infarction Heart failure Efficacy and Survival Study
ER	endoplasmic reticulum
FS	fractional shortening
G6P	glucose-6-phosphate
GAPDH	glyceraldehyde-3-phosphate dehydrogenase
G-CSF	granulocyte colony-stimulating factor
GM-CSF	granulocyte-macrophage colony-stimulating factor
GPCR	G protein coupled receptors
GR	glucocorticoid receptor
GRE	glucocorticoid response elements
H6PDH	hexose-6-phosphate dehydrogenase
HCl	hydrochloric acid
H&E	haematoxylin and eosin
HIER	heat-induced antigen retrieval

HIF-1α	hypoxia inducible factor-1α
HPA axis	hypothalamic-pituitary adrenal axis
HSP	heat shock protein
IB	infarct border
ICAM-1	intercellular adhesion molecule-1
IκB	inhibitor-κB
IFN	interferon
IGF-1	insulin-like growth factor-1
IL	interleukin
IP-10	interferon γ inducible protein
KC	keratinocyte chemoattractant
LV	left ventricle
LVEDA	left ventricle end diastolic area
LVEDD	left ventricle end diastolic diameter
LVESA	left ventricle end systolic area
LVESD	left ventricle end systolic diameter
MCP-1	monocyte chemoattractant protein-1
M-CSF	macrophage colony-stimulating factor
MI	myocardial infarction
MIP	macrophage inflammatory protein
MMP	matrix metalloprotease
MR	mineralocorticoid receptor

MRI	magnetic resonance imaging
NAD	nicotinamide adenine dinucleotide
NADPH	nicotinamide adenine dinucleotide phosphate
NF-κB	nuclear factor-κB
NK	natural killer cells
PAS	Periodic Acid Schiff reaction
PBS	phosphate buffered saline
PCR	polymerase chain reaction
PDGF	platelet-derived growth factor
PDGFR	platelet derived growth factor receptor
PECAM-1	platelet-endothelial cell adhesion molecule-1
PIER	proteolytic-induced antigen retrieval
PMN	polymorphonuclear cells
PSR	Picrosirius Red
PWD	posterior wall thickness at diastole
PWS	posterior wall thickness at systole
qRT PCR	quantative real time polymerase chain reaction
RALES	Randomised ALdactone Evaluation Study
RANTES	regulation on activation, normal T cell expressed and secreted
ROS	reactive oxygen species
RV	right ventricle
SAME	syndrome of apparent mineralocorticoid excess

SDF-1α	stromal cell-derived factor-1α
SCF	stem cell factor
SEM	standard error of the mean
SPA	scintillation proximity assay
TBS	tris buffered saline
TGF-β	transforming growth factor-β
TIMPS	tissue inhibitors of matrix metalloproteases
TLR	toll-like receptor
TNF-α	tumour necrosis factor-α
TSP-1	thrombospondin-1
TTC	triphenyltetrazolium chloride
u-PA	urokinase-plasminogen activator
VCAM-1	vascular cell adhesion molecule-1
VEGF	vascular endothelial growth factor

Table of Contents

List of Figures

List of Tables

Chapter 1 Introduction

1.1 Cardiovascular disease in the UK

Cardiovascular disease (CVD) is responsible for 198,000 deaths per year in the United Kingdom alone and is a major cause of premature death (British Heart Foundation, 2008). The term CVD encompasses myocardial infarction (MI), angina, stroke, transient ischaemic attack and coronary heart disease. The resultant cardiac damage from ischaemic heart disease can result in the development of heart failure, an illness in which the cardiac output is insufficient for the body's needs. The Hillingdon Heart Study estimates that 140 men per 100,000 in the UK have heart failure, with MI being the most common cause (Cowie et al., 1999).

Myocardial infarct size is an important determinant of outcome post MI and its limitation can be achieved by conditioning, reperfusion and revascularisation therapies (Ishii et al., 2008, Ferdinandy et al., 2007). Pre-conditioning (brief ischaemic events just prior to MI) reduces infarct size and subsequent remodelling in MI patients (Nakagawa et al., 1995). Additionally brief bouts of ischaemia in the moments succeeding reperfusion (restoration of blood flow to the ischaemic myocardium) has also been shown to be beneficial in the clinic (Staat et al., 2005). The advent of reperfusion therapy in the 1980's has resulted in an increase in post-infarct survival (Ferdinandy et al., 2007). However, this was also accompanied by an increase in the number of patients developing heart failure; improved survival may have increased the pool of people at risk of developing heart failure (Velagaleti et al., 2008). Furthermore, reperfusion therapy has the potential to cause irreversible tissue injury depending on the duration of ischaemia (Ferdinandy et al., 2007). Current therapeutics aimed at reducing post-infarct remodelling after reperfusion include β-blockers, diuretics, ACE inhibitors and more recently mineralocorticoid receptor antagonists, but despite these interventions the prognosis is still poor (van der Horst et al., 2007). There is plentiful evidence to suggest that enhancement of angiogenesis on the infarct border can improve heart function and

prevent the progression to heart failure (Jujo et al., 2008, Meyer et al., 2006, Yau et al., 2005) . The work described in this thesis will address the possibility that manipulation of post-infarct angiogenesis by glucocorticoids generated in the myocardium may provide a new therapeutic option.

1.2 Myocardial infarction

1.2.1 Cell death

MI occurs predominantly as a result of occlusion of a coronary vessel by a thrombus, a consequence of atherosclerotic plaque rupture. The reduction of local oxygen supply prevents aerobic respiration in the cardiac cell resulting in death. Cardiomyocytes are susceptible to 3 types of cell death: necrosis, apoptosis and autophagy, with the level of energy depletion determining the form of death (Mani, 2008). Necrotic cell death is observed in the infarct core where conditions are anoxic. It relies on intrinsic signalling by DNA damage and extrinsic signalling via death receptors (Mani, 2008). Necrosis is a result of mitochondrial dysfunction typified by energy depletion, Ca^{2+} accumulation and an increase in reactive oxygen species (ROS), and is mediated by cathepsin activation (Syntichaki et al., 2002, Holler et al., 2000). This form of cell death is characterised by loss of membrane integrity and spillage of cellular contents which can evoke a powerful inflammatory response (Schweichel and Merker, 1973). Apoptosis, on the other hand, is found in the infarct border where oxygen is present in low concentrations, and in the remote regions of the heart that are under haemodynamic and humoural stress (Mani, 2008, Olivetti et al., 1996, Scarabelli et al., 2001). Like necrosis, it is mediated by intrinsic (via the mitochondrial pathway) and extrinsic (via death receptor) signalling. These stimuli are integrated by the caspase proteolytic enzymes that cleave intracellular proteins and result in morphological changes (Thornberry and Lazebnik, 1998). Apoptosis is characterised by chromatin condensation and bulges in the cellular membrane, known as blebbing (Potts et al., 2005, Klionsky and Emr, 2000). The role of cell autophagy after MI is uncertain but is linked to apoptosis. Recycling of nutrients

from old organelles can ensure cell viability in stress states and is, thus, protective (Klionsky and Emr, 2000). However, it may also provide ATP which is necessary in apoptotic death (Mani, 2008). Insufficient knowledge about necrosis and autophagy means that they are not yet targeted therapeutically. On the other hand, inhibitors of the apoptosis cascade, by targeting Bax and the caspases, reduce infarct size in experimental models and have been associated with preservation of cardiac function indicating that preventing early cell death may be beneficial (Hochhauser et al., 2003, Yaoita et al., 1998). The therapeutic implications of long term inhibition of apoptosis are yet to be determined but there is cause for concern as apoptosis does have a homeostatic role (Mani, 2008).

1.3 Post-infarct inflammation

1.3.1 Trigger for inflammation

Necrosis is a powerful trigger for the inflammatory response. Release of DNA and RNA from necrotic cells can activate toll-like receptors (TLR) (Elkon, 2007, Chen et al., 2007). Subsequent induction of interleukin-1β (IL-1β), keratinocyte chemoattractant (KC/IL-8) and macrophage inflammatory protein-2 (MIP-2) can attract neutrophils to the site of necrosis (Frangogiannis et al., 2002) . The pathological role of TLR activation in infarct healing has been demonstrated by reduced fibrosis and improved cardiac function in TLR2 knock-out mice relative to controls (Shishido et al., 2003). Necrosis also results in exposure of mitochondrial proteins, such as cardiolipin, which can trigger the complement (C) cascade (Sumitra et al., 2005, Rossen et al., 1994). This cascade consists of serine proteases that activate each other sequentially in the hours following MI. These proteins are associated with destruction of the cardiac architecture, accounting for a significant proportion of ischaemic injury (Rossen et al., 1994, Sumitra et al., 2005).

ROS, such as hydrogen peroxide, superoxide radicals, hydroxyl radicals and peroxynitrite are another trigger for the inflammatory response (Dhalla et al., 2000, Levonen et al., 2008). They are a vital part of normal cell signalling but excessive production post-MI can overwhelm endogenous antioxidants leading to cell injury (Levonen et al., 2008, Kevin et al., 2005). NADPH oxidase is a source of superoxide and its expression increases after MI (Zhao et al., 2009). However, deficiency of NADPH oxidase does not prevent post-infarct oxidative stress due to compensatory superoxide producers (Zhao et al., 2009). Other sources of oxidative stress include xanthine oxidase, uncoupled endothelial nitric oxide synthase (eNOS) and mitochondrial dysfunction (Levonen et al., 2008). ROS themselves can cause necrosis by damage of the cell membrane via lipid peroxidation and can enhance apoptosis. Furthermore they have a role in activating TLR and causing vascular dysfunction and cardiac arrhythmias (Kevin et al., 2005, Shishido et al., 2003). Chronic elevation of ROS in the myocardium can aid in the progression to heart failure (Dhalla et al., 1996). Antioxidant therapy can prevent the adverse effects of oxidative stress; however such therapy has to be highly directed so not to affect normal cell signalling (Levonen et al., 2008, Dhalla et al., 2000).

1.3.2 Cytokine and chemokine upregulation

Cytokines are small (less than 30kDa in size), soluble proteins that regulate cell function and are regulated themselves by nuclear factor-κB (NF-κB) (Borish and Steinke, 2003). NF-κB is normally found in the cytoplasm in a complex with inhibitor-κB (IκB). ROS, IL-1β and tumour necrosis factor α (TNFα) activate pathways that converge on Iκ kinase enabling its phosphorylation and subsequent degradation of IκB (Stancovski and Baltimore, 1997). NF-κB is then able to translocate to the nucleus where it can regulate genes involved in inflammation, cell proliferation and survival (Lenardo and Baltimore, 1989). Preventing activation of NF-κB by targeted deletion of the NF-κB subunit p50 reduces inflammatory cell infiltration to the myocardium 24 hours after ischaemia reperfusion injury demonstrating its vital role in inflammatory cell recruitment (Frantz et

al., 2007). Mast cell degranulation has also been implicated in the initiation of the post-infarct cytokine cascade (Frangogiannis et al., 2002, Dewald et al., 2004).

Upregulation of inflammatory cytokines occurs within hours of MI and declines over several days (Nian et al., 2004). Persistent cytokine activation can be damaging to the myocardium (Nian et al., 2004). Cytokines mediate their actions by dimerisation of tyrosine kinase receptors producing intracellular signalling cascades (Borish and Steinke, 2003). They can induce myocyte expression of integrins and alter the endothelial cell phenotype to an inflammatory or angiogenic one (Nian et al., 2004). Anti-cytokine therapy has had limited success in the treatment of heart failure. Etanercept, a TNFα inhibitor, lowers plasma TNFα but has no beneficial effect on mortality or rate of hospitalisation (Mann et al., 2004).

Chemokines are small (8-14kDa) chemoattractants that contain 2-4 conserved cysteine residues, the bonding of which determines their 3 dimensional structure and, therefore, their actions (Borish and Steinke, 2003, Frangogiannis and Entman, 2005). The two main classes of chemokine are the CXC family, including IL-8 and IP-10 (CXCL10), and the CC chemokines, such as monocyte chemoattractant protein-1 (MCP-1) and MIP-1β (Frangogiannis and Entman, 2005). Their effects are mediated by G protein coupled receptors (GPCRs) and they have roles in inflammation, wound healing and homeostasis (Borish and Steinke, 2003). Their principal targets are bone marrow derived cells. Like cytokines, chemokines can be upregulated by ROS, complement activation and NF-κB activation and this upregulation is rapid and transient (Frangogiannis and Entman, 2005, Lakshminarayanan et al., 2001). Chemokine inhibitors impair recruitment of monocytes/macrophages, T cells and B cells to inflamed sites and are under development for the treatment of atherosclerosis and autoimmune disorders (Reckless et al., 2005, Reckless et al., 2001).

1.3.3 Neutrophil infiltration

Neutrophils are polymorphonuclear cells that mediate the early inflammatory response to injury (see Figure 1.1). They destroy and remove pathogens along with cell debris (Frangogiannis et al., 2002). In the absence of inflammation neutrophils circulate in the blood without interacting with the vessel wall (Frangogiannis et al., 2002). Inflammatory stimuli, such as IL-6, IL-8 and TNF-α prime neutrophils and the endothelium for translocation into the injured tissue (Jordan et al., 1999, van Es and Devreotes, 1999, Sekido et al., 1993, Kukielka et al., 1995b). An inflammatory environment promotes expression of the adhesion molecules; P-selectin and intercellular adhesion molecule-1 (ICAM-1); on endothelial cells, which can interact with the L-selectin and β_2-integrins constitutively expressed on neutrophils (Kukielka et al., 1995b, Frangogiannis et al., 2002, Jordan et al., 1999). The selectin adhesion molecules mediate the initial contact as the neutrophils roll along the endothelium and migrate towards chemoattractants. Firm adherence is mediated by ICAM-1 and β_2-integrins (Kukielka et al., 1995b, Jordan et al., 1999, Frangogiannis et al., 2002). Adherence of neutrophils to the endothelium alone is sufficient to induce damage and can cause vasoconstriction (Ma et al., 1991). Platelet-endothelial cell adhesion molecule-1 (PECAM-1) is expressed on endothelial cells and is reported to be involved in neutrophil translocation through the endothelial cell layer, the subendothelial matrix and on to the site of inflammation (Muller et al., 1993, Thompson et al., 2001). Additionally, local stimuli, such as IL-8 can induce the metamorphosis of these neutrophils which can block blood vessels, (Thelen et al., 1988). The 'no-reflow' phenomenon in reperfusion injury may be mediated by accumulation of neutrophils and platelets in the vasculature (Jordan et al., 1999, Frangogiannis et al., 2002).

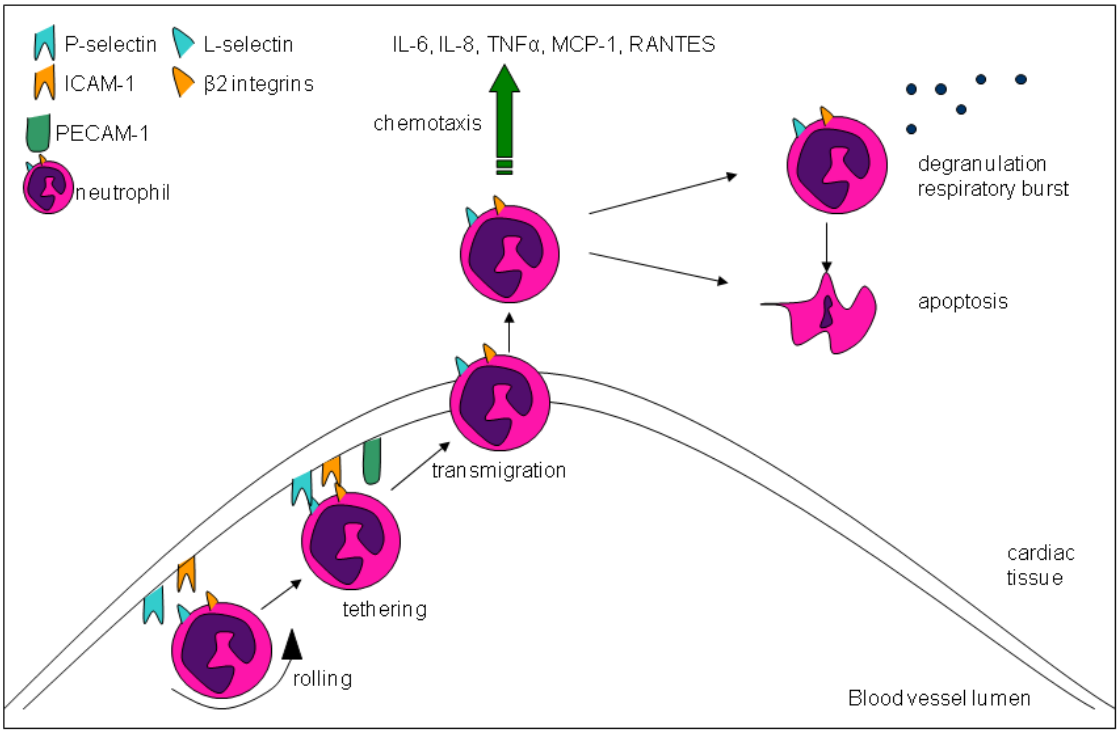

Figure 1-1 Infiltration of neutrophils into the heart after myocardial infarction

Adhesion molecules such as B-selectin and intercellular adhesion molecule-1 (ICAM-1) are upregulated in response to inflammatory stimuli. They bind to the L-selectin and β2 integrins constitutively expressed on neutrophils, aiding neutrophil rolling and tethering to the vascular endothelium. Subsequently neutrophils transmigrate into the heart with the additional help of platelet cell adhesion molecule-1 (PECAM-1), otherwise known as CD31. Neutrophils are attracted to the site of injury, migrating towards gradients of cytokines and chemokines such as IL-6 (interleukin-6), IL-8, TNFα (tumour necrosis factor α), MCP-1 (monocyte chemoattractant protein-1) and RANTES (regulation on activation, normal T cell expressed and secreted). At the infarct, neutrophils propagate the inflammatory response by degranulation (releasing proteases and inflammatory mediators) and release of reactive oxygen species during the respiratory burst. Lastly neutrophils undergo apoptosis, providing a stimulus for macrophage infiltration. Figure adapted from Frangogiannis et al., 2002.

Increased expression of IL-6 and IL-8 in the hours after MI attracts neutrophils to the infarct (Frangogiannis et al., 2002, Kukielka et al., 1995b, Kukielka et al., 1995a, Rollins, 1997, Ivey et al., 1995). Such neutrophil attractants can be secreted from mononuclear phagocytes, endothelial cells, T cells, fibroblasts, myocytes and neutrophils themselves (Borish and Steinke, 2003). Neutrophils infiltration into the myocardium peaks 24-48 hours after MI, in murine and canine models, and declines rapidly, with very few neutrophils being present at 7 days (Tao et al., 2004, Dewald et al., 2004). Genetic ablation of IL-6 shows its importance in neutrophil recruitment and wound healing (Gallucci et al., 2000, Cuzzocrea et al., 1999). IL-8 is not expressed in mice but its homologue has been identified to be keratinocyte chemoattractant (KC). For the purposes of this thesis the homologue will be referred to as IL-8 (Frangogiannis and Entman, 2005). Reduction in IL-8 expression or blockade of CXCR2 (the receptor for IL-8) results in reduced neutrophil recruitment post-MI and in other ischaemic injuries demonstrating its importance in recruiting neutrophils (Kilgore et al., 1998, Kukielka et al., 1995a, Coelho et al., 2008, Sekido et al., 1993). The role of IL-8 extends beyond that of attracting neutrophils to the site of injury. This chemokine has also been shown to induce neutrophil shape change, making them less deformable, and stimulating their inflammatory functions (Frangogiannis, 2004, Thelen et al., 1988).

Once in the tissue neutrophils degranulate releasing damaging proteases, arachidonic acid metabolites (such as leukotriene B_4 which is itself a neutrophil chemoattractant), and other inflammatory mediators (Jordan et al., 1999). Neutrophils are also able to phagocytose particles and undergo a ‘respiratory burst’ mediated by NADPH oxidase activity. Free radical production from this process can cause further tissue damage and propagate the inflammatory response (Rossi, 1986). The vascular endothelium is particularly sensitive to free radicals, which can increase adhesion molecule expression by endothelial cells and vascular permeability (Deisher et al., 1993, Svendsen and Bjerrum, 1992). Neutrophils themselves also die in the infarct and provide a stimulus for monocyte infiltration (Savill et al., 1989a, Savill et al., 1989b). Overall the action of

neutrophils amplifies the inflammatory response and provides a stimulus for other inflammatory cell infiltration.

Neutrophils can enhance cell death and, in the clinic, high circulating IL-6 and neutrophil levels are associated with increased mortality (Kin et al., 2006, Jaremo and Nilsson, 2008). In a murine model of MI, depletion of neutrophils using an anti-PMN antibody results in reduced apoptosis potentially by reduced NF-κB signalling (Kin et al., 2006). It is likely that the ability of neutrophils to enhance cell death is related to their ability to produce free radicals, as discussed above (Kin et al., 2006). However, neutrophils also provide a vital stimulus for subsequent wound healing which is required to stabilise the healing infarct. Depletion of neutrophils (prior to and continued after injury) results in impairment of necrotic cell removal in mice 7 days post-MI (Heymans et al., 1999).

1.3.4 Macrophage infiltration

Monocytes are derived from bone marrow myeloid progenitor cells that have the potential to give rise to a variety of inflammatory cells. Under basal conditions monocytes are released into the blood where they remain or they enter the tissue and mature to become long-lived, tissue specific macrophages, such as Kupffer cells in the liver and osteoclasts in the bone (Mosser and Edwards, 2008). Monocytes patrol the vessel wall relying on β_2-integrin and CX_3CR1-fractalkine-mediated adhesion (Auffray et al., 2007). They can extravasate within an hour in response to relevant inflammatory stimuli which are released from resident tissue cells, such as myocytes and endothelial cells, or from other inflammatory cells, such as neutrophils (see Figure 1.2) (Auffray et al., 2007, Lambert et al., 2008).

Monocytes are recruited by chemoattraction to MCP-1 and MIP-1α, -1β and 2, with MCP-1 being the most potent (Frangogiannis et al., 2002, Kakio et al., 2000). MCP-1 is localised to the microvascular endothelium, binds to CCR2 and can also attract natural

killer (NK) cells and T cells (Lakshminarayanan et al., 2001). These factors increase within hours after MI; subsequent macrophage infiltration starts from 2 days after MI, peaks between 4 and 7 days, after which it declines (Dewald et al., 2004, Tao et al., 2004). MCP-1 is involved in several diseases that have monocyte rich infiltrates, such as atherosclerosis and rheumatoid arthritis (Nelken et al., 1991, Koch et al., 1992). While continuous cardiomyocyte specific over-expression of MCP-1 leads to heart failure and premature death which is mediated by enhanced apoptosis (Zhou et al., 2006), transient over-expression in a murine model of MI is beneficial and is associated with enhanced macrophage infiltration and reduced scar size (Morimoto et al., 2006).

Monocyte adherence to the extracellular matrix of the infarct can encourage further cytokine upregulation (Sunderkotter et al., 1994). Monocytes differentiate into macrophages, stimulated by macrophage colony-stimulating factor (M-CSF) and caspases, proteolytic enzymes involved in the apoptosis cascade (Figure 1.2, Frangogiannis et al., 2002). The beneficial role of this process in infarct healing has been indicated by the demonstration that intra-peritoneal injection of M-CSF leads to enhanced macrophage infiltration, improved left ventricular function and infarct repair in a rat model of MI (Yano et al., 2006b). Macrophages can secrete additional MCP-1, amplifying the inflammatory response (Morimoto et al., 2006, MacKinnon et al., 2008, Kakio et al., 2000, Frangogiannis et al., 1998, Cathelin et al., 2006). Furthermore, over 150 secretory proteins have been identified from macrophage cultures including IL-1α, IL-1β, IL-6, TNFα, MIP-1α, MIP-1β, MIP-2α, MIP-2β, MCP-1, IL-8, thrombospondin-1 (TSP-1), platelet derived growth factor (PDGF), proteases, matrix metalloproteases (MMPs), M-CSF, basic fibroblast growth factor (bFGF), vascular endothelial growth factor (VEGF), transforming growth factor (TGF) α and β, and urokinase-plasminogen activator (u-PA) (Lambert et al., 2008, Sunderkotter et al., 1994). This underlines the pivotal role of macrophages in the inflammatory response. The roles of macrophages in myocardial infarct healing include phagocytosis to remove cell debris, stimulation of angiogenesis and scar formation. Depletion of macrophages, using an anti-macrophage serum, has demonstrated that they are a vital part of wound healing (Cohen et al., 1987).

Detection of necrotic cell debris in the ischaemic core can produce a dramatic change in macrophage physiology, including enhancing cytokine production (Mosser and Edwards, 2008). On the other hand, phagocytosis of apoptotic cells increases secretion of TGF-β which can mediate a decrease in macrophage secretion of a range of pro-inflammatory cytokines including, IL-1β, IL-8 and TNFα (Fadok et al., 1998). This demonstrates the importance of the type of cell death after MI.

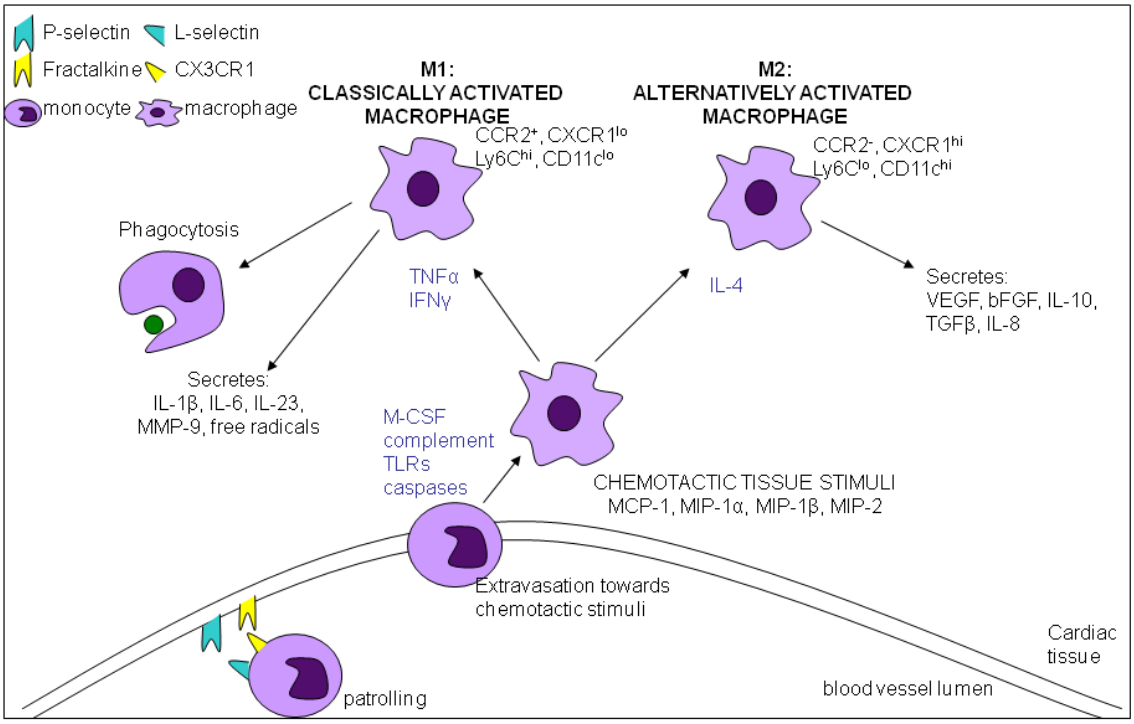

Figure 1-2 Macrophage action post-MI

Interaction of monocytes with the vessel wall is mediated by β2 integrins and CX3CR1-fractalkine-mediated adhesion. They transmigrate into the infarct in response to inflammatory stimuli. Macrophage colony-stimulating factor (M-CSF), the complement cascade and toll like receptors (TLRs) stimulate the differentiation of monocytes to macrophages in the tissue subsequently enabling their migration towards chemotactic stimuli (monocyte chemoattractant protein-1 (MCP-1) and macrophage inflammatory proteins (MIP)).The local environment can prime macrophages to become M1 (classically-activated macrophages) or M2 (alternatively-activated macrophages). Tumour necrosis factor α (TNFα) and interferon γ (IFNγ) encourage the M1; CCR2+, CXCR1lo, Ly6Chi, CD11clo phenotype while interleukin-4 (IL-4) encourages the M2; CCR2-, CXCR1hi, Ly6Clo, CD11chi phenotype. Typical M1 behaviour includes phagocytosis, secretion of inflammatory mediators such as IL-1β, IL-6, IL-23 and free radicals along with matrix metalloprotease-9 (MMP-9). M2 macrophages secrete pro-angiogenic and pro-resolution factors such as vascular endothelial growth factor (VEGF), basic fibroblast growth factor (bFGF), IL-10, transforming growth factor β (TGFβ) and IL-8. By secreting such factors alternatively-activated macrophages stimulate angiogenesis and wound healing. Figure adapted from Lambert et al., 2008 and Mosser and Edwards, 2008

1.3.4.1 Macrophage subtypes

As indicated (above), monocytes and macrophages can be subdivided into regulatory, classically-activated (M1) and alternatively-activated (M2) categories (see Figure 1.2). However it has recently been acknowledged that instead of each subtype being distinct from one another, their activation state should be considered more of a continuous 'spectrum' of phenotypes and that their phenotype can change (Mosser and Edwards, 2008)..

Circulating monocytes are a relatively heterogeneous population; however Sunderkötter *et al* have demonstrated that monocytes that have been recently liberated from the bone marrow initially have an inflammatory ly6C^{hi} phenotype (Sunderkötter et al., 2004). Under steady state conditions these monocytes downregulate ly6C (a monocyte/macrophage and endothelial cell differentiation antigen) as they mature. These monocytes have a high proliferative capacity and migrate into tissue when there is peripheral inflammation (Sunderkotter et al., 2004). Activation of such monocytes by TNF and interferon-γ (IFNγ) produces classically-activated macrophages that are characterised by their expression levels of the specific cell markers as follows; CCR2^{+}, CX3CR1^{lo}, ly6C^{hi,} CD11c^{lo} (Nahrendorf et al., 2007, Sunderkotter et al., 2004). CCR2 is the receptor for MCP-1 and, therefore, these macrophages migrate along its gradient (Sunderkotter et al., 2004, Sunderkotter et al., 1994). These classically-activated macrophages are primed to secrete pro-inflammatory cytokines, such as IL-1, IL-6 and IL-23, and produce free radicals amplifying the inflammatory response (Sunderkotter et al., 2004). Excessive production of these cytokines by macrophages may lead to autoimmune responses and are, therefore, damaging rather than protective (Sunderkotter et al., 2004). In post-infarct healing classically-activated macrophages phagocytose cell debris enabling granulation and scar tissue formation and, thus, stabilising the infarct (Nahrendorf et al., 2007, van Amerongen et al., 2007). M1 macrophages can activate MMP-9 thus favouring degradation of the ECM (Nahrendorf et al., 2007).

The role of alternatively-activated macrophages (M2) is to inhibit inflammation (by secretion of the anti-inflammatory cytokines TGF-β and IL-10), aid in wound healing and to stimulate angiogenesis (Lambert et al., 2008, Mosser and Edwards, 2008, Nahrendorf et al., 2007, van Amerongen et al., 2007). M2 activation is dependent on IL-4, which can be secreted by mast cells and neutrophils (Loke et al., 2002, Brandt et al., 2000). M2 macrophages have a gene expression profile that is distinct from other macrophage types. Nematode infections stimulate a typical M2 response and lead to the upregulation of FIZZ1 (RELMα), YM1 and arginase 1 in the macrophages (Nair et al., 2006, Kreider et al., 2007). FIZZ1 is a resistin-like molecule that can antagonise insulin action. The chitinase like activity of YM1 can aid in matrix reorganisation and wound healing, and arginase activity enables production precursors of collagen, contributing to the extracellular matrix and scar formation (Loke et al., 2002, Lambert et al., 2008, Nair et al., 2005, Kreider et al., 2007).

Macrophage infiltration and angiogenesis are positively correlated in several injury and disease models, including stroke and cancer (Manoonkitiwongsa et al., 2001, Banciu et al., 2008). The role of alternatively-activated macrophages in angiogenesis involves their ability to secrete angiogenic cytokines such as IL-8 (which can also act in an inflammatory capacity as mentioned previously), VEGF and bFGF. Macrophages must be activated in order to stimulate angiogenesis as it enables them to secrete angiogenic cytokines (Polverini et al., 1977, Leor et al., 2006). Activated, but not unstimulated, macrophages can stimulate neovascularisation in corneal explant assays (Polverini et al., 1977). Additionally, intra-cardiac injection of human, activated macrophages after coronary artery occlusion in rats enhances vessel density, relative to control, after 5 weeks' recovery (Leor et al., 2006). *In vitro* IL-8 can enhance endothelial cell proliferation and capillary formation, and also increase the expression of MMP-2, MMP-9 and anti-apoptotic genes (Li et al., 2003). Furthermore, *in vivo* IL-8 can enhance recruitment of bone marrow derived cells to the ischaemic myocardium and contributes to neovascularisation (Kocher et al., 2006). Both bFGF and VEGF can stimulate endothelial cell migration, proliferation and capillary tube sprouting (reviewed in

Sunderkotter et al., 1994). Over-expression of MCP-1 also results in augmentation of capillary density and preserves heart function (Morimoto et al., 2006). Macrophages are also a source of factors that enhance angiogenesis indirectly, such a prostaglandins and angiotensin-converting enzyme (ACE). Paradoxically they also secrete angiostatic factors such as TSP1 and IFNγ (Sunderkotter et al., 1994).

1.3.4.2 Macrophage subtype in injury and disease

Both M1 and M2 macrophages have been implicated in a variety of diseases including atherosclerosis, cancer and diabetes (Galkina and Ley, 2009, Mosser and Edwards, 2008, Lambert et al., 2008, Martin-Fuentes et al., 2007). An M1 macrophage phenotype may aid in the progression of atherosclerosis, whereas encouraging M2 activation may improve plaque stability (Martin-Fuentes et al., 2007, Mosser and Edwards, 2008). Classically-activated macrophages are implicated in cancer initiation with a switch to alternatively-activated macrophages aiding in tumour progression and angiogenesis (Sica et al., 2006). Moreover, in a murine model of liver fibrosis M2 macrophages were shown to have a dual role in injury and repair. Conditional ablation of M2 monocytes during liver injury reduces fibrosis, indicating that M2 macrophages are harmful. However, depletion during the recovery phase prevents resolution of fibrosis, suggesting they have an important role in healing (Duffield et al., 2005).

In myocardial infarct healing Nahrendorf et al. have shown that classically-activated ly6C^{hi}/CD11c^{lo} monocytes infiltrate the myocardial infarct maximally by 3 days, after which they decline (Nahrendorf et al., 2007). This peak was associated with enhanced MCP-1 expression. Genetic deletion of the receptor for MCP-1 (CCR2) resulted in reduced recruitment of M1 macrophages early in myocardial infarct healing (Nahrendorf et al., 2007). This was, in part, due to decreased liberation of ly6C^{hi} monocytes from the bone marrow. Infiltration of M2 (ly6C^{lo}/CD11c^{hi}) monocytes peaks between 5 and 7 days post-MI and is associated with increased VEGF expression and reduced protease activity (Nahrendorf et al., 2007). Genetic deletion of CX3CR2, the fractalkine receptor,

impairs recruitment of ly6C^{lo} monocytes to the healing infarct at 5-7 days indicating that it has a vital role in recruiting this type of monocyte (Nahrendorf et al., 2007).

The crucial role of both classically-activated and alternatively-activated macrophages during myocardial infarct healing has been demonstrated using selective depletion with clodronate. Depletion of classically-activated monocytes by administering clodronate immediately after MI increases cell debris and necrotic tissue area 7 days after MI (Nahrendorf et al., 2007). On the other hand, selective depletion of M2 macrophages from day 3 decreases the number of CD31-positive endothelial cells, α smooth muscle actin-positive smooth muscle cells and collagen deposition (Nahrendorf et al., 2007). Furthermore, in a cryo-injury model of left ventricular damage macrophage depletion increased 4 week mortality by 28% (van Amerongen et al., 2007). Surviving mice had a greater necrotic area, reduced neovascularisation and collagen deposition. This was associated with increased ventricular dilation and wall thinning (van Amerongen et al., 2007) lending support for the requirement of an organised co-ordinated inflammatory response in infarct healing. The balance of M1 and M2 activation may determine the outcome of post-infarct healing.

1.3.5 Resolution of inflammation

The processes governing the resolution of inflammation are unclear. There is conflicting evidence regarding the effect of deficiency in IL-10, a cytokine reported to inhibit production of inflammatory cytokines. While one study reports that IL-10 deficiency increases inflammation and necrosis in a murine model of MI (Yang et al., 2000) another has shown that it has a limited effect on inflammation in terms of abundance, timing and resolution (Zymek et al., 2007). The importance of inflammatory resolution has been shown where the anti-inflammatory and anti-angiogenic TSP-1 has been knocked out. Deficiency of TSP-1 post-MI elevates and extends inflammation and is associated with scar expansion and adverse remodelling (Frangogiannis et al., 2005). Additionally, excessive inflammation can lead to cardiac rupture (Nian et al., 2004).

TGF-β is secreted by macrophages and is reported to act as a 'stop signal' for inflammation. Apoptotic neutrophils are phagocytosed by macrophages while there is speculation regarding the fate of the infiltrated macrophages. They may die locally, migrate out of the tissue or mature into resident macrophages or dendritic cells.

1.4 Angiogenesis in MI

Neovascularisation encompasses 3 processes that are vital both in embryo growth and in adulthood; vasculogenesis, angiogenesis and arteriogenesis (Carmeliet, 2000, Jain, 2003, Conway et al., 2001). Vasculogenesis, the production of blood vessels in discrete locations by differentiation of progenitor cells, is vital in generating vasculature during embryo development but is also possible in adulthood. The expansion of this primitive vasculature is mediated by sprouting of new vessels from existing ones and is known as angiogenesis. The term arteriogenesis encompasses maturation of pre-existing vessels or *de novo* growth of collateral vessels producing large muscular arteries (Jain, 2003, Conway et al., 2001). All three processes require well orchestrated expression of growth factors, adhesion molecules and modulators of the extracellular matrix. Lack of co-ordination may produce abnormal, pathological vasculature (Jain, 2003). Angiogenesis has been observed in a variety of disease models, including cancer, haemangioma and retinopathy (Folkman and Shing, 1992, Hynes, 2002, Patan, 2000, Carmeliet and Jain, 2000). Therefore inhibition of this process is an attractive therapeutic target. However, angiogenesis is also a vital part of wound healing and enhancing new vessel growth is also attractive after limb ischaemia and MI (Sasaki et al., 2007, Payne et al., 2007, Orlic et al., 2001, Law et al., 2004, Maulik and Thirunavukkarasu, 2008, Meyer et al., 2006, Cheng et al., 2007). Angiogenesis is a complex event requiring co-ordinated signalling from the vessel wall and the extracellular matrix that results in increased vessel permeability, endothelial cell proliferation, migration, vessel stabilisation and eventually pruning, processes that temporally overlap and is described here (Figure 1.3) (Jain, 2003).

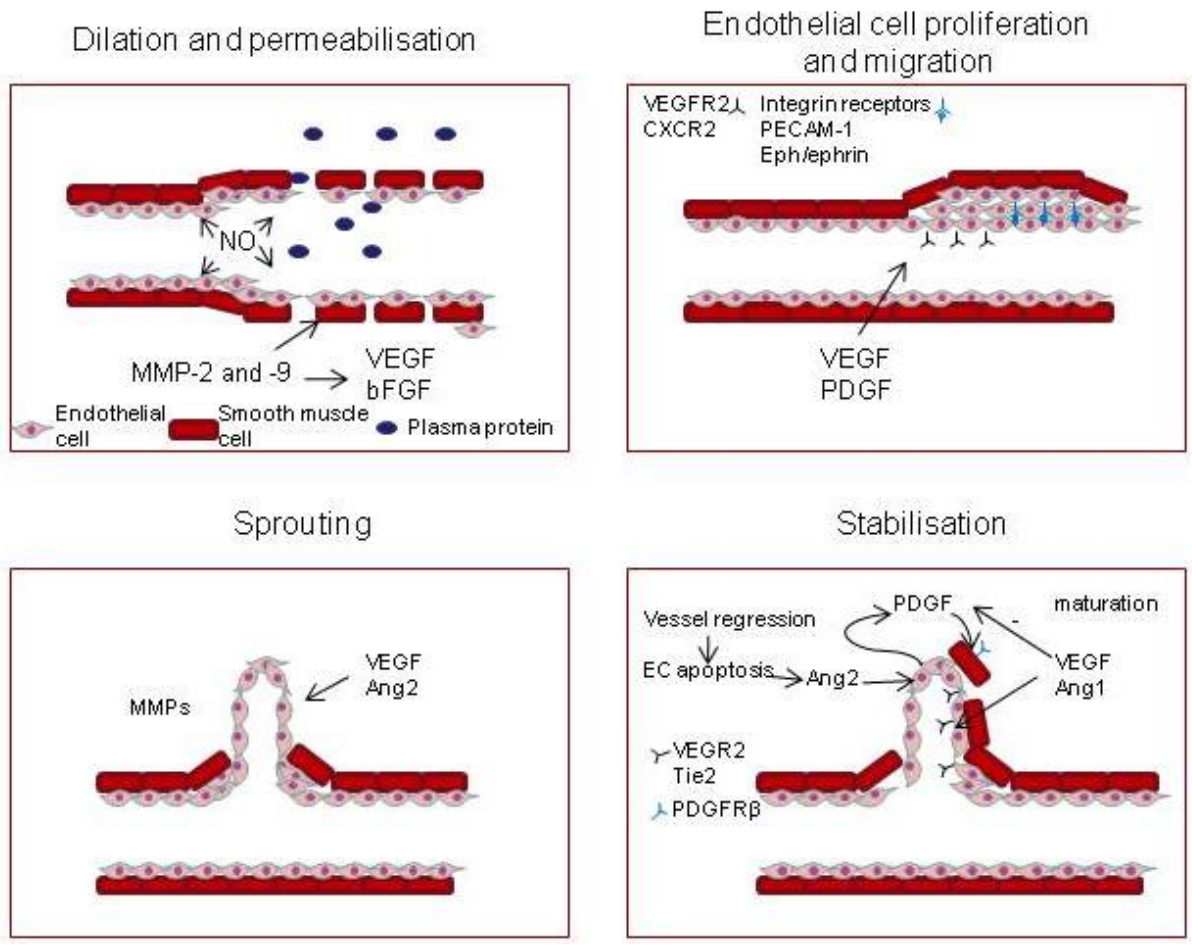

Figure 1-3 Angiogenesis

The first step of angiogenesis involves the dilation and permeabilisation of a mother vessel. Nitric oxide mediates an increase in vessel diameter which is followed by degradation of the basement membrane by the matrix metalloproteases MMP-2 and MMP-9. Such degradation liberates matrix bound growth factors such as VEGF (vascular endothelial growth factor) and bFGF (basic fibroblast growth factor). The second step consists of endothelial cell proliferation and migration which is mediated by VEGF and PDGF (platelet derived growth factor) acting on their cognate endothelial cell receptors, VEGFR2 and CXCR2. Integrin receptors, adhesion molecules (such as PECAM-1, platelet cell adhesion molecule) and Eph/ephrin receptor ligand pairs aid in endothelial cell migration towards sites of angiogenesis. The third step is vessel sprouting. In areas of extracellular matrix degradation endothelial cells sprout from capillaries, guided by VEGF and Ang2 (Angiopoietin 2). The loops formed by these sprouts will become the new vessels. Finally, the angiogenic vessel must be stabilised (step 4). Vessel pruning is

mediated by Ang2-induced endothelial cell apoptosis. Appropriate pruning, along with vessel maturation, promotes the formation of an organised vascular network. VEGF and Ang1 promote endothelial cell survival. Additionally the interaction of Ang1 with the Tie2 receptor tightens cell to cell junctions making the vessels leak resistant. PDGF is secreted by endothelial cells and recruits smooth muscle cells and pericytes to the vessel wall via interactions with its receptor, PDGFRβ, expressed on these cells. Figure adapted from Murdoch et al (2008).

1.4.1 Stimulation of angiogenesis

Angiogenesis is mediated by the upregulation of angiogenic factors and modulators of the extracellular matrix, along with down-regulation of anti-angiogenic factors. These changes can be stimulated by ischaemia (Conway et al., 2001, Steinbrech et al., 2000, Shohet and Garcia, 2007). Under hypoxic conditions reduced degradation of hypoxia inducible factor-1α (HIF-1α) enables it to translocate to the nucleus where it can up-regulate its target genes which encode factors involved in angiogenesis, such as VEGF, angiopoietin 1 (Ang-1), angiopoietin 2 (Ang-2) and PDGF (Kido et al., 2005, Bates and Harper, 2002, Steinbrech et al., 2000). Knock out of HIF-1α impairs development of the vasculature whereas over-expression after MI increases vessel density whilst reducing infarct size (Kido et al., 2005, Shohet and Garcia, 2007). Hypoxia also leads to the upregulation of aminopeptidase-N (APN)/CD13, a marker of angiogenic vessels *in vitro* (Bhagwat et al., 2001).

Ischaemia can trigger both angiogenesis and inflammation. It is, therefore, difficult to determine the contribution of direct (HIF-1α) and indirect (inflammation) effects of ischaemia on post-MI angiogenesis. As mentioned previously, macrophages are known to secrete a host of factors, including angiogenic cytokines such as MCP-1, VEGF and PDGF (Kayisli et al., 2002, Lambert et al., 2008, Sunderkotter et al., 1994). A non-inflammatory model of angiogenesis of the cornea, in immuno-deficient mice, demonstrates the efficiency of VEGF and FGF as angiogenic agents in the absence of inflammation (Kenyon et al., 1996). However, chemokines such as IL-8 can act in both an inflammatory manner, recruiting neutrophils to sites of inflammation, and in an angiogenic manner, by stimulating endothelial cell chemotaxis and proliferation (Sekido et al., 1993, Thelen et al., 1988, Kayisli et al., 2002). Attempts have been made to dissect out the contribution of inflammation to angiogenesis using a variety of intervention studies. Depletion of neutrophils early in tumour development reduces angiogenesis and tumour growth (Nozawa et al., 2006). Macrophage depletion, with clodronate reduces angiogenesis after MI and in aortic ring explants (Fraccarollo et al.,

2008, Nahrendorf et al., 2007, van Amerongen et al., 2007, Gelati et al., 2008). In addition, in a tumour model, depletion of macrophages can reduce angiogenic cytokine production and tumour size (Banciu et al., 2008). Additionally, as discussed above, polarisation of macrophages to the M2 resolution phenotype may also promote angiogenesis (Mosser and Edwards, 2008).

1.4.2 Dilation and permeability

The constituents of blood vessels can include endothelial cells, smooth muscle cells and pericytes (collectively known as mural cells) and an extracellular matrix/basement membrane which provides support (Jain, 2003). This organised structure needs to be permeablised to enable capillary growth. Initially, vascular nitric oxide dilates blood vessels and can increase VEGF expression (see Figure 1.3) (Patan, 2000, Jain, 2003, Carmeliet, 2000). Subsequent redistribution of endothelial cell adhesion molecules, along with degradation of the basement membrane and extracellular matrix by MMP-2 and MMP-9, increases vessel permeability (Patan, 2000, Jain, 2003, Haas et al., 2000). The composition of the extracellular matrix can modulate endothelial cell shape, thus influencing their response to growth factors (Sottile, 2004). MMPs liberate matrix bound growth factors, such as VEGF and bFGF but also release angiostatic molecules such as angiostatin and tumstatin (Haas et al., 2000). However, MMPs are generally considered to be pro-angiogenic and the angiostatic factor TSP-1 is thought to reduce angiogenesis through inhibition of MMPs (Conway et al., 2001). The dilated and permeable nature of these nacscent vessels enables plasma protein leakage and subsequent production of a new provisional matrix (Carmeliet, 2000, Conway et al., 2001).

1.4.3 Endothelial cell proliferation, migration and vessel sprouting

Several factors, such as those from the VEGF and FGF families along with IL-8 and TNF-α, are involved in enhancing endothelial cell proliferation and it is likely that there is some redundancy (Risau, 1997, Maulik and Thirunavukkarasu, 2008, Virag and Murry, 2003). VEGF acts on the VEGF receptor 2 on endothelial cells promoting endothelial cell proliferation, migration and tube formation (see Figure 1.3) (Maulik and Thirunavukkarasu, 2008, Gu et al., 1999, Nahrendorf et al., 2007). Blockade of CXCR2, the receptor for IL-8 prevents vessel sprouting in aortic rings highlighting its role in angiogenesis (Gelati et al., 2008). Such factors, produced by endothelial cells and inflammatory cells, may also stimulate the proliferation of smooth muscle cells (Folkman and Shing, 1992). Endothelial cell migration requires matrix degradation by MMPs and u-PA (Haas et al., 2000, Cheng et al., 2007, Sunderkotter et al., 1994, Heymans et al., 1999, Sottile, 2004). Depletion of MMP-2 reduces angiogenesis *in vivo* in a hindlimb ischaemia model and *in vitro* in aortic ring cultures (Cheng et al., 2007). Heymans et al. demonstrated that deficiency of u-PA in a murine model of MI reduced cardiac VEGF expression and angiogenesis and this could not be resolved fully by VEGF therapy (Heymans et al., 1999). These studies demonstrate that angiogenesis requires more than just growth factors (Heymans et al., 1999, Greenberg et al., 2008).

Migration of endothelial cells is mediated by the integrin receptors ($\alpha_v\beta_3$ and $\alpha_5\beta_1$), adhesion molecules (PECAM-1), and Eph/ephrin receptor ligand pairs (Jain, 2003). The role of integrins in angiogenesis is somewhat controversial as knockout mice and antagonists directed against integrins do not necessarily have reduced angiogenesis. Indeed, these manipulations have been associated with enhanced angiogenesis (reviewed in (Hynes, 2002). Gap junctions, such as VE-cadherin and connexins, link endothelial cells as they form the endothelial layer however, some appear to be more important than others (Jain, 2003, Stalmans et al., 2002). Knockout of VE-cadherin and connexin 43 are embryonically lethal whilst deficiency of connexion 40 results in impaired cardiac function (reviewed in Jain, 2003). In contrast, PECAM-1 (CD31) null mice develop normally suggesting that loss of action is compensated for by other adhesion molecules

during development (Solowiej et al., 2003). As expected, Solowiej et al. found that PECAM-1 knockout mice have reduced vessel density in sponge implants (Solowiej et al., 2003). Transfer of wild type bone marrow to these mice restores their angiogenic ability suggesting that bone marrow cells contribute to the neovascularisation (Solowiej et al., 2003). Similarly, mice deficient for aminopeptidase-N (otherwise known as CD13), another cell adhesion molecule, develop normally but have reduced angiogenesis in low oxygen-induced retinopathy and gelfoams embedded with growth factors (Rangel et al., 2007).

Sprout formation from pre-existing capillaries in areas of matrix degradation is stimulated by cues provided by the extracellular matrix such as co-expression of Ang2 and VEGF (Patan, 2000, Carmeliet, 2000, Conway et al., 2001). These sprouts form the loops and networks that will become the capillary bed. The lumen diameter is determined by various isoforms of VEGF and Ang1 (Patan, 2000, Carmeliet, 2000, Conway et al., 2001).

1.4.4 Stabilisation and maturation

The longevity of neovascularisation depends on the local balance of pro-angiogenic and anti-angiogenic factors (Patan, 2000, Carmeliet, 2000, Conway et al., 2001). While survival of the new vessel may be advantageous, vessel pruning is also important. Endothelial cell survival is vital for maintenance of these nascent vessels and is encouraged by VEGF acting on the VEGF receptor (Conway et al., 2001). The interaction of Ang1 with its receptor, Tie 2, stabilises vessels by tightening cell to cell junctions making them leak resistant (see Figure 1.3) (Thurston et al., 1999). Additionally, Ang1 promotes cell survival (Conway et al., 2001). The factors that play a role in vessel regression, such as Ang2, eliminate excess vessels by endothelial cell apoptosis promoting an organised vessel network prior to addition of the stabilising mural cell coat (Conway et al., 2001, Patan, 2000, Maisonpierre et al., 1997). Interestingly, Ang 2, which also binds to Tie 2 receptors, has a dual role in angiogenesis.

In the presence of VEGF Ang 2 stimulates vessel sprouting. However, in its absence vessel regression is favoured via destabilisation (Jain, 2003).

PDGF is secreted by endothelial cells and recruits smooth muscle cells and pericytes, expressing the PDGF receptor (PDGRβ) to the vessel wall (Greenberg et al., 2008). Lack of PDGF or its receptor is embryonically lethal, demonstrating its vital role in neovascularisation (Lindahl et al., 1997). Intriguingly, VEGF has been shown to be a negative regulator of PDGF-mediated pericyte recruitment in matrigel implantation models and in the chorioallantoic membrane of chick embryos (Greenberg et al., 2008). Such findings may explain why cancerous tumours, characterised by high VEGF levels, have leaky abnormal vasculature and why anti-VEGF therapy results in pericyte coverage and vessel normalisation in tumour models (Greenberg et al., 2008).

Vessel plasticity declines as pericyte/smooth muscle coverage is gained. Therefore, superfluous vessel regression or, alternatively, further endothelial cell proliferation and migration may be prevented (Conway et al., 2001). Whilst vessel destabilisation of mature vessels may still occur (by removal of pericytes/smooth muscle cells) it is much less likely than in an immature vessel (Jain, 2003).

There has been some debate regarding the origin of pericytes. It has been suggested that they may differentiate from mesenchymal stem cells (Bexell et al., 2009), mononuclear cells (Conway et al., 2001), epicardial cells (Dettman et al., 1998) or fibroblasts (Njauw et al., 2008). TGF-β initiates differentiation of these cells to pericytes (Bergers and Song, 2005). The receptor for TGF-β is endoglyn (CD105) which is expressed on endothelial cells. Homozygous deletion of endoglyn results in embryonic lethality due to impaired angiogenesis, whereas mice heterozygous for endoglyn have reduced angiogenesis and impaired cardiac function after MI (van Laake et al., 2006). Pericytes are commonly associated with vessel stability but they have many more diverse functions. Like smooth muscle cells, pericytes can alter vessel tone in response to vasoactive substances (Kutcher and Herman, 2009, Kawamura et al., 2004). Indeed pericytes can secrete vasoactive substances, growth factors and cytokines thus

influencing vascular function (Conway et al., 2001). They are found in high density at the blood-brain barrier where they form a tight boundary (Ramsauer et al., 2002, Thomas, 1999). Interestingly in this location pericytes can exhibit macrophage-like phagocytic behaviour (Thomas, 1999). Some have hypothesised that they could indeed be brain macrophage precursors (Bergers and Song, 2005, Thomas, 1999).

1.4.5 Post-infarct angiogenesis

Initially after MI the number of vessels across the left ventricle decreases due to loss of part of the myocardium (Grass et al., 2006). Additionally, angiostatic chemokines, such as interferon γ inducible protein (IP-10), are upregulated to prevent vessel formation before the wound is 'debrided' (Frangogiannis et al., 2001, Grass et al., 2006). From 4 days post-MI a capillary plexus is formed around the infarct (Ren et al., 2002). As infarct healing advances from the inflammatory phase to the proliferative phase there is an increase in endothelial cell proliferation and angiogenic cytokines (Virag and Murry, 2003). Subsequently, the infarct border vessel density is augmented by 7 days after MI (Ren et al., 2002, Grass et al., 2006, Lutgens et al., 1999, Virag and Murry, 2003). As the infarct scar matures the neovessels are pruned, a process that is normally complete by 4 weeks post-MI (Ren et al., 2002, Grass et al., 2006, Dewald et al., 2004). Interventions that result in increased vessel density on the infarct border also improve heart function (Kido et al., 2005, Kocher et al., 2001, Liu et al., 2007, Sasaki et al., 2007, Orlic et al., 2001, Nahrendorf et al., 2007, Engel et al., 2006). Enhancing perfusion here may prevent the infarct from spreading into the healthy myocardium by salvaging cardiomyocytes (Liu et al., 2007). While cardiac angiogenesis after MI is beneficial, angiogenesis in the absence of injury is deleterious and results in hypertrophy (Tirziu et al., 2007). In human infarcted hearts capillary density is negatively correlated with scar size and infarct-related artery stenosis showing that increased vessel density is associated with more favourable remodelling (Prech et al., 2006).

1.4.6 Therapeutic angiogenesis

Experimentally, use of only one growth factor to enhance angiogenesis leads to the production of aberrant, disorganised, leaky vasculature (Korpisalo et al., 2008, Greenberg et al., 2008). Angiogenesis in cancerous tumours is often a result of VEGF over-expression and the vessels produced are disorganised and leaky, characteristic of VEGF-induced neovascularisation (Murdoch et al., 2008). However, VEGF therapy has been shown to be beneficial. Animal models demonstrate that injection of VEGF into the myocardium of infarcted hearts can reduce infarct size, enhance angiogenesis and improve cardiac function (Ruixing et al., 2007, Yau et al., 2005). However, in a rabbit hindlimb model of ischaemia both VEGF and PDGF were required to improve perfusion (Korpisalo et al., 2008, Greenberg et al., 2008). PDGF which is required for pericyte priming, aiding in vessel maturation and reducing vessel leakage, can work synergistically with VEGF (Greenberg et al., 2008, Korpisalo et al., 2008). Additionally, injection of cells engineered to over-express VEGF with IGF-1 into a rodent heart after MI improves infarct healing better than VEGF alone (Yau et al., 2005). Several strategies may be employed to induce angiogenesis. These include delivery of growth factors (individually or in a cocktail) or perhaps more attractively delivery of transcription factors that induce expression of several angiogenic factors. The latter approach may be more likely to induce the full physiological angiogenic cascade (Jain, 2003). Unfortunately, injection of growth factors has had limited success to date (Simons, 2005, Losordo et al., 1998, Ellis et al., 2006).

There is increasing evidence that bone marrow-derived cells, including endothelial progenitor cells and mononuclear cells, mobilised after injury or injected into the myocardium or circulation after injury, may enhance neovascularisation (Orlic et al., 2001, Kocher et al., 2001, Sesti et al., 2005, Kastrup et al., 2006, Sasaki et al., 2007, Simons, 2005, Fazel et al., 2006, Takahashi et al., 1999, Takahashi et al., 2006). Fazel et al. reported that c-kit+ cells found in the heart after MI originated from the bone marrow (Fazel et al., 2006). In the heart these cells contributed to angiogenesis by increasing VEGF and altering the ratio of angiopoietin 1 to angiopoietin 2 providing an

environment that favours angiogenesis (Fazel et al., 2006). There is also evidence that these c-kit cells are also resident in the myocardium (Beltrami et al., 2003). Whilst some studies report that these mobilised progenitors can incorporate into the healing heart post-infarction regenerating it (Orlic et al., 2001) others suggest that their beneficial actions are mediated by enhancing neovascularisation on the infarct border (Kocher et al., 2001). Daily injection of granulocyte colony-stimulating factor (G-CSF) or stem cell factor (SCF) which liberate bone marrow-derived cells, improves post-infarct heart function in rats independently of improved neovascularisation at 8 weeks. Thus the function of bone marrow-derived cells in this context is not entirely clear (Sesti et al., 2005). There is confusion in this field as there are also a number of experimental studies that report that such factors and cells have no effect on post-infarct healing (Maekawa et al., 2004, Terrovitis et al., 2004). A current hypothesis is that homing of progenitors to the heart may not contribute directly to cardiac healing by incorporation into the muscle or vasculature but act via a paracrine mechanism (Sesti et al., 2005, Takahashi et al., 2006). The BOOST clinical trial (BOne marrOw transfer to enhance ST-elevation infarct regeneration) attempted to determine the effect of intracoronary infusion of bone marrow cells (harvested from and given back to) on MI patients undergoing percutaneous coronary intervention with stent implantation. This resulted in a small, sustained improvement in ejection fraction, but not left ventricular systolic function, at 18 month follow-up (Meyer et al., 2006). This is currently being followed up with BOOST 2 in which a more comprehensive assessment of the mechanism of early improved ejection fraction is being conducted.

1.4.7 'Vascular mimicry'

It has been acknowledged that rapidly growing tumours are able to enhance perfusion independent of angiogenesis by a process called 'vascular mimicry' (Maniotis et al., 1999). "Tunnels" have been identified in the myocardium that do not express endothelial cell markers, but are positive for elastase. Some of these tunnels contained blood

components, such as erythrocytes, with others comprising of endothelial cell-like cells. It was hypothesised that this tunnel formation was mediated by macrophages (Moldovan et al., 2000, Bendeck, 2000). A similar phenomenon has also been described in the heart in cardiac specific MCP-1 overexpressing mice. This was associated with increased macrophage infiltration and the development of heart failure as the mice aged (Moldovan et al., 2000). However this phenomenon is not reported extensively in the literature during post-infarct healing.

1.5 Fibroblasts in MI

Fibroblasts are derived from mesenchymal cells, are found in close association with cardiomyocytes and between myocardial tissue layers and have a homeostatic role in maintaining the extracellular matrix (ECM) (Camelliti et al., 2005). They can respond to mechanical and biochemical stimuli leading to enhanced cell proliferation, production of extracellular matrix and growth factors (Camelliti et al., 2005). One of the components of the post-MI healing response involves the differentiation of quiescent fibroblasts to myofibroblasts, enabling fibrosis (see Figure 1.4). In the myocardium post-infarct myofibroblasts are derived from resident fibroblasts but in extra-cardiac sites fibrosis is reported to be mediated by bone marrow-derived fibroblasts (Yano et al., 2005, Forbes et al., 2004). Typical fibroblast markers include vimentin and Discoidin Domain Receptor 2, (Osborn et al., 1984, Camelliti et al., 2005). However, after differentiation they secrete α smooth muscle actin (Dewald et al., 2004, Virag and Murry, 2003). Transformation of fibroblasts can be mediated by reactive oxygen species and TGF-β, produced by macrophages (Desmouliere et al., 1993, Fadok et al., 1998, Cleutjens et al., 1995). TGF-β mRNA expression is enhanced from 1 day post-MI and remains elevated for a further 6 days (Dewald et al., 2004). Myofibroblast activation follows this with it increasing from 3 days post-MI and remaining elevated until day 7, before declining (Dewald et al., 2004, Virag and Murry, 2003, Yang et al., 2002, Tao et al., 2004). In this activated state myofibroblasts proliferate and can secrete collagen, MMPs, tissue

inhibitors of matrix metalloproteases (TIMPS), TGF-β and TNFα (Virag and Murry, 2003, Squires et al., 2005). These proteases and cytokines can modulate the extracellular matrix and promote scar formation.

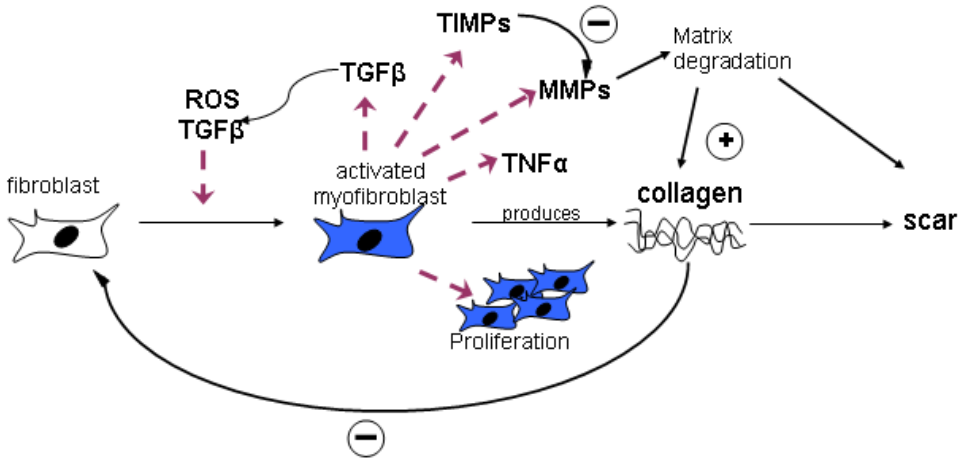

Figure 1-4 Fibroblast activation after myocardial infarction

The increase in cardiac reactive oxygen species (ROS) and transforming growth factor β (TGF β) as a result of MI mediates the transformation of fibroblasts to myofibroblasts. In this activated state fibroblasts proliferate and secrete factors such as matrix metalloproteases (MMPs), tumour necrosis factor α (TNFα), TGFβ, which acts in a positive feedback loop to further enhance fibroblast transformation, and tissue inhibitor of metalloproteases (TIMPs) which inhibit MMPs. Collagen secretion by myofibroblasts and matrix degradation by MMPs permits scar formation in the healing myocardial infarct. Negative feedback by collagen prevents excessive fibroblast-mediated fibrosis. Figure adapted from Camelliti et al., 2005.

1.6 The extracellular matrix in MI

The dynamic, highly organised extracellular matrix provides structural and mechanical support to tissues along with interacting with cells to modulate their behaviour (Dobaczewski et al., 2009, Porter and Turner, 2009). The intense inflammatory response associated with MI results in disruption of this influential matrix. This enables inflammatory cell infiltration in the inflammatory phase and then infiltration of other cell types in the proliferative phase (Cleutjens et al., 1995, Sottile, 2004). Matrix degradation liberates matrix bound growth factors such as bFGF, aiding in promotion of angiogenesis (Sunderkotter et al., 1994). Within 3 hours of reperfusion, extravasation of plasma proteins, via increased vascular permeability, produces a temporary fibrin/fibrinogen matrix in the infarcted myocardium, providing support for proliferating and migrating cells (Dobaczewski et al., 2006). The basement membrane and extracellular matrix constituents laminin and hyaluronan are fragmented within 24 hours and replaced with a 'second order' provisional matrix made of fibronectin (Dobaczewski et al., 2006). Fragments of collagen and hyaluronan can act as neutrophil chemoattractants and induce inflammatory gene expression in endothelial cells and macrophages respectively (Dobaczewski et al., 2009, Weathington et al., 2006, Taylor et al., 2004, Dobaczewski et al., 2006).

The ECM is degraded by the zinc-dependent proteases known as MMPs that are secreted during the inflammatory phase of infarct healing (Tao et al., 2004, Sun et al., 2000). Activation of MMPs occurs as early as 10 minutes after ischaemia and these enzymes, along with serine proteases, can then degrade collagen which is a constituent of the extracellular matrix (Etoh et al., 2001, Dobaczewski et al., 2009). MMP-1 and MMP-8 are gelatinases that break down intact collagen and enable subsequent collagen degradation by MMP-2 and MMP-9 (Birkedal-Hansen et al., 1993, Sun et al., 2000, Romanic et al., 2001). MMP-9 has been localised to neutrophils and macrophages, with MMP-2 being expressed in macrophages, myocytes, vascular endothelial cells and smooth muscle cells (Heymans et al., 1999, Vanhoutte et al., 2006, Romanic et al., 2001,

Cheng et al., 2007). Furthermore the temporal expression profiles of MMP-9 and MMP-2 correspond with neutrophil and macrophage infiltration, respectively (Tao et al., 2004). MMPs are a vital part of angiogenesis. In a hind limb model of ischaemia and in an *ex vivo* aortic ring culture, deficiency of MMP-2 reduced angiogenesis due to reduced migratory and angiogenic capacity of endothelial cells. This was associated with reduced inflammation and VEGF expression (Cheng et al., 2007).

MMP activation can also be damaging. Hearts from patients that had dilated cardiomyopathy had increased cardiac levels of MMP-2, MMP-9 and collagen relative to control healthy tissue (Sivakumar et al., 2008). Peak expression of MMPs in animal models of MI is correlated with the timing of cardiac rupture (Tao et al., 2004), which may be mediated by inappropriate removal of the ECM (Vanhoutte et al., 2006). The plasminogen system regulates post-infarct ECM turnover and involves MMPs and plasminogen activators (Heymans et al., 1999). Reduced matrix degradation in u-PA and MMP-9 knockout mice both reduces inflammatory cell infiltration and the incidence of cardiac rupture (Heymans et al., 1999). However, this is associated with reduced angiogenesis and impaired scar formation (Heymans et al., 1999). While preventing cardiac rupture is beneficial, an adequate scar is required to maintain structural integrity thus stabilising the infarct and maintaining function (Sun and Weber, 2000). This indicates that there is a fine balance in MMP activation being beneficial or detrimental, much like inflammation.

During the post-MI proliferative phase myofibroblast production of TIMPs inhibits the actions of MMPs and favours collagen deposition rather than breakdown (Bujak and Frangogiannis, 2007, Sun and Weber, 2000). TIMP I, II and III are upregulated from 3 days post MI, remain elevated at day 28, and their expression is negatively correlated with MMP expression (Sun et al., 2000). The role of TIMPs post-MI is reported to extend beyond that of just inhibiting MMPs. They have also been implicated in cell growth and preventing apoptosis (Vanhoutte et al., 2006).

1.7 Scar formation in MI

Cardiac fibrosis is determined by the balance of collagen synthesis and degradation by the MMPs. Myofibroblasts are activated by factors produced by macrophages. They then secrete collagen, with deposition being observed from 3 days post-MI and increasing progressively up to 180 days after infarction (Dobaczewski et al., 2006, Dean et al., 2005, Porter and Turner, 2009, Yang et al., 2002, Virag and Murry, 2003, Sun et al., 2000, Cleutjens et al., 1995). Infusion of galectin 3 (a lectin that has a role in cell interactions) into the rat myocardium induces cardiac fibroblast proliferation and collagen deposition while depletion of macrophages impairs scar formation by reducing collagen deposition, demonstrating the importance of inflammation in the initiation of the fibrotic response (van Amerongen et al., 2007, Sharma et al., 2004). Fibrillar and non-fibrillar collagen is found in the myocardium with fibrillar collagen type I being the most abundant (Shamhart and Meszaros, 2009). In cardiac pathology the abundance of strong, stiff collagen I and elastic collagen III increases (Pauschinger et al., 1999). Furthermore, the proportion of collagen I relative to III increases, favouring production of a stiffer scar (Pauschinger et al., 1999). Cross-linking of collagen is vital in providing tensile strength and structural integrity to the weakened myocardium (Virag and Murry, 2003, Dean et al., 2005, Weber, 1989). Direct injection of collagen into the myocardium immediately after MI has a beneficial outcome in a rodent model of MI. Six weeks after treatment rats injected with collagen had thicker infarcts, reduced infarct expansion index and improved ejection fraction (Dai et al., 2005). A thicker scar may be protective against cardiac rupture (Nahrendorf et al., 2006).

The production of collagen may also serve to promote the quiescent phenotype of fibroblasts thus providing a negative feedback mechanism. Dermal fibroblasts stimulated with TGF-β show decreased collagen production in response to a collagen-rich environment (Clark et al., 1995). This may prevent excessive fibrosis, which may facilitate cardiac arrhythmias (Zannad and Radauceanu, 2005, Li et al., 1999, Kostin et al., 2002). High cardiac collagen production has been associated with left ventricular

dysfunction in rats (Sharma et al., 2004). Dysfunction was associated with an increase in stiff collagen I relative to elastic collagen III. (Sharma et al., 2004).

The infarct scar, as a result of experimental MI, is found in the apical region of the myocardium which is the most vulnerable as it is relatively thin with the greatest curvature. Damage here leads to a more pronounced decline in heart function (Pfeffer and Braunwald, 1990). Modification of the scar size independent of actual size is well reported in the literature (Nahrendorf et al., 2006, Garcia et al., 2007, Hammerman et al., 1983a, Hammerman et al., 1983b, Brown et al., 1983). Infarct expansion increases the scar size and, in humans, is greatest in patients with elevated blood pressure and increased vascular resistance. These patients are more likely to develop complications (Pfeffer and Braunwald, 1990, Pierard et al., 1987).

1.8 Cardiac hypertrophy and remodelling

The initial post-infarct decline in cardiac function is mediated by systolic dysfunction which worsens with time (Shioura et al., 2007). In humans, end systolic volume is a powerful predictor of death (Pfeffer and Braunwald, 1990, White et al., 1987). The tissue loss and hormonal stimulation associated with MI can mediate hypertrophy and remodelling, compensatory processes that may maintain normal function (Pfeffer and Braunwald, 1990). The extent of this remodelling depends on size and position of infarct, collaterals and the patency of the occluded coronary artery (Stanley et al., 2004).

After MI, cardiomyocytes in the infarct core die while those at the infarct border change to a distorted, irregular shape (Kocher et al., 2001). Increased wall stress and subsequent upregulation of genes, such as those encoding TNFα, TGF-β and endothelin, alter cardiomyocyte expression of cardiac-specific genes, in particular those involved in the foetal gene programme (atrial natriuretc factor, ANP, and β myosin heavy chain, β MHC) (MacLellan and Schneider, 2000, Kapadia et al., 1997, Sadoshima et al., 1992, Sadoshima and Izumo, 1993). Such expression is characteristic of cardiomyocyte

hypertrophy, a mechanism occurring after MI to compensate for myocytes loss. This means that post-MI, after an initial decline, cardiac muscle mass starts to increase again through cell hypertrophy (Stanley et al., 2004).

Infarct damage results in slippage of cardiomyocytes leading to wall thinning, ventricle dilation and a decline in diastolic function (Pfeffer and Braunwald, 1990, Shioura et al., 2007, Yang et al., 2000). Gaps between capillaries and myocytes widen and may result in subendocardial ischaemia (Stanley et al., 2004). Chamber dilation creates a volume overload state and cardiac output decreases (Stanley et al., 2004). During remodelling the remote region (part of heart not affected by the MI) undergoes morphological changes too. The ventricle changes shape from its normal elliptical shape to become more spherical (Athanasuleas et al., 2004). The increased left ventricle cavity size and its distorted shape bestow a mechanical burden on the failing heart exacerbating remodelling and cardiac function may decline further (Douglas et al., 1989). Current therapeutics given to MI patients, such as ACE inhibitors, β blockers and mineralocorticoid receptor (MR) antagonists, can prevent ventricular dilation, decrease left ventricle volume and mass, and reduce collagen turnover to a certain extent but do not always prevent progression to heart failure (Stanley et al., 2004).

1.9 Glucocorticoids

Glucocorticoids have a plethora of physiological functions including modulating metabolism, the stress response, inflammation and blood pressure. The first use of glucocorticoids clinically was in the 1940's when Hench et al. demonstrated their use as anti-inflammatory agents to treat rheumatoid arthritis (Hench et al., 1950). Since then glucocorticoids have revolutionised the treatment of a variety of disorders including asthma and arthritis and can be used to prevent acute transplant rejection.

1.9.1 Synthesis, release and metabolism

Glucocorticoids are steroid hormones that are synthesised in the zonae fasciculate/reticularis of the adrenal cortex in response to a regulated hormone network between endocrine tissues (Buckingham, 2006). The precursor for glucocorticoids is cholesterol which undergoes side-chain cleavage by cytochrome P450 enzymes to produce pregnenolone (Lin and Achermann, 2004). Sequential hydroxylations lead to the production of cortisol in humans and corticosterone in rodents (Lin and Achermann, 2004). Rodent and human glucocorticoids differ due to the lack of 17α-hydroxylase (the enzyme that catalyses the production of cortisol) in the rodent adrenal glands (Lin and Achermann, 2004).

Glucocorticoid release is under the control of the hypothalamic pituitary adrenal (HPA) axis. Corticotrophin-releasing factor (CRF) is secreted from the hypothalamus (fuelled by stimuli such as excessive temperatures, infections or injury) and stimulates the release of adrenocorticotrophic hormone (ACTH) from the anterior pituitary gland (Aguilera et al., 2001, Jacobson, 2005). ACTH in turn stimulates glucocorticoid synthesis and release from the adrenal cortex. The HPA axis has negative feedback mechanisms, including ACTH on hypothalamic CRF production and glucocorticoids on both hypothalamic CRF and anterior pituitary gland ACTH release (Aguilera et al., 2001, Jacobson and Sapolsky, 1991, Jacobson, 2005, Buckingham, 2006). Vasopressin,

also known as antidiuretic hormone may also exert stimulatory actions on glucocorticoid synthesis and release by promoting ACTH release (Aguilera et al., 2001, Jacobson and Sapolsky, 1991). ACTH can also stimulate mineralocorticoid production and release from the adrenal gland but such production is also regulated by the renin-angiotensin system and the electrolyte composition of the blood. In healthy adult humans, approximately 15mg of cortisol are secreted by the adrenal gland into the bloodstream every day (Esteban et al., 1991) in a pulsatile fashion (Buckingham, 2006). There is a diurnal pattern to this secretion with it peaking in humans on waking and being very low in the evening (the opposite is true in rodents due to their nocturnal nature) (Kerrigan et al., 1993, Jacobson, 2005).

Circulating glucocorticoids are normally bound to corticosteroid-binding globulin (CBG) which sequesters them preventing access to receptors. Normally 95% of glucocorticoid will be bound to the CBG and this will buffer the glucocorticoid levels (Hammond et al., 1990, Buckingham, 2006). Glucocorticoids can be metabolised by a variety of routes. The major route involves the reduction of carbons 4-5 of the A ring by hepatic 5α or 5β reductases (Figure 1.5) (Tomlinson et al., 2004). Alternatively, glucocorticoids may be metabolised via reduction by 20α- or 20β- hydroxysteroid dehydrogenase, oxidative side chain removal, hepatic hydroxylation producing 6β-hydroxycortisol/corticosterone, or inter-conversion of active cortisol/corticosterone with inactive cortisone/11-dehydrocorticosterone by the 11β-hydroxysteroid dehydrogenase enzymes (Tomlinson et al., 2004). The latter route of metabolism is the subject of this thesis (Figure 1.5).

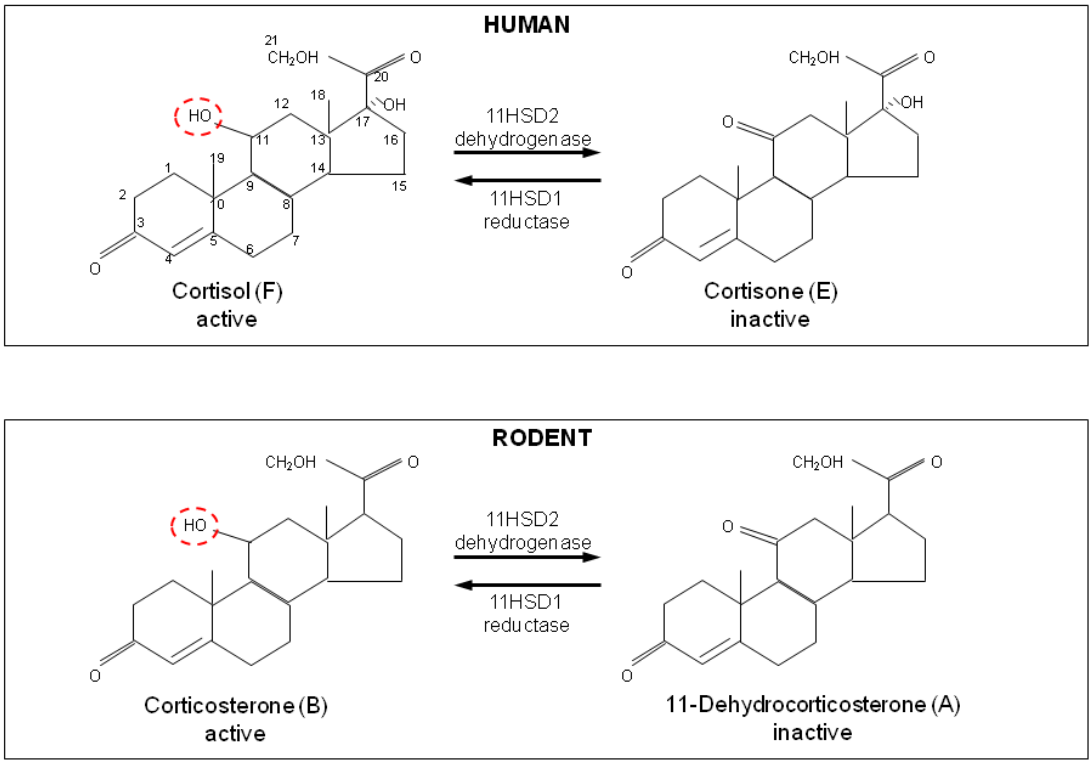

Figure 1-5 Glucocorticoid structures

The predominant glucocorticoids cortisol, in humans, and corticosterone, in rodents, are inactivated by the dehydrogenase activity of 11β-hydroxysteroid dehydrogenase type 2 (11HSD2) that removes a hydroxyl group from carbon-11. Inactive cortisone and 11-dehydrocorticosterone are reactivated by the reductase activity of 11HSD1. Carbon numbers are labelled on cortisol structure only. Figure adapted from Walker and Seckl (2003).

1.9.2 The glucocorticoid receptor

Glucocorticoids mediate their actions via intracellular nuclear receptors called glucocorticoid receptors (GR). They have high sequence homology to other steroid receptors particularly in the DNA binding domain (Funder, 1997, Buckingham, 2006). GR is rendered inactive in the cytoplasm by a 300kDa complex that binds to it. This complex is made up of a 90kDa heatshock protein (hsp90), hsp70, p23 and immunophilins (Pratt, 1993). Hsp90 acts as a chaperone and prevents the unoccupied GR translocating to the nucleus. Upon ligand binding this complex dissociates enabling receptor dimerisation by hydrophobic interactions, nuclear localisation and modulation of gene transcription (see Figure 1.6) (Bledsoe et al., 2004). Some glucocorticoid target genes encode glucocorticoid response elements (GREs) in their promoters. These GREs are imperfect palindromic sequences that are 2 hexamer half sites that are separated by a 3bp and are recognised by the activated GR homodimer (Barnes, 1998). Varying compositions of the GREs, transcription factors present and the transcription regulatory proteins recruited can modulate whether GR binding to the GRE will enhance or repress gene transcription (Barnes, 1998). For example, GRs and transcription factors can bind to the co-activator CREB binding protein which can acetylate histones thus opening up the DNA structure and enabling gene transcription. However GR can also bind to co-repressors that favour tight coiling of the DNA around histones therefore preventing gene transcription (Barnes, 1998). GR may also influence gene transcription independently of DNA binding by interacting with transcription factors (Jonat et al., 1990). Alternate splicing of the GR transcript produces 2 isoforms of the receptor that differ at the C terminus; GRα and GRβ. GRβ may act as a dominant negative inhibitor of GRα as it does not bind glucocorticoids but can bind to DNA preventing access of ligand activated GRα (Oakley et al., 1996, Barnes, 1998).

Due to the nature of nuclear receptors it can take hours for the effects of GR activation to appear (Losel and Wehling, 2003). However, there are glucocorticoid-mediated responses that take a matter of seconds or minutes that suggests there is another

mechanism by which glucocorticoids act (Losel and Wehling, 2003). This is by binding to membrane bound or cytoplasmic receptors and can result in modulation of calcium influx and the inflammatory response (Losel and Wehling, 2003). The role of membrane bound GR is not fully understood.

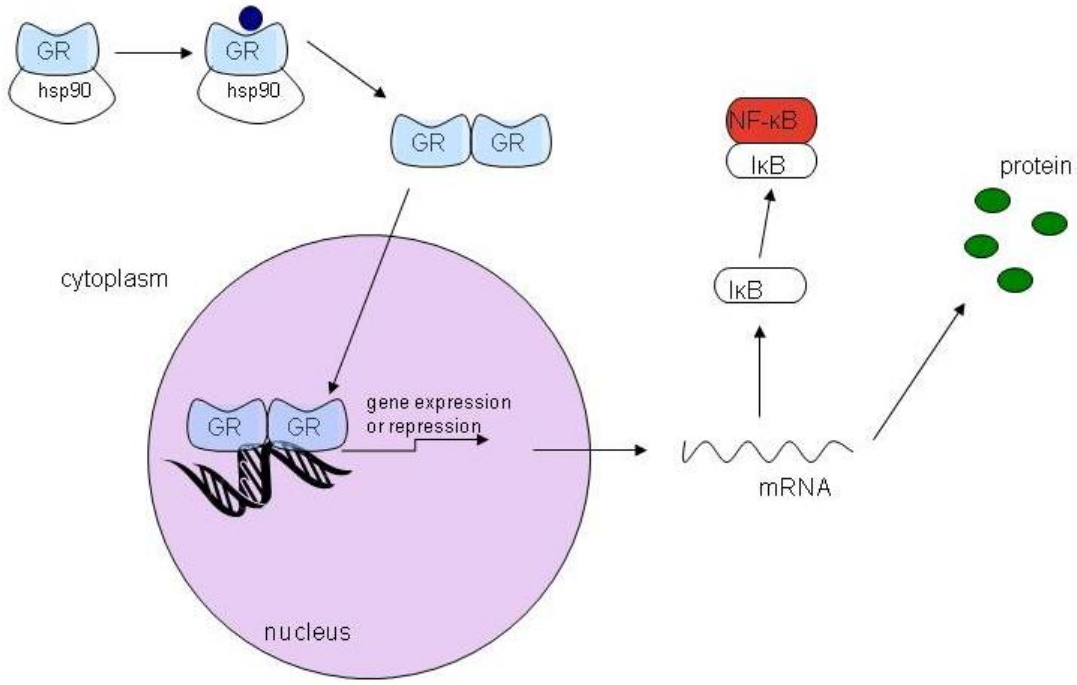

Figure 1-6 Glucocorticoid receptor activation

The glucocorticoid receptor (GR) is rendered inactive in the cytoplasm by the binding of a complex that is made up of proteins including heatshock protein 90 (hsp90). Upon ligand binding the complex is dissociated, GR dimerize and they subsequently translocate to the nucleus. In the nucleus GR pairs interact with glucocorticoid response elements in the DNA thus enabling gene transcription or gene repression. Gene transcription leads to the production of mRNA which is translated into proteins. One such protein is IκB. IκB binds to NF-κB rendering it inactive in the cytoplasm and preventing it from translocating to the nucleus and activating transcription of inflammatory genes. Figure adapted from Sternberg et al (2006).

1.9.3 Glucocorticoids and the corticosteroid receptors

Glucocorticoids can also mediate their actions via the mineralocorticoid receptors (MR) (Buckingham, 2006). The expression of GR and MR is tissue specific. Expression of GR is ubiquitous in glucocorticoid target tissues such as the liver, brain, cells of the immune system and the lungs. In the cardiovascular system GR has been found in cardiomyocytes, cardiac fibroblasts, vascular smooth muscle cells and the vascular endothelium (Hadoke et al., 2006, Ullian, 1999). It has low affinity for glucocorticoids having a K_D of 10-20nM for cortisol and corticosterone, and shows no binding of the mineralocorticoid, aldosterone. MR, on the other hand, has high affinity for both glucocorticoids and mineralocorticoids (K_D for both is approximately 0.5-2nM) (Buckingham, 2006). The distribution of MR is restricted in comparison to that of GR. MR are found in mineralocorticoid target tissues such as, the distal tubule of the kidney, sweat glands, colon and brain. In the cardiovascular system MR has also been identified in cardiomyocytes and the vascular endothelium and smooth muscle cells (Milik et al., 2007, Buckingham, 2006,(Hadoke et al., 2009). As circulating levels of cortisol/corticosterone are 100 fold greater than those of aldosterone, and the level of glucocorticoid in the tissue is likely to be 0.5-1nM at the diurnal nadir, it is likely that under basal conditions where both receptors are expressed MR, rather than GR, will be occupied by glucocorticoids (Esteban et al., 1991, Funder, 1997). It has been suggested that in epithelial tissues glucocorticoids act as MR agonists whereas in non-epithelial tissues they act as antagonists (Gomez-Sanchez et al., 1990, Funder, 1997). This view is still somewhat controversial and requires further investigation. To confer aldosterone specificity the MR must be protected from illicit activation by glucocorticoids. This is achieved by pre-receptor metabolism of glucocorticoids by the 11β-hydroxysteroid dehydrogenase enzymes (11HSD).

1.10 11β-hydroxysteroid dehydrogenase enzymes

The 11β-hydroxysteroid dehydrogenase enzymes were initially thought to be one enzyme that changes the direction of its activity depending on its environment. However in the 1980's and 1990's the two distinct isoforms of the enzyme were identified and characterised (Stewart and Krozowski, 1999, Seckl and Walker, 2001). These isozymes belong to the short-chain dehydrogenase/reductase superfamily that has over 3000 members (Tomlinson et al., 2004).

1.10.1 11β-hydroxysteroid dehydrogenase type 1

11β-hydroxysteroid dehydrogenase type 1 (11HSD1) catalyses the conversion of inactive cortisone and 11-dehydrocorticosterone to active cortisol and corticosterone, in humans and rodents respectively (see Figure 1.7). The biological activity of cortisol and corticosterone results from the presence of a hydroxyl group on carbon-11 of the glucocorticoid structure. 11HSD1 reduces the oxygen at carbon-11 thus reactivating the glucocorticoid and amplifying it locally. Since GR are relatively low affinity receptors the presence of 11HSD1 may increase their activation by generating high concentrations of the appropriate ligand in target tissues (Walker and Seckl, 2003). The direction of 11HSD1 activity has been the subject of some debate. In tissue homogenates and microsomes the enzyme can act as a dehydrogenase or reductase but in intact tissues and organs it predominantly catalyses the reductase reaction (Gao et al., 1997, Seckl, 2004). Analyses of enzyme kinetics have demonstrated that rat 11HSD1 has a Km of 1.83±0.06μM for corticosterone and 17.3±2.24μM for cortisol (Draper and Stewart, 2005, Stewart and Krozowski, 1999). For this reason it is termed a low affinity enzyme as the Km is relatively high compared to the circulating levels of free corticosterone (in the nM range).

11HSD1 is found in the endoplasmic reticulum (ER) with its catalytic domain in the ER lumen. It is found in proximity to hexose-6-phosphate dehydrogenase (H6PDH) which

catalyses the conversion of glucose-6-phosphate to 6-phosphogluconolactonate, producing NADPH, the vital cofactor for 11HSD1 activity, in the process. Deletion of H6PDH has shown that this enzyme is crucial to the reductase activity of 11HSD1 (Lavery et al., 2006). The structure of 11HSD1 is highly conserved across species, particularly in the cofactor binding site and the catalytic domain (Tomlinson et al., 2004) Like the GR, 11HSD1 has a wide expression including in the liver, kidney, brain adipose, bone, gastrointestinal tract, vasculature, heart and the gonads (Walker and Seckl, 2003, Tomlinson et al., 2004). Its expression and activity is regulated by a wide range of factors that include cytokines, growth factors, insulin, sex steroids and glucocorticoids themselves (Tomlinson et al., 2004).

The role of 11HSD1 has been studied using genetically-modified mice. In transgenic mice overexpressing 11HSD1 specifically in the adipose (to a similar extent as observed in the adipose of obese humans) adipose corticosterone levels are increased and this is associated with increased central fat mass (Masuzaki et al., 2001, Rask et al., 2001). Mice with liver-specific over expression of 11HSD1 exhibit insulin resistance, fatty liver and dyslipidemia without changes in adipose mass (Paterson et al., 2005). Additionally, mice with targeted disruption of the 11HSD1 allele have been generated. Homozygous 'knockout' mice ($^{-/-}$) are viable, producing normal pups, show no detectable changes in blood pressure and generally are phenotypically normal (Kotelevtsev et al., 1997). While adrenalectomised wild type mice can convert 11-dehydrocorticosterone (from implanted pellets) to corticosterone, 11HSD1$^{-/-}$ mice could not (Kotelevtsev et al., 1997). This shows that 11HSD1 is the only enzyme capable of regenerating inactive glucocorticoids (Kotelevtsev et al., 1997). The adrenal glands of 11HSD1$^{-/-}$ mice on the MF1/129 background, but not those on the C57Bl6 background, are enlarged and morphometric analysis shows that this is due to adrenocortical hyperplasia (Harris et al., 2001, Paterson et al., 2006, Kotelevtsev et al., 1997, Paterson et al., 2007). This may be a result of diminished negative feedback to the HPA axis (Harris et al., 2001). Peak levels, however, are not different from wild type litter mates (Kotelevtsev et al., 1997, Harris et al., 2001). Deficiency of 11HSD1 in mice produces a plethora of potentially beneficial

effects that include resistance to diabetes and obesity (Morton et al., 2004, Morton et al., 2001). 11HSD1$^{-/-}$ mice have an improved lipid profile, increased liver insulin sensitivity and improved glucose tolerance (Morton et al., 2001, Kotelevtsev et al., 1997). Furthermore, these mice have reduced visceral fat accumulation, when on a high fat diet compared with wild type mice and resist development of diabetes when fed a hyper-calorific diet (Morton et al., 2004). These beneficial metabolic effects were associated with reduced expression of phosphoenolpyruvate carboxykinase (PEPCK, a rate limiting enzyme involved in gluconeogenesis) and increased expression of enzymes involved in lipid oxidation in the liver (Kotelevtsev et al., 1997, Morton et al., 2001). The beneficial effects of 11HSD1 knockout extend beyond that of improving metabolic parameters. 11HSD1$^{-/-}$ mice also are protected against age associated cognitive decline (Yau et al., 2001). Of particular interest to the work described in this thesis is that 11HSD1$^{-/-}$ mice exhibit enhanced angiogenesis in MI wound healing and improved cardiac function 7 days post-MI (Small, 2005, Small et al., 2005).

Cortisone reductase deficiency is a rare disorder that represents the "putative human 11HSD1 knockout" and is typified by hyperandrogenism and in some cases, obesity (Tomlinson et al., 2004). There is increased metabolic clearance of cortisol resulting in increased ACTH secretion as an effort to maintain cortisol levels but this is at the expense of a subsequent increase in androgen synthesis (Tomlinson et al., 2004). Treatment with the synthetic glucocorticoid, dexamethasone, suppresses this increase in androgens (Tomlinson et al., 2004).

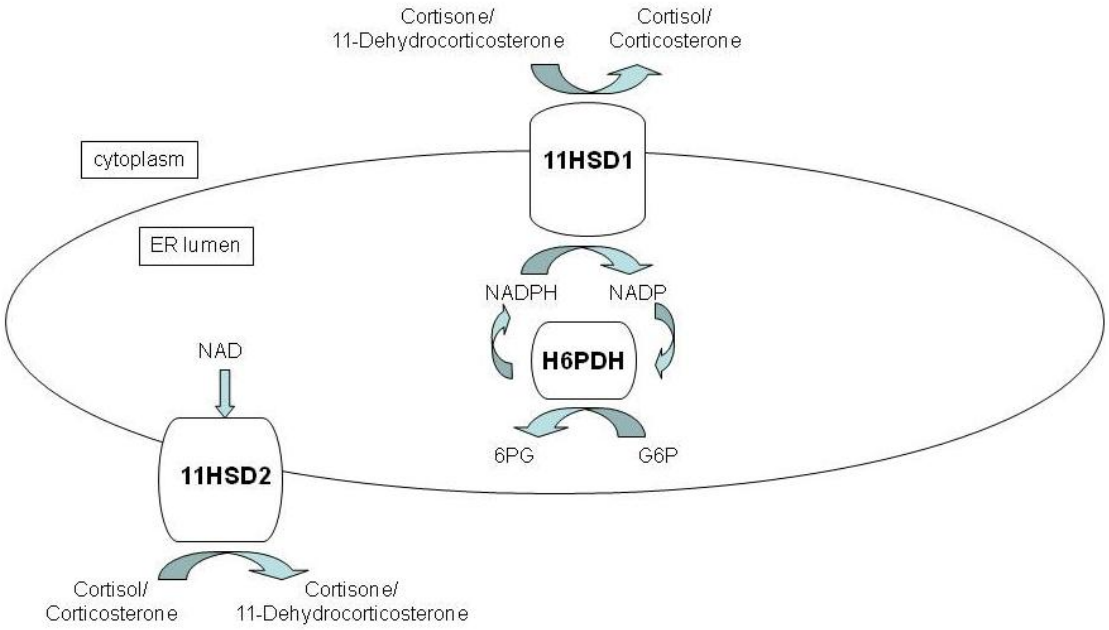

Figure 1-7 The 11β-hydroxysteroid dehydrogenase (11HSD) isozymes

Both 11HSD isozymes are found in the endoplasmic reticulum (ER). The catalytic site of 11HSD1 is situated in the ER lumen in proximity to hexose-6-phosohate dehydrogenase (H6PDH) which catalyses the conversion of glucose-6-phosphate (G6P) to 6-phosphogluconolactoneate (6PG), producing NADPH (nicotinamide adenine dinucleotide phosphate) in the process. NADPH is a cofactor required for the reductase activity of 11HSD1, which reactivates glucocorticoids locally. 11HSD2 catalyses the opposite reaction, inactivating glucocorticoids, with its dehydrogenase activity aided by the cofactor NAD (nicotinamide adenine dinucleotide). Figure adapted from Draper et al (2005).

1.10.2 11β-hydroxysteroid dehydrogenase type 2

11β-hydroxysteroid dehydrogenase type 2 (11HSD2) catalyses the inactivation of glucocorticoids; cortisol and corticosterone are converted to cortisone and 11-dehydrocorticosterone in humans and rodents respectively (see Figure 1.7). Its main role is to reduce the concentration of local glucocorticoids thus preventing elicit activation of high affinity MR. Aldosterone, in contrast, is not a substrate for 11HSD2 (Funder, 1997). Like 11HSD1, 11HSD2 is found in the ER but the bulk of this enzyme is in the cell cytoplasm rather than in the ER lumen (Draper and Stewart, 2005). NAD is the required cofactor for 11HSD2 which is an exclusive dehydrogenase. This enzyme has high affinity for its substrate with a Km of 50nM for cortisol and 5nM for corticosterone (Draper and Stewart, 2005, Stewart and Krozowski, 1999). Corresponding with its role, 11HSD2 is expressed in mineralocorticoid target tissues including the collecting ducts and medulla of the kidney, the colon and the placenta (Brown et al., 1996, Edwards et al., 1988). In the kidney 11HSD2 prevents illicit activation of the renal MR by glucocorticoids enabling the reabsorption of sodium in the distal tubules and increased secretion of potassium. $11HSD2^{-/-}$ mice have been generated however, 50% die within 48 hours of birth due to motor weakness (Kotelevtsev et al., 1999). The surviving mice are characterised by enlarged kidneys, hypokalaemia, hypotonic polyuria, increased blood pressure and impaired vascular function compared to wild types (Kotelevtsev et al., 1999, Hadoke et al., 2001). The presence of 11HSD2 in MR expressing cells confers mineralocorticoid specificity on the MR. This enzyme is present in the placenta and has a vital role preventing glucocorticoids passing from mother to foetus. Glucose intolerance is observed in offspring exposed to high levels of glucocorticoid *in utero* (Nyirenda et al., 1998).

Mutations in the human 11HSD2 gene result in the syndrome of apparent mineralocorticoid excess (SAME). The symptoms of this disease resemble those seen in the $11HSD2^{-/-}$ mice and include hypertension, sodium retention and hypokalaemia (Draper and Stewart, 2005). However, the name of this disease is deceptive as this is not

truly a disorder of mineralocorticoid excess. Aldosterone is actually reduced, but defective glucocorticoid deactivation results in excessive MR activation by glucocorticoids (Draper and Stewart, 2005).

1.10.3 Inhibitors of the 11HSDs

The therapeutic benefit of pharmacological 11HSD1 inhibition was initially shown with liquorice derivatives that are relatively non-selective (Monder et al., 1989). Carbenoxolone reduces plasma cholesterol levels, glucose production and improves insulin sensitivity in humans. However, it also has detrimental effects that are consistent with inhibition of 11HSD2 (Walker et al., 1995, Andrews et al., 2003). More recently, selective inhibitors of 11HSD1 have been developed including compound 544 (Merck), BVT.14225 (Biovitrum) and compound 2922 (Amgen) which have IC_{50} values of 97nM, 52nM and 161±23nM respectively, indicating high potency (Hermanowski-Vosatka et al., 2005, Barf et al., 2002, Lloyd et al., 2009). Hermanowski-Vosatka et al. have shown that administration of compound 544 is beneficial in murine models of obesity, diabetes and atherosclerosis (Hermanowski-Vosatka et al., 2005). In diet-induced obesity the drug lowers body weight, insulin, fasting glucose, triglycerides and cholesterol while in a model of type 2 diabetes fasting glucose, insulin, glucagon, triglycerides and free fatty acids are reduced and glucose tolerance improved (Hermanowski-Vosatka et al., 2005). Furthermore, compound 544 slows atherosclerotic plaque progression in ApoE deficient mice (Hermanowski-Vosatka et al., 2005). Selective inhibitors are currently in Phase II clinical trials for the treatment of diabetes. Additional development of 11HSD1 inhibitors is required before progression of such inhibitors to the clinic.

1.11 Glucocorticoid-related human diseases

Maladaptive glucocorticoid responses form the basis of several human disorders. Excess glucocorticoids are associated with metabolic syndrome which includes visceral obesity, hypertension, insulin resistance and alterations in glucose and lipid metabolism (Walker and Seckl, 2003, Draper and Stewart, 2005). In idiopathic obesity tissue cortisol is increased independently of plasma levels and this is associated with increased 11HSD1 activity in the adipose (De Bosscher et al., 2003). Cortisol can stimulate the differentiation of preadipocytes to adipocytes which may enable expansion of the adipose tissue (Kleiman and Tuckermann, 2007, Draper and Stewart, 2005, Tomlinson et al., 2004). As there is strong evidence for a genetic component to obesity investigators are currently attempting to identify polymorphisms in the 11HSD1 gene of obese patients (Walker and Seckl, 2003). Cushing's syndrome is a disease of cortisol excess and the symptoms resemble metabolic syndrome. It is typified by increased abdominal fat, muscle wasting, skin thinning and poor wound healing (De Bosscher et al., 2003). Metabolic syndrome may represent a low cortisol Cushing's syndrome. The opposite of this is the rare disease known as chronic adrenal insufficeincy or Addison's disease. Insufficient corticosteroid production by the adrenal glands results in reduced blood pressure, fatigue and weight loss.

1.12 Glucocorticoids and the cardiovascular system

Treatment with glucocorticoids has been correlated with increased risk of cardiovascular disease (Souverein et al., 2004, Wei et al., 2004). GR and MR are expressed in a variety of different cell types across the cardiovascular system. Firstly if we consider the vasculature; GR and MR are expressed in smooth muscle cells and endothelial cells, (Walker et al., 1991, Takeda et al., 2007, Hadoke et al., 2006, Ullian, 1999, Yang and Zhang, 2004). While glucocorticoids (both local and systemic) have a role in maintaining blood pressure under pathological situations they can also promote hypertension (Ullian, 1999, Whitworth, 1994, Whitworth et al., 2002, Yang and Zhang,

2004). Glucocorticoids can suppress the local production of vasodilators, such as nitric oxide and prostacyclin, along with potentiating the actions of vasoconstrictor hormones such as α adrenoreceptor agonists and endothelin (Whitworth et al., 2002, Yang and Zhang, 2004, Ullian, 1999, Hadoke et al., 2006). Additionally, local glucocorticoids may also induce vascular remodelling by enhancing vascular smooth muscle cell hypertrophy in response to angiotensin II (Ullian, 1999, Hadoke et al., 2006) and by inhibiting angiogenesis (Small et al., 2005).

In the myocardium GR expression has been localised to cardiomyocytes and fibroblasts while MR are located in cardiomyocytes (Walker et al., 1991, Slight et al., 1993, Takeda et al., 2007, Slight et al., 1996, Pujols et al., 2002, Lombes et al., 1992). Genetic manipulation of corticosteroid receptors in the heart has demonstrated their importance physiologically. Ninety percent of GR knockout mice die at birth due to delays in lung maturation while conditional cardiac over-expression of GR is associated with bradycardia and atrio-venricular block (Cole et al., 1995, Sainte-Marie et al., 2007). Conditional cardiac knock-down of MR induces severe heart disease and premature death (Beggah et al., 2002). Conversely, conditional cardiac over-expression of MR leads to early sudden death and, in those mice surviving, cardiac arrhythmias (Ouvrard-Pascaud et al., 2005). This could be related to the modulation of electrical and mechanical activities of the heart that have been attributed to glucocorticoids. For example, the contractile force of rat papillary muscles is reduced after adrenalectomy, but this can be prevented by dexamethasone treatment (Lefer et al., 1968). As increased glucocorticoids have been associated with adverse cardiovascular outcomes, such as heart failure for example (Wei et al., 2004), reducing their actions is attractive in the setting of cardiovascular disease. However, systemic blockade of the GR can result in compensatory increases in the HPA axis, and therefore in circulating glucocorticoids, making direct inhibition of the GR an unsuitable therapeutic approach (Bamberger and Chrousos, 1995, Spiga et al., 2007).

Co-expression of the corticosteroid receptors with 11HSD1 or 11HSD2 amplifies and reduces local glucocorticoid action respectively (see Figure 1.8). In the vasculature

11HSD1 is expressed in smooth muscle cells while 11HSD2 is expressed in endothelial cells (Slight et al., 1996, Walker et al., 1991, Takeda et al., 2007, Hadoke et al., 2006, Christy et al., 2003). Distribution of the 11HSDs varies depending on the vascular territory (Hadoke et al., 2006). In the myocardium 11HSD1 is expressed in cardiomyocytes and fibroblasts and 11HSD2 is expressed in cardiac fibroblasts only (Morton et al., 2004, Masuzaki et al., 2001, Vliegen et al., 1991, Slight et al., 1993, Slight et al., 1996). Mice with selective 11HSD1 isozyme deletion have been used to determine the influence of the 11HSDs on the cardiovascular system. $11HSD2^{-/-}$ mice develop hypertension, endothelial dysfunction and cardiac hypertrophy (Christy et al., 2003, Hadoke et al., 2001, Kotelevtsev et al., 1999). The role of 11HSD2 in the vascular wall and the myocardium may be to prevent the detrimental effects of local MR activation by glucocorticoids. However, it is difficult to determine the direct local effects of glucocorticoids on the cardiovascular system relative to those mediated by the increase in blood pressure (systemic glucocorticoid). In contrast, inactivation of 11HSD1 has no effect on vascular function and blood pressure (Kotelevtsev et al., 1997, Hadoke et al., 2001). While 11HSD1 does not appear to have a role in basal vascular function (Hadoke et al., 2001) it may have a role in vascular inflammation. Treatment of apoE deficient mice with an 11HSD1 inhibitor prevented atherosclerotic plaque progression that was associated with reduced expression of the inflammatory cytokine, MCP-1 (Hermanowski-Vosatka et al., 2005). However, in a more recent study by Lloyd et al., pharmacological inhibition of 11HSD1 had no effect on pro-inflammatory cytokines or atherosclerosis (Lloyd et al., 2009). The mechanism by which 11HSD1 inhibition reduces plaque size requires further investigation.

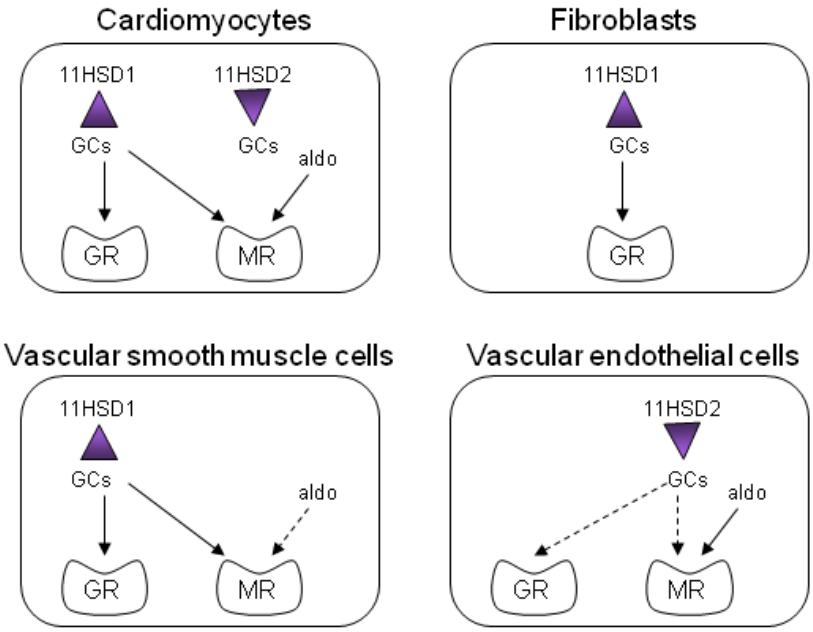

Figure 1-8 Occupancy of GR and MR in cells of the cardiovascular system

The presence of both 11β-hydroxysteroid dehydrogenase (11HSD) type 1 and type 2 in cardiomyocytes means that glucocorticoids (GC) can be both inactivated and reactivated in the same cell. For this reason it is likely that both the glucocorticoid receptor (GR) and mineralocorticoid receptor (MR) are activated by glucocorticoids, with the mineralocorticoid aldosterone, activating MR only. The presence of 11HSD1 in cardiac fibroblasts will amplify glucocorticoids locally thus enhancing GR activation. In vascular smooth muscle cells 11HSD1 amplification of glucocorticoids will ensure activation of both GR and MR by the steroid. Aldosterone has to compete for the MR. On the other hand vascular endothelial cells express 11HSD2 which will prevent MR activation by glucocorticoids and will favour that by aldosterone. Solid arrows represent the predominant activation and dashed represent the less likely activation route. Figure adapted from Walker (2007).

1.12.1 Glucocorticoids and inflammation

Glucocorticoids have a role in mediating the fine balance between a beneficial robust inflammatory response immediately after injury, a type 2 resolution response (part of the inflammatory response) and in preventing chronic inflammation (McEwen et al., 1997). This is achieved in part by programming. For example, sustained increase in glucocorticoid secretion by the HPA axis can programme the inflammatory system to be predominantly pro-resolution, preventing chronic inflammation. While quick resolution of inflammation may be beneficial, a robust type 1 inflammatory response is required in many situations to clear cell debris and pathogens (McEwen et al., 1997).

Glucocorticoids are immunomodulatory molecules that can exert their actions by a genomic and non genomic mechanisms (Barnes, 1998). They inhibit the production of a range of inflammatory cytokines including IL-1β, IL-2, IL-3, IL-6, IL-11, TNF-α, and chemokines such as IL-8, RANTES, MCP-1 and MIP-1α (Galon et al., 2002, Cupps and Fauci, 1982, Barnes, 1998). In parallel, GR activation up-regulates anti-inflammatory genes, such as IL-10 and lipocortin-1 (Barnes, 1998, Galon et al., 2002, Cupps and Fauci, 1982). For many of these inflammatory mediators GREs are not present upstream of their promoters, suggesting that modulation of their expression is not due to direct GR mediated alteration of transcription. GR can enhance synthesis of IκB, which renders NF-κB inactive in the cytoplasm preventing it from augmenting inflammation (please refer to Section 1.2.3 and Figure 1.6) (Barnes, 1998). Inhibition of NF-κB activity by glucocorticoids can also diminish the synthesis of nitric oxide, which can also reduce inflammation (Barnes, 1998). Additionally, GR can interact with activator protein-1 (AP-1) preventing it from mediating its inflammatory actions (Barnes, 1998, Jonat et al., 1990, Buckingham, 2006, De Bosscher et al., 2003). Non-genomic actions of glucocorticoids are apparent, as their effects on inflammation occur within minutes rather than hours. *In vitro,* high doses of corticosterone can inhibit macrophage phagocytosis in less than 30 minutes (Long et al., 2005) and high doses of 6-α methylprednisolone prevent neutrophil degranulation within 5 minutes (Liu et al., 2005).

Furthermore glucocorticoids can arbitrate mRNA breakdown, as seen with granulocyte-macrophage colony-stimulating factor (GM-CSF) (Barnes, 1998).

Glucocorticoids can mediate their effects on the inflammatory system due to the wide expression of their receptors and 11HSD1. GR and MR are expressed in inflammatory cells such as macrophages and lymphocytes, as is 11HSD1 (Gilmour et al., 2006, Brereton et al., 2001, Thieringer et al., 2001). Exposure of monocytes to glucocorticoids as they mature into macrophages programmes them to be phagocytic and anti-inflammatory (Heasman et al., 2003). 11HSD1 is up-regulated upon differentiation of monocytes to macrophages, serving to amplify glucocorticoids in areas of inflammation (Gilmour et al., 2006, Chapman et al., 2006). Within 3 hours of a thioglycollate injection into the peritoneum (a model of sterile peritonitis) there is an increase in 11HSD1 activity in cells recruited to the area (Gilmour et al., 2006). The elastase produced by neutrophils has been shown to cleave cortisol from CBG (Hammond et al., 1990). This process aids in delivery of the anti-inflammatory glucocorticoid to sites of inflammation (Hammond et al., 1990). This local increase in glucocorticoids in an inflamed site may place a 'brake' on the self-amplifying process of inflammation preventing overshoot which may threaten homeostasis (Munck et al., 1984). Several cytokines such as, IL-4, IL6, MCP-1 and TNF-α up-regulate 11HSD1 in inflammatory cells and vascular smooth muscle cells (Thieringer et al., 2001, Cai et al., 2001). This is not associated with a parallel increase in 11HSD2 activity (Cai et al., 2001).

Synthetic glucocorticoids can enhance macrophage phagocytosis of apoptotic cells. In agreement with this Gilmour et al. demonstrated a delay in macrophages gaining phagocytic competence in $11HSD1^{-/-}$ mice (Liu et al., 1999, Gilmour et al., 2006). Glucocorticoids also accelerate eosinophil apoptosis while also enhancing neutrophil survival and modulating the secretion of pro- and anti- inflammatory mediators from inflammatory cells (Barnes, 1998, John et al., 1998).

1.12.2 Glucocorticoids and angiogenesis

Angiogenesis is a tightly regulated process and can be inhibited by glucocorticoids. As mentioned previously, GR, MR and the 11HSD enzymes are found in the vessel wall (Hadoke et al., 2006, Hadoke et al., 2001, Christy et al., 2003, Ullian, 1999, Walker et al., 1991, Yang and Zhang, 2004). Corticosterone and 11-dehydrocorticosterone inhibit angiogenesis *in vitro* in aortic ring angiogenesis assays and *in vivo* in sponge models (Small et al., 2005). While corticosterone can reduce vessel sprouting in $11HSD1^{-/-}$ mice, the inactive molecule, 11-dehydrocorticosterone cannot (Small et al., 2005). This compliments results from a sponge implant model using the human glucocorticoids, cortisol and cortisone (Small et al., 2005). Angiogenesis is enhanced by addition of RU38486 (Mifepristone), a GR antagonist, suggesting that the angiostatic effects of glucocorticoids are mediated by the GR (Small et al., 2005). $11HSD1^{-/-}$ mice and RU38486 treated mice also have enhanced neovascularisation of cutaneous surgical wounds (Small et al., 2005). It follows that individuals with Cushing's syndrome, who have excess glucocorticoids, have impaired wound healing (Gordon et al., 1994). Particularly relevant to the work presented in this thesis is that the observation that $11HSD1^{-/-}$ mice have enhanced cardiac angiogenesis 7 days post-MI (Small et al., 2005). Rat osteocarcinoma cells transfected with 11HSD1, but not 11HSD2, are sensitive to the angiostatic effects of cortisol (Rabbitt et al., 2002). 11HSD2 transfected cells show an increase in cell proliferation suggesting that endogenous glucocorticoids have a tonic angiostatic effect (Rabbitt et al., 2002, Rabbitt et al., 2003). In agreement with these findings, vascularised tumours express 11HSD2 and not 11HSD1 which acts in an anti-inflammatory, pro-differentiation manner (Rabbitt et al., 2003).

There are several mechanisms by which glucocorticoids might exert their angiostatic effect. Firstly, this may be by reducing angiogenic cytokine production or secretion. Dexamethasone can block the increase in VEGF expression in response to hypoxia (Steinbrech et al., 2000) and Hori et al. found that steroids produced a dose-dependent decrease in sponge angiogenesis that was associated with decreased expression of TNF-α and IL-6 (Hori et al., 1996). Furthermore, in an *in vivo* tumour model, GR mediated

suppression of cancer growth and angiogenesis occurred in conjunction with reduced expression of IL-8 and VEGF (Yano et al., 2006a). Glucocorticoids also inhibit PDGF-induced VEGF expression in human aortic vascular smooth muscle cells (Nauck et al., 1998). Finally they can inhibit nitric oxide production which is involved in the initiation of angiogenesis (Ullian, 1999).

Glucocorticoids may also hinder cell proliferation. Incorporation of [^{3}H]-thymidine into the nuclei of replicating endothelial cells and skin fibroblasts is reduced by glucocorticoid treatment *in vitro* (Sakamoto et al., 1987, (Derbyshire et al., 1996). Glucocorticoids, but not aldosterone, inhibit smooth muscle cell and endothelial cell growth suggesting that the anti-angiogenic behaviour of glucocorticoids is mediated by their activation of GR rather than MR (Longenecker et al., 1982, Longenecker et al., 1984). Haemangiomas are tumours of the microvasculature that form due to proliferation of endothelial cells, but are mostly harmless. Removed haemangiomas that are subsequently cultured show decreased capillary growth in response to a variety of glucocorticoids, including dexamethasone and methylprednisolone (Hasan et al., 2003). This is associated with a reduction in IL-6 transcripts and enhanced expression of the apoptotic gene clusterin/apolipoprotein J suggesting that reduced inflammation and enhanced cell death played a role (Hasan et al., 2003). This inhibition of cell proliferation is achieved by preventing transition from the G1 phase (cells increase in size and prepare for division) to the S phase (DNA synthesis). Two different mechanisms that are cell specific have been proposed for this anti-mitotic activity. Firstly, glucocorticoids up-regulate the cyclin-dependent kinase inhibitors (CKIs), p27 and p21 (Rogatsky et al., 1997). CDKIs bind to cyclin-cyclin dependent kinase (CDK) complexes, preventing their catalytic activity, and ultimately, their progression through the cell cycle (Rogatsky et al., 1997). Secondly, glucocorticoids repress mitogenic factors, including cyclin D3, CDK4 and CDK6, that are required for the cell cycle programme (Rogatsky et al., 1997).

Alternative ways in which steroids may restrain angiogenesis include alteration of endothelial cell morphology (Folkman and Ingber, 1987) and promotion of vessel regression. Glucocorticoids have been shown to reduce MMP-2 production and secretion and to enhance TIMP-2 secretion in rat smooth muscle cells (Pross et al., 2002). Small immature vessels are favoured by glucocorticoids for involution and this is mediated by basement membrane degradation and subsequent detachment of endothelial cells from the vessel wall leading to their death (Folkman and Ingber, 1987). In new vessels it is likely that the basement membrane is less stable and has a greater turnover, leaving it susceptible to degradation (Folkman and Ingber, 1987). In the chick chorioallantoic membrane model glucocorticoids reduce collagen synthesis (Maragoudakis et al., 1989). Furthermore, co-administration of collagen production inhibitors with steroid synergises their angiostatic actions (Folkman and Ingber, 1987).

Conversely to the previously reported literature it has been suggested that steroids can be angiostatic independent of their ability to activate GR or MR (Folkman and Ingber, 1987). Tetrahydrocortisol is an inactive glucocorticoid and is angiostatic. Folkman et al. suggest that the distribution of hydroxyl groups across the steroid structure is vital in determining its angiostatic ability (Folkman and Ingber, 1987). However there is overwhelming evidence (as mentioned above) that the corticosteroid receptors are involved therefore, these reports should be taken with caution.

1.13 Glucocorticoids and MI

It has been demonstrated that glucocorticoids can decrease inflammation and angiogenesis, processes that are vital in the MI healing response and therefore modulation of glucocorticoids after MI may have adverse effects on the recovery process. Indeed, exogenous glucocorticoid therapy is associated with a greater risk of MI and heart failure (Wei et al., 2004, Souverein et al., 2004). However, in the 1970's glucocorticoid administration post-MI was proposed to have a favourable outcome. Libby et al. showed, in dogs, that a single dose of methylprednisolone given 30 minutes

or 6 hours after MI reduces ischaemic cell death (Libby et al., 1973). This was followed by clinical studies that found that a single dose of glucocorticoid within 2 days of MI decreases mortality and infarct size (Barzilai et al., 1972, Morrison et al., 1976). The protective influence of these drugs was hypothesised to be due to stabilisation of lysosomal membranes preventing their rupture and subsequent release of their damaging digestive enzymes (Lefer et al., 1980, Libby et al., 1973). More recently Hafezi-Moghadam et al. reported that a single high dose of dexamethasone (40mg/kg) given to mice 1 hour prior to MI reduced infarct size at 24 hours (Hafezi-Moghadam et al., 2002). It was postulated that this protection was bestowed by enhanced nitric oxide synthesis which may have enhanced coronary blood flow (Hafezi-Moghadam et al., 2002). These protective effects were mediated by GR as RU38486 abrogated the beneficial effects of dexamethasone (Hafezi-Moghadam et al., 2002). It has also been proposed that the cardioprotective effects may involve inhibition of NF-κB and activation of protein kinase Akt (Thiemermann, 2002). Conversely, several clinical studies conducted in the 1970's also reported no effects or even detrimental effects of glucocorticoids post-MI (Madias and Hood, 1982). Roberts et al. found that 8 doses of methylprednisolone given after MI increased infarct size and contributed to ventricular arrhythmias (Roberts, 1976). Additionally chronic corticosterone therapy was associated with an increased infarct size in rats (Scheuer and Mifflin, 1997). Taken together, these data suggest that glucocorticoids are beneficial early in infarct healing as they limit the infarct size. However, when such therapy continues into the healing phase it is detrimental. This may be mediated by the anti-inflammatory and anti-angiogenic effects of glucocorticoids. The inflammatory response is required for adequate scar formation and prevention of this can lead to the development of cardiac aneurysms and rupture (Hammerman et al., 1984). Systemic blockade of glucocorticoids after MI and, during infarct healing is not a realistic therapeutic strategy as it may lead to an Addisonian crisis or reduced negative feedback on the HPA axis.

In humans serum levels of glucocorticoids increase post-MI and remain elevated for several days (Ceremuzynski, 1981). It has been speculated that the sudden increase in

circulating glucocorticoids may overwhelm the CBG that normally renders it inactive, thus increasing the effects of glucocorticoids (Ceremuzynski, 1981). Extrapolating from the exogenous glucocorticoid evidence it may be hypothesised that this release is protective. Aldosterone is also reported to be increased post-MI and is correlated with poorer outcome (Ceremuzynski, 1981). It is also well known that catecholamines are increased immediately after MI (Gazes et al., 1959). The relationship between glucocorticoids and catecholamines is a reciprocal one. Glucocorticoids can regulate catecholamine synthesis in the adrenal medulla but catecholamines can stimulate adrenocorticotrophin release from the anterior pituitary, which can then stimulate glucocorticoid release from the adrenal cortex (Axelrod and Reisine, 1984). After this transient increase in systemic glucocorticoids levels the modulation of glucocorticoid concentration locally by 11HSD1 may play a role in dermining the infarct healing response.

1.14 Hypotheses

The 11HSD1$^{-/-}$ mouse has been well characterised in terms of its metabolic and vascular phenotype. However, very little is known about the effect of its deletion on the function of the heart. Any differences in the basal cardiac phenotype of these mice may have an effect on the post-MI outcome.

The **first hypothesis** that is investigated, therefore, is that the cardiac architecture of 11HSD1$^{-/-}$ mice is similar to that of C57Bl6 control mice and this is associated with comparable heart function. In addition, the localisation of 11HSD1 protein is to be confirmed.

The literature suggests that glucocorticoids are beneficial immediately after MI but continued administration of exogenous glucocorticoids in the healing phase is detrimental. This effect may be mediated by the ability of glucocorticoids to reduce inflammation and angiogenesis, processes that are vital in the healing response. It was

previously shown by Small et al. that 11HSD1$^{-/-}$ mice have enhanced angiogenesis 7 days after MI and this was associated with improved cardiac function (Small et al., 2005). However the stimulus for this was unknown.

The **second hypothesis** is that the initial systemic increase in corticosterone post-MI is sufficient to confer protection on the heart from ischaemic damage despite the lack of intracellular regeneration of glucocorticoids in 11HSD1$^{-/-}$ mice. Furthermore, it is proposed that the mechanism for the post-infarct enhancement in vessel density in 11HSD1$^{-/-}$ mice involves an enhanced inflammatory response and promotion of associated pro-angiogenic signalling during early infarct healing.

Despite there being enhanced vessel density 7 days after MI in 11HSD1$^{-/-}$ mice the longevity of these vessels was not established. It is reasonable to expect that the augmented vessel density is required for sustained improvement in cardiac function following infarction. Vessels undergo pruning 14-21 days after MI becoming stable and mature by 28 days (Grass et al., 2006, Ren et al., 2002).

The **third hypothesis** is that the enhanced vessel density previously reported 7 days after MI in 11HSD1$^{-/-}$ mice is retained when infarct healing is complete (28 days) and is associated with sustained improvement in cardiac function. Furthermore, it is postulated that the enhanced blood supply will reduce scar formation.

Finally, it is desirable that the beneficial effects of 11HSD1 inhibition demonstrated in a transgenic mouse model can be translated to the clinic. Selective 11HSD1 inhibitors are in development for treatment of a variety of disorders including diabetes, obesity and atherosclerosis.

The **fourth hypothesis** is that administration of a selective inhibitor of 11HSD1 (compound 544) will recapitulate the effect of genetic deletion of 11HSD1. Drug treated mice will be expected to show enhanced inflammation and angiogenesis, and improved cardiac function 7 days after MI.

2 Methods

2.1 Animals

11HSD1 knock-out (11HSD1$^{-/-}$ colony bred in-house) and C57Bl6 (Harlan, UK) mice used in experiments were 10-16 weeks old, unless otherwise stated. The mice were maintained on a 12 hour light/ 12 hour dark cycle in a room with regulated temperature (21±2°C) and humidity (50±10%). Animals had free access to standard chow (or vehicle/drug diet in the inhibitor study) and water. All breeding, maintenance and experimental protocols were approved by the University of Edinburgh ethics committee and performed in accordance with the Animals (Scientific Procedure) Act (UK) 1986 under project licence number 60/3570 and personal licence number 60/10361.

2.1 Colony management

2.1.1 Breeding strategy

11HSD1 ($^{-/-}$) mice were generated in-house by Yuri Koteletsev (see Figure 2.1 for a simplified scheme of the knockout strategy) (Kotelevtsev et al., 1997, Morton et al., 2004). Initially 3 males heterozygous for 11HSD1 were mated with 3 females null for 11HSD1 to produce litters of 11HSD1 heterozygotes and null mice. Subsequent matings were conducted as straight knock-out crosses to avoid surplus mice being produced. C57Bl6 male mice (Harlan) served as controls

2.1.2 DNA extraction

DNA was extracted from ear clips taken from mice at weaning. Ear clips were digested overnight with 300µl tail buffer (0.05M Tris HCl pH 8.0, 0.1M EDTA pH 8.0, 0.1M NaCl, 1%SDS) and 17.5µl Proteinase K (10mg/ml) at 55°C. 10µl RNase (20µg/ml) was

added and incubated for a further hour at 37°C. Samples were placed on ice for 10 minutes to precipitate the SDS then centrifuged at 9660g for 2 minutes. 300µl of isopropanolol was added to the supernatant and rotated for 6 minutes. Tubes were centrifuged for a further 2 minutes at 9660g. The supernatant was removed to leave the DNA pellet. Pellets were washed with 70% ethanol and centrifuged again. Ethanol was removed and the DNA pellet was suspended in 50µl TE buffer (0.1mM Tris.Cl pH 8, 0.002mM EDTA). DNA was allowed to dissolve for 45 minutes at 37°C before storage at -20°C.

2.1.3 Polymerase Chain reaction to genotype

The polymerase chain reaction (PCR) enables the amplification of specific sequences of DNA, using specific primers, which can be run on a gel and the product identified by its size. Three primers were used to genotype the mice: 5'-TTC TTC GTG TGT CCT ACA GG-3', 5'-CCC GCC TTG ACA ATA AAT TG-3' and 5'-CAC TGC ATT CTA GTT GTC GTT TGT CC-3'. 1µl of extracted DNA was used for a 20µl reaction volume that also contained 1x buffer, 0.05mM dNTPs, 1U Taq Polymerase, 10ρM of each primer and 11.2µl autoclaved water. PCR was initiated in a MJ Research PTC Peltier Thermocycler with a 5 minute DNA denaturing step at 98°C. Following this there were 36 cycles of: 95°C for 1 minute (denaturing and activating the Taq Polymerase enzyme), 61°C for 1 minute (primer annealing), 72°C for 2 minutes and 10 seconds (primer extension). Final extension was conducted at 72°C for 10 minutes and finally samples were held at 4°C until ran on a 2% agarose gel. Ethidium bromide was used to visualise bands on the gel in an Uvitec box. Mice heterozygous for 11HSD1 had 2 bands between 900 and 1000 base pairs with the knockout having a single band closer to 900 when compared to a DNA ladder (Figure 2.1).

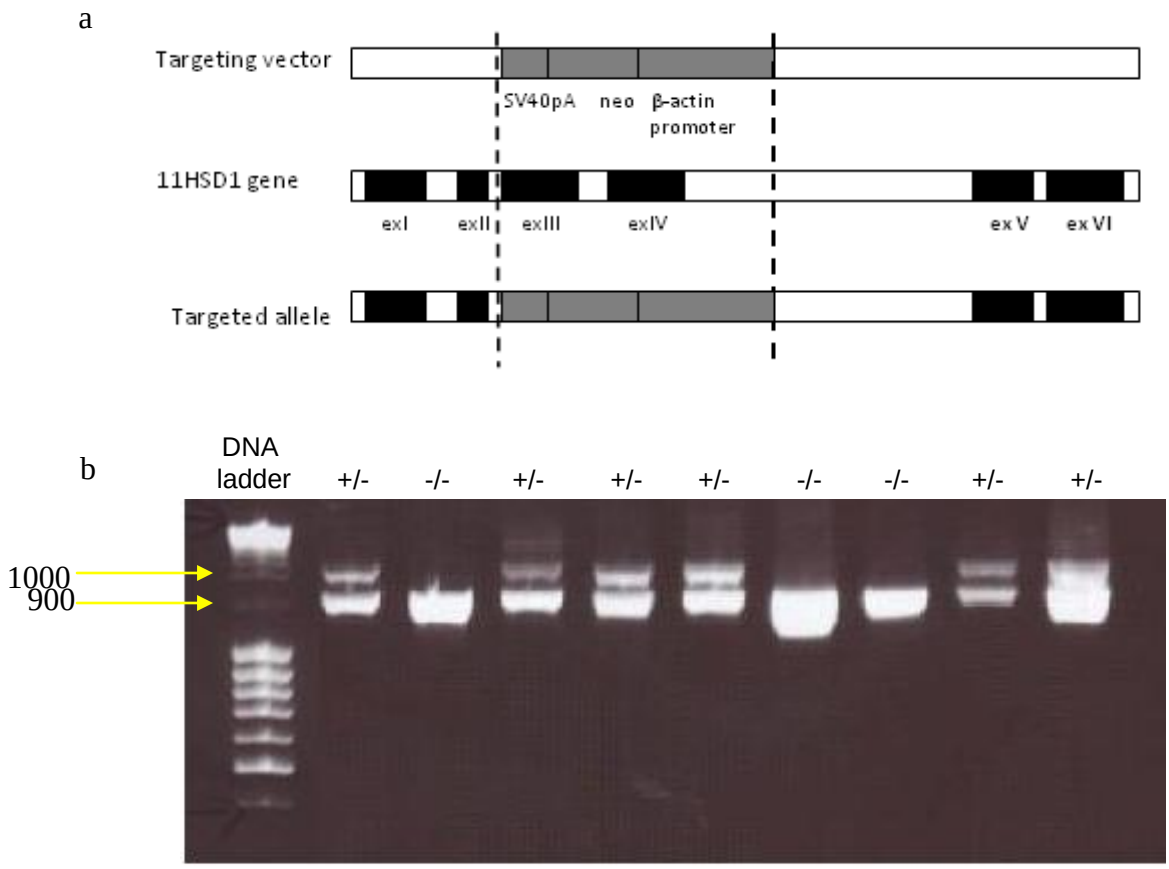

Figure 2-1 Production and Identification of 11HSD1$^{-/-}$ mice by genotyping using the polymerase chain reaction

(a) Simplified diagram of the 11HSD1 knockout strategy adapted from Kotelevstev et al., 1997. A targeting vetor containing a neomycin resistance cassette was used to excise exons encoding the catalytic domain of 11HSD1. The targeted allele was electroporated into embryonic stem cells, neomycin resistant clones were selected and injected into C57BL6 blastocytes before being transferred into a foster mother. Chimeras were bred to MF1 mice and the progeny were genotyped for the knockout. (b) Samples of DNA were run on an ethidium bromide gel. Mice heterozygote for 11HSD1 ($^{+/-}$) are identified by the presence of 2 bands between 900 and 1000 base pairs. In contrast 11HSD1 knock-out mice ($^{-/-}$) exhibit only 1 band at 900 base pairs.

2.2 In Vivo work

2.2.1 Coronary artery ligation

There are several murine models of myocardial infarction (MI) including cyro-injury, coronary artery cauterization and coronary artery ligation. Cryo-injury is achieved by applying a cryo-probe to the anterior left ventricle free wall for approximately 10 seconds followed by removal using saline at room temperature. This produces transmural infarction that reduces fractional shortening and left ventricular contractility (van den Bos et al., 2005). However there are several limitations to this model. The infarct area is small, there is little left ventricular remodelling and the injury is not ischaemic, therefore not exemplary of clinical MI (van den Bos et al., 2005). Coronary artery cauterization is more representative of MI as the injury is caused by ischaemia, but there is substantial secondary damage to the heart rendering this model inutile (Moskowitz et al., 1979). Coronary artery ligation is a well established model of ischaemic myocardial infarction that produces a consistent infarct size in the same location. The left descending main coronary artery is ligated with a suture, either permanently or transiently before reperfusion. Ischaemia followed by reperfusion is more clinically relevant but results in less remodelling than permanent occlusion. The effect of an experimental intervention is therefore less likely to be seen after reperfusion which may result in the need for larger experimental groups (Vandervelde et al., 2006). For this reason the permanent occlusion model, which has become the standard, was used for the work described herein for consistency with previous studies from our laboratory and with published work.

Male, 10-16 week old 11HSD1$^{-/-}$ and C57BL6 (Harlan) mice were weighed and anaesthetised with an intraperitoneal injection of medetomidine (1mg/kg), ketamine (75mg/kg) and atropine (600µg/kg). Upon induction of anaesthesia buprenorphine (0.05mg/kg) was administered subcutaneously as an analgesic. Doses were repeated

every 12 hours for 24 hours. Whilst under anaesthesia mice were kept on a heating pad at 37°C to maintain temperature. The skin on the chest was shaved and cleaned with an alcohol wipe. Mice were placed in a supine position with limbs taped down onto the heating pad. The trachea was intubated with a blunted 12g needle and mechanical ventilation began with room air (stroke volume 200µl, stroke rate 120 per min, Hugo Sachs Elektronik Minivent Harvard Apparatus). Eyes were coated with Lacri-Lube gel (Genusexpress, Aberdeen) to prevent desiccation. A 1cm subcutaneous incision was made over the left thorax extending medially and the subcutaneous tissue was separated from the muscle layers by blunt dissection. The major and minor pectoral muscles were separated and retracted with 5.0 Mersilk sutures (Ethicon, Livingstone) exposing the ribs. The left thorax was opened at the 4^{th} intercostal space by blunt dissection. The chest was held open using a 1cm chest retractor and a hole was made in the pericardium above the left atria and ventricle. The left main descending coronary artery was found beneath the left atrial notch in the left ventricle where pulsation of the vessel was visible. A 6.0 Proline suture (Ethicon, Livingstone) was pulled underneath the artery, as close to the atrium as possible and avoiding entering the left ventricular cavity. The needle was brought out approximately 1-2mm from the incision site and the suture was tied, ligating the artery. Successful ligation was evident from blanching of the left ventricle. In sham operated animals the suture was pulled under the artery but not tied. The pericardium was replaced over the heart and 2 single stitches with 5.0 Mersilk sutures were used to close the thoracic wall. Muscles were replaced into their former positions and the skin was stitched with continuous 5.0 Mersilk sutures. To speed recovery animals received atipamazole (Antisedan, an α_2 antagonist 5mg/kg) and 1.5ml sterile saline intraperitoneally along with air supplemented with 20% oxygen through a funnel in which the mouse's head was placed. Recovery was evident by self breathing movement, whiskers twitching and myoclonic jerks at which point the intubation was removed. Animals recovered on a heating pad before being returned to their cages.

2.2.2 Echocardiography

Myocardial function in mice can be assessed invasively by the pressure volume loop (P-V) using a specialised conductance catheter placed into the left ventricle, or non-invasively by magnetic resonance imaging (MRI) or ultrasound (echocardiography). A benefit of the P-V method is that it enables simultaneous measurements of the left ventricle pressure and volume giving a comprehensive assessment of heart function (Shioura et al., 2007). However non-invasive methods are advantageous as they are technically less difficult and the assessment of cardiac function can be performed serially in the same mouse. MRI images which can be clarified with use of a contrast agent, give excellent spatial resolution and enable assessment of regional contractile function, cardiac dimensions and infarct size (Van Laake, 2007). However, this technique requires prolonged periods of imaging and is expensive. On the other hand, echocardiography requires a short imaging time under light anaesthesia and is less expensive. Until recently echocardiography has been limited by its resolution and its 1 dimensional view. However advances in high resolution ultrasound (such as with the Vevo 770 or Vevo 2100, VisualSonics) are increasing the number of parameters that can be measured, making ultrasound more comparable to MRI. Ventricle dimensions may be measured using echocardiography enabling calculation of ejection fraction (the fraction of blood that is pumped out of the ventricle with each heart beat) and fractional shortening (the change in ventricle diameter between the contracted and relaxed state). When the heart is failing a decrease in ejection fraction (EF) and fractional shortening (FS) are seen (Van Laake, 2007, Sasaki et al., 2007, Orlic et al., 2001, Engel et al., 2006). In the current study mice were anaesthetised with isofluorane and echocardiography was conducted using a Diasus ultrasound machine (10-22MHz probe Dynamic Imaging, Livingstone UK). The chest was shaved and the transducer, coated in Henleys ultrasound gel (Dunlops Veterinary Supplies, Dumfries) was placed alongside the sternum (parasternally) to obtain a 2D image of the myocardium taken at the mid-papillary muscle level. Images were saved and analysed offline using Diasus software

(Dynamic Imaging). The ejection fraction ((LVEDA-LVESA)/LVEDA x 100) and fractional shortening ((LVEDD-LVESD)/LVEDD x 100) measurements enabled assessment of left ventricular function (Table 2.1).

Left ventricle parameter	Abbreviation
Left ventricle end diastolic area	LVEDA
Left ventricle end systolic area	LVESA
Left ventricle end diastolic diameter	LVEDD
Left ventricle end systolic diameter	LVESD
Posterior wall thickness at diastole	PWD
Posterior wall thickness at systole	PWS
Fractional shortening	FS
Ejection fraction	EF

Table 2-1 Left ventricle parameters assessed from echocardiography

Left ventricular parameters were measured offline using Diasus software. Measurements were taken at the mid papillary muscle level.

2.2.3 Blood sampling

Plasma samples were required to analyse circulating corticosterone levels after MI. Samples were taken at 7:30am, the diurnal nadir, as differences between C57Bl6 and 11HSD1$^{-/-}$ mice would be more pronounced (Harris et al., 2001). 2mm was cut from the end of the tail using surgical scissors. The tail was then milked for blood into an EDTA coated, capillary tube (Microvette CB300, Sarstedt, Leicester) as the mouse moved freely for a maximum of 1 minute. Blood sample were obtained quickly in order to prevent the stress response to handling confounding the corticosterone levels. Tubes were spun at 6000g for 10 minutes. The upper plasma layer was taken carefully and frozen at -20°C. Samples for flow cytometric analysis were taken just prior to culling via cardiac puncture. A 26g EDTA (5%) coated needle was placed into the left ventricle and blood was collected steadily. Samples were placed in Eppendorf tubes on ice. Approximately 1 ml of blood can be obtained using this method while the mouse is anaesthetised under isofluorane.

2.2.4 Drug dosing

For experiments described in Chapter 6 an 11HSD1 inhibitor, compound 544 (3-(1-adamantyl)-6,7,8,9-tetrahydro-5H-[1,2,4] triazolo [4,3-α] azepine, Enamine Ltd, Ukraine), was administered to mice in their food. Previous work by Merck and in our laboratory showed that this was an effective method of dosing (Hermanowski-Vosatka et al., 2005). During this study drug was to be administered after induction of MI therefore any dosing that may increase stress levels, such as repeated intraperitoneal injections and gavaging, was not feasible. Prior to surgery and dosing mice were separated into pairs and weighed daily, along with their food, in order to determine their daily food intake. For 500g diet 180g powdered diet (normal chow mix) was combined with 19g gelatine dissolved in 151ml hot water and 150ml drug carrier solution. Compound 544 was dissolved in methylcellulose (0.5%) and Tween 80 (5%) and mixed thoroughly with the

food. Vehicle diet contained the methylcellulose and Tween 80 only. The drug was administered at 30mg/kg/day assuming a food intake of 10g daily calculated from pre-surgery observations. Food was packed tightly into 60ml tubes and placed in the cages. Food tubes and mice were weighed daily after the commencement of the study to monitor drug intake. Food tubes were changed when empty or when signs of mould were detected.

2.3 Histology

After mice had been culled via cervical dislocation hearts were removed from the body and washed with ice cold PBS. Hearts for triphenyltetrazolium staining were frozen on dry ice then stored at -80°C.

For histology and immunohistochemistry the tissue must be preserved by fixation in solutions such as 10% neutral buffered formalin and zinc fixative (Ramos-Vara, 2005, Ismail et al., 2003). Fixation prevents autolysis, stabilises the tissue and stops bacterial growth. However this process also can distort the tissue and may create excessive protein cross linking that may mask the antigen and thus prevent antibody binding (see Section 2.5 Immunohistochemistry). To prevent over fixation tissues were fixed in 10% neutral buffered formalin (Sigma, Dorset, UK) for 24 hours then placed in 70% ethanol until processing. Whilst ethanol itself is also considered a fixative it has low penetration and therefore is more commonly used in this capacity in immunocytochemistry. An alternative approach to preserving antigen availability is to use frozen tissue sectioned with a cryostat. Better antigen preservation is seen where cryostat tissue sections are used. However, resolution is lower in frozen sections than fixed ones due to greater section thickness, and morphological changes during the freezing process may produce artefacts (Chiu et al., 1994). Fixation in formalin and subsequent embedding in paraffin wax is a superior way to preserve the tissue in terms of stability and morphology, and therefore was the option taken here. Fixed tissue was passed through as series of graded ethanols and xylene to clear and infiltrate the tissue prior to embedding in paraffin wax.

Tissue was carefully positioned during embedding in paraffin wax to ensure the best orientation for sectioning along the longitudinal axis of the heart. Paraffin blocks were placed in the freezer prior to cutting 5µm sections from each embedded heart using a Leitz Weltzlar 1512 microtome. Sections were floated in a Thermo water bath set at 40°C to remove wrinkles prior to mounting on charged glass slides (VH Bio, Tyne and Wear). Sections were then baked at 37°C overnight.

2.3.1 Triphenyltetrazolium staining

Triphenyltetrazolium chloride (TTC) reacts with dehydrogenase enzymes and cofactors to stain healthy tissue a bright red colour whereas necrotic tissue, which lacks such activity, remains unstained (Ytrehus et al., 1994). Frozen hearts were defrosted and cut into 5 transverse sections using surgical blades and each section was incubated (15 minutes; 37°C) in 1% TTC (Sigma, Dorset, UK) dissolved in PBS. Sections were then incubated for a further 10 minutes in 10% neutral buffered formalin at room temperature to enhance contrast of the stain. Hearts were blotted dry on tissue paper and digitally photographed at 10x magnification (Leica). For each section the area of infarct (unstained) as a percent of the left ventricle (stained red) was calculated using MCID software (Interfocus Imaging Ltd, Cambridge).

2.3.2 Haematoxylin and Eosin (H&E) stain

An H&E stain was utilised to identify neutrophils which have distinctive multi-lobed nuclei. Nuclei appear purple with the cytoplasm being pink (Figure 2.2). The staining protocol was as follows. Slides were deparaffinised and rehydrated in xylene (solution 1) for 10 minutes, xylene (solution 2) for 30 seconds, 100% ethanol for 1 minute, 2 x 1 minute incubations in 74 OP (ethanol) then 5 minutes in running tap water. Sections were stained by placing in Gill's haematoxylin (Sigma) for 1 minute followed by

washing in running tap water and placing in alkaline tap water (see Appendix 1) for a further 1 minute. The nuclei were differentiated by placing in acid alcohol (see Appendix 1) for 5 seconds followed by washing. Slides were then placed in 70% ethanol followed by Eosin Y (alcoholic; Sigma) for 30 seconds. After a further tap water wash slides were dehydrated through graded alcohols (74 OP; 2 x 1 minute incubations 100% ethanol; 1 minute) to xylene (2 x 2minutes). Slides were mounted and coverslipped with DPX.

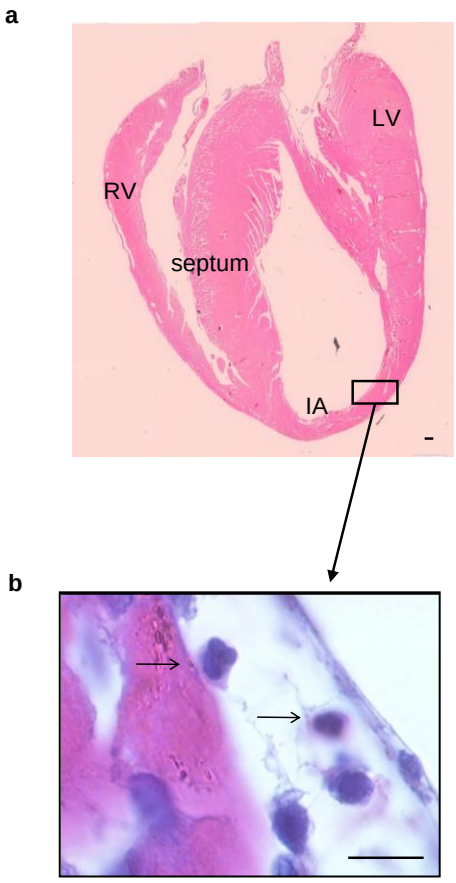

Figure 2-2 Haematoxylin and eosin stained heart section

Typical examples of (a) a longitudinal section and (b) high magnification detail from a haematoxylin and eosin-stained heart from a C57Bl6 mouse 2 days after myocardial infarction surgery. IA is the infarct area and arrows point to neutrophils present within the infarcted area. LV, left ventricle; RV, right ventricle. Scale bar is 10µm.

2.3.3 Periodic Acid Schiff Reaction (PAS)

The Periodic Acid Schiff Reaction (PAS) is used to assess the extracellular matrix. It stains glycogen and other carbohydrates in the basement membrane (magenta) and the nuclei (blue). Sections were stained by Susan Harvey (Medical Research Council/Centre for Inflammation Research Histology Service). Slides were deparaffinised and rehydrated as before then placed in water prior to oxidation in 1% Periodic acid for 5 minutes. Slides were then washed in water followed by incubation in Schiff's reagent (Sigma) for 15-20 minutes and then another wash in water for 10 minutes. Nuclei were stained with Harris's haematoxylin (Sigma) for 2.5 minutes and sections were then rinsed in water. Nuclear staining was differentiated with acid alcohol as in H&E staining. Slides were washed again before being dehydrated and coverslipped as previously.

2.3.4 Picrosirius Red staining (PSR)

Collagen deposition in the left ventricle is a measure of fibrosis but it is found in the heart under normal conditions as part of the basement membrane. Picrosirius red (PSR) stains collagen fibres pink/red with a yellow background. Sections were stained by Susan Harvey (Medical Research Council/Centre for Inflammation Research Histology Service). Slides were deparaffinised and rehydrated (as for H&E), incubated in Weigert's haematoxylin (see Appendix 1) for 8 minutes then washed under tap water for 10 minutes. Slides were then placed in Picrosirius Red (prepared in-house, see Appendix 1) for 1 hour followed by 2 washes in acidified water. Finally slides were dehydrated and coverslipped as before.

2.3.5 Masson's Trichrome stain

Masson's Trichrome is a standard stain used to assess infarct size in hearts (Kido et al., 2005). This stain distinguishes collagen fibres (blue) and nuclei (black) from the background (red). Sections were stained by Susan Harvey (Medical Research Council/Centre for Inflammation Research Histology Service). Slides were deparaffinised and rehydrated as before, washed in distilled water, then placed in Weigert's iron haematoxylin for 10 minutes. Sections were rinsed in warm running tap water for 10 minutes followed by further washing in distilled water. Staining was differentiated in phosphomolybdic-phosphotungstic acid solution (see Appendix 1) until collagen was no longer red (approximately 15 minutes). Subsequently sections were incubated in aniline blue solution (see Appendix 1) for 10 minutes, washed, then placed in 1% acetic acid for 2-5 minutes. After more washing in distilled water slides were dehydrated and coverslipped.

2.3.6 Quantification

Qualitative assessment of gross heart structure, the extracellular matrix and basal collagen from H&E, PAS and PSR staining in un-operated hearts was conducted by David Brownstein, an expert rodent pathologist. Quantification of neutrophils, collagen deposition and scar size after MI or sham operation were conducted using Image Pro6.2, Stereologer Analyser 6 MediaCybernetics (Buckinghamshire, UK) with sections being tiled at x50 or x100 magnification. The entire left ventricle (including the apex and posterior and anterior wall) was identified as an area of interest using the Image Pro6.2 computer programme after image acquisition. Neutrophils were identified by their distinctive multi-lobed nuclei at x1000 magnification. Cells were counted in the left ventricle and expressed as the average number (from 10 randomly selected areas) per $40\mu m^2$. Collagen deposition and scar size were quantified as a percentage of the total area of the left ventricle. Scar thickness was calculated from the thickness of 3 points along the scar and averaged. Endocardial and epicardial infarct lengths were calculated

as a percentage of the total circumference of the left ventricle using the following equation:

Infarct length (%) = infarct length/ left ventricle circumference x 100 (Kido et al., 2005). Histological stains were conducted on 1 slide per animal and each stain was run on sequential slides.

2.4 Immunohistochemistry

Immunohistochemistry allows the visualisation of antigens in a tissue by the application of an antibody specific for that antigen enabling assessment of antigen localisation and expression. Please refer to Section 2.4 Histology for details of fixation, embedding and sectioning. For immunohistochemistry 2 sections were placed on each microscope slide giving an adjacent negative control. Sections were then baked at 37°C overnight and for a further 30 minutes at 55°C immediately prior to staining to ensure good section adherence to the slide. Slides were taken through a series of xylenes (3 x 5 minutes) and graded ethanol (100% for 5 minutes and 74OP 2 x 5 minutes) to remove the wax and rehydrate the tissue.

As described in Section 2.4 (Histology) tissue fixation may result in protein cross-linking that may mask the antigen of interest. Unmasking cross-linked antigens can be achieved using antigen retrieval steps which involve exposing the tissue to high temperatures or to enzymatic digestion (Ramos-Vara, 2005). Heat-induced epitope retrieval (HIER) involves heating the sections in the microwave in either low or high pH buffers such as citrate pH6 buffer and Tris-EDTA pH9 buffer. Buffers are heated to boiling, slides are added and placed in the microwave on high power for 10 minutes. Slides are subsequently cooled in the buffer for a further 20 minutes. Proteolytic-induced epitope retrieval (PIER) uses enzymes such as trypsin and Proteinase K to unmask the antigen (see Appendix 1 for recipe). Slides are incubated with these enzymes usually at 37°C for 20 minutes.

Antibodies are immunoglobulins found in the serum and plasma. They are made by introducing the relevant antigen into a host, preferably a different species, causing the production of antibodies. Blood is collected and the antibody is isolated and purified. Polyclonal antibodies recognise several epitopes of the antigen and have relatively low specificity and high variation between batches. Monoclonal antibodies do not have this drawback as they are immunochemically identical. After the host has been immunised B cells (cells that produce the antibody) are harvested, fused with myeloma cells producing an immortal cell line that yield the antibody of interest (Ramos-Vara, 2005). However one disadvantage of such antibodies is that if fixation has cross-linked the specific antigen that the particular monoclonal antibody recognises it may not bind. As polyclonal antibodies recognise an array of epitopes they will be more likely to adhere. Both polyclonal and monoclonal antibodies have been used in the current work.

All of the immunohistochemistry protocols used in this study use avidin biotin technology for detection (Figure 2.3). The unconjugated primary antibody binds to the antigen. A biotinylated secondary antibody directed against the primary is applied followed by extravidin peroxidase which recognises the biotin of the secondary antibody. Subsequent incubation with the chromagen (3, 3'-diaminobenzidine; DAB), results in the development of a brown colour (due to peroxidase activity) at sites where extravidin peroxidase is bound. This system enables amplification of the target antigen as the secondary antibody and extravidin peroxidase can bind to several epitopes of the primary antibody and secondary antibody respectively, thus increasing sensitivity. However, such amplification may also amplify background staining which may have several sources. Endogenous peroxidase activity is seen in tissue containing haemoproteins (e.g. haemoglobin, myogloblin) and may produce background staining by reacting with DAB. In the present study, endogenous peroxidase activity was quenched by application of 3% hydrogen peroxide for 15 minutes. Some tissues also express endogenous biotin and, therefore, require blocking by pre-treating with avidin followed by saturating with biotin. Fixation of tissues increases hydrophobicity. Both hydrophobic and ionic non-specific interactions between the tissue and antibodies may

cause background staining. This may be reduced by incubation with non-fat dry milk and bovine serum albumin (BSA) as a separate step and/or addition of BSA (1-5%) in the diluting buffer. Inappropriate binding of the secondary antibody to the tissue is prevented using serum from the species in which the secondary antibody was raised. Substantial background staining is seen when an antibody is directed against the same species in which it was raised. To prevent this incubation with a mouse-on-mouse blocking kit for 1 hour was conducted and proved successful. Furthermore thorough washing between all incubation steps, with the exception of milk/BSA, serum blocking and mouse on mouse blocking, with buffer (either PBS or TBS-Tween) prevents inappropriate background staining.

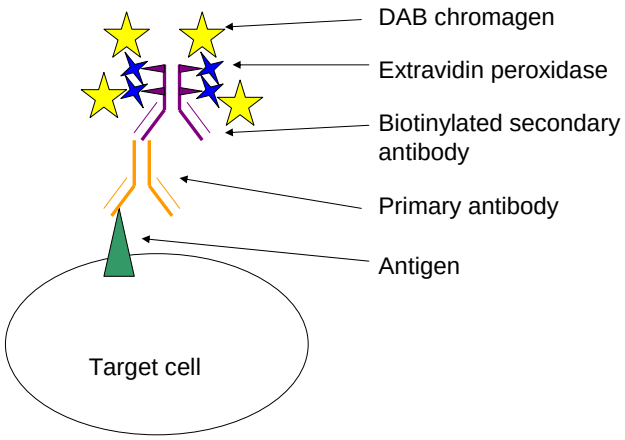

Figure 2-3 Schematic of immunohistochemistry using avidin biotin technology

Immunohistochemistry is used to label specific antigens in tissue sections by application of a relevant antibody. Addition of a biotinylated secondary antibody that recognises the primary antibody but not the host tissue is applied, after removal of the excess primary. The secondary is removed by washing and extravidin peroxidase is added to recognise the biotinylation of the previous antibody. DAB recognised the peroxidase activity of the extravidin peroxidase and reacts to give a brown colour.

2.4.1 Protocols

A brief overview of the protocols is given in Table 2.2. Each different antibody was stained for on 1 slide per animal. Where several different antibodies were used in a study sequential slides were used where possible. For all immunohistochemistry protocols 5µm sections were deparaffinised in xylene and rehydrated through various concentrations of ethanol then placed in running tap water. Endogenous peroxidase activity was blocked using 3% hydrogen peroxide diluted in distilled water for up to 15 minutes. Primary antibody concentrations were determined after pilot experiments using a range of antibody dilutions around those suggested by the manufacturer. Control antibodies (immunoglobulins from pre-immune animals) were diluted as the primary antibody (Table 2.3). After application of the secondary antibody, sections were washed in PBS or TBS and incubated with extravidin peroxidase (Sigma) diluted 1/200 in buffer for 30 minutes. After more washing the sections were incubated with DAB Substrate (Vector, Peterborough, UK) for the relevant time. DAB was placed on one positive slide from each experiment and watched under the microscope until the brown colour developed. The length of time required for this was then used for the rest of the slides. Sections were washed for 5 minutes in tap water then counterstained with haematoxylin, dehydrated and coverslipped using DPX.

CELL TYPE	ANTIBODY	ANTIGEN RETRIEVAL	BLOCKING	PRIMARY ANTIBODY DILUTION	PRIMARY ANTIBODY INCUBATION	SECONDARY ANTIBODY
Macrophage	Monoclonal rat anti-mouse Mac 2 (Cedarlane)	No	10% normal goat serum	1/6000 in PBS/1%BSA	Overnight 4°C	Biotinylated goat anti-rat (Vector), 1/400, 1 hour
Alternatively activated macrophage	Polyclonal rabbit anti-mouse YM-1 (Stem Cell Technologies)	Citrate buffer pH6 microwave	Avidin-biotin, 10% normal goat serum	1/50 in PBS/1%BSA	1 hour room temperature	Biotinylated goat anti-rabbit (Vector), 1/200, 30 minutes
T Cell	Polyclonal rabbit anti-human CD3 (Dako)	Tris-EDTA pH9 microwave	20% normal goat serum	1/400 in PBS/1%BSA	1 hour room temperature	Biotinylated goat anti-rabbit (Vector) 1/200, 30 minutes
B Cell	Monoclonal rat anti-mouse CD45R (BD Bioscience)	No	10% normal rabbit serum	1/400 in PBS/1%BSA	30 minutes room temperature	Biotinylated rabbit anti-rat (Vector) 1/200, 30 minutes
Endothelial cells	Monoclonal rat anti-mouse CD31 (BD Bioscience)	Proteinase K 37°C	20% normal rabbit serum	1/50 in PBS/1%BSA	Overnight 4°C	Biotinylated rabbit anti-rat (Vector) 1/200, 30 minutes

CELL TYPE	ANTIBODY	ANTIGEN RETRIEVAL	BLOCKING	PRIMARY ANTIBODY DILUTION	PRIMARY ANTIBODY INCUBATION	SECONDARY ANTIBODY
Proliferating cells	Monoclonal mouse anti-mouse BrdU (Sigma)	Trypsin 37°C, 2N HCl 37°C	Avidin-biotin, mouse on mouse	1/1000 in TBS/10% NGS/5%BSA	1 hour 37°C	Biotinylated goat anti-mouse (Vector) 1/200, 30 minutes
Activated myofibroblast /smooth muscle	Monoclonal mouse anti-mouse α smooth muscle actin (Sigma)	No	2.5%milk/2.5 %BSA,mouse on mouse, 10% normal goat serum	1/400 in PBS/1%BSA	1 hour room temperature	Biotinylated goat anti-mouse (Vector) 1/200, 30 minutes
11HSD1	Polyclonal sheep anti-mouse anti 11HSD1 (generated in house)	No	2.5%milk/2.5 % BSA, 10% normal rabbit serum	1/2000 in PBS/5% BSA	Overnight 4°C	Biotinylated rabbit anti sheep (Vector) 1/200, 30 minutes

Table 2-2 Protocols for immunohistochemistry

Brief details of the immunohistochemistry protocols used including antigen retrieval, blocking, primary and secondary antibody incubations. BSA=bovine serum albumin; PBS= phosphate buffered saline TBS= tris buffered saline, 11HSD1= 11β-hydroxysteroid dehydrogenase, NGS= normal goat serum

Primary antibodies	Control antibodies (same concentration as primary)
Mac 2, CD45R, CD31	Rat IgGa κ
BrdU, α smooth muscle actin	Mouse ascites fluid
YM1, CD3	Rabbit IgG
11HSD1	Sheep IgG

Table 2-3 Relevant control antibodies for immunohistochemistry

Control antibodies (immunoglobulins from pre-immune animals) were diluted and applied in the same manner as the primary antibodies.

2.4.2 Identification of macrophages

A variety of macrophage markers are used in immunohistochemistry, including F4/80, mac 3, factor VIIIa and mac 2. F4/80 is a widely expressed on monocytes and macrophages, and antibodies directed against it have been used for immunohistochemistry frozen tissue or in tissue fixed in Methyl Carnoys solution (Morimoto et al., 2006, Henderson et al., 2008). In the current study tissues were fixed in 10% formalin, and despite attempts to optimise the protocol, F4/80 staining was not sufficiently clear for quantification (Figure 2.4). Mac 2, otherwise known as galectin 3, is another well-characterised cell surface marker that is expressed and secreted by activated macrophages, and was used successfully in the current study in identifying macrophages (MacKinnon et al., 2008). After peroxidase blocking, sections were incubated with 10% normal goat serum (Vector) diluted in PBS for 30 minutes. The monoclonal rat anti-mouse mac 2 primary antibody (VH Bio) was diluted 1/6000 in PBS/1%BSA and incubated with the sections overnight at 4°C. After PBS washes the biotinylated goat anti-rat antibody (Vector) was added in a 1/200 dilution in PBS/1%BSA for 60 minutes.

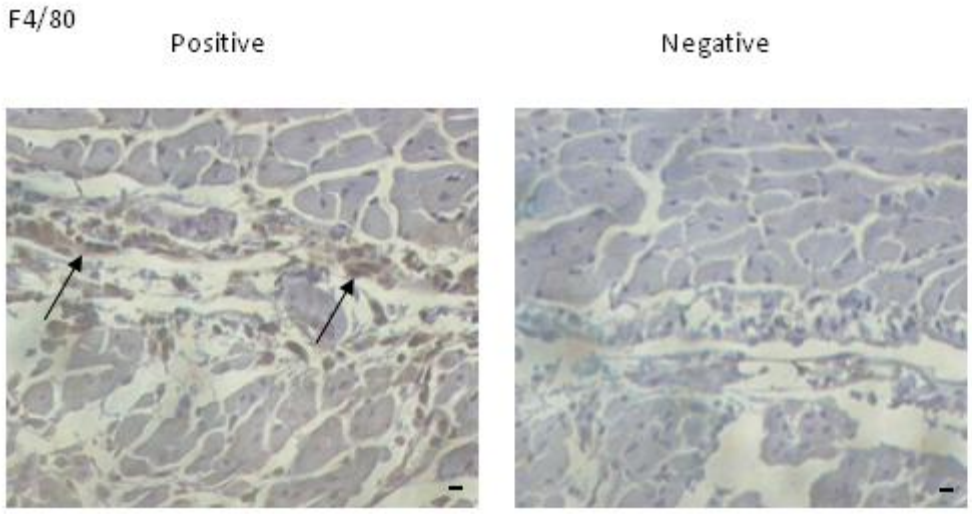

Figure 2-4 Immunohistochemistry for the macrophage marker F4/80

Mouse heart tissue 7 days post-MI demonstrating typical F4/80 positive and negative staining which was insufficiently clear for quantification. Bar is 10µm.

2.4.3 Identification of alternatively activated macrophages

Anti-RELMα/FIZZ1 (a resistin-like molecule) and YM1 (a chitinase-like lectin) antibodies have been used to detect alternatively activated macrophages using immunohistochemistry (Loke et al., 2002, Nair et al., 2005). Immunohistochemistry for RELMα showed cell staining in positive control sections (nematode infected lungs) but not in hearts after MI. YM1 on the other hand was expressed in both positive control tissue and in infarcted hearts (for examples see Section 4, Figure 4.13). Therefore this marker was chosen to detect alternatively activated macrophages in the healing infarcts. HIER was conducted by microwaving slides in hot citrate buffer pH 6.0 (see Appendix 1) for 5 minutes followed by cooling for a further 20 minutes. After peroxidase blocking, sections were incubated with Avidin/Biotin blocking solutions (Vector), following manufacturer's instructions, and 10% normal goat serum (Vector) diluted in PBS (30 minutes). The polyclonal rabbit anti-mouse YM1 primary antibody (Stem Cell Technology, France) was diluted 1/50 in PBS/1%BSA and incubated with sections for 60 minutes at room temperature. After washes with PBS sections were incubated with the biotinylated goat anti-rabbit secondary antibody (Vector) diluted 1/400 in PBS/1%BSA for 30 minutes.

2.4.4 Identification of other inflammatory cells

For immunohistochemistry to detect T-cells, antigens were retrieved by heating in Tris-EDTA buffer pH9.0 (see Appendix 1) for 10 minutes in the microwave, followed by cooling. After peroxidase blocking, sections were incubated in 20% normal goat serum (Vector) diluted in PBS for 30 minutes. The polyclonal rabbit anti-human CD3 primary antibody (Dako, Cambridgeshire) was diluted 1/400 in PBS/1%BSA and incubated for 60 minutes at room temperature. After washing the biotinylated goat anti-rabbit secondary antibody (Vector) was diluted 1/200 in PBS/1%BSA and incubated with the sections for 30 minutes. For B cell staining sections were blocked in 10% normal rabbit

serum (Vector) in PBS for 30 minutes. The monoclonal rat ant-mouse CD45R primary antibody (BD Bioscience, Oxford) was diluted 1/50 in PBS/1%BSA and incubated with sections for 30 minutes at room temperature. Slides were washed then incubated with a biotinylated rabbit anti rat secondary antibody (Vector) diluted 1/200 in PBS/1%BSA.

2.4.5 Identification of neovascularisation

A number of endothelial cell markers have been used for immunohistochemical detection of endothelial cells, including isolectin B_4, CD34, von Willebrand factor and Tie-2. Ismail et al conducted an extensive comparison of several endothelial cell markers in tissues prepared in a variety of fixatives (Ismail et al., 2003). They found that CD31, otherwise known as platelet endothelial cell adhesion molecule-1 (PECAM-1), was a superior endothelial cell marker in formalin fixed paraffin embedded tissue as it detects both macro- and micro-vessels (Ismail et al., 2003). This makes it ideal to assess neovascularisation. The CD31 antigen was retrieved by proteolytic tissue digestion in Proteinase K (20µg/ml in TE buffer, Roche, West Sussex, UK) for 20 minutes at 37°C and a further 20 minutes cooling. After peroxidase blocking sections were blocked further by incubation with 20% normal rabbit serum (Vector) in PBS for 30 minutes. The monoclonal rat anti mouse CD31 primary antibody (BD Bioscience) was diluted 1/50 in PBS/1%BSA and incubated with sections overnight at 4°C. After washing the biotinylated rabbit anti-rat secondary antibody (Vector) was diluted 1/200 in PBS/1%BSA and incubated with the sections for 30 minutes.

2.4.6 Identification of cell proliferation

Proliferating cells can be identified by exposure to bromodeoxyuridine (BrdU) which is incorporated into the nucleus during replication and can subsequently be detected with a specific antibody. Injecting a bolus dose of BrdU *in vivo* enables assessment of cell

proliferation from time of injection. In this study BrdU (2.5mg in warmed saline, 5mg/ml, Sigma) was injected into the peritoneum of mice 1 hour prior to sacrifice to allow incorporation into the nuclei of replicating cells. In heart sections, antigens were retrieved by incubating slides in 2N HCl (see Appendix 1) for 15 minutes at 37°C followed by trypsin digestion (see Appendix 1) for 30 minutes at 37°C. All washes were with TBS-Tween (see Appendix 1) to reduce background staining due to hydrophobic interactions. Blocking of non-specific antibody binding was by incubation with an Avidin/Biotin blocking kit and mouse-on-mouse blocking kit as per manufacturer's instructions (Vector). The monoclonal mouse anti-mouse primary antibody was diluted 1/1000 (Sigma) in TBS/10% normal goat serum/5%BSA and incubated for 1 hour at 37°C. After washing with TBS-Tween sections were incubated with the biotinylated goat anti-mouse secondary antibody (Vector) diluted 1/200 in TBS/1%BSA for 30 minutes.

2.4.7 Double immunohistochemistry

The study described in Chapter 4 was designed to identify which cells were proliferating. In order to achieve double immuno-labelling for mac2 positive macrophages and BrdU positive proliferating cells the protocols were run sequentially. Mac 2 immunohistochemistry was run first followed by the BrdU protocol immediately after the DAB step. BrdU was visualised using a SG substrate kit following manufacturer's instructions (Vector) to produce a blue/grey colour. Sections were then washed (counterstaining with haematoxylin was omitted) and dehydrated as with other protocols. Attempts to co-localise BrdU with CD31 were unsuccessful when protocols were run sequentially or in parallel.

2.4.8 Myofibroblast activation

Blocking of non-specific background staining was achieved by incubating sections with 2.5%milk/2.5%BSA in PBS for 1 hour followed by a mouse-on-mouse blocking kit for a further hour and 10% normal goat serum (both Vector) in PBS for 30 minutes. The monoclonal mouse anti-mouse α-smooth muscle actin (αSMA) primary antibody (Sigma) was diluted 1/400 in PBS/1%BSA and incubated with the tissue at room temperature for 60 minutes. After washing the biotinylated goat anti-mouse secondary antibody (Vector) was diluted 1/200 in PBS/1%BSA and incubated with the slides for 30 minutes.

2.4.9 11HSD1 expression

Attempts to achieve immunostaining with commercially bought 11HSD1 and 11HSD2 (Cayman Chemicals, Michigan, USA) were unsuccessful. However, an antibody generated in-house against a murine 11HSD1 fragment over-expressed in E.coli (raised in sheep) was available. The sheep plasma was purified by Fu Yang (Centre for Cardiovascular Science, The University of Edinburgh) using a Hightrap protein G column (GE Healthcare). In heart and positive control tissue (liver and kidney) background staining was blocked by incubating sections for 1 hour in 2.5% powdered milk/2.5% BSA in PBS followed by 30 minutes in 10% normal rabbit serum (Vector). The polyclonal sheep anti-mouse 11HSD1 was diluted 1/2000 in PBS/5%BSA and incubated with sections overnight at 4°C. After washing in PBS the biotinylated rabbit anti-sheep secondary antibody (Vector) diluted 1/200 in PBS/1%BSA was added for a further 30 minutes.

2.4.10 Quantification

Quantification of immunohistochemistry was conducted using Image Pro 6.2, Stereologer Anaylser 6 MediaCybernetics. Sections were tiled at x100 and the entire left ventricle (including the apex and posterior and anterior wall) or infarct border (area between the infarcted tissue and the healthy myocardium) were selected as the area of interest (after image acquisition using Image Pro 6.2) in which all measurements were made. Macrophage infiltration (both mac 2 and YM1) was quantified as the percent of infarct border stained. The area was assessed automatically after a threshold had been set manually. Small vessels (<200 μm^2 diameter) positively stained for the endothelial cell marker, CD31, were counted in the left ventricle as the number per 400μm^2 and expressed as an average of 10 areas in the left ventricle randomly selected by the computer programme. Counting was conducted during acquisition on the computer using a scale bar. BrdU positive cells were counted in the left ventricle and expressed as number of cells per mm^2. Activated myofibroblast activation was quantified as percentage staining in the left ventricle.

2.5 Biochemical and molecular techniques

2.5.1 Corticosterone Radioimmunoassay

The corticosterone radioimmunoassay, developed in-house, is a competition assay that has been used here to determine plasma levels of corticosterone after myocardial infarction. Samples are incubated with radiolabelled corticosterone (^{3}H-B), a primary antibody directed against corticosterone, and a secondary antibody directed against the primary conjugated to scintillation proximity (SPA) beads. When these SPA beads are in close proximity to the ^{3}H-B light is emitted and can be detected by scintillation counters. When there is little unlabelled corticosterone in the sample most of the primary antibody will bind to the radiolabelled corticosterone stimulating the SPA beads to emit light after exposure to the secondary antibody (Figure 2.5). Where there is more unlabelled

corticosterone (i.e. more corticosterone in the sample) this will compete for the primary antibody, reducing the amount of the ^{3}H-B in proximity to the SPA bead conjugated secondary antibody and, therefore, will reduce SPA stimulation (Figure 2.5).

At the diurnal nadir (7:30am) blood was collected by tail tip from the mice as described in Section 2.3.3. Samples were spun at 6000g at 4°C and the plasma was removed to a fresh tube before freezing at -20°C. When ready to assay samples were diluted 1 in 5 with borate buffer (se Appendix 1). The majority of plasma corticosterone is normally bound to corticosterone binding globulin and this was liberated by denaturing at 75° for 1 hour. Samples were then kept on ice until ready to assay. Standards of 0, 0.3, 0.6, 1.25, 2.5, 5, 10, 20, 40, 80, 160 and 320nM corticosterone were made from concentrated stock solution (32µM) in borate buffer. 20µl of sample or standard were added to wells in a 96 well flexible plates in duplicate. 50µl of the radiolabelled corticosterone (radiation count of 8-12000 counts per minute (CPM), 1.5nM) and the primary antibody (rabbit anti-mouse corticosterone antibody made in-house by Dr Chris Kenyon, Centre for Cardiovascular Science, The University of Edinburgh) diluted 1/100 in borate buffer was added to each well. Plates were incubated at room temperature for 2 hours before adding 50µl anti-rabbit SPA beads (5mg/ml made up in borate buffer) to each well. Plates were inverted to mix. Emitted light was measured in the Wallac 1450 Microbeta Scintillation Counter after further 16 hour incubation. The standards (x axis) were plotted against the CPM (y axis) to generate a standard curve. Sample corticosterone concentrations were calculated by interpolation on the standard curve (Figure 2.6).

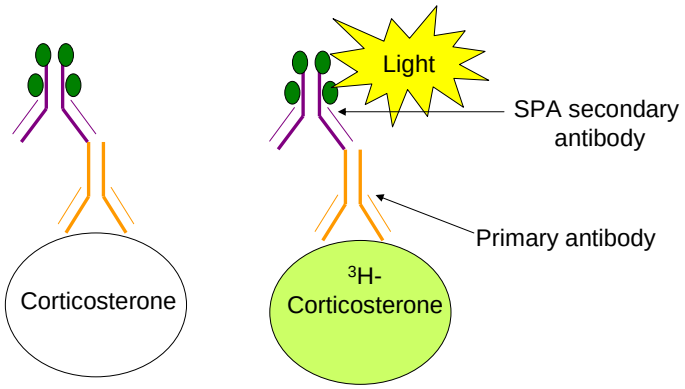

Figure 2-5 Corticosterone radioimmunoassay

Corticosterone in the sample competes with ^{3}H-corticosterone for the primary antibody and subsequently the complex binds to the SPA secondary. Light is emitted when the SPA is in proximity to ^{3}H-corticosterone which is measured in a beta counter. SPA= scintillation proximity assay.

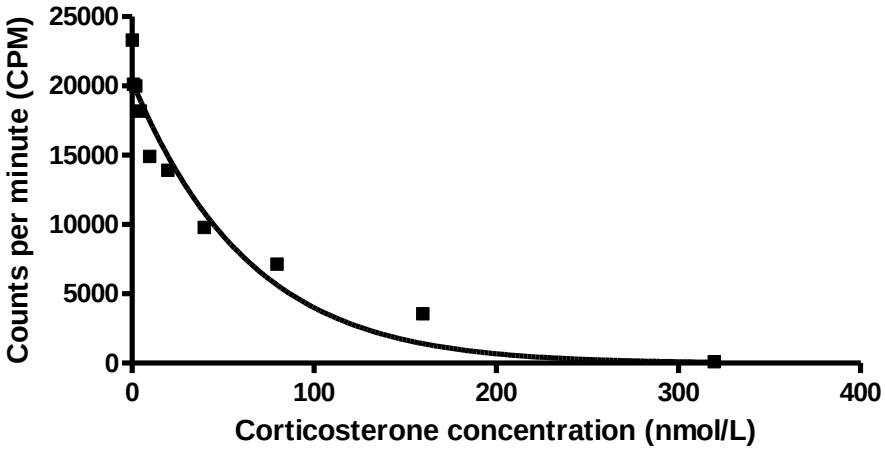

Figure 2-6 Corticosterone standard curve

A standard curve was generated for each corticosterone radioimmunoassay plate in order to determine the corticosterone concentration in plasma samples.

2.5.2 RNA extraction

Heart tissue was excised, washed in ice cold PBS and bisected before freezing on dry ice. Samples were stored at -80°C before being used. Trizol (Invitrogen) was used to extract RNA from the tissue. Half of a heart was homogenised in 1ml Trizol using 3mm Retsch metal beads in a Retsch MM301 ball miller at room temperature (Retsch, Leeds). Full homogenisation was achieved after 3.5 minutes at 25Hz. Samples were then moved to a fresh autoclaved eppendorf and spun at 12000g for 10 minutes at 4°C. This extra isolation step removed insoluble material such as collagen. The supernatant was removed to a fresh tube and incubated at room temperature for 5 minutes. 0.2ml chloroform was added, samples were shaken vigorously then incubated at room temperature for 3 minutes. Samples were spun at 12000g for 15 minutes at 4°C. The colourless upper aqueous phase contained the RNA and was removed to a fresh tube. 0.5ml isopropanolol was added to precipitate the RNA over a 10 minute incubation period. After another spinning step (12000g for 10 minutes at 4°C), a gel-like RNA pellet was formed. The pellets were washed with 70% ethanol in DEPC water and spun again (7500g for 5 minutes at 4°C). The ethanol was removed and the pellets dried before re-dissolving the RNA in 30-50µl DEPC treated water (see Appendix 1). RNA quantity and quality in 2µl were analysed using the Nanodrop 2000 analyser (Wilmington, USA). All RNA had an A260/A280 ratio of 1.8-2.2 which suggests high quality RNA with low contamination with carbohydrates or proteins. RNA was treated with DNase I amplification grade (Invitrogen) to prevent degradation by endogenous DNases. Briefly, 1µg RNA was incubated with 1x DNase reaction buffer and 1 unit DNase Amp Grade for 15 minutes at room temperature. The reaction was inactivated by adding 2.5mM EDTA and incubating at 65°C for 10 minutes. Samples were kept at -80°C until ready to transcribe to cDNA.

2.5.3 cDNA synthesis

RNA cannot be used in PCR and for this reason it is converted to single stranded cDNA using reverse transcription. This was achieved using the High Capacity cDNA Reverse Transcription kit (Applied Biosystems, Warrington). A mastermix containing 1x RT buffer, 1 x dNTPs, 1x RT random primers (short primers that give uniform amplification of RNA), 1µl multiscribe RT, 1µl RNase inhibitor and 3.2µl nuclease free water was mixed together on ice. RNase inhibitors were used to prevent RNA degradation. 10µl of this mastermix was added to eppendorf tubes along with 10µl DNase-treated RNA (approximately 1µg). Solutions were mixed using a pipette before being loaded onto a Thermocycler. The reverse transcription was carried out under the following conditions; 25°C for 10 minutes, 37°C for 120 minutes, 85°C for 5 minutes. cDNA was subsequently transferred to a freezer at -20°C for storage. To check that the reverse transcription had worked a GAPDH PCR was conducted. GAPDH is a housekeeping gene expressed in all cell types and therefore should be present in cDNA samples. A mastermix containing 1x buffer, 0.05mM dNTP mix, 1 unit Taq Polymerase, 10ρmol of the forward and reverse primers (forward 5'-TCA AGA AGG TGG TGA AGC AGG C-3', backward 5'-CTC TCT TGC TCA GTG TCC TTG C-3') and autoclaved water. A 25µl reaction mixture was produced by adding 1µl DNA to the mastermix. The PCR reaction was initiated with a denaturing step (95°C, 4 minutes) followed by 30 cycles of 94°C for 1 minute, 53°C for 1 minute and 72°C 2 minutes. Final extension was achieved with 10 minute incubation at 72°C. Samples were run on a 2% agarose gel containing ethidium bromide and visualised using an Uvitec box. A DNA ladder was used to identify GAPDH bands at 280 base pairs.

2.5.4 Quantitative Real Time PCR

Quantitative real time PCR (qRT PCR) is a highly sensitive method that enables the quantitative analysis of tissue mRNA levels. It is similar to conventional end point PCR in that there are cycles of primer annealing, extension and target amplification.

However, unlike end point PCR, detection of mRNA is achieved as the reaction occurs giving higher sensitivity and resolution. In this study a Roche Lightcycler was used for qRT-PCR. This method utilises fluorescent resonance energy transfer (FRET) where the primer-probe contains a 5' high energy reporter that is attached to a 3'low energy quencher. When the probe and primer are close together energy is transferred from the high energy reporter to the quencher upon light excitation. During the PCR reaction the primer-probe becomes annealed to complementary strands of cDNA. As the Taq Polymerase enzyme copies the cDNA its 5' nuclease activity cleaves the primer-probe preventing the energy transfer. Fluorescent emission from the reporter is captured by the Lightcycler instrument. Emissions are detected over several cycles of primer annealing, extension and amplification. The detection system produces an amplification plot which shows the fluorescence level and cycle number (Figure 2.7). From this a crossing point (CP) value may be extrapolated. This value is the cycle at which the level of fluorescence in the reaction is distinguishable from the background. The lower the CP value the fewer the number of cycles required to get a significant level of fluorescence indicating a greater mRNA abundance. This is normalised to a housekeeping gene/endogenous control, in this case GAPDH, to compensate for potential differences in the amount of cDNA put into the reaction. GAPDH was a suitable candidate as it was not altered by infarction (as seen from data from the current study) and remained similar across the samples.

Initially a small volume of cDNA from a variety of experimental groups was pooled then serially diluted to produce a standard curve. The amount of cDNA required for the qRT PCR reaction was optimised from this standard curve for each gene. cDNA for IL-6, MCP-1 and IL-8 qRT PCR was used undiluted. cDNA for VEGF, GR, MR and 11HSD1 was diluted 1 in 5 in PCR grade water just prior to use. Each reaction included 2µl cDNA, 1x Lightcycler Probes Master, 4x primer probe (Applied Biosystems pre-optimised probes) and PCR grade water to a volume of 10µl. The primer probes are listed below in Table 2.4. The programme used on the Lightcycler 480 was: pre incubation at 95°C for 10 minutes (ramp rate 4.8°C/s); 40 cycles of amplification 95°C

for 10 seconds (ramp rate 4.8°C/s), 60°C for 20 seconds (ramp rate 2.5°C/s), 72°C for 20 seconds (ramp rate 4.8°C/s single acquisition); cooling 40°C for 10 seconds (ramp rate 2.5°C/s).

The volumes used are very small thus increasing the likelihood of a pipetting error. Therefore samples were run in triplicate. Triplicates were averaged unless there were discrepancies (greater than 10%) between values. In such cases the inconsistent value was removed. These average CP values were then expressed as a fold change relative to the GAPDH CP value. Expression was normalized for GAPDH expression and expressed as fold increases over control sham-operated mice.

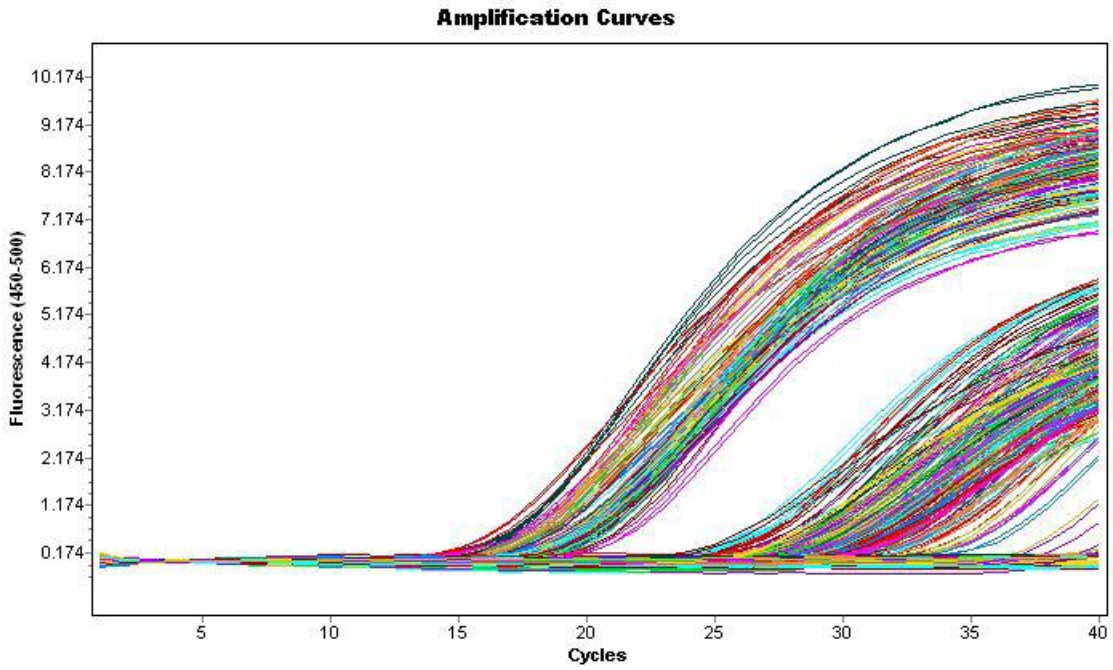

Figure 2-7 Typical amplification curve produced by qRT-PCR

In samples where the gene of interest is expressed fluorescent emissions increase beyond that of the background (shown by an upward curve). The cycle (crossing point, CP, where the line ascends) indicates how much of that mRNA is present.

Gene	Assay ID
Interleukin-6 (IL-6)	Mm99999064_m1
Monocyte chemoattractant protein 1 (MCP-1)	Mm00441242_m1
Interleukin 8 (IL-8)	Mm00433859_m1
Vascular endothelial growth factor A (VEGF A)	Mm00437306_m1
Glucocorticoid receptor (GR)	Mm00433832_m1
Mineralocorticoid receptor (MR)	Mm01241596_m1
11β-hydroxysteroid dehydrogenase type 1 (11HSD1)	Mm00476182_m1

Table 2-4 Primer-probes used for qRT-PCR

TAQman ® Gene Expression Assays were used to detect mRNA levels of IL-6, MCP-1, IL-8, VEGFa, GR, MR and 11HSD1. The table shows their Applied Biosystems assay IDs.

2.6 Power Calculations and Statistical Analysis

Sample size was determined on the basis of cardiac function (ejection fraction i.e., the fraction of blood pumped out of the left ventricle in one beat, assessed by echocardiography) as the primary end point. Based on previous work in the laboratory and published work, I assumed ejection fraction to be 30% 7 days after MI (normal ejection fraction is approximately 65%) and that increasing angiogenesis may improve ejection fraction by 10% (to 40%) with a standard deviation of 8%. This would necessitate a sample size of ≥6 mice per MI group tested for there to be 80% power in the experiment. As the difference in sham and MI values for ejection fraction are relatively large (normally >30%) the sample size required in the sham-operated groups is much lower (≥3 mice per goup tested). Sample size was determined using GraphPad Statmate 2.

Statistical analysis was conducted using GraphPad Prism software. In each Chapter all data are expressed as mean ± SEM. Analysis of mortality and cause of death data were conducted using Fisher's exact test and the Chi squared test. Other comparisons are by unpaired Student's t test, 1 way ANOVA and 2 way ANOVA. Please see individual Chapters for full details. P values less than 0.05 were considered significant.

2.7 Materials

APPLIED BIOSYSTEMS, WARRINGTON, UK

High capacity cDNA reverse transcription kit, TAQman ® Gene Expression Assays; Interleukin-6 (Il-6) Mm99999064_m1, Monocyte chemoattractant protein 1(MCP-1) Mm00441242_m1**,** Interleukin 8 (Il-8) Mm00433859_m1, Vascular endothelial growth factor A (VEGF A) Mm00437306_m1, Glucocorticoid receptor (GR) Mm00433832_m1, Mineralocorticoid receptor (MR) Mm01241596_m1 and 11 β hydroxysteroid dehydrogenase type 1 Mm00476182_m1, mouse GAPDH endogenous control (FAM/MGB probe non primer limited)

BD BIOSCIENCES, OXFORD, UK

Monoclonal rat anti mouse CD31 antibody , rat $IgG2_{a,k}$ control antibody,

CEDARLANE, SUPPLIED THROUGH VH BIO, TYNE AND WEAR, UK

Monoclonal rat anti mouse mac 2

DAKO, CAMBRIDGESHIRE, UK

Polyclonal rabbit anti human CD3 antibody

DUNLOP'S VETERINARY SUPPLIES, DUMFRIES, UK

Henleys Ultrasound gel

ENAMINE LTD, UKRAINE

Compound T5293658

ETHICON, LIVINGSTONE, UK

Mersilk sutures 5/0 75cm (W581), Prolene sutures 6/0 (W8712)

FISHER SCIENTIFIC, LEICESTERSHIRE, UK

Tris HCl, Tris base, sodium chloride (NaCl), 74 O.P, Hydrochloric acid, potassium dihydrogen orthophosphate (KH_2PO_4), calcium chloride ($CaCl_3$), sodium hydrogen carbonate ($NaHCO_3$), Shandon MB35 Premier microtome blades

GE AMERSHAM, BUCKINGHAMSHIRE, UK

Anti-Rabbit YSi SPA Scintillation Beads, ^{3}H- Corticosterone,

GENUSEXPRESS, ABERDEEN, UK

Lacri-lube gel

INVITROGEN, PAISLEY, UK

Rat anti mouse CD11b PE antibody, hamster anti mouse CD11c-APC antibody, Trizol, DNase I amplification grade

INTERFOCUS IMAGING LTD, CAMBRIDGE, UK

MCID software

LONZA, SLOUGH, UK

Dulbecco's PBS without magnesium or calcium

PROMEGA, SOUTHAMPTON, UK

RNase, agarose, 100bp DNA ladder, loading buffer, GoTaq DNA Polymerase, dNTPs

RATHBURN CHEMICALS LTD, WALKERBURN, UK

Chloroform

REAGENA, FINLAND

Reastain Quick Diff kit

RETCSH, LEEDS, UK

3mm cone balls

ROCHE, WEST SUSSEX, UK

Proteinase K, Collagenase (type), Lightcycler 480 multiwell plates 384, Lightcycler 480 Probes Master

SAINSBURY'S, UK

Gelatin, non fat dried milk

SARSTEDT, LEICESTER, UK

Microvette CB300 blood collection tubes

SIGMA, DORSET UK

EDTA, Isopropanolol, SDS, Ethidium Bromide, 10% neutral buffered saline, triphenyltetrazolium chloride, Harris's Haematoxylin, Gill's Haematoxylin, Weigert's Haematoxylin, Eosin Y, DPX (Fluka), BrdU (Fluka), mouse anti mouse BrdU antibody, mouse anti mouse α smooth muscle actin antibody, control mouse ascites fluid, bovine serum albumin fraction V, bovine serum albumin, Extravidin peroxidase, 30% hydrogen peroxide, ammonia hydroxide, methylcellulose, Tween 80, citric acid, boric acid (B6768), potassium chloride (KCl), corticosterone, diethyl pyrocarbonate (DEPC), Bradford reagent, Direct Red, Collagenase type IA-S (C-5894), magnesium sulphate ($MgSO_4$), ammonium chloride (NH_4Cl), Ethylenediaminetetraacetic acid disodium salt dehydrate (Na_2EDTA), Potassium bicarbonate ($KHCO_3$), Periodic acid, Schiff's Reagent, Collagenase Type IA-S.

STEM CELL TECHNOLOGIES, GRENOBLE, FRANCE

Polyclonal rabbit anti mouse YM-1

VECTOR, PETERBOROUGH, UK

Normal goat serum, normal rabbit serum, biotinylated goat anti rat secondary antibody, biotinylated goat anti rabbit secondary antibody, biotinylated goat anti mouse secondary antibody, biotinylated rabbit anti rat antibody, biotinylated rabbit anti sheep, avidin biotin blocking kit, M.O.M mouse IgG blocking reagent (PK-2200), DAB substrate kit (SK-4100), rabbit IgG, sheep IgG

VH BIO, TYNE AND WEAR, UK

11HSD1 primers 5'-TTC TTC GTG TGT CCT ACA GG-3', 5'-CCC GCC TTG ACA ATA AAT TG-3' and 5'-CAC TGC ATT CTA GTT GTC GTT TGT CC-3'

GAPDH primers: forward 5'-TCA AGA AGG TGG TGA AGC AGG C-3', backward 5'-CTC TCT TGC TCA GTG TCC TTG C-3'

VWR-BDH, LEICESTERSHIRE, UK

Superfrost slides, absolute ethanol, Xylene, calcium chloride

3 Basal cardiac phenotype of the 11HSD1 deficient mouse

3.1 Introduction

Glucocorticoids have a plethora of physiological functions including modulating metabolism, the stress response, inflammation and blood pressure. However, pathological excess of glucocorticoids is correlated with adverse cardiovascular effects (Kerrigan et al., 1993). Their action is mediated by activation of either low affinity glucocorticoid (GR) or high affinity mineralocorticoid (MR) receptors that are expressed across the cardiovascular system, including in the heart and vasculature (Sheppard and Autelitano, 2002, Lombes et al., 1995, Hadoke et al., 2006, Yoshikawa et al., 2009, Takeda et al., 2007). These receptors are often co-expressed with the 11β-hydroxysteroid dehydrogenase (11HSD) enzymes which are also present in the myocardium and vasculature (Hadoke et al., 2006, Slight et al., 1993, Slight et al., 1996, Christy et al., 2003, Takeda et al., 2007, Walker et al., 1991). 11β-hydroxysteroid dehydrogenase type 1 (11HSD1) reactivates cortisone in humans and 11-dehydrocorticosterone in rodents, to cortisol and corticosterone respectively, by its ability to act as a reductase. It is found in glucocorticoid target tissues and amplifies glucocorticoids locally. Conversely, protection of the MR from illicit activation by glucocorticoids is achieved via 'pre-receptor' inactivation of cortisol/corticosterone by 11β-hydroxysteroid dehydrogenase type 2 (11HSD2).

Glucocorticoids have a diverse array of effects in the myocardium including regulation of electrical and mechanical activities of the heart (Yoshikawa et al., 2009). Dexamethasone, a synthetic glucocorticoid, can increase cardiac L-type Ca^{2+} channel currents, increase contraction and relaxation velocities, and in healthy human volunteers can reduce resting heart rate (Whitehurst et al., 1999, Penefsky and Kahn, 1971, Brotman et al., 2005). However, studies have also shown that MR activation can modulate electrical activities of the heart (Ouvrard-Pascaud et al., 2005) and fibrosis

(Benard et al., 2009). A recent comprehensive study of the specific role of GR activation on metabolism in rat cardiomyocytes was conducted by Yoshikawa et al. using the GR selective agonist cortivazol and the GR antagonist RU-38486 (Yoshikawa et al., 2009). Selective GR activation upregulated pro-hypertrophic and pro-apoptotic genes which may increase cell size and increase cell death (Yoshikawa et al., 2009).

As excess endogenous glucocorticoids have been associated with adverse cardiovascular outcomes reducing their actions is attractive in the setting of cardiovascular disease. However, systemic blockade of the GR can result in compensatory increases in the activity of the hypothalamic-pituitary-adrenal (HPA) axis, and therefore in circulating glucocorticoids, making direct inhibition of the GR an unsuitable therapeutic target (Spiga et al., 2007, Bamberger and Chrousos, 1995). Manipulation of local levels of glucocorticoids without this adverse effect on the HPA axis can be achieved by inhibition of 11HSD1. Until recently there were no selective inhibitors of 11HSD1 and so to investigate the effect of its deficiency a mouse with selective disruption of the HSD1B1 gene ($11HSD1^{-/-}$) mouse was generated (Kotelevtsev et al., 1997). $11HSD1^{-/-}$ mice are viable, producing normal pups, show no detectable changes in blood pressure and cannot regenerate corticosterone from 11-dehydrocortiosterone, indicating that 11HSD1 is the only enzyme responsible for reactivating glucocorticoids (Kotelevtsev et al., 1997). The adrenal glands of $11HSD1^{-/-}$ mice are enlarged and morphometric analysis showed that this is due to adrenocortical hyperplasia. The functional significance of this is demonstrated by enhanced basal corticosterone levels in these mice although peak corticosterone levels are not different from wild-type litter mates (Kotelevtsev et al., 1997, Harris et al., 2001). $11HSD1^{-/-}$ mice are resistant to diet-induced obesity, are protected against age-related cognitive decline and have improved insulin sensitivity (reviewed in (Paterson et al., 2005, Tomlinson and Stewart, 2005)). It has also been shown previously that $11HSD1^{-/-}$ mice have enhanced cardiac angiogenesis and improved heart function 7 days after myocardial infarction (MI) (Small et al., 2005, Small, 2005). Despite these interesting observations very little is known about the basal cardiac phenotype of $11HSD1^{-/-}$ mice with published papers merely reporting that there

is no difference in organ weights (Kotelevtsev et al., 1997, Morton et al., 2004). As 11HSD1$^{-/-}$ mice have improved heart function 7 days after MI it is vital to know whether this is because of some basal differences in cardiac architecture and function. Furthermore, there is a lack of consistency in the literature regarding the localisation of 11HSD1 in the myocardium. It is hypothesised that the cardiac architecture of 11HSD1$^{-/-}$ mice is similar to that of C57Bl6 controls and that this is associated with comparable cardiac function. Simultaneously, the localisation of 11HSD1 within the myocardium is investigated with the hypothesis that expression is localised to cardiomyocytes, fibroblasts and smooth muscle cells.

3.2 Methods

3.2.1 Mice

Male C57Bl6 (Harlan, UK) and 11HSD1 homozygous null ($^{-/-}$) mice (bred from an in-house colony on a C57Bl6 background) (Kotelevtsev et al., 1997, Morton et al., 2004) aged 10-12 weeks were used. Mice were killed by cervical dislocation. For histological analysis hearts were bisected transversely while for immunohistological analysis hearts were bisected down the longitudinal axis. This was followed by fixation, processing and embedding in paraffin wax as described in Section 2.4.

3.2.2 Immunohistochemistry

Identification of 11HSD1 was conducted using a polyclonal sheep anti-mouse 11HSD1 antibody generated in-house diluted 1/2000 in PBS/5% BSA. For details of the procedure please refer to Section 2.5 and 2.5.9 and Table 2.2. Immuno-reactivity for 11HSD1 yielded weak staining and, therefore, it was not quantifiable. 3 sections of heart taken from each genotype (C57Bl6 and 11HSD1$^{-/-}$ mice) were stained with liver sections serving as a positive control.

3.2.3 Echocardiography

Cardiac function was assessed by echocardiography as described in section 2.3.2. The observer was blinded to surgery and genotype for the purpose of echocardiography measurements.

3.2.4 Histology

Haematoxylin and eosin staining was used to assess the gross cardiac structure. The cardiac endomysial, epimysial and adventitial matrix were assessed using Picrosirius Red and Periodic-Acid-Schiff staining. These stains highlight collagen and tissue glycogen respectively. Staining was conducted by Susan Harvey (Medical Research Council/ Centre for Inflammation Research Histology Service) and was assessed by Dr David Brownstein, a pathologist. Please refer to Section 2.4.3 and 2.4.5 for further details.

3.2.5 Statistics

All values are expressed as mean ± SEM. Comparisons of body weight, heart weight and echocardiography are by unpaired Student's t-test. P values less than 0.05 were considered significant.

3.3 Results

Expression of 11HSD1 in the myocardium

Immunohistochemistry for 11HSD1 showed high levels of immunoreactivity in the liver of C57Bl6 mice which was used as a positive control (Figure 3.1). The negative control showed no immunoreactivity. In the heart vascular smooth muscle cells, but not endothelial cells, expressed 11HSD1 as seen in Figure 3.1. This was seen in vessels of varying size. Cardiomyocytes stained weakly for 11HSD1 (Figure 3.1). Cardiac fibroblasts are found interstitially, have ovoid nuclei with drawn out cytoplasm and can form fibres. They also stained positively for 11HSD1 and were distributed evenly across the myocardium (Figure 3.1). The 11HSD1$^{-/-}$ mice did show some weaker staining in liver positive control sections, cardiac smooth muscle cells, cardiomyocytes and cardiac fibroblasts (Figure 3.1). Staining was similar in all sections examined.

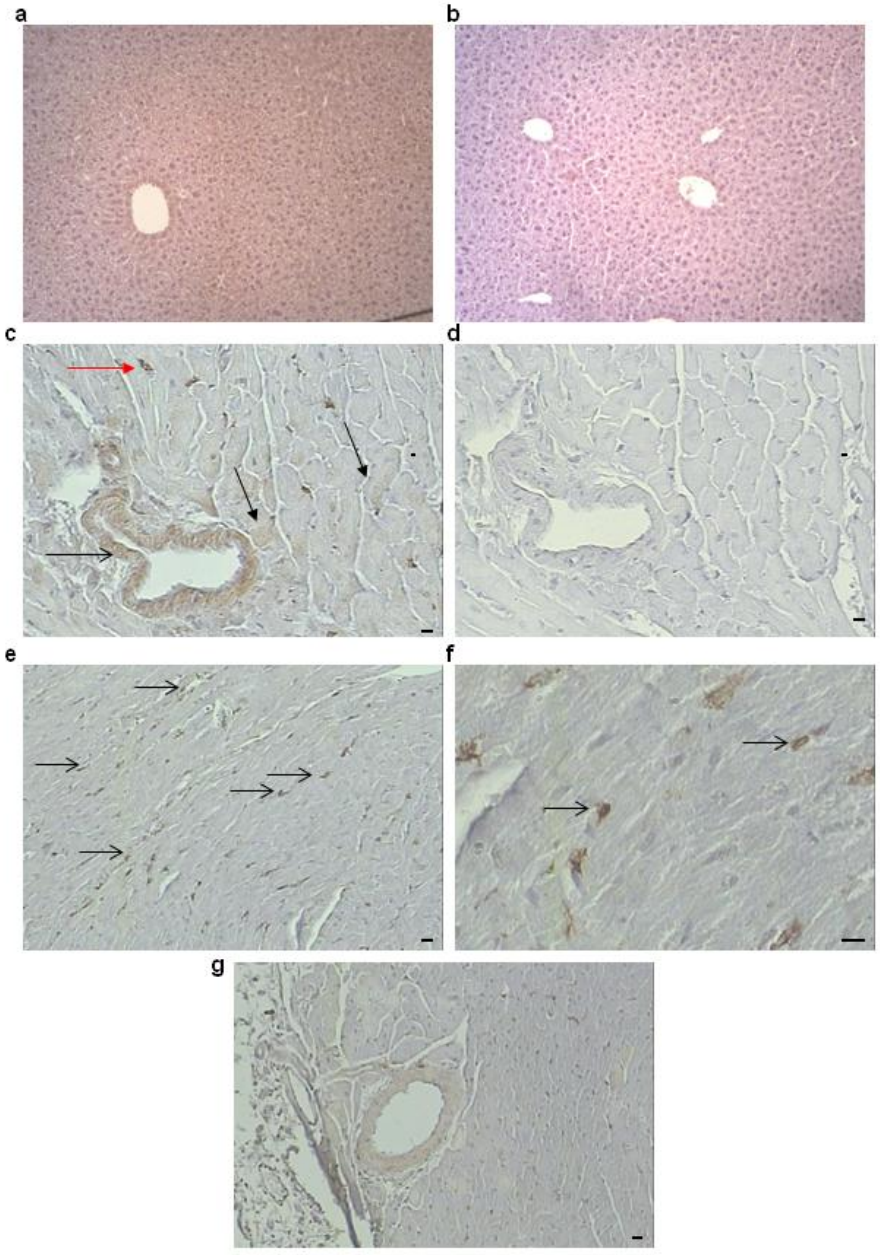

Figure 3-1 Immunohistochemistry for 11HSD1

A sheep anti-mouse 11HSD1 antibody was used to identify 11HSD1 in murine heart tissue. Liver was used as a positive control for 11HSD1 immunoreactivity (a) with the negative control showing no staining (b). (c) Immunoreactivity is evident in the smooth muscle of coronary vasculature and fibroblasts with weaker staining in cardiomyocytes of heart tissue (identified morphologically, open arrow point to vascular smooth muscle cells, red arrow points to fibroblasts, closed arrows point to cardiomyocytes). (d) No staining was observed in the negative

control. (e and f) Arrows point to positive cells staining in heart sections that are likely to be fibroblasts. 11HSD1$^{-/-}$ mice show weak staining (g). Pictures are representative of sections taken from 3 mice. Bar is 10μm.

Body and heart weight

Male 10-12 week old C57Bl6 and 11HSD1$^{-/-}$ mice had similar body weights (Figure 3.2). In contrast, heart weight was significantly lower in 11HSD1$^{-/-}$ mice compared with C57Bl6 controls (Figure 3.2; $P<0.05$). This relationship remained when expressed relative to body weight (Figure 3.2). There was no difference in other organ weights.

Histopathogical analysis of the myocardium

Gross inspection of hearts from C57Bl6 and 11HSD1$^{-/-}$ mice showed that there were no obvious malformations in the hearts of 11HSD1$^{-/-}$ mice (Figure 3.3). This was confirmed by cross-sections of the heart which were stained with haematoxylin and eosin (Figure 3.4). Periodic Acid Schiff showed that deficiency of 11HSD1 had no effect on the endomysial, epimysial or adventitial matrix in the heart (Figure 3.5). Histological assessment by the independent pathologist found that there was a tendency for 11HSD1$^{-/-}$ mice to have smaller cardiomyocytes upon gross observation although this was not measured. The pathologist found no other differences between hearts from C57Bl6 and 11HSD1$^{-/-}$ mice.

Cardiac function

C57Bl6 and 11HSD1$^{-/-}$ mice had comparable left ventricular dimensions as assessed by echocardiography (Table 3.1). Furthermore heart function expressed as ejection fraction (EF) and fractional shortening (FS) were similar in both groups (Figure 3.6).

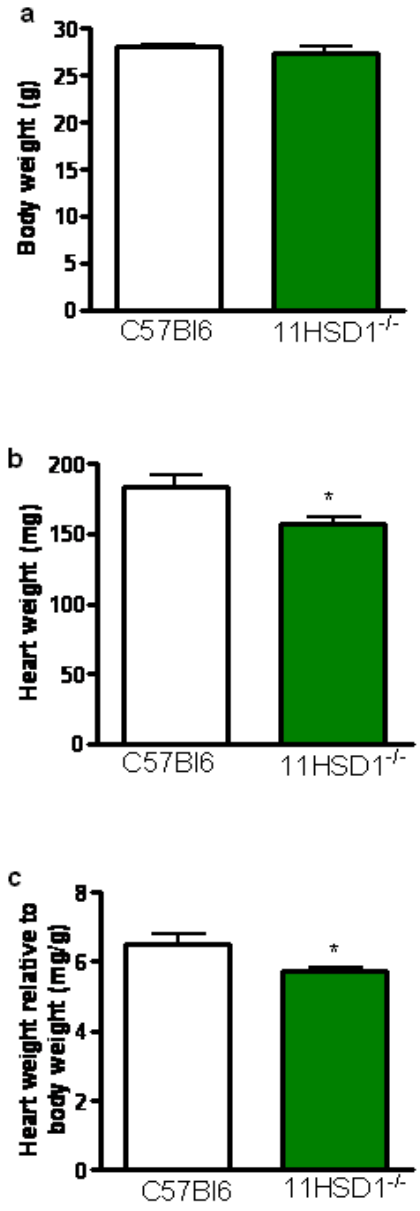

Figure 3-2 The influence of transgenic deletion of 11HSD1 on mouse body weight and heart weight

$11HSD1^{-/-}$ mice (male, 10-12 weeks old, C57Bl6 n=10, $11HSD1^{-/-}$ n=8) were a similar weight to age matched C57Bl6 control mice (a). Despite this, heart weight (b) was significantly reduced in the $11HSD1^{-/-}$ mice compared with controls. The reduction in heart weight was also evident when expressed relative to body weight (c). Data are expressed as mean ± SEM. *P<0.05 when compared with C57Bl6 controls using a Student's unpaired t test.

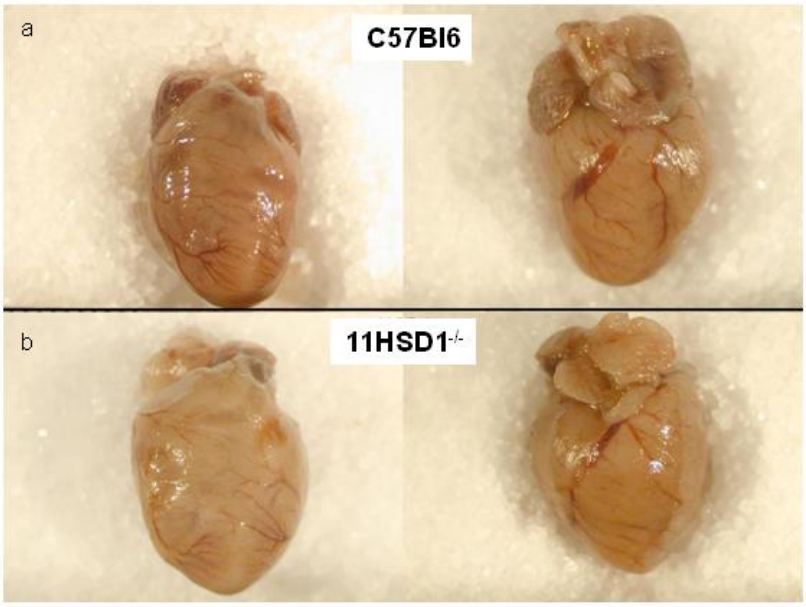

Figure 3-3 Gross comparisons of hearts from 11HSD1-/- and C57Bl6 mice

Photographs of frontal and dorsal views of typical hearts excised from C57Bl6 (a) and 11HSD1$^{-/-}$ (b) mice showing that there are no overt structural abnormalities observable with the naked eye.

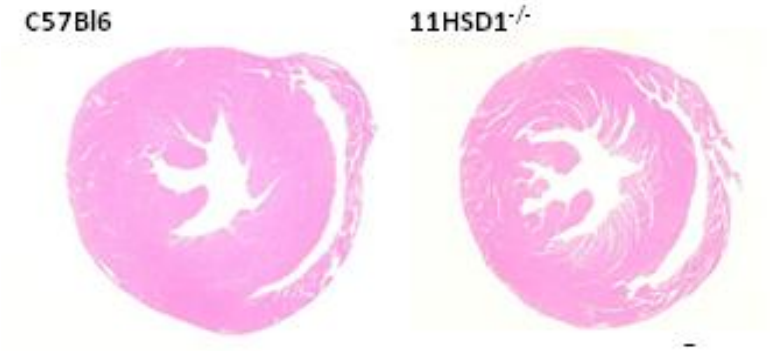

Figure 3-4 Haematoxylin and eosin stained hearts

Typical cross sections of haematoxylin and eosin stained sections obtained from hearts of C57Bl6 and 11HSD1$^{-/-}$ mice demonstrating no overt structural abnormalities between the groups. Scale bar is 10µm.

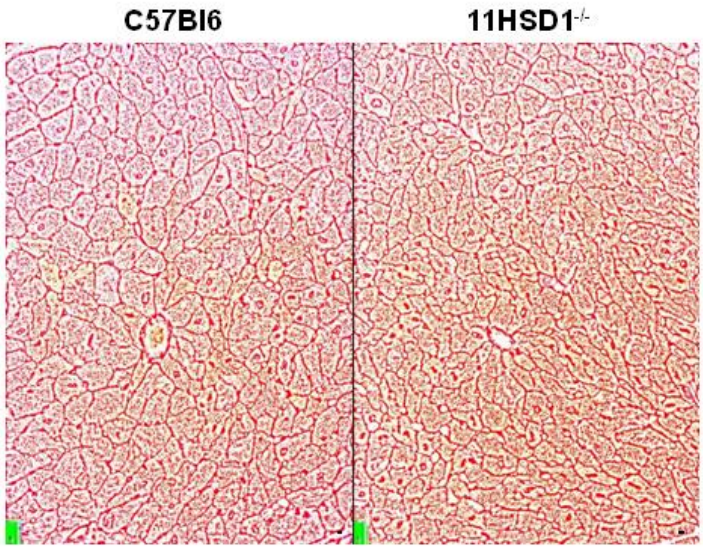

Figure 3-5 Picrosirius Red staining of the myocardium

Cross sections of hearts from C57Bl6 and 11HSD1$^{-/-}$ mice following Picrosirius Red staining. The section has been digitally inverted, filtered and equalised in order to bring up the endomysium. There are no differences in the extracellular matrix between C57Bl6 and 11HSD1$^{-/-}$ mice. Cardiomyocyte cross-sectional area appears to be reduced. Bar is 10µm.

	C57Bl6	11HSD1$^{-/-}$
LVEDA	19.92 ± 1.12	17.81 ± 0.48
LVESA	6.25 ± 0.74	5.61 ± 0.86
LVEDD	4.33 ± 0.28	3.73 ± 0.14
LVESD	2.54 ± 0.18	2.44 ± 0.17
PWD	0.85 ± 0.05	0.79 ± 0.07
PWS	1.28 ± 0.11	1.12 ± 0.08
EF (%)	69.74 ± 2.68	66.4 ± 3.94
FS (%)	41.37 ± 2.27	34.95 ± 3.42

Table 3-1 Left ventricle dimensions by echocardiography

LVEDA (left ventricle end diastolic area), LVESA (left ventricle end systolic area), LVEDD (left ventricle end diastolic diameter), LVESD (left ventricle end systolic diameter), PWD (posterior wall thickness at diastole), PWS (posterior wall thickness at systole), EF (ejection fraction) and FS (fractional shortening) were assessed in isofluorane anaesthetised C57Bl6 and 11HSD1$^{-/-}$ mice. Genotype had no influence on any parameter assessed by echocardiography. Data are expressed as mean ± SEM. n=10 C57Bl6, n=8 11HSD1$^{-/-}$.

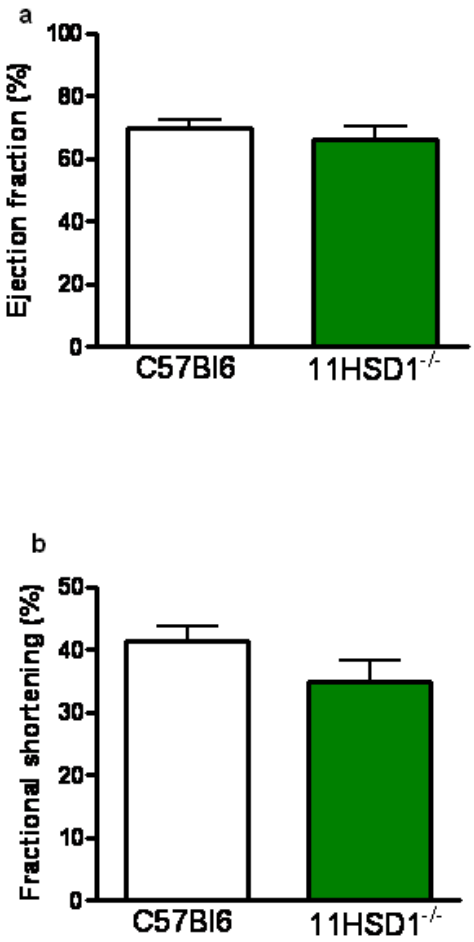

Figure 3-6 Quantified data from echocardiography of C57Bl6 and 11HSD1$^{-/-}$ mice.

Ejection fraction (a) was calculated from the left ventricle end diastolic area (LVEDA) and left ventricle end systolic area (LVESA) and expressed as a percent. Fractional shortening (b) was calculated from the left ventricle end diastolic diameter (LVEDD) and left ventricle end systolic diameter (LVESD) and expressed as a percent. Genotype has no influence on basal cardiac function. Data are expressed as mean ± SEM. n=10 C57Bl6, n=8 11HSD1$^{-/-}$.

3.4 Discussion

Previous work has shown that 11HSD1$^{-/-}$ mice have enhanced angiogenesis and improved heart function 7 days after MI but the basal cardiac phenotype of these mice has not been described (Small, 2005, Small et al., 2005). The aim of the current work was to investigate the distribution of the 11HSD1 protein in the myocardium and determine the consequences of 11HSD1 deletion on cardiac structure and function. 11HSD1 immunoreactivity was localised to cardiac fibroblasts, vascular smooth muscle cells and cardiomyocytes. Whilst there was a decrease in heart weight in the 11HSD1$^{-/-}$ mice compared to C57Bl6 controls, the cardiac architecture and function was comparable.

11HSD1 Expression

Expression of both corticosteroid receptors and both 11HSD isozymes has been described previously in the myocardium and vessel wall (Walker, 2007b, Hadoke et al., 2006). Furthermore 11HSD1 activity has been detected in the rodent myocardium and artery wall (Small, 2005, Klusonova et al., 2009, Hadoke et al., 2001). GR expression has been localised to cardiomyocytes, cardiac fibroblasts and the vasculature (smooth muscle and endothelial cells) with MR expression also being found in cardiomyocytes and the vasculature (Walker et al., 1991, Slight et al., 1993, Takeda et al., 2007, Slight et al., 1996). Consistent with these previous investigations 11HSD1 immunoreactivity was observed in the cardiac fibroblasts and vascular smooth muscle cells with faint staining also evident in cardiomyocytes (but not endothelial cells) (Small, 2005, Morton et al., 2004, Masuzaki et al., 2001, Deuchar, 2009, Camelliti et al., 2005, Christy et al., 2003, Vliegen et al., 1991). 11HSD2 distribution was not examined here but previous studies have shown it to be expressed in cardiomyocytes and vascular endothelial cells (Slight et al., 1996, Christy et al., 2003, Takeda et al., 2007). Interestingly the 11HSD1$^{-/-}$ mice still showed some positive staining for 11HSD1 although this was much fainter than the C57Bl6 controls. Previous studies from this laboratory have shown that a truncated form

of the 11HSD1 protein can still be translated in the 11HSD1$^{-/-}$ mice with approximately 5% enzyme activity in the liver (Tijana Mitic, personal communication). This is in line with previous work that has demonstrated that 11HSD1$^{-/-}$ mice on the MF1/129 background have no enzyme activity in the brain, less that 5% enzyme activity in the liver and 6.36% activity in thoracic aortas (Kotelevtsev et al., 1997, Hadoke et al., 2001). This great reduction in 11HSD1 activity is the result of targeted replacement exon 3 and 4 (which encode the catalytic domain of the enzyme) with a neomycin resistance cassette during the production of the knockout (see Figure 2.1 for the knockout strategy) (Kotelevstev et al., 1997, Tomlinson et al., 2004). The truncated proeitn, therefore, does not contain this vital domain (Kotelevstev et al., 1997, Tomlinson et al., 2004). The in-house produced antibody is polyclonal, recognises several epitopes of the antigen and, thus, can bind to several sites on the 11HSD1 protein. It is possible that some but not of these epitopes are present on the truncated form of 11HSD1 explaining the weaker staining in the 11HSD1$^{-/-}$ mice.

Pathology

The results presented here replicate those found previously; showing that in male mice aged 10-12 weeks old there was no difference in body weight between C57Bl6 and 11HSD1$^{-/-}$ mice (Kotelevtsev et al., 1997, Morton et al., 2004). Interestingly 11HSD1$^{-/-}$ mice have been shown to resist diet-induced obesity whereas over-expression of 11HSD1 in adipocytes (to a level comparable to that seen in obese humans) results in the development of features of metabolic syndrome, including visceral obesity (Morton et al., 2004, Masuzaki et al., 2001). The mice used in the current study were maintained on standard chow diet and had not, therefore, been metabolically challenged.

In the present study, 11HSD1$^{-/-}$ mice were shown for the first time to have significantly decreased heart weight relative to C57Bl6 controls. Mice with high tissue levels of corticosterone, due to deficiency of 11HSD2 have enlarged hearts (Deuchar, 2009). Furthermore, in neonatal hearts, high corticosterone levels increased heart weight (Reini

et al., 2008). This effect could be reversed by an MR but not a GR, antagonist, suggesting that glucocorticoid-dependent changes in heart weight may be mediated by MR activation (Reini et al., 2008). Tissue glucocorticoid levels were not determined in this study, but we would predict that they are reduced in the 11HSD1$^{-/-}$ mice compared to C57Bl6 control as they would not be locally regenerated within the target tissues. The independent pathologist suggested that the decrease in heart weight in 11HSD1$^{-/-}$ mice may be due to a decrease in cardiomyocyte cross-sectional area (Dr. David Brownstein, personal communication) and we have demonstrated here that cardiomyocytes have weak expression of the 11HSD1 protein. Glucocorticoids stimulate pro-hypertrophic genes and we can speculate that a local reduction in corticosterone might reduce cardiomyocyte size via this mechanism (Yoshikawa et al., 2009). Additionally activation of GR can modulate the electrical and mechanical activities of the heart. This suggests that preventing cardiac regeneration of corticosterone may alter basal cardiac phenotype (Yoshikawa et al., 2009). Despite hearts from 11HSD1$^{-/-}$ weighing 10% less than those from their C57Bl6 counterparts, gross inspection and qualitative histological analysis showed that the structure of the myocardium was comparable suggesting no overt structural abnormalities.

Although 75% of the myocardium consists of cardiomyocytes but this translates to only 30-40% of total cell number (Camelliti et al., 2005, Vliegen et al., 1991). Other cells found in the heart under normal conditions include fibroblasts, endothelial cells and vascular smooth muscle cells. 11HSD1 protein has been detected in cardiomyocytes, fibroblasts and vascular smooth muscle cells but not in endothelial cells (Porter and Turner, 2009, Camelliti et al., 2005). Fibroblasts account for approximately 60% of the total cardiac cell number and are regulators of extracellular matrix production (Porter and Turner, 2009). They lie between muscle layers providing continuity between cells (Porter and Turner, 2009). The significance of reduced glucocorticoid activity in cardiac fibroblasts of 11HSD1$^{-/-}$ mice is yet to be determined. The relative abundance of fibroblasts in the myocardium, their secretion of a diverse array of cytokines and growth factors and their proximity to cardiomyocytes suggests that modulating fibroblast

function may be important to recovery after MI (Porter and Turner, 2009). Glucocorticoids have been shown to reduce fibroblast proliferation, growth and can inhibit secretion of pro-inflammatory proteins (Pratt, 1978, Porter and Turner, 2009, Hardy, 2008). Under basal conditions 11HSD1 deficiency does not alter the extracellular matrix, suggesting it has limited impact on basal fibroblast function.

It may be predicted that lack of 11HSD1 in the vasculature might modulate vascular tone since stimulation of GR in the vascular smooth muscle can increase contractility (Walker et al., 1992, Sudhir et al., 1989) and in endothelial cells can impair vasodilatation (Mangos et al., 2000). However, despite the ability of 11HSD1 to amplify glucocorticoids locally within the vascular smooth muscle, its deficiency has no effect on vessel function or blood pressure (Kotelevtsev et al., 1997, Hadoke et al., 2001).

Cardiac function

The results of histological analysis of the C57Bl6 and 11HSD1$^{-/-}$ myocardium correspond with the echocardiography data. 11HSD1$^{-/-}$ has no detectable impact on left ventricle dimensions or heart function as assessed by ejection fraction and fractional shortening. As 11HSD1$^{-/-}$ mice have reduced heart weight, with potentially smaller cardiomyocytes it is possible that the individual cardiomyocyte function is altered in these animals. Whilst this was not studied in the work presented here it would be interesting to determine whether the expression of contractile proteins and the response to hypertrophic stimuli were the same in 11HSD1$^{-/-}$ mice and C57Bl6 controls.

Studies in which the expression of GR and MR have been manipulated show their importance physiologically. Conditional cardiac over-expression of GR is associated with bradycardia and atrio-venricular block, whilst 90% of GR knockout mice die at birth due to delays in lung maturation (Cole et al., 1995, Sainte-Marie et al., 2007). On

the other hand, conditional cardiac knock-down of MR induces severe heart disease and premature death (Beggah et al., 2002) whereas conditional cardiac over-expression of MR leads to early sudden death and (in those mice surviving) cardiac arrhythmias (Ouvrard-Pascaud et al., 2005). We have not observed an obvious cardiac phenotype in the 11HSD1$^{-/-}$ mice such as those when the receptors for corticosterone are modulated. However, when 11HSD2, the enzyme that inactivates glucocorticoids, is knocked out mice become hypertensive, develop severe cardiac enlargement and have impaired vascular function independent of renal sodium retention (Deuchar, 2009, Hadoke et al., 2001).

The activation of cardiac MR is likely to be mediated by both aldosterone and corticosterone. Corticosterone circulates in concentrations 100 fold greater than those of aldosterone. This together with the expression of 11HSD1 in fibroblasts, cardiomyocytes and vascular smooth muscles suggests that MR in the heart may be exposed to high concentrations of corticosterone (Esteban et al., 1991, Linde et al., 1981). There is also evidence that the enzymes capable of *de novo* synthesis of corticosterone and aldosterone are present in the myocardium. However, the contribution of this to total tissue levels appears to be small (Kayes-Wandover and White, 2000, Takeda et al., 1994, Silvestre et al., 1999).

Pharmaco-epidemiological data suggests that individuals treated with glucocorticoids may be at increased risk of developing cardiovascular disease (Wei et al., 2004, Walker, 2007b). Moreover, the use of glucocorticoids is associated with the development of heart failure (Souverein et al., 2004). Deficiency of 11HSD1 has proved beneficial in murine models of obesity, diabetes and atherosclerosis (Hermanowski-Vosatka et al., 2005). It has also been shown previously that mice with 11HSD1 deletion have augmented angiogenesis and improved heart function 7 days post MI (Small, 2005, Small et al., 2005). The mechanism for this and the downstream effect of these observations is uncertain. The data presented in the current Chapter have demonstrated that the enhanced angiogenesis and improved heart function observed 7 days after MI in 11HSD1$^{-/-}$ mice is not due to an underlying cardiac phenotype.

4 Characterisation of the response to myocardial infarction in 11HSD1 deficient mice

4.1 Introduction

11HSD1 is expressed in myocardial fibroblasts, in the smooth muscle of the cardiac vasculature and cardiomyocytes (Chapter 3) (Sheppard and Autelitano, 2002, Klusonova et al., 2009). Deficiency of 11HSD1 has no effect on basal cardiac pathology and heart function (Chapter 3). However, 7 days after MI $11HSD1^{-/-}$ mice have enhanced angiogenesis (Small et al., 2005) and improved heart function (Small, 2005). The mechanisms underlying these alterations have yet to be determined. These form the basis of the work described in this Chapter.

Infarct size is an important determinant of outcome following MI (Yang et al., 2002). Therapeutic strategies aimed at reducing infarct size (such as reperfusion) have led to reduction of acute mortality post-MI but patients still develop heart failure (Ferdinandy et al., 2007, Velagaleti et al., 2008). A number of experimental studies have demonstrated that reduction of infarct expansion by enhancing blood supply to the infarct border reduces remodelling and improves heart function post-MI (Engel et al., 2006, Sasaki et al., 2007, Orlic et al., 2001). Improving perfusion can provide vital oxygen and nutrients required for tissue survival. This has been achieved by direct injection of putative cell progenitors or pro-angiogenic factors into the myocardium (Sasaki et al., 2007, Orlic et al., 2001). However, translation of these strategies to the clinic has had limited success to date (Kastrup et al., 2006, Lasala and Minguell, 2009, Meyer et al., 2006). An alternative approach is to manipulate endogenous mechanisms involved in infarct healing so that the associated angiogenic response is enhanced.

Neovascularisation by angiogenesis (the synthesis of new blood vessels from pre-existing vasculature) is a complex series of events that occurs on the infarct border in response to pro-angiogenic signals from adjacent cells in the infarct. The vessels are

usually formed transiently and are pruned after maturation of the infarct scar (Grass et al., 2006, Ren et al., 2002). Glucocorticoids are recognised inhibitors of angiogenesis reducing new blood vessel growth *in vivo* after implantation of sponges beneath the skin, in tumour models and *ex vivo* in aortic ring cultures (Small et al., 2005, Hori et al., 1996, Banciu et al., 2008b). Inhibition of angiogenesis during infarct healing increases the area of necrosis and depresses cardiac function highlighting its importance after MI (Heymans et al., 1999). Since 11HSD1$^{-/-}$ mice exhibit enhanced angiogenesis in response to other stimuli (Small et al., 2005), it was proposed that locally-generated glucocorticoids have an angiostatic influence in the heart following injury. Consequently, inhibition of 11HSD1 may provide a means to improve blood supply, reduce cardiomyocyte loss and improve function post-MI.

Glucocorticoids are released into the systemic circulation acutely after MI (Donald et al., 1994) and initially appear to be cardioprotective, as glucocorticoid receptor (GR) antagonism can increase infarct size (Libby et al., 1973, Morrison et al., 1976, Hafezi-Moghadam et al., 2002). In contrast, when glucocorticoids are given chronically in the healing phase post-MI they are detrimental. Chronic glucocorticoid therapy increases infarct size in experimental and clinical studies (Scheuer and Mifflin, 1997, Roberts, 1976), an effect that may be mediated by glucocorticoid action on the mineralocorticoid receptor (MR). In the EPHESUS clinical trial treatment with epleronone (an MR antagonist) starting 3-14 days after MI reduced the risk of cardiovascular mortality. Similarly, epleronone reduced scar thinning and improved heart function in a rat model of this condition (Pitt et al., 2005, Fraccarollo et al., 2008). The deleterious effects of chronic glucocorticoid administration after MI may be due to their ability to inhibit inflammation (Gilmour et al., 2006, Chapman et al., 2009, Cupps and Fauci, 1982, Galon et al., 2002) and angiogenesis (Small et al., 2005, Small, 2005, McNatt et al., 1999, Hasan et al., 2000, Hori et al., 1996, Folkman and Ingber, 1987), processes that are vital to the healing response.

The post-infarct inflammatory response consists of neutrophil influx into the myocardium which subsequently results in recruitment of monocytes to the area.

Monocytes then differentiate into classically-activated and alternatively-activated macrophages, which enables them to fulfil two vital roles. The first of these, fulfilled by classically-activated macrophages, is to remove cell debris by phagocytosis (Nahrendorf et al., 2007, van Amerongen et al., 2007). Secondly, alternatively-activated macrophages stimulate angiogenesis by secretion of pro-angiogenic factors such as VEGF and IL-8 (Loke et al., 2002, Mosser and Edwards, 2008). Recent work showing that 11HSD1$^{-/-}$ mice have increased macrophage infiltration into sites of inflammation in peritonitis, pleurisy and serum arthritis models has highlighted the anti-inflammatory role of 11HSD1 (Gilmour et al., 2006, Chapman et al., 2009, Coutinho et al., 2009).

Sponge implant and tumour models of angiogenesis have a clear inflammatory component which may contribute to vessel formation. There is recent evidence that angiogenesis in the aortic ring model may also involve inflammation; depletion of adventitial macrophages reduces VEGF expression and vessel sprouting (Gelati et al., 2008). The inextricable link between inflammation and angiogenesis in post-infarct healing is well documented. Selective depletion of macrophages after MI reduces angiogenesis and results in impaired scar formation and heart function (van Amerongen et al., 2007). Scar formation by collagen deposition is another vital component of the healing response and is mediated by the transformation of fibroblasts to myofibroblasts. Reactive oxygen species, hypoxia and transforming growth factor-β (TGF-β) secreted from macrophages all contribute to fibroblast transformation (Cleutjens et al., 1995, Desmouliere et al., 1993, Fadok et al., 1998). Preventing adequate collagen deposition can also impair cardiac function (van Amerongen et al., 2007).

While the effects of manipulating systemic glucocorticoids after MI have been investigated by other groups the effect of reducing local levels is undetermined (Scheuer and Mifflin, 1997, Roberts, 1976, Morrison et al., 1976, Libby et al., 1973, Hafezi-Moghadam et al., 2002). The current study aimed to establish whether the high systemic corticosterone level, immediately and acutely after MI, swamps the contribution of local glucocorticoid regeneration by 11HSD1 and, therefore, lack of 11HSD1 in the early phase does not diminish the protective action of glucocorticoids on reducing ischaemic

damage. Once the systemic hypercorticosteronaemia has settled 11HSD1 is likely to play a role in infarct recovery. It is hypothesised that the mechanism for the post-infarct enhancement of vessel density in 11HSD1$^{-/-}$ mice involves an enhanced inflammatory response post-MI and promotion of associated pro-angiogenic signalling in early infarct healing. Furthermore, it is proposed that enhancement of vessel density leads to an improvement in heart function following MI.

4.2 Methods

4.2.1 Coronary artery ligation

Male C57Bl6 mice (Harlan, UK) and 11HSD1 homozygous null ($^{-/-}$) mice (bred from an in-house colony on a C57Bl6 background) aged 10-12 weeks were used for all experiments. Mice underwent coronary artery ligation for induction of MI with sham-operated mice serving as controls, as described in Section 2.3.1.

4.2.2 Echocardiography

Cardiac function was assessed by echocardiography as described in Section 2.3.2. Mice underwent echocardiography 2, 4 and 7 days after surgery in order to obtain measurements of ventricular dimensions. The observer was blinded for the purpose of echocardiography measurements and all other subsequent analysis of tissue.

4.2.3 Tissue collection

For analysis of circulating corticosterone levels blood was taken 24 hours post-surgery, by tail tip at 7:30am (the diurnal nadir) as described in Section 2.3.3. The mice were then killed cervical dislocation. Mice killed at days 2, 4 and 7 after surgery were given an intraperitoneal injection of 2.5mg BrdU, dissolved in saline, 1 hour prior to cervical dislocation. The heart was excised and washed in ice cold PBS. For infarct size assessment the whole heart was frozen on dry ice prior to storage at -80°C. For other analyses, hearts were bisected down the longitudinal axis (apex to base) and one half fixed in 10% neutral buffered saline as described in Section 2.4. The other half was frozen immediately on dry ice prior to storage at -80°C.

4.2.4 Infarct size measurements

Hearts were stained with triphenyltetrazolium chloride (TTC) in order to determine infarct size, as described in Section 2.4.1.

4.2.5 Circulating corticosterone

A corticosterone radioimmunoassay was conducted on plasma samples to determine circulating levels of corticosterone after myocardial infarction, as described in Section 2.5.1.

4.2.6 Histology

Sections were stained with haematoxylin and eosin to allow identification of neutrophils by their distinctive multi-lobed nuclei, as described in Section 2.4.2. Quantification of the number of neutrophils in the left ventricle was conducted using Image Pro6.2, Stereologer Analyser 6 MediaCybernetics, as described in Section 2.4.6.

4.2.7 Immunohistochemistry

Identification of blood vessels was conducted using a monoclonal rat anti-mouse CD31 primary antibody (BD Bioscience) diluted 1/50 in PBS/1%BSA. Cell proliferation was detected using a monoclonal mouse anti-mouse BrdU antibody (Sigma) diluted 1/1000 in TBS/10% normal goat serum/5%BSA. Macrophages and alternatively-activated macrophages were recognised with a monoclonal rat anti-mouse mac 2 primary antibody (Cedarlane) diluted 1/6000 in PBS/1%BSA and a polyclonal rabbit anti-mouse YM1 primary antibody (Stem Cell Technologies) diluted 1/50 in PBS/1%BSA respectively. T

and B cells were identified with a polyclonal rabbit anti-human CD3 primary antibody (Dako) diluted 1/400 in PBS/1%BSA and a monoclonal rat ant-mouse CD45R primary antibody (BD Bioscience) diluted 1/50 in PBS/1%BSA, respectively. Identification of activated myofibroblasts was conducted using a monoclonal mouse anti-mouse α smooth muscle actin (αSMA) primary antibody (Sigma) diluted 1/400 in PBS/1%BSA. 11HSD1 was detected using an in-house polyclonal sheep anti-mouse 11HSD1 antibody diluted 1/2000 in PBS/5%BSA. For details of the procedures please see to Section 2.5. Quantification of immunohistochemistry was conducted using Image Pro 6.2, Stereologer Anaylser 6 MediaCybernetics. See Section 2.5.10 for details.

4.2.8 Quantitative real time polymerase chain reaction (qRT-PCR)

Heart tissue was homogenised and RNA was extracted by the Trizol method as described in Section 2.5.2. RNA was reverse transcribed into cDNA as described in Section 2.5.3 and subsequent qRT-PCR was conducted as explained in Section 2.5.4.

4.2.9 Statistics

All values are expressed as mean ±SEM. Comparisons of survival and cause of death were by Fisher's exact test and Chi square test respectively. Comparisons of echocardiography, circulating corticosterone, histology and immunohistochemistry for 2, 4 and 7 day data are by 2-way ANOVA with Bonferroni post-hoc tests with comparisons between genotype and surgery. Post-hoc tests were conducted when the ANOVA showed a genotype difference to $P<0.05$. An unpaired Student's t test was used to compare triphenyltetrazolium infarct size. Comparisons of real time qRT-PCR were with Kruskal-Wallis testing. P values <0.05 denote statistical significance.

4.3 Results

Mortality

There was no difference in mortality between C57Bl6 and 11HSD1$^{-/-}$ mice after coronary artery ligation with survival being 76% and 78%, respectively (Table 4.1). No mortality was observed after sham operation. The number of unsuccessful surgeries, due to ligating the coronary artery below its branches thus causing an infarct of variable size was similar in C57Bl6 and 11HSD1$^{-/-}$ mice (Table 4.1). Death occurring during or immediately after surgery was due to too much tissue damage or blood loss (7% in C57Bl6 and 9% in 11HSD1$^{-/-}$). Mortality occurring 4-7 days after MI was due to cardiac rupture (blood in the chest cavity) or heart failure (enlarged heart) as determined by post mortem and was similar in C57Bl6 and 11HSD1$^{-/-}$ mice.

	C57Bl6	11HSD1$^{-/-}$
Survival (%)	76% (63/83)	78% (35/45)
No MI (%)	4% (3/83)	4% (2/45)
Mice used in study	72% (60/83)	73% (33/45)
Cause of death (% of all mice)		
Surgery	7% (6/83)	9% (4/45)
Cardiac rupture	8% (7/83)	7% (3/45)
Heart failure	8% (7/83)	7% (3/45)

Table 4-1 Mortality after myocardial infarction surgery

Survival, proportion of unsuccessful coronary artery ligation surgeries and cause of mortality were similar between C57Bl6 and 11HSD1$^{-/-}$ mice up to 7 days after MI surgery. Raw numbers are in brackets.

The impact of surgery on body and heart weight

Body weight declined 1 day after sham and MI surgery to a similar extent in C57Bl6 and 11HSD1$^{-/-}$ mice (Figure 4.1). Weight recuperation was seen at day 4 and 7 but did not return to pre-operative levels in sham or MI mice. Heart weight was similar in all groups post-surgery with the exception of 11HSD1$^{-/-}$ mice which had significantly heavier hearts than C57Bl6 controls 2 days after MI ($P<0.05$, Table 4.2). However when heart weight was corrected for body weight this relationship was no longer seen.

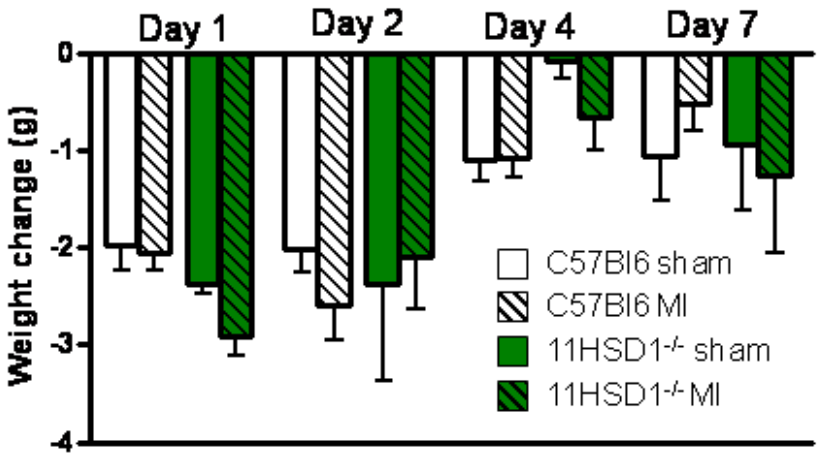

Figure 4-1 Body weight changes after myocardial infarction or sham surgery

Body weight declined immediately after induction of myocardial infarction (MI) or sham operation in C57Bl6 and 11HSD1$^{-/-}$ mice relative to pre-operative weight. Body weight was regained from day 4 in all groups. n=8 C57BL6 sham, n=12 C57BL6 MI, n=4 11HSD1$^{-/-}$ sham, n=6 11HSD1$^{-/-}$ MI. Data are expressed as mean ± SEM.

	Heart weight (g)				Heart weight/body weight (mg/g)			
	C57Bl6		11HSD1 $^{-/-}$		C57Bl6		11HSD1 $^{-/-}$	
	Sham	MI	Sham	MI	Sham	MI	Sham	MI
Day 1	0.19 ±0.02	0.20 ±0.02	0.16 ±0.02	0.19 ±0.01	7.17 ±0.59	7.55 ±0.41	5.99 ±0.41	7.01 ±0.32
Day 2	0.14 ±0.01	0.15 ±0.01	0.16 ±0.01	0.19 ±0.01*	6.00 ±0.12	6.55 ±0.26	6.06 ±0.26	6.99 ±0.47
Day 4	0.14 ±0.01	0.16 ±0.01	0.17 ±0.01	0.16 ±0.01	5.85 ±0.21	6.06 ±0.17	5.73 ±0.44	5.80 ±0.39
Day 7	0.17 ±0.01	0.17 ±0.02	0.16 ±0.01	0.18 ±0.01	5.82 ±0.22	6.29 ±0.41	5.59 ±0.28	6.60 ±0.67

Table 4-2 Raw heart weights and heart weight relative to body weight in C57Bl6 and 11HSD1$^{-/-}$ mice

MI did not alter raw heart weights or the heart weight: body weight ratio. n=8 C57BL6 sham, n=12 C57BL6 MI, n=4 11HSD1$^{-/-}$ sham, n=6 11HSD1$^{-/-}$ MI. Data are expressed as mean ± SEM. * P<0.05 C57Bl6 vs. 11HSD1$^{-/-}$ by 2 way ANOVA.

Circulating corticosterone

Plasma corticosterone levels in C57Bl6 mice were similar 1 day after sham or MI operation (Figure 4.2). Whilst MI significantly elevated circulating corticosterone in 11HSD1$^{-/-}$ mice relative to sham ($P<0.05$) there was no difference between C57Bl6 and 11HSD1$^{-/-}$ mice.

Infarct size

Infarct size was assessed from TTC stained hearts. Hearts taken from sham operated mice were completely stained red indicating no ischaemic cell death. At day 1 the extent of left ventricular damage was comparable in C57Bl6 and 11HSD1$^{-/-}$ mice (35.1 ± 1.0 vs. 37.8 ± 2.4 % of left ventricle, n=6 Figure 4.3).

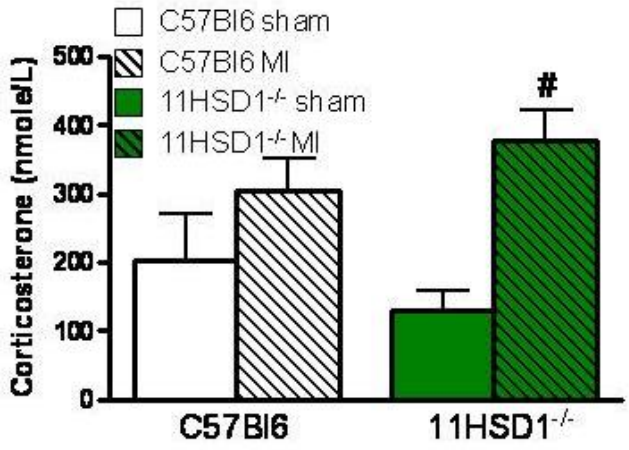

Figure 4-2 Circulating corticosterone after MI or sham surgery

Circulating corticosterone levels 1 day after surgery, measured using a corticosterone radioimmunoassay. Genotype had no influence on circulating corticosterone levels after sham or MI surgery. n=8 C57BL6 sham, n=12 C57BL6 MI, n=4 11HSD1$^{-/-}$ sham, n=6 11HSD1$^{-/-}$ MI. Data are expressed as mean ± SEM. # P<0.05 sham vs. MI by 2 way ANOVA.

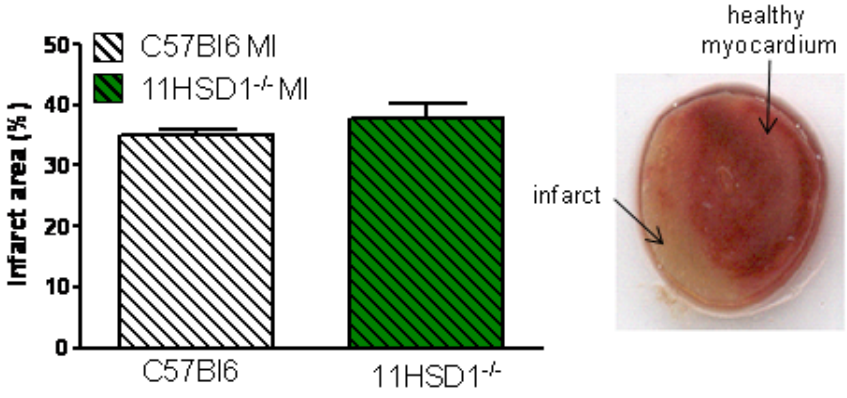

Figure 4-3 Infarct size after MI

Infarct size, assessed by TTC staining (expressed as a percent of the left ventricle) was the same in C57Bl6 and 11HSD1$^{-/-}$ mice 1 day after coronary artery ligation surgery (n=6). Data are expressed as mean ± SEM.

Post infarct neovascularisation

The number of CD31 positive blood vessels (<200µm in diameter) in the left ventricle remained stable in sham and MI animals up to 4 days after surgery (Figure 4.4). At day 7 after MI there was a significant increase in the number of CD31 positive vessels in C57Bl6 and 11HSD1$^{-/-}$ mice relative to sham operated controls ($P<0.001$). These vessels were pericyte poor (Figure 4.5). The number of vessels was significantly greater in 11HSD1$^{-/-}$ mice at this time ($P<0.05$). It was notable that some vessels did not stain with CD31. These were distributed evenly across the myocardium and there was a similar number in all groups (Figure 4.4). Expression of the pro-angiogenic cytokine IL-8 was significantly greater in the myocardium of 11HSD1$^{-/-}$ mice compared with C57Bl6 controls at day 7 (Figure 4.6, $P<0.01$). However, expression of VEGFa mRNA was not different between C57BL6 and 11HSD1$^{-/-}$ mice (Table 4.4).

Cell proliferation, assessed by BrdU incorporation into replicating nuclei, was increased after MI in C57Bl6 and 11HSD1$^{-/-}$ mice relative to sham-operated controls (Figures 4.4 and 4.5). Positive cell staining was distributed across the left ventricle with the highest density of proliferating cells being seen on the infarct border. Coinciding with the increase in vessel density, cell proliferation was greater in 11HSD1$^{-/-}$ mice than in C57Bl6 mice ($P<0.01$). At 4 and 7 days post MI there was some non-vessel CD31 positive cell staining on the infarct border. Attempts to co-localize BrdU with CD31, to determine whether the endothelial cells were proliferating cells were unsuccessful. Double staining sections with BrdU and the macrophage marker, mac 2, showed that these markers were not expressed together demonstrating that the cells proliferating are not macrophages (Figure 4.5).

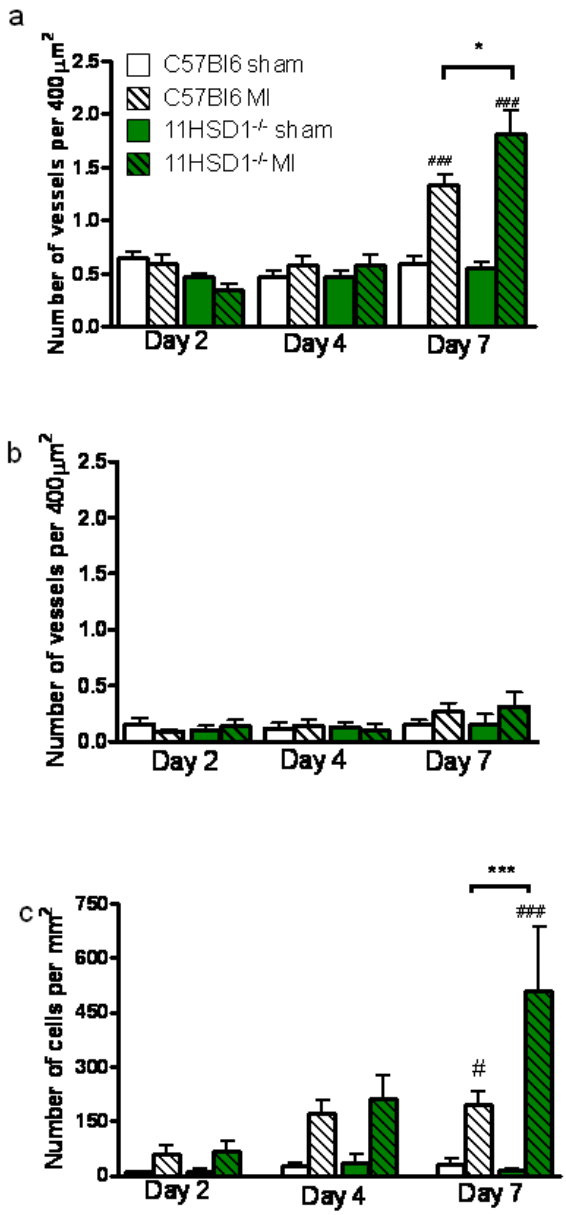

Figure 4-4 Angiogenesis after MI or sham surgery

Vessel density was assessed by immunohistochemistry for the endothelial cell marker, CD31, and quantified by counting small (<200µm diameter), CD31 positive vessels in the left ventricle (n=4-12). Vessel density increases 7 days after MI compared with sham operated mice (a). Furthermore 11HSD1$^{-/-}$ mice have enhanced vessel density relative to C57Bl6 mice at this time. The number of CD31 negative vessels was similar across the groups (b). Cell proliferation, assessed by BrdU incorporation into replicating nuclei, was increased after MI at day 7 in 11HSD1$^{-/-}$ mice compared to C57Bl6 controls (c). n=8 C57BL6 sham, n=12 C57BL6 MI, n=4

11HSD1$^{-/-}$ sham, n=6 11HSD1$^{-/-}$ MI. Data are expressed as mean ± SEM. #P<0.05 ### P<0.001 Sham vs. MI, * P<0.05, *** P<0.001 C57Bl6 vs. 11HSD1$^{-/-}$ by 2 way ANOVA.

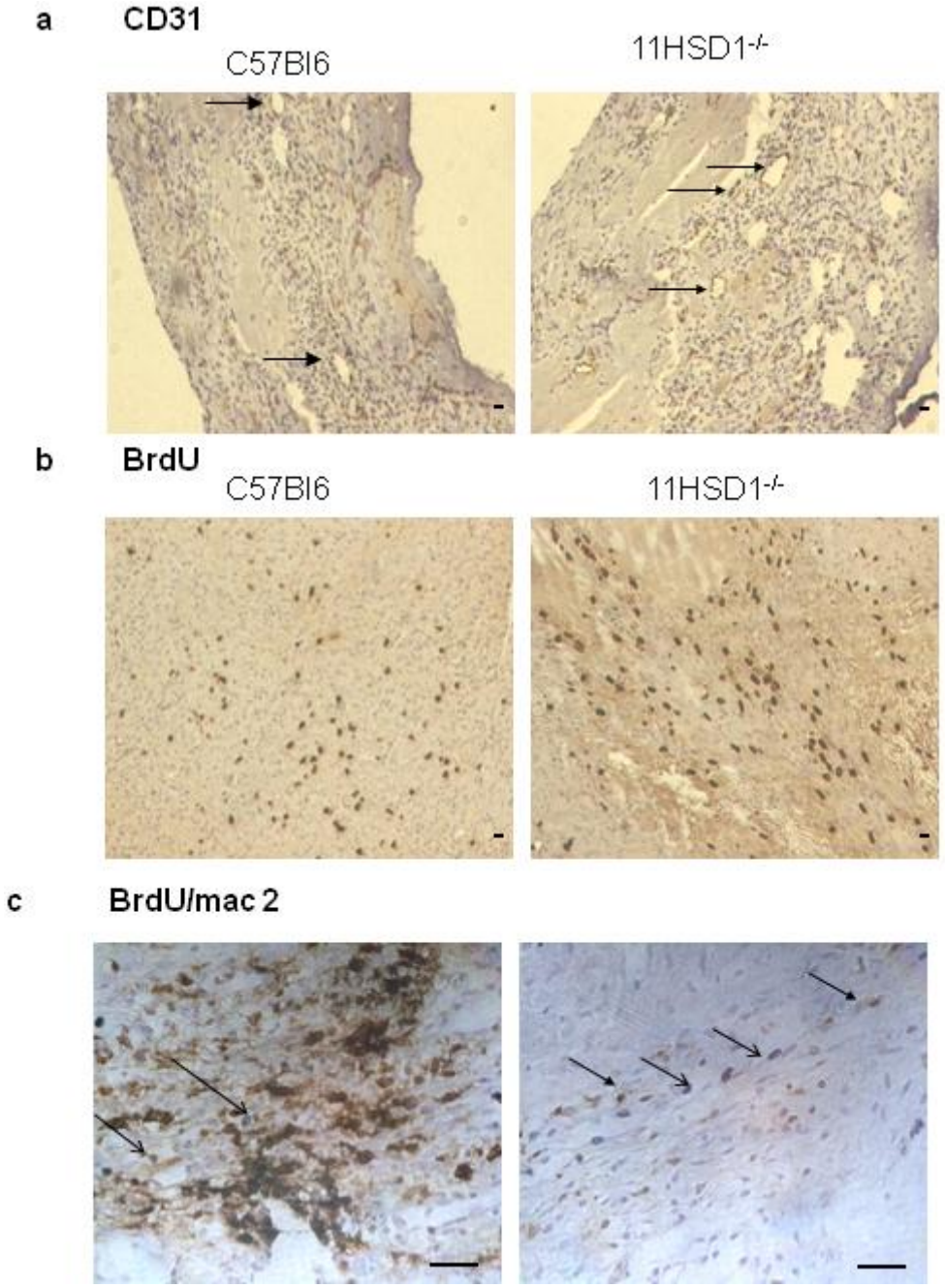

Figure 4-5 Immunohistological analysis of cardiac neovascularisation

Arrows point to CD31 positive vessels in the infarct border (a). BrdU positive nuclei stained brown 7 days post MI (b). Sections were counterstained with haematoxylin. Colocalisation of

BrdU (blue/grey, open arrows) with mac 2 (brown, closed arrows) positive cells in the infarct border (c). Bars are 10µm.

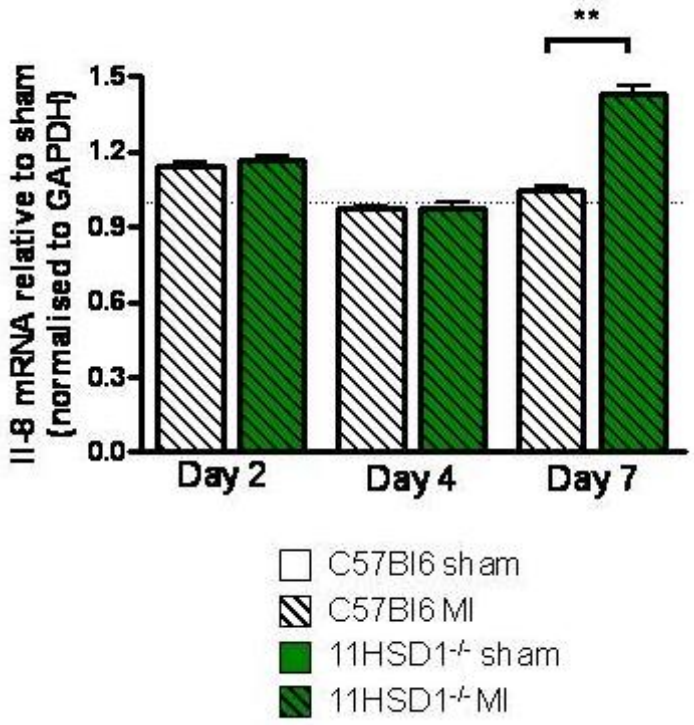

Figure 4-6 Interleukin-8 mRNA after MI or sham surgery

Interleukin-8 (IL-8) mRNA expression (relative to sham-operated) and normalised to GAPDH housekeeping gene (n=6). IL-8 was increased in the 11HSD1$^{-/-}$ mice relative to C57Bl6 controls at day 7. Data are expressed at mean ± SEM ** P<0.01 C57Bl6 vs. 11HSD1$^{-/-}$ by Kruskal-Wallis.

Neutrophil infiltration

Neutrophils were identified in the infarct and on the infarct border in haematoxylin and eosin stained sections (Figure 4.7). In sham-operated mice the number of neutrophils in the left ventricle was very low and remained the same over 7 days (Figure 4.8). In C57Bl6 mice 2 days after MI there was a significant increase in neutrophils in the heart compared with sham-operated controls ($P<0.01$). At days 4 and 7 the neutrophil count declined to similar numbers as the shams. $11HSD1^{-/-}$ mice had significantly greater neutrophil influx 2 days after MI compared with C57Bl6 mice ($P<0.01$). Numbers declined to sham levels 4 days post-MI. Expression of the neutrophil chemoattractants, IL-6 and IL-8, did not differ between the groups at 2 days (Figures 4.6 and 4.8).

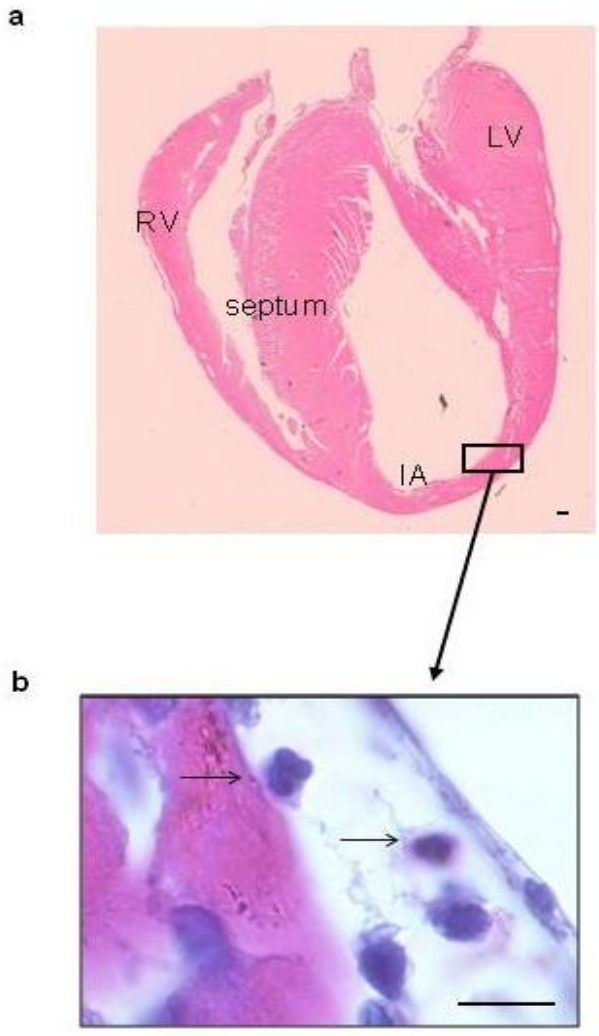

Figure 4-7 Identification of neutrophils in haematoxylin and eosin stained sections

Neutrophils were identified by their distinctive multi-lobed nuclei in haematoxylin and eosin (H&E) stained sections. Tiled H&E stained section (a). LV= left ventricle, RV= right ventricle, IA= infarct area. High power view of neutrophils in the left ventricle (black arrows) (b). Bar is 10µm.

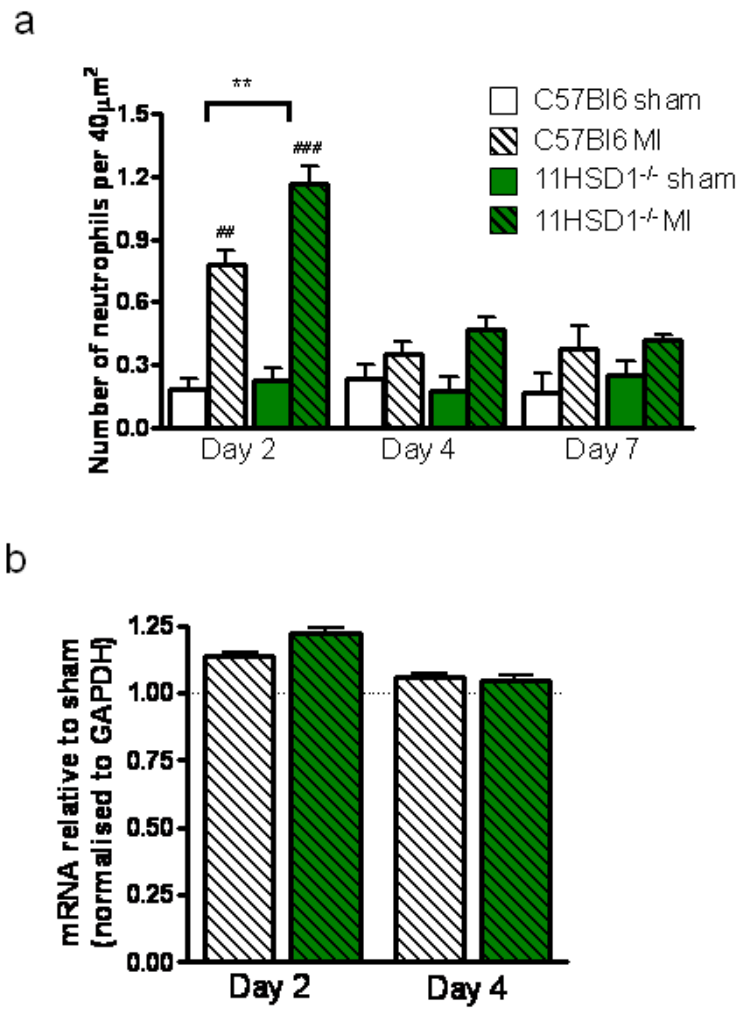

Figure 4-8 Neutrophil influx after MI or sham surgery

Neutrophils in the left ventricle were counted in haematoxylin and eosin stained sections and expressed as number per 40µm^2 (a). Neutrophil numbers were increased after MI compared with sham-operated mice and this increase was greater in 11HSD1$^{-/-}$ mice. Interleukin-6 (IL-6) mRNA expression relative to sham and normalised to GAPDH housekeeping gene was not different between the groups (b). n=8 C57BL6 sham, n=12 C57BL6 MI, n=4 11HSD1$^{-/-}$ sham, n=6 11HSD1$^{-/-}$ MI. For RT-PCR n=6 per group. Data are expressed as mean ± SEM. ## P<0.01, ###P<0.001 sham vs. MI **P<0.01 C57Bl6 vs. 11HSD1$^{-/-}$ by 2 way ANOVA.

Macrophage infiltration

Macrophage infiltration, shown by mac 2 immunoreactivity, was seen predominantly in the infarct and border zone (Figure 4.9). Staining was low in all sham operated groups. Mac 2 positive cells were detected 2 days after MI with significant increases in staining observed 4 and 7 days post-MI relative to sham in both strains of mice ($P<0.001$, Figure 4.10). At 7 days after infarction macrophage staining was significantly augmented in $11HSD1^{-/-}$ mice compared with C57Bl6 controls ($P<0.001$). Myocardial expression of monocyte chemoattractant protein-1 (MCP-1) mRNA, a chemokine involved in macrophage recruitment, was elevated 7 days after MI in the hearts of $11HSD1^{-/-}$ mice versus C57Bl6 mice ($P<0.01$, Figure 4.10).

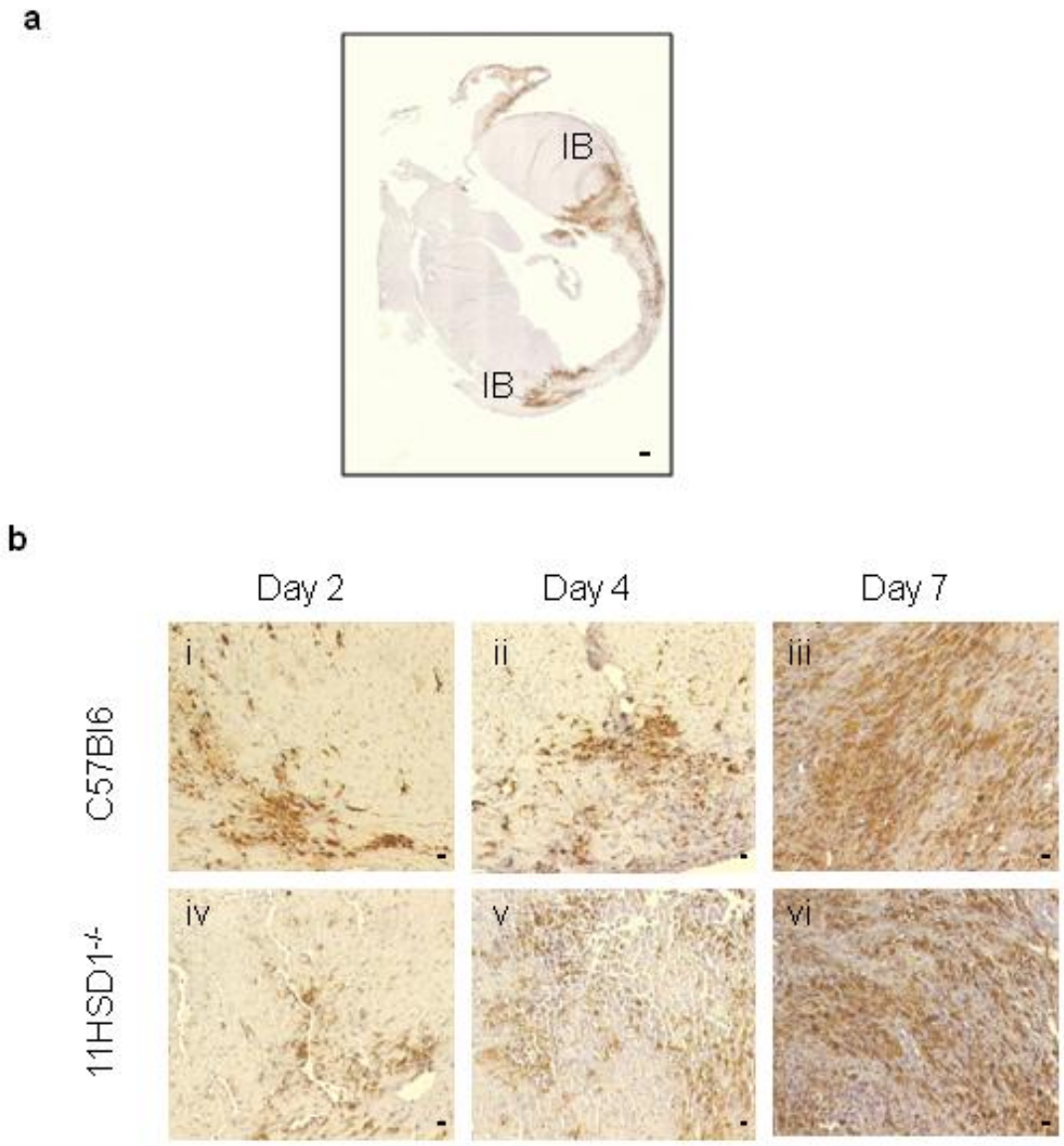

Figure 4-9 Identification of macrophages in heart sections

Tiled section of a heart that has been immunolabelled with anti-mac 2 antibody to identify macrophages (brown) in the infarct border (IB) and counter-stained with haematoxylin (a). Pictures of mac 2 immunohistochemistry in the infarct border in C57Bl6 and 11HSD1$^{-/-}$ mice 2, 4 and 7 days after MI (b). Bar is 10µm.

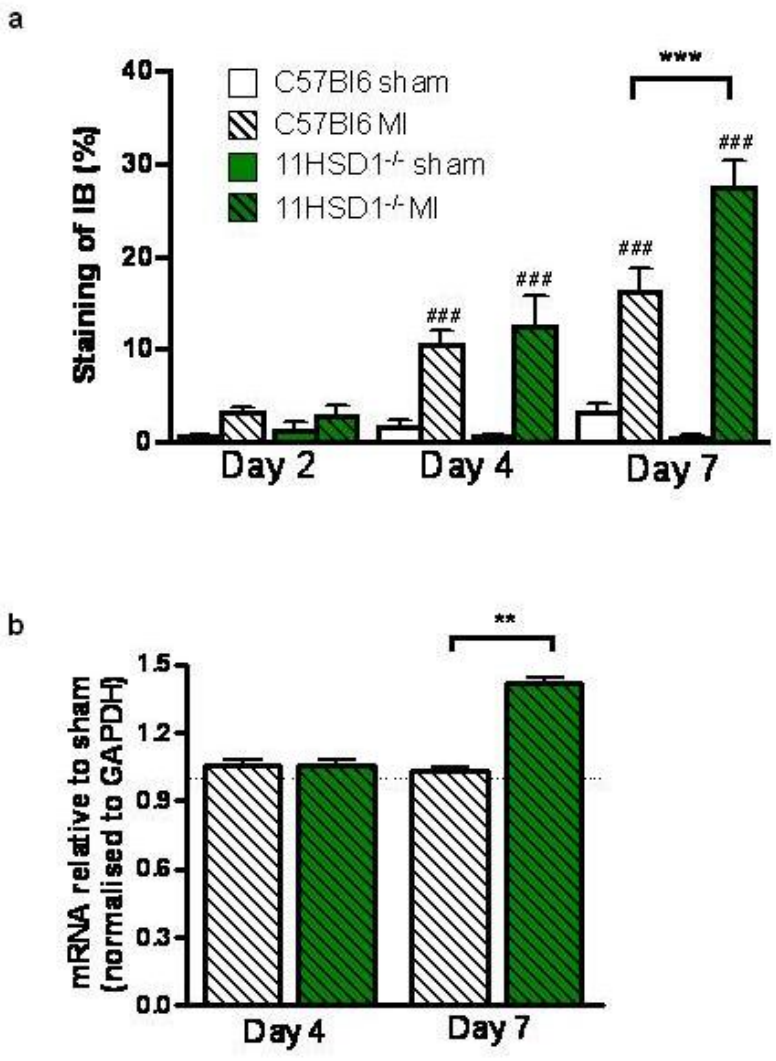

Figure 4-10 Macrophage infiltration after MI or sham surgery

Macrophage infiltration shown by mac 2 immunoreactivity was quantified as percent of the infarct border (IB) stained (a). Mac 2 immunoreactivity increased over the week post-MI with there being significantly more mac 2 positive cells in the infarct border of 11HSD1$^{-/-}$ mice compared with C57Bl6 controls at day 7. b) Monocyte chemoattractant protein-1 (MCP-1) mRNA expression relative to sham and normalised to GAPDH housekeeping gene. MCP-1 was increased in the 11HSD1$^{-/-}$ mice relative to sham at day 7. n=8 C57BL6 sham, n=12 C57BL6 MI, n=4 11HSD1$^{-/-}$ sham, n=6 11HSD1$^{-/-}$ MI. For RT-PCR n=6 per group. Data are expressed at mean ± SEM. ### P<0.001 sham vs. MI, **P<0.01, *** P<0.001 C57Bl6 vs. 11HSD1$^{-/-}$ by 2 way ANOVA and Kruskal-Wallis.

Alternatively-activated macrophages

The number of cells immunopositive for the alternatively activated macrophage marker, YM1, was elevated 4 and 7 days post-MI in both strains of mice, relative to sham-operated controls in which staining was negligible (Figures 4.11 and 4.12). The pattern of staining was similar to that of mac 2 positive cells. $11HSD1^{-/-}$ mice had significantly more YM1 positive macrophages at 4 days after MI compared with C57Bl6 controls ($P<0.05$) with a similar trend at day 7. This relationship remained when expressed relative to the total number of macrophages (Figure 4.12).

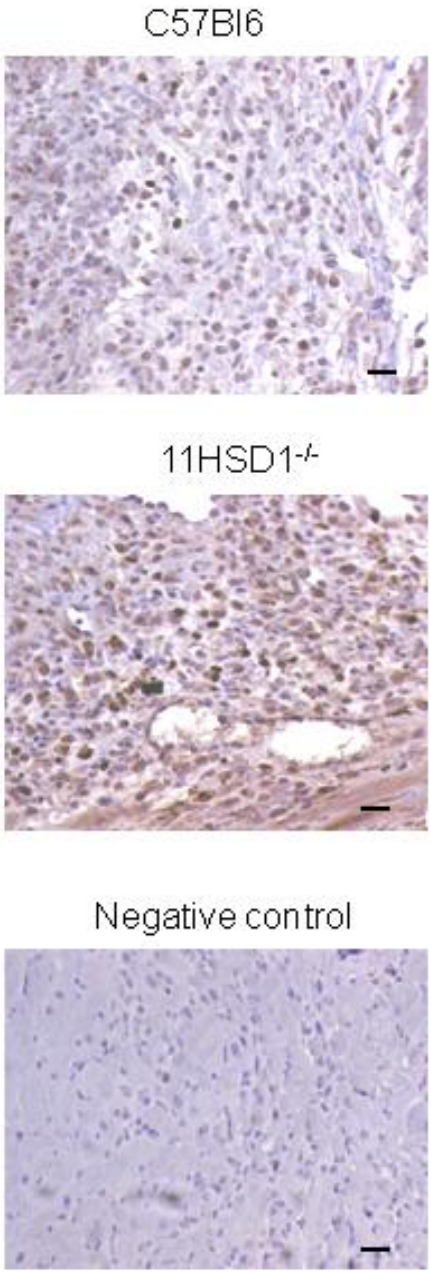

Figure 4-11 Identification of alternatively-activated macrophages by immunohistochemistry

Alternatively activated macrophages were identified by immunohistochemistry for YM1. Sections were counterstained with haematoxylin. Bar is 10µm.

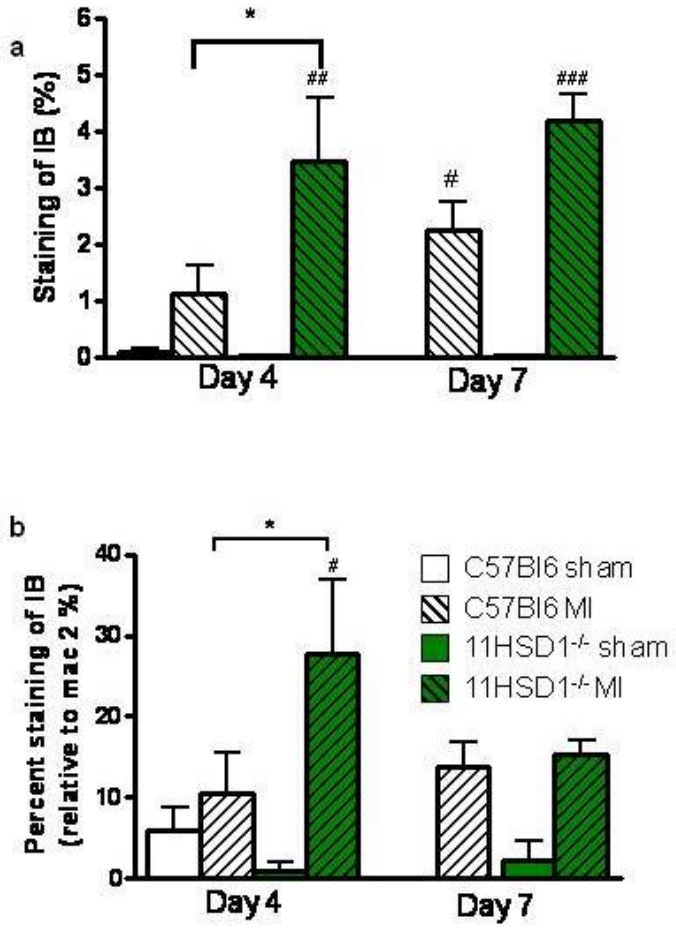

Figure 4-12 Alternatively-activated macrophage infiltration after MI or sham operation

Alternatively-activated macrophage infiltration demonstrated by YM1 immunoreactivity was quantified as percentage of the infarct border (IB) stained (a). YM1 positive cells were also expressed as a percentage of mac2 positive macrophages in the infarct border (b). Immunoreactivity for YM1 was increased 4 and 7 days after MI. Moreover there were more YM1 positive cells in the infarct borders of 11HSD1$^{-/-}$ mice relative to C57Bl6 controls at day 4. n=8 C57BL6 sham, n=12 C57BL6 MI, n=4 11HSD1$^{-/-}$ sham, n=6 11HSD1$^{-/-}$ MI. Data are expressed as mean ± SEM. # P<0.05, ## P<0.01 sham vs. MI, * P<0.05 C57Bl6 vs. 11HSD1$^{-/-}$ by 2 way ANOVA.

Other inflammatory cells post MI

Expression of the T cell marker, CD3, was seen in the infarct and border zone but not in hearts from sham-operated animals (Figure 4.13). The amount of staining was low relative to that of macrophages with maximum staining at day 2. Immunohistochemistry for the B cell marker, CD45R, stained a small number of cells in infarcted hearts only (Figure 4.13). The cells were located diffusely across the left ventricle. There were no observable differences between T and B cell staining in C57Bl6 or 11HSD1$^{-/-}$ mice.

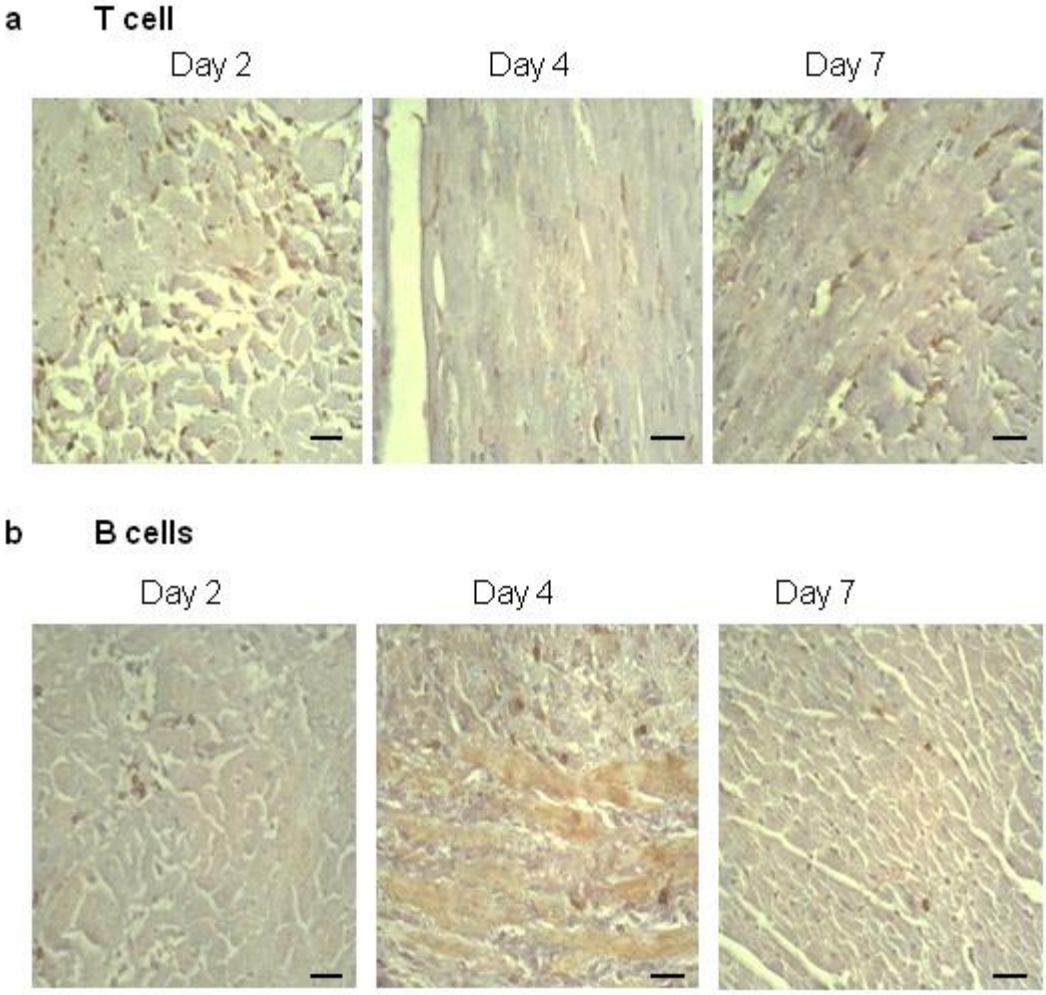

Figure 4-13 Immunohistochemistry for inflammatory cells

(a) Immunohistochemistry with an anti-CD3 antibody showed that T cells infiltrate the myocardium of MI mice only. (b) Immunohistochemistry with an anti-CD45R antibody showed a small number of B cells in the heart after ligation only. Sections were counterstained with haematoxylin. Sections shown here are from C57Bl6 mice. Bar is 10 µm.

Myofibroblast activation

Immunohistochemistry detected α smooth muscle actin (αSMA) secreted from activated myofibroblasts in the infarct and border zone after myocardial infarction (Figure 4.14). It also detects the smooth muscle layer of vessels; however after MI the majority of staining was related to myofibroblasts (identified by its staining pattern). αSMA staining in the left ventricle was increased after MI at day 4 and 7 in C57Bl6 and 11HSD1$^{-/-}$ mice ($P<0.05$). Genotype had no influence on αSMA immunoreactivity.

Expression of GR, MR and 11HSD1 mRNAin the heart

Expression of GR and MR mRNA in the hearts was comparable between C57Bl6 and 11HSD1$^{-/-}$ mice (Table 4.3) with MI having no effect. 11HSD1 mRNA was detected in C57Bl6 mice and infarction did not affect its expression. The CP values for 11HSD1 mRNA in the 11HSD1$^{-/-}$ mice were very high (34.5->35). Therefore it was not possible to accurately assess the amount of 11HSD1 mRNA. However these values do show that levels of the transcript were very low, almost beyond detection.

Expression of 11HSD1 protein

In sham operated mice 11HSD1 immuno-reactivity was restricted to cardiac fibroblasts and the smooth muscle of the cardiac vasculature (please refer to Chapter 3).11HSD1 protein expression after MI was similar to sham-operated controls but was also detected in inflammatory cells at all time-points (Figure 4.15). Upon close inspection, these inflammatory cells were identified as macrophages (Figure 4.15). Due to the quality of staining this was not quantifiable.

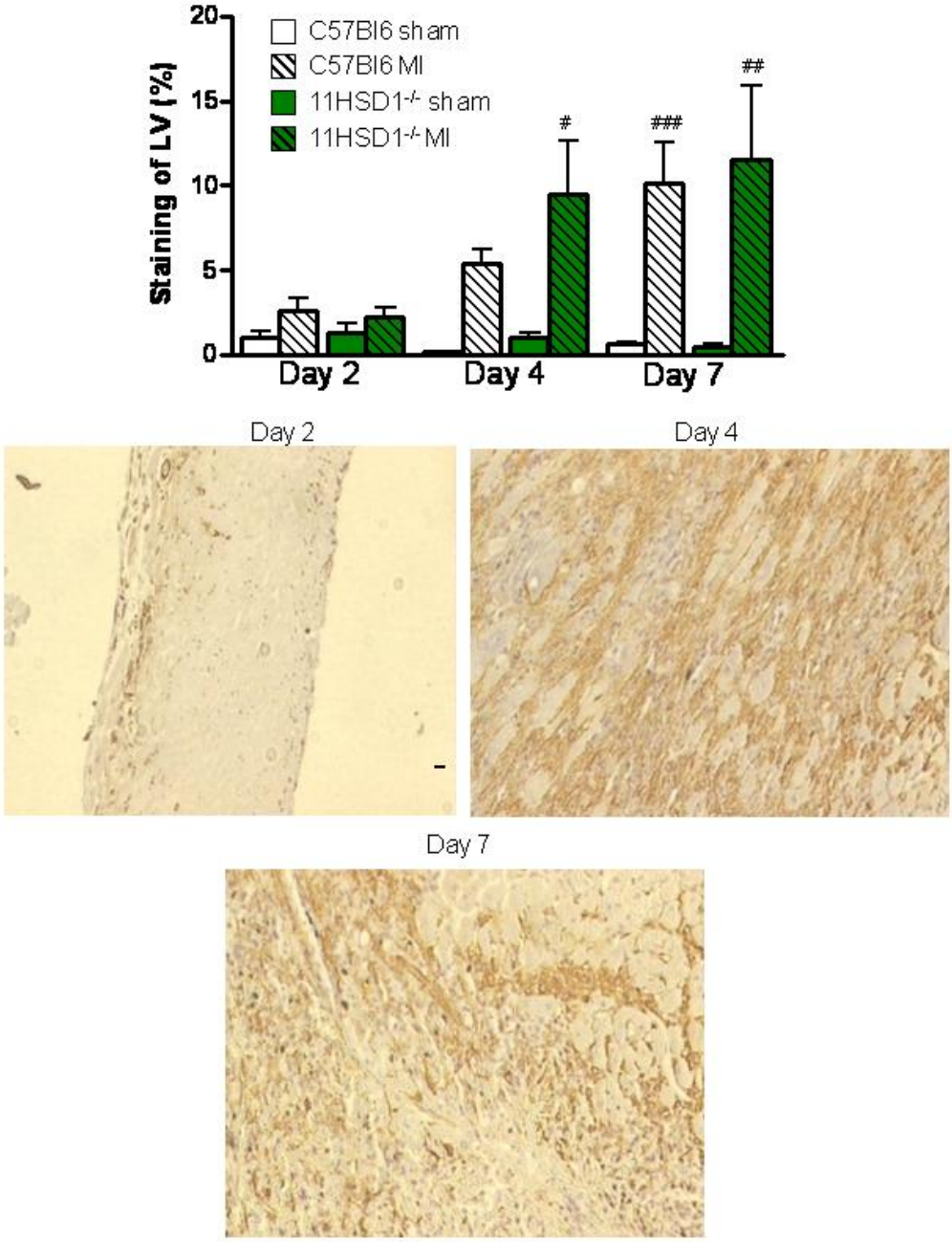

Figure 4-14 Fibroblast activation to myofibroblasts after MI or sham surgery

Activated myofibroblasts were detected using immunohistochemistry for α smooth muscle actin. Positive staining increased after MI over 7 days. Sections were counterstained with haematoxylin. n=8 C57BL6 sham, n=12 C57BL6 MI, n=4 11HSD1$^{-/-}$ sham, n=6 11HSD1$^{-/-}$ MI.

Data are expressed as mean ± SEM. Bar is 10µm. # P<0.05, ##P<0.01, ##P<0.001 sham vs. MI by 2 way ANOVA.

	VEGFa		GR		MR		11HSD1	
	C57Bl6	11HSD1 -/-	C57Bl6	11HSD1 -/-	C57Bl6	11HSD1 -/-	C57Bl6	11HSD1 -/-
Day 2	1.02 ± 0.01	1.02 ± 0.01	1.02 ± 0.01	1.00 ± 0.01	1.00 ± 0.01	0.96 ± 0.01	0.99 ± 0.01	N/D
Day 4	1.00 ± 0.01	1.00 ± 0.02	0.99 ± 0.01	1.01 ± 0.01	1.00 ± 0.01	0.98 ± 0.02	1.00 ± 0.01	N/D
Day 7	1.01 ± 0.02	1.00 ± 0.01	1.00 ± 0.02	1.02 ± 0.01	1.00 ± 0.02	1.01 ± 0.01	0.98 ± 0.01	N/D

Table 4-3 Expression of VEGFa, GR, MR and 11HSD1 mRNAs after MI surgery.

Post-infarct expression of VEGFa, GR, MR and 11HSD1 in the heart relative to sham surgery and normalised to GAPDH (n=6). There were no changes observed across the groups. N/D is not detected. Data are expressed as mean ± SEM.

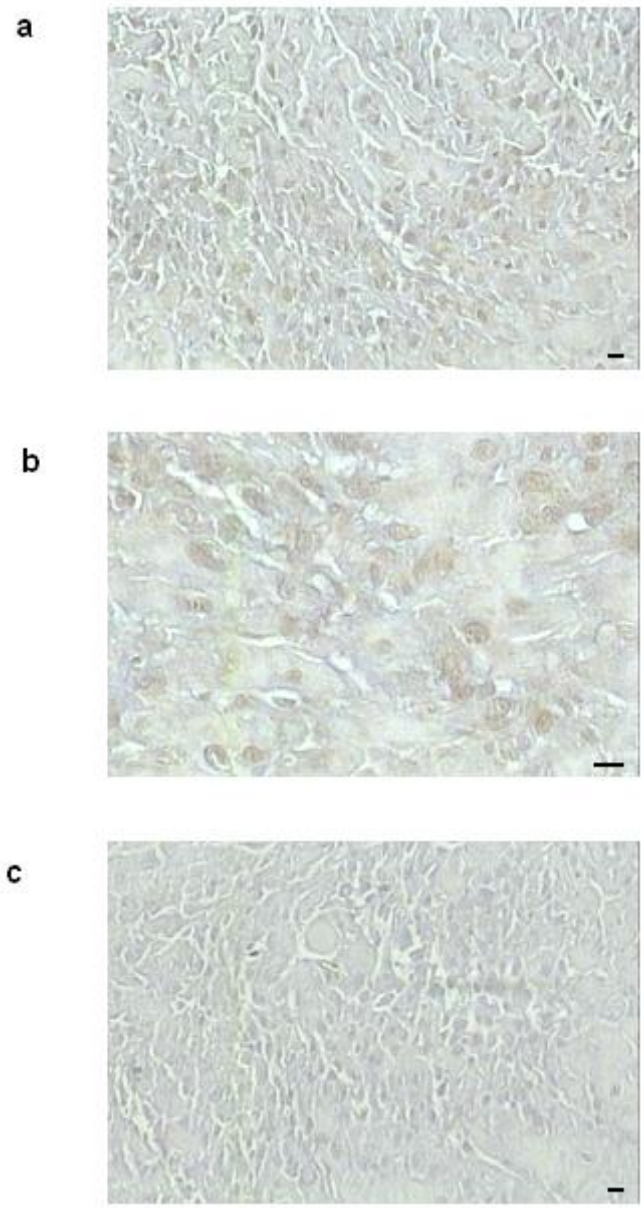

Figure 4-15 Immunohistochemistry for 11HSD1 after MI surgery

11HSD1 immunohistochemistry showed positive cell staining in inflammatory cells (a, b) that upon close inspection resemble macrophages. c) negative control. Sections were counterstained with haematoxylin. Bar is 10µm.

Left ventricle dimensions and cardiac function

There were no differences in left ventricle end diastolic area (LVEDA) at any time point between all groups suggesting that up to a week post-MI there has been no ventricular dilation (Table 4.4). Left ventricle end systolic area (LVESA) was significantly increased in C57Bl6 mice 4 and 7 days after MI compared to sham-operated controls suggesting systolic dysfunction and at day 2 and 4 in the $11HSD1^{-/-}$ mice. There were no differences in left ventricle end diastolic diameter (LVEDD) and end systolic diameter (LVESD) up to 4 days post MI between C57Bl6 and $11HSD1^{-/-}$ mice. At day 7 LVEDD was significantly elevated after MI in the C57Bl6 mice compared with sham but not relative to $11HSD1^{-/-}$ mice. In C57Bl6 mice MI was associated with a reduction in fractional shortening (FS) and ejection fraction (EF) compared with sham, that was evident from 2 days after coronary artery ligation; this did not change significantly up to 7 days post surgery (Table 4.4 and Figure 4.16). In $11HSD1^{-/-}$ mice FS and EF were reduced from 2 days after MI to a similar extent as C57Bl6 mice. However from 7 days post MI there was a trend for improved FS whilst EF was significantly enhanced in $11HSD1^{-/-}$ compared with control mice ($P<0.05$).

	Day 2				Day 4				Day 7			
	C57Bl6		11HSD1$^{-/-}$		C57Bl6		11HSD1$^{-/-}$		C57Bl6		11HSD1$^{-/-}$	
	Sham	**MI**	**Sham**	**MI**	**Sham**	**MI**	**Sham**	**MI**	**Sham**	**MI**	**Sham**	**MI**
LVEDA	15.6 ±1.7	13.5 ±1.3	10.7 ±1.7	13.1 ±2.7	12.9 ±1.1	13.2 ±1.4	16.0 ±4.2	13.0 ±1.9	14.3 ±1.5	16.4 ±2.4	12.7 ±1.5	11.4 ±0.9
LVESA	5.9 ±1.0	9.7 ±0.9	2.3 ±0.4	8.7 ±1.9 #	3.9 ±0.5	9.4 ±1.0 #	4.7 ±1.1	8.8 ±1.1#	5.1 ±0.7	12.1 ±2.1 #	4.3 ±0.7	6.8 ±0.5
LVEDD	3.6 ±0.1	3.6 ±0.2	3.3 ±0.1	3.6 ±0.4	3.7 ±0.2	3.6 ±0.2	3.9 ±0.6	3.7 ±0.2	3.5 ±0.2	4.1 ±0.2 #	3.7 ±0.2	3.8 ±0.2
LVESD	2.1 ±0.2	2.7 ±0.2	1.9 ±0.1	2.9 ±0.4	2.3 ±0.1	2.8 ±0.2	2.4 ±0.5	2.8 ±0.2	2.2 ±0.1	3.2 ±0.2	2.3 ±0.2	2.9 ±0.1
PWD	0.9 ±0.1	0.9 ±0.1	0.9 ±0.2	0.8 ±0.1	0.9 ±0.1	0.9 ±0.1	1.2 ±0.2	1.0 ±0.1	1.0 ±0.1	1.0 ±0.1	1.0 ±0.1	0.9 ±0.1
PWS	1.2 ±0.1	1.1 ±0.1	1.1 ±0.2	1.1 ±0.2	1.2 ±0.1	1.2 ±0.1	1.6 ±0.2	1.3 ±0.1	1.3 ±0.1	1.2 ±0.1	1.2 ±0.1	1.2 ±0.1
EF (%)	63.1 ±2.8	27.8 ±2.4 ###	78.8 ±1.5	32.9 ±3.5 ###	69.6 ±2.5	28.7 ±1.6 ###	67.0 ±5.0	31.8 ±1.6###	63.6 ±4.5	29.1 ±2.7###	65.4 ±4.0	40.1 ±1.6##*
FS (%)	40.5 ±4.6	25.5 ±2.0###	42.5 ±3.0	21.9 ±1.7###	38.7 ±2.1	22.7 ±2.9###	41.2 ±3.8	25.1 ±3.9 ##	35.7 ±2.5	21.6 ±2.0###	37.4 ±2.5	25.2 ±2.6 #

Table 4-4 Left ventricle dimensions after MI or sham surgery

There were no differences in left ventricle (LV) end diastolic area (EDA), end systolic diameter (ESD), posterior wall thickness at diastole (PWD) or posterior wall at systole (PWS) between the groups at any time point. A decline in LV end systolic area (ESA) was seen after MI

suggesting systolic dysfunction. LV end diastolic diameter (EDD) was significantly increased 7 days post-MI in C57Bl6 mice compared with shams. Ejection fraction (EF%) was significantly decreased at all time points after MI. 11HSD1$^{-/-}$ mice had significantly improved heart function 7 days post MI relative to C57Bl6 controls. Fractional shortening (FS%) was decreased after MI at all time points. n=8 C57BL6 sham, n=12 C57BL6 MI, n=4 11HSD1$^{-/-}$ sham, n=6 11HSD1$^{-/-}$ MI. Data are expressed as mean ± SEM> # P<0.05, ## P<0.01, ###P<0.001 sham vs. MI, * P<0.05 C57Bl6 vs. 11HSD1$^{-/-}$ by 2 way ANOVA.

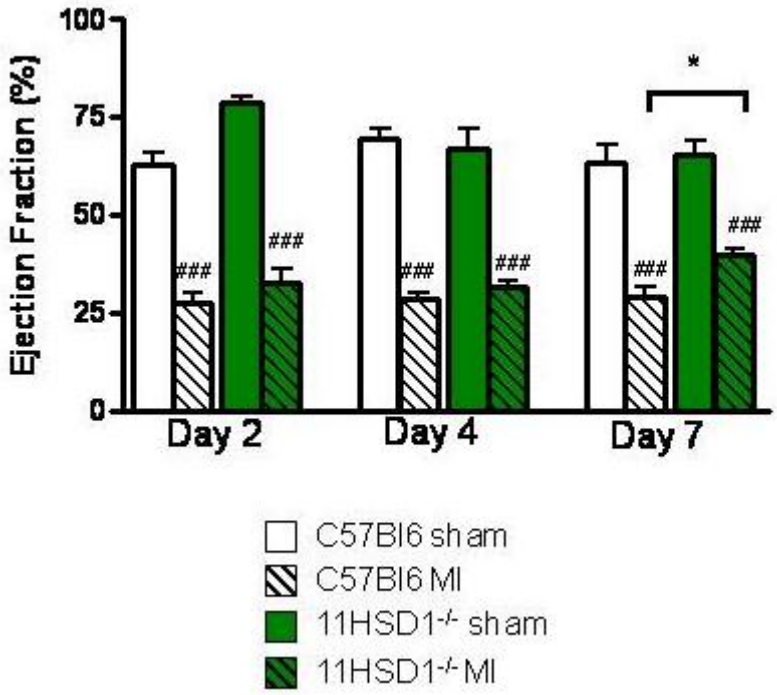

Figure 4-16 Left ventricle ejection fraction after sham or MI surgery

Left ventricle function was expressed as ejection fraction using the equation (left ventricle end diastolic area- left ventricle end systolic area)/ left ventricle end diastolic area x 100. Ejection fraction declined after MI. 11HSD1$^{-/-}$ mice showed improved heart function 7 days after MI compared with C57Bl6. n=8 C57BL6 sham, n=12 C57BL6 MI, n=4 11HSD1$^{-/-}$ sham, n=6 11HSD1$^{-/-}$ MI. Data are expressed as mean ± SEM. ## P<0.01, ###P<0.001 sham vs. MI, * P<0.05 C57Bl6 vs. 11HSD1$^{-/-}$ by 2 way ANOVA.

4.4 Discussion

The aim of the current study was to determine whether the high circulating corticosterone immediately after MI is sufficient to protect the heart from initial ischaemic damage in 11HSD1$^{-/-}$ mice. Furthermore, it addressed the mechanism of the previously reported enhancement of angiogenesis in these animals (Small et al., 2005, Small, 2005). The data presented here confirm this previous observation that vessel density is enhanced 7 days after MI in 11HSD1$^{-/-}$ mice compared with C57Bl6 controls. This was associated with increased cell proliferation and augmented tissue IL-8 mRNA levels. Further investigation demonstrated that both the systemic stress-mediated release of corticosterone and the infarct size were comparable in 11HSD1$^{-/-}$ and C57Bl6 control mice and, therefore, are unlikely to account for the changes in vessel density. 11HSD1$^{-/-}$ mice have enhanced neutrophil and macrophage infiltration 2 and 7 days post-MI respectively. Moreover this was associated with an increase in alternatively-activated, reparative macrophage influx. By 7 days after MI, at the time when increased vessel density was clearly evident, there was an improvement in cardiac function in 11HSD1$^{-/-}$ mice. The 11HSD1 protein expression was detected in invading inflammatory cells along with cardiomyocytes, cardiac fibroblasts and vascular smooth muscle cells. The relative contribution of these cells types in mediating this altered healing response in the 11HSD1$^{-/-}$ mice is relatively unknown however.

Recovery from surgery

Previous characterisation has shown that 11HSD1$^{-/-}$ mice have no underlying cardiac phenotype with normal cardiac architecture and function (Kotelevtsev et al., 1997) (please refer to Chapter 3). Mortality rates and cause of death were similar in both strains of mice as was weight gain after surgery, demonstrating that early in infarct healing the mice do not develop a grossly abnormal phenotype. Weight loss was rapid

after surgery and regain of weight began 2 days after surgery as the mice recovered from the stress of the surgery. Evidence from Chapter 3 shows that 11HSD1$^{-/-}$ mice have lower basal heart weight than C57Bl6 controls. However, no such difference was observed after surgery.

Initial ischaemic damage

11HSD1$^{-/-}$ mice on the C57Bl6 background have no alteration in the function of the HPA axis relative to wild type controls (Paterson et al., 2006). In the current study circulating corticosterone levels were comparable between C57Bl6 and 11HSD1$^{-/-}$ mice after MI or sham surgery. Glucocorticoids reduce ischaemic cell death when administered early and acutely after MI. A single dose of methylprednisolone, given 30 minutes or 6 hours after MI, reduced ischaemic damage in a dog model (Libby et al., 1973). Furthermore in a clinical study a single dose of methylprednisolone reduced infarct size and mortality (Libby et al., 1973, Morrison et al., 1976). The protective influence of glucocorticoids may be due to their ability to stabilise lysosymal membranes preventing the release of their damaging digestive enzymes into the cell (Lefer et al., 1980). Alternatively their positive effects may be attributed to their ability to activate endothelial nitric oxide synthase (eNOS) causing vasorelaxation and therefore increased coronary blood flow (Hafezi-Moghadam et al., 2002, Lefer et al., 1980). Although 11HSD1$^{-/-}$ mice are unable to regenerate corticosterone in the heart, infarct size was comparable between strains suggesting that the systemic release of corticosterone is sufficient to protect the heart from initial ischaemic cell death.

Neovascularisation

Angiogenesis, formation of new blood vessels from pre-existing vasculature, is a complex series of events involving cell proliferation, migration, capillary sprouting,

pruning and maturation (Simons, 2005, Ren et al., 2002, Grass et al., 2006). It is stimulated by a number of cytokines including IL-8, VEGF, platelet derived growth factor (PDGF) and fibroblast growth factor (FGF) as a response to hypoxia or inflammation (Xu et al., 2007, Korpisalo et al., 2008, Yau et al., 2005, Payne et al., 2007, Ruixing et al., 2007, Greenberg et al., 2008, Fernandez et al., 2000). The results presented here reproduce the previously reported enhancement in vessel density 7 days post MI in the 11HSD1$^{-/-}$ mice relative to C57Bl6 controls (Small et al., 2005). In the present study this was found to be associated with increased cell proliferation, assessed by BrdU incorporation, and augmented tissue IL-8 mRNA expression. Vessels on the infarct border lacked pericytes at this stage (CD31 positive only), consistent with reports in the literature (Ren et al., 2002, Arras et al., 1998). A limitation of CD31 immunohistochemistry was that in all groups some vessel structures showed no CD31 immunoreactivity to this marker; potentially because expression of the antigen can alter as the cells mature (Ismail et al., 2003). Non-stained vessels were equivalent to a small but consistent proportion to those that stained positive for CD31 at all time points and, as such, was not a confounding variable in the current study. CD31 is a pan-endothelial cell marker and, therefore, it cannot distinguish between old and new vessels. Aminopeptidase N/CD13 is a specific marker of angiogenic vasculature but detection by immunohistochemistry requires gentle tissue fixation (Rangel et al., 2007, Bhagwat et al., 2001). Unfortunately, as the tissue was fixed in formalin, use of this marker was not possible. Alternatively, tagging of cNGR (a peptide sequence that homes to CD13 positive cells) with a fluorophore has demonstrated its localisation to angiogenic sites on the infarct border 4 and 7 days after experimental MI (Buehler et al., 2006). Assessment of CD13 expression in tissue less heavily fixed, assessing endoglin/CD105 expression (another angiogenic endothelial cell marker) (van Laake et al., 2006) or using fluorescently-labelled cNGR should be considered for future studies.

While it has been shown that 11HSD1$^{-/-}$ mice have enhanced vessel density 7 days post-MI the functionality of these vessels is yet to be elucidated. Assessment of perfusion can be made using micro-angiography (Cheng et al., 2007) but resolution is too low for

accurate quantification (Bondke et al., 2007). Laser Doppler is an alternative but this method also has limitations as penetration depth is low (Scholz et al., 2002, Bondke et al., 2007). Perfusion of fluorescently-labelled microspheres, ultrasound contrast microbubbles or microbubbles tagged with endothelial cell specific antibodies are alternatives that could be considered in future studies (Liu et al., 2007, Dickie et al., 2006).

The increase in cell proliferation in 11HSD1$^{-/-}$ mice is in line with a study by El-Helou et al. who show that dexamethasone treatment decreases post-infarct cell proliferation (El-Helou et al., 2008). In order to identify which cells were proliferating double immunohistochemistry (traditional and confocal using fluorescently conjugated secondary antibodies) was attempted with limited success. BrdU and mac 2 were not co-expressed indicating that macrophages were not proliferating. Unfortunately double labelling BrdU with CD31 (endothelial cells) or αSMA (fibroblasts) was unsuccessful. Based on evidence in the literature it is likely that the proliferation mostly involved endothelial cells and cardiac fibroblasts, with possibly a small contribution from cardiomyocytes (Virag and Murry, 2003, Lutgens et al., 1999). Increased proliferation of endothelial cells is consistent with the occurrence of increased angiogenesis, that has been previously shown in 11HSD1$^{-/-}$ mice *in vivo* and *in vitro* (Small et al., 2005).

In the current study 11HSD1$^{-/-}$ mice exhibited enhanced IL-8 expression 7 days after MI compared with C57Bl6 controls. IL-8 is secreted by macrophages and endothelial cells in the healing infarcts, acts as a chemoattractant for bone marrow-derived endothelial progenitor cells and can promote endothelial cell proliferation (Li et al., 2003, Kocher et al., 2006). Blockade of CXCR2, the receptor for IL-8, prevents vessel sprouting in aortic rings highlighting its role in angiogenesis (Gelati et al., 2008). Other factors involved in liberation of bone marrow-derived cells, such as stromal cell-derived factor (SDF)-1α, may be involved in enhancing angiogenesis in 11HSD1$^{-/-}$ mice and warrant further investigation (Sasaki et al., 2007).

VEGF, another pro-angiogenic cytokine, is produced by cardiomyocytes, macrophages and vascular smooth muscle cells. It acts on the VEGF 2 receptor on endothelial cells promoting endothelial cell proliferation, migration and tube formation (Gu et al., 1999, Nahrendorf et al., 2007, Maulik and Thirunavukkarasu, 2008). Exogenous administration and endogenous upregulation of VEGFa following myocardial hypoxia is reported to mobilise endothelial progenitor cells and stimulate angiogenesis resulting in reduced infarct size and improved heart function (Kalka et al., 2000, Kido et al., 2005, Payne et al., 2007, Ruixing et al., 2007, Yau et al., 2005). In the present study no changes in VEGFa levels were observed suggesting that it is not an important contributory factor in this model. Vandervelde et al. found that VEGFa gene expression was unaltered up to 28 days after MI with the exception of at 7 days when it was decreased (Vandervelde et al., 2007). It was hypothesised that this was due to constitutively high VEGFa expression in control hearts and therefore their absolute mRNA quantities may still be high (Vandervelde et al., 2007). VEGF is not the only contributor to adult angiogenesis as alone it stimulates the production of aberrant, disorganised leaky vasculature and must be regulated to optimise its therapeutic potential (Bates and Harper, 2002, Payne et al., 2007). In a rabbit hindlimb model of ischaemia both VEGF and PDGF were required to improve perfusion (Korpisalo et al., 2008). Furthermore PDGF is required for pericyte priming (aiding in vessel maturation, reducing vessel leakage) and can work synergistically with VEGF (Greenberg et al., 2008). Other growth factors were not examined in this study and require further attention.

Upregulation of angiogenic cytokines may be mediated directly through ischaemia. Under hypoxic conditions degradation of hypoxia inducible factor (HIF)-1α is blocked enabling it to translocate to the nucleus where it up-regulates its target genes involved in angiogenesis (Kido et al., 2005, Forsythe et al., 1996). Knockout of HIF-1α impairs development of the vasculature whereas over-expression after MI is associated with reduced infarct size and increased vessel density (Shohet and Garcia, 2007, Kido et al., 2005). Angiogenesis can, therefore, be induced independent of inflammation (van Laake

et al., 2006). Although the weight of evidence points to inflammation as a mechanism for increased vessel density of 11HSD1$^{-/-}$ mice after MI, activation of HIF-1α merits further consideration.

Post infarct inflammation

Ischaemia from coronary artery occlusion evokes a powerful inflammatory response. This is mediated by reactive oxygen species, and activation of toll-like receptors (TLR) and the complement cascade resulting in production of a plethora of cytokines and chemokines (Shishido et al., 2003, Sumitra et al., 2005). Glucocorticoids inhibit the production of a range of inflammatory cytokines including IL-1β, IL-2, IL-3, IL-6, IL-11, TNF-α, interferon (IFN)-α and chemokines such as IL-8, RANTES, MCP-1 and MIP-1α (Barnes, 1998, Cupps and Fauci, 1982, Galon et al., 2002, Park et al., 2009). In parallel, GR activation up-regulates anti-inflammatory mediators such as IL-10, TGF-β and lipocortin-1 and can modulate phagocytosis by macrophages (Galon et al., 2002, Cupps and Fauci, 1982, Barnes, 1998, Gilmour et al., 2006, Park et al., 2009). Leukocytes, macrophages, smooth muscle cells and cardiac fibroblasts express 11HSD1 and the enzyme is upregulated in macrophages after activation (Gilmour et al., 2006, Thieringer et al., 2001, Brereton et al., 2001, Walker et al., 1991). 11HSD1 amplifies glucocorticoids locally and may serve to curtail the inflammatory response. In 11HSD1$^{-/-}$ mice macrophage infiltration into sites of inflammation in peritonitis, pleurisy and serum arthritis models is increased (Gilmour et al., 2006, Chapman et al., 2009, Coutinho 2009). Excessive inflammation after MI can be detrimental and lead to cardiac rupture (Nian et al., 2004) but a certain amount is required for adequate scar formation (van Amerongen et al., 2007).

In the absence of inflammation neutrophils circulate in blood without interacting with the vessel wall (Frangogiannis et al., 2002). From 6 hours after infarction inflammatory mediators such as IL-6, IL-8 and TNF-α are up-regulated in the myocardium and act as potent neutrophil chemoattractants (Vandervelde et al., 2007, Dewald et al., 2004,

Fielding et al., 2008, Coelho et al., 2008, Frangogiannis et al., 2002). Concurrent with the increase in inflammatory cytokines, there is also an increase in anti-inflammatory and anti-angiogenic mediators such as IL-10 and interferon-γ inducible protein (IP)-10 which have roles in preventing immature granulation tissue deposition and angiogenesis (Vandervelde et al., 2007, Yang et al., 2000, Frangogiannis et al., 2001). In this model there was no difference in expression of IL-6 and IL-8 two days after infarction. Previous studies have shown that acute surgical trauma can result in cytokine expression, making detection of local changes difficult to detect until at least 3 days post surgery (Nossuli et al., 2000). Surgical trauma may therefore have interfered with detection of changes in cytokine expression in the current study. In addition cytokine expression was assessed in pieces of heart tissue that contained both the infarct and healthy tissue. It is possible that including the healthy tissue diluted the expression of the cytokines making it less likely to detect changes.

When an inflammatory stimulus is present neutrophils roll slowly along the post capillary venules, before becoming tethered to the endothelium in a process mediated by adhesion molecule expression (Frangogiannis et al., 2002). Local stimuli, such as IL-8, can induce neutrophil metamorphosis prior to translocation into the tissue (Thelen et al., 1988). The results presented here show that neutrophil infiltration peaked early after infarction (day 2) and declined to sham levels by day 4; consistent with the current literature (Dewald et al., 2004). Furthermore the peak of neutrophil infiltration was significantly augmented in $11HSD1^{-/-}$ mice. Mice deficient in glucocorticoids following adrenalectomy have increased expression of the adhesion molecules (L-selectin on neutrophils and ICAM-1 and VCAM-1 on endothelial cells) that have a role in tethering neutrophils to the endothelium (Cavalcanti et al., 2007). Reduced availability of glucocorticoids in the $11HSD1^{-/-}$ mice may provide a similar stimulus for enhanced attraction of neutrophils post-MI. Expression of adhesion molecules early after infarction requires further investigation. Glucocorticoids reduce neutrophil apoptosis *in vitro* suggesting that the increase seen in intact neutrophil numbers in the $11HSD1^{-/-}$ mice is unlikely to be due to delayed apoptosis (Ruiz et al., 2002).

There is conflicting evidence regarding the influence of neutrophils on infarct healing. Neutrophils are an important source of oxidant stress and, therefore, can increase cardiomyocyte death in the infarct; particularly when they enter the heart after reperfusion (Kin et al., 2006, Rossi, 1986, Jordan et al., 1999). Administration of a neutrophil-neutralising antibody to rats just prior to MI reduces apoptosis diminishing the extent of the infarct. Furthermore, in patients high circulating IL-6 and neutrophil counts are associated with increased mortality after MI (Kin et al., 2006, Jaremo and Nilsson, 2008). However, neutrophils also remove necrotic cells and provide a stimulus for monocyte infiltration and angiogenesis, both of which are vital in infarct healing (Frangogiannis et al., 2002, Savill et al., 1989a, Nozawa et al., 2006). Thus selective neutrophil depletion 1 day before and for the 4 days following MI was reported to impair necrotic cell removal in mice 7 days post-MI (Heymans et al., 1999). Timing is likely to be important in the eventual influence of neutrophils. In the present study, increased alternate macrophage activation and angiogenesis is consistent with the beneficial influence of neutrophils in the heart 2 days after infarction. Investigation of IL-4 expression, as the major neutrophil derived mediator of these outcomes (Brandt et al., 2000, Loke et al., 2002), would be worthwhile to establish its potential contribution in 11HSD1$^{-/-}$ mice.

Under basal conditions monocytes patrol the vessel wall and extravasate within an hour in response to the relevant inflammatory stimuli (Auffray et al., 2007). In the myocardial infarct they are recruited by chemokines such as MCP-1, MIP-1α, MIP-1β and MIP-2, with MCP-1 being substantially the most potent (Frangogiannis et al., 2002). Over-expression of MCP-1 is associated with increased macrophage infiltration and a reduction in scar size in a murine model of MI (Morimoto et al., 2006). Once in the infarct monocytes differentiate into macrophages, which can then secrete additional MCP-1 (Morimoto et al., 2006, Kakio et al., 2000, MacKinnon et al., 2008). The results presented here show that, in C57Bl6 and 11HSD1$^{-/-}$ mice, infiltration by mac 2 positive cells increased over the week following MI. Furthermore 11HSD1$^{-/-}$ mice had enhanced

macrophage staining and increased MCP-1 mRNA expression 7 days after MI compared with C57Bl6 mice.

Nahrendorf et al. suggested that there is a particular subset of monocytes involved in infarct healing that are 'alternatively-activated' and pro-angiogenic. These cells are characterised by low expression of ly6C (a monocyte/macrophage and endothelial cell differentiation cell surface antigen) and high expression of CD11c (an integrin expressed on monocytes, macrophages and dendritic cells) (Nahrendorf et al., 2007). Unlike classically-activated macrophages that secrete pro-inflammatory mediators and display phagocytic behaviour, alternatively-activated macrophages secrete anti-inflammatory and pro-angiogenic cytokines such as IL-4 and IL-8 (Loke et al., 2002, Mosser and Edwards, 2008). In the study by Nahrendorf et al. the number of inflammatory $ly6C^{hi}/CD11c^{lo}$ monocytes in the infarcted heart peaked 3 days after MI whilst pro-angiogenic $ly6C^{lo}/CD11c^{hi}$ monocytes peaked 5-7 days post-MI (Nahrendorf et al., 2007). Using a different approach (immunohistochemistry) I found that $11HSD1^{-/-}$ mice have significantly more YM1 immuno-positive, alternatively activated macrophages in the infarct border 4 days post-MI. At day 7 after MI these changes were still evident but no longer significant. This observation suggests that in $11HSD1^{-/-}$ mice alternate macrophage activation may take place at an earlier time point than in wild type mice. Characterisation of hearts 4 and 7 days after MI by flow cytometry may provide more evidence for this. Alternatively-activated macrophages are the likely source of IL-8, expression of which was increased at the time of angiogenesis in the $11HSD1^{-/-}$ mice. These macrophages have also been associated with myofibroblast accumulation and wound healing (Nahrendorf et al., 2007), and thus may have an effect on scar formation (please refer to Chapter 5).

The importance of inflammatory cells in angiogenesis has been demonstrated by several intervention studies. Deficiency of neutrophils in a cancer model prior to the 'angiogenic switch' reduces angiogenesis and tumour growth (Nozawa et al., 2006). Macrophage depletion, achieved by administration of liposome-encapsulated clodronate which is lethal upon phagocytosis, reduces angiogenesis after MI and in aortic ring explants

(Nahrendorf et al., 2007, Fraccarollo et al., 2008, van Amerongen et al., 2007, Gelati et al., 2008). This effect in aortic rings is reversed by replenishment with bone marrow-derived macrophages suggesting that vessel sprouting is strongly influenced by the presence of inflammatory cells (Gelati et al., 2008). Macrophages have been shown to be a vital component of tumour angiogenesis as depletion reduces angiogenic factor production and tumour size to a similar extent to glucocorticoid treatment (Banciu et al., 2008a). Furthermore over-expression of MCP-1 augments capillary density and preserves heart function (Morimoto et al., 2006). The inflammatory response also has a vital role in other infarct healing processes. Scar formation is impaired and cardiac function is depressed when monocytes are depleted (van Amerongen et al., 2007, Fraccarollo et al., 2008, Nahrendorf et al., 2007) . Moreover direct injection of a human activated macrophage suspension into rat hearts immediately after infarction increases vessel density, reduces ventricular dilation and an improves heart function 5 weeks post-MI (Leor et al., 2006). It would be very interesting to investigate whether monocyte depletion by clodronate administration (Fraccarollo et al., 2008, Nahrendorf et al., 2007, van Amerongen et al., 2007) or conditional ablation of CD11b cells mediated by the diphtheria toxin receptor (Duffield et al., 2005) would prevent the enhanced vessel density in the $11HSD1^{-/-}$ mice compared with C57Bl6 controls.

Studies examining renal ischaemia/reperfusion injury suggest that T and B cells might have a vital role in the healing response in the kidney (Burne-Taney et al., 2005). Furthermore, T cells secrete IL-4, a cytokine known to programme macrophages to the alternatively-activated phenotype (Loke et al., 2002). The role of these lymphocytes is relatively unknown after cardiac ischaemia but they are present during the healing phase (Liao and Cheng, 2006). Immunohistochemistry for T cells showed that the peak in infiltration was 2 days post-MI while few cells showed B cell immunoreactivity suggesting that, whilst these cells are part of infarct healing, their role may be limited. Due to the relatively low numbers of cells this avenue of investigation was not pursued.

Myofibroblast activation

Another component in the healing response post-MI involves the differentiation of cardiac fibroblasts to myofibroblasts. Such transformation, stimulated by reactive oxygen species and TGF-β produced by macrophages, leads to the secretion of factors able to modulate the extracellular matrix, mediate inflammation and increases collagen synthesis (Cleutjens et al., 1995, Desmouliere et al., 1993, Fadok et al., 1998, Porter and Turner, 2009). Myofibroblast activation, assessed by immunostaining for the secreted α smooth muscle actin, increased over the week after infarction, peaking at day 7. There was no evidence for a difference in staining between the strains despite 11HSD1$^{-/-}$ mice having increased infiltration of macrophages which can aid in fibroblast activation (Desmouliere et al., 1993, Cleutjens et al., 1995, Fadok et al., 1998). This has important implications when considering the long-term outcome in 11HSD1$^{-/-}$ mice after MI (see Chapter 5). Activation of myofibroblast MR has been implicated to exacerbate fibrosis (Brilla et al., 1993, Lijnen and Petrov, 2000) and, therefore, reduced glucocorticoid generation in 11HSD1$^{-/-}$ mice might prevent this (see Chapter 5).

Expression of steroid-related genes

GR expression has been localised to cardiomyocytes, cardiac fibroblasts, vascular smooth muscle cells and endothelial cells, whilst MR expression has been found in cardiomyocytes, vascular smooth muscle cells and endothelial cells (Sheppard and Autelitano, 2002, Lombes et al., 1995, Walker, 2007b, Yang and Zhang, 2004, Takeda et al., 2007, Ullian, 1999, Hadoke et al., 2006, Christy et al., 2003). Cardiac GR mRNA expression does not change after MI (Silvestre et al., 1999). Expression of MR, in contrast, has been shown to be upregulated 14 and 28 days after infarction respectively (Milik et al., 2007, Takeda et al., 2007). However, Silvestre et al. found no such difference (Takeda et al., 2007, Milik et al., 2007, Silvestre et al., 1999). The results presented here show no change in the expression of mRNA for either receptor at any of the time points post infarction and in either genotype. In the current study activation of GR and MR were not assessed.

11HSD1 is reported to be expressed at a basal level in myocardial fibroblasts, cardiomyocytes and smooth muscle of the cardiac vasculature (please refer to Chapter 3) (Sheppard and Autelitano, 2002, Klusonova et al., 2009). MI had no effect on 11HSD1 mRNA expression at any time point in C57Bl6 mice. This result is consistent with previous work from this laboratory that found no difference in 11HSD1 activity 7 days post-MI, and with reports that activity is not altered in failing human hearts (Slight et al., 1996, Small, 2005). Here we observed immunoreactive 11HSD1 in infiltrating macrophages which may alter their phenotype in the heart. 11HSD2 is also reported to be expressed in the myocardium in fibroblasts (Slight et al., 1993, Slight et al., 1996, Takeda et al., 2007). In the current study 11HSD2 mRNA and protein expression were not investigated due to lack of satisfactory primers for qRT-PCR and antibodies for immunohistochemistry. The limited literature suggests that 11HSD2 mRNA expression increases 14 days post-MI and after chronic intermittent hypoxia but there is no difference in failing human hearts (Takeda et al., 2007, Slight et al., 1996, Klusonova et al., 2009). It is difficult to make definitive conclusions regarding expression of GR, MR and the 11HSD enzymes post-MI due to the lack of data and consistency in the literature.

As mentioned previously glucocorticoids are potent immuno-modulatory hormones. As hypothesised, 11HSD1$^{-/-}$ mice exhibit enhanced inflammation which is in agreement with previous work that showing that these mice have worse inflammation in models of sterile peritonitis and arthritis (Gilmour et al., 2006, Coutinho 2009). Glucocorticoids are also known inhibit angiogenesis *in vitro* and *in vivo* via the glucocorticoid receptor. It has been shown that aldosterone does not affect angiogenesis in human bone marrow derived-endothelial cells (Chen et al., 2004). In aortic ring cultures the decrease in angiogenesis produced by glucocorticoids can be prevented by a glucocorticoid, but not by a mineralocorticoid receptor antagonist (Small et al., 2005). In addition, the GR antagonist, RU38486, reduces angiogenesis 7 days post-MI relative to vehicle treated controls (Small et al., 2005). These studies suggest that enhanced angiogenesis in the 11HSD1$^{-/-}$ mouse is not mediated by reduced glucocorticoid signalling via the MR but

rather via the GR. However, Fraccarollo et al. demonstrate that the MR antagonist epleronone can enhance angiogenesis 7 days after MI (Fraccarollo et al., 2008). It is possible that the angiostatic effect of glucocorticoids may be mediated by activation of both the GR and MR. Many studies that have shown glucocorticoids can inhibit angiogenesis but cannot conclude definitively that this is independent of inflammation.

Cardiac function

It is clear from the literature that enhanced angiogenesis on the infarct border post-MI improves heart function (Engel et al., 2006, Liu et al., 2007, Sasaki et al., 2007, Orlic et al., 2001, Kido et al., 2005, Kocher et al., 2006). Whilst ejection fraction was not different between control and 11HSD1$^{-/-}$ mice early after infarction, by 7 days after MI, at the time when increased vessel density was clear there was an improvement in ejection fraction. Fractional shortening showed the same trend but did not reach significance reflecting the inferior accuracy of the measurement of ventricle diameter. The initial decline in heart function is mediated due to systolic dysfunction as seen here and in previous studies (Shioura et al., 2007). Dysfunction of the myocardium may reflect the loss of viable tissue and altered calcium handling in those cells remaining on the infarct border (Mork et al., 2009, Shioura et al., 2007). Cardiomyocytes isolated from the septum of hearts 7 days post-MI have longer contractions and calcium transients relative to sham and are associated with impaired cardiac function (Mork et al., 2009). It is probable that increasing blood supply to the infarct border will improve cardiomyocyte contractility and prevent infarct expansion by salvage of cardiomyocytes (Liu et al., 2007).

Improving heart function by enhancing angiogenesis is well established within the field and various approaches are being taken to investigate this. Translation of strategies such as direct myocardial injection of putative cell progenitors or angiogenic factors have had limited clinical success to date (Sasaki et al., 2007, Orlic et al., 2001, Kastrup et al., 2006, Lasala and Minguell, 2009, Meyer et al., 2006). An alternative approach is to

manipulate endogenous mechanisms involved in infarct healing so that the associated angiogenic response is enhanced. The results presented here show that 11HSD1$^{-/-}$ mice have enhanced vessel density and improved heart function that is preceded by augmented inflammation and, in particular, by alternatively-activated macrophage infiltration. It is interesting to draw parallels from this study to one by Wagner et al. who found, in a murine model of left pulmonary artery ligation, that dexamethasone treatment reduced inflammation and angiogenesis (Wagner et al., 2008). One must bear in mind that angiogenesis is a dynamic process that involves vessel pruning and maturation and, therefore, the enhancement in vessel density in the 11HSD1$^{-/-}$ mice may not be maintained. Vessel pruning and maturation is complete 4 weeks after MI therefore this is a vital time-point to reassess vessel density (Ren et al., 2002, Grass et al., 2006). Infarct healing is also complete by this time and it is important to know whether these early differences in infarct healing can alter scar formation and cardiac function. These issues are tackled in the next chapter.

5 The effect of 11HSD1 deficiency on longer term infarct healing

5.1 Introduction

Cytokines and growth factors act in concert to regulate the dynamic process of angiogenesis that includes vessel formation, pruning and maturation. The stimulation of post-infarct angiogenesis has been the primary focus of work by many laboratories while the remodelling of such vessels has been relatively overlooked (Small et al., 2005, Kido et al., 2005, Kocher et al., 2006, Engel et al., 2006). 11HSD1 deficiency has been shown to augment angiogenesis in a variety of models, including after MI at 7 days (Chapter 4 (Small et al., 2005, Small, 2005)) however, whether the vessels are retained is yet to be determined and is the subject of this chapter.

During neovascularisation the complex interplay of growth factors leads to the production of highly organised vasculature that can be capable of perfusion (Conway et al., 2001, Greenberg et al., 2008, Korpisalo et al., 2008, Risau, 1997). Stimulation of angiogenesis with exogenous administration of single growth factors, such as VEGF, does increase vessel density but it produces aberrant, disorganised and leaky vasculature (Kocher et al., 2006, Kido et al., 2005, Conway et al., 2001). Factors such as PDGF, Ang-1, the Tie 2 receptor and TGF-β1 stabilise vessels by recruitment of pericytes and by tightening smooth muscle cell interactions during vessel maturation (Conway et al., 2001, Greenberg et al., 2008, Korpisalo et al., 2008, Thurston et al., 1999, Ramsauer et al., 2002). The addition of a pericyte coat to immature vessels is vital in stabilisation as it can inhibit further endothelial cell proliferation and migration (Conway et al., 2001). However, factors involved in vessel regression (such as Ang-2) also play an essential role in angiogenesis; eliminating excess vessels by endothelial cell death and promoting an organised vessel network (Conway et al., 2001, Patan, 2000, Grass et al., 2006, Maisonpierre et al., 1997). Vessel stability increases with pericyte coverage and this prevents superfluous vessel regression. Post-infarct angiogenesis is established 7 days after MI (Chapter 4 and (Small et al., 2005, Grass et al., 2006, Ren et al., 2002)) with

vessel pruning occurring between 7 and 21 days, and full maturation complete 28 days after infarction (Ren et al., 2002, Grass et al., 2006); accompanying this process is the completion of infarct healing and scar formation. It is possible that the increase in vessel density in the 11HSD1$^{-/-}$ mice is transient and not subject to pruning (Jujo et al., 2008, Grass et al., 2006). Sustained enhancement of vessel density is associated with improved cardiac function therefore, establishment of the longevity of these vessels is vital (Liu et al., 2007, Sasaki et al., 2007). Improving perfusion to the infarct border may prevent infarct expansion by salvaging cardiomyocytes, along with improving cardiomyocyte contractility (Maulik and Thirunavukkarasu, 2008, Sasaki et al., 2007, Payne et al., 2007).

Fibrosis is stimulated by the post-infarct inflammatory response, which is enhanced in 11HSD1$^{-/-}$ mice (Chapter 4). Macrophage secretion of transforming growth factor-β (TGF-β) activates myofibroblast production of collagen (Desmouliere et al., 1993, Cleutjens et al., 1995, Fadok et al., 1998). Subsequent collagen production starts from 3-7 days after infarction and increases further by 28 days (Dean et al., 2005, Virag and Murry, 2003). Collagen deposition in the infarct scar is vital for stabilising damaged tissue (van Amerongen et al., 2007). Conversely, increased ventricular stiffness resulting from fibrosis can impair cardiac function (van Heerebeek et al., 2008, Du et al., 2003). There is a fine balance between inadequate and excessive fibrosis (Du et al., 2003, Schellings et al., 2009). 11HSD1$^{-/-}$ mice have enhanced macrophage infiltration 7 days after MI (Chapter 4) suggesting that the subsequent fibrotic response might be enhanced. However, enhanced angiogenesis has been associated with beneficial effects on scar characteristics as it can reduce scar thinning and left ventricle chamber dilation (Engel et al., 2006, Kido et al., 2005, Orlic et al., 2001).

In the current study it is hypothesised that the enhanced vessel density previously reported at 7 days after MI in 11HSD1$^{-/-}$ mice (Chapter 4 (Small et al., 2005)) is retained after healing is complete at 28 days and that this translates into sustained improvement in cardiac function. Furthermore, it is investigated whether the increase in vessel density is associated with modification of scar formation.

5.2 Methods

5.2.1 Coronary artery ligation

Male C57Bl6 mice (Harlan, UK) and 11HSD1 homozygous null ($^{-/-}$) mice aged 10-12 weeks were used for all experiments. Mice underwent coronary artery ligation for induction of MI with sham-operated mice serving as controls, as described in Section 2.3.1.

5.2.2 Echocardiography

Cardiac function was assessed by echocardiography as described in Section 2.3.2. Mice underwent echocardiography 7, 14, 21 and 28 days after surgery in order to obtain serial measurements of ventricular dimensions. The observer was blinded for the purpose of echocardiography measurements and all other subsequent analysis of tissue.

5.2.3 Tissue collection

For analysis of circulating corticosterone levels blood was taken weekly, prior to echocardiography, by tail tip at 7:30am (the diurnal nadir) as described in Section 2.3.3. Mice were killed by cervical dislocation after echocardiography. The hearts were excised, washed in ice-cold PBS, weighed then bisected down the longitudinal axis. It was fixed in 10% neutral buffered formalin for 24 hours for use in histology and immunohistochemistry.

5.2.4 Circulating corticosterone

A corticosterone radioimmunoassay was conducted on plasma samples to determine circulating levels of corticosterone after myocardial infarction, as described in Section 2.5.1.

5.2.5 Immunohistochemistry

Identification of CD31 positive and α smooth muscle actin (αSMA) positive vessels was conducted using a monoclonal rat anti-mouse CD31 primary antibody (BD Bioscience) diluted 1/50 in PBS/1%BSA, and a monoclonal mouse anti-mouse αSMA primary antibody (Sigma) diluted 1/400 in PBS/1%BSA, respectively. For details of the procedure please see Section 2.5.1. Small immuno-positive vessels (<200μm diameter) were counted in the left ventricle using Image Pro 6.2, Stereologer Anaylser 6 MediaCybernetics as described in Section 2.5.2.

5.2.6 Histology

Collagen deposition and assessment of infarct scar characteristics were assessed from heart sections stained with Picrosirius Red and Masson's Trichrome by Susan Harvey (Medical Research Council/ Centre for Inflammation Research Histology Service). Quantative assessment of collagen deposition, scar size, scar thickness and epicardial or endocardial infarct lengths was conducted using Image Pro6.2, Stereologer Analyser 6 MediaCybernetics. Please refer to Sections 2.4.3, 2.4.4 and 2.4.5 for further details.

5.2.7 Statistics

All values are expressed as mean ± SEM. Analysis of mortality and cause of death data were conducted using Fisher's exact test and the Chi squared test. Comparisons of body weight, organ weight, echocardiography and circulating corticosterone are by 2-way ANOVA with Bonferroni post-hoc tests comparing genotype and time. Repeated measures test were used to compare the measurements made at various time points. Unpaired Student's t tests were used to compare histology and immunohistochemistry.

5.3 Results

Mortality and the impact of surgery on body and organ weight

Mortality and its cause after MI were similar to that presented in Chapter 4 (Table 5.1) Survival until the end of the study was 76% and 64% for C57Bl6 and 11HSD1$^{-/-}$ mice respectively (p=NS). C57Bl6 mice started to gain weight relative to their pre-surgery weight from 14 days after induction of MI (Figure 5.1). In contrast 11HSD1$^{-/-}$ mice did not regain the post-operative weight loss for the duration for the 28 day study ($P<0.05$). However, 11HSD1$^{-/-}$ mice were significantly heavier than their C57Bl6 counterparts before the surgery and up to 7 days later despite being the same age ($P<0.05$, Figure 5.1). Heart, lung, liver and kidney weights were similar between C57Bl6 and 11HSD1$^{-/-}$ mice, whether expressed in grams or relative to body weight, at 28 days after MI (Table 5.2). However, spleen weight was significantly lower 28 days post infarction in 11HSD1$^{-/-}$ mice compared with C57Bl6 controls.

	C57Bl6	11HSD1$^{-/-}$
Survival	76.9% (10/13)	64.3% (9/14)
Cause of death (% of all mice)		
Surgery	15.4% (2/13)	14.3% (2/14)
Cardiac rupture	0% (0/13)	7.1% (1/14)
Heart failure	7.7% (1/13)	14.3% (2/14)

Table 5-1 Mortality after myocardial infarction surgery

Survival and cause of death were similar between C57Bl6 and 11HSD1$^{-/-}$ mice up to 28 days after surgery. Raw numbers are in brackets.

	Weight (g)		Weight relative to body weight (mg/g)	
	C57Bl6	11HSD1$^{-/-}$	C57Bl6	11HSD1$^{-/-}$
Heart	0.16 ± 0.01	0.17 ± 0.01	6.10 ± 0.42	5.87 ± 0.22
Lung	0.17 ± 0.01	0.17 ± 0.01	6.22 ± 0.39	5.84 ± 0.27
Kidney	0.34 ± 0.01	0.36± 002	12.54 ± 0.75	12.29 ± 0.54
Liver	1.34 ± 0.08	1.17 ± 0.05	50.28 ± 4.08	40.63 ± 2.20
Spleen	0.12 ± 0.01	0.08 ± 0.01 *	4.63 ± 0.59	2.88 ± 0.30 *

Table 5-2 Organ weights 28 days after MI surgery

Heart, lung, liver, kidney and spleen weights were measured 28 days after surgery and expressed relative to body weight. 11HSD1$^{-/-}$ mice had significantly lighter spleens than C57Bl6 mice at this time point. n= 10 C57BL6 MI, n=9 11HSD1$^{-/-}$ MI. Data are expressed as mean ± SEM. *P<0.05 C57Bl6 vs. 11HSD1$^{-/-}$ unpaired Student's t test.

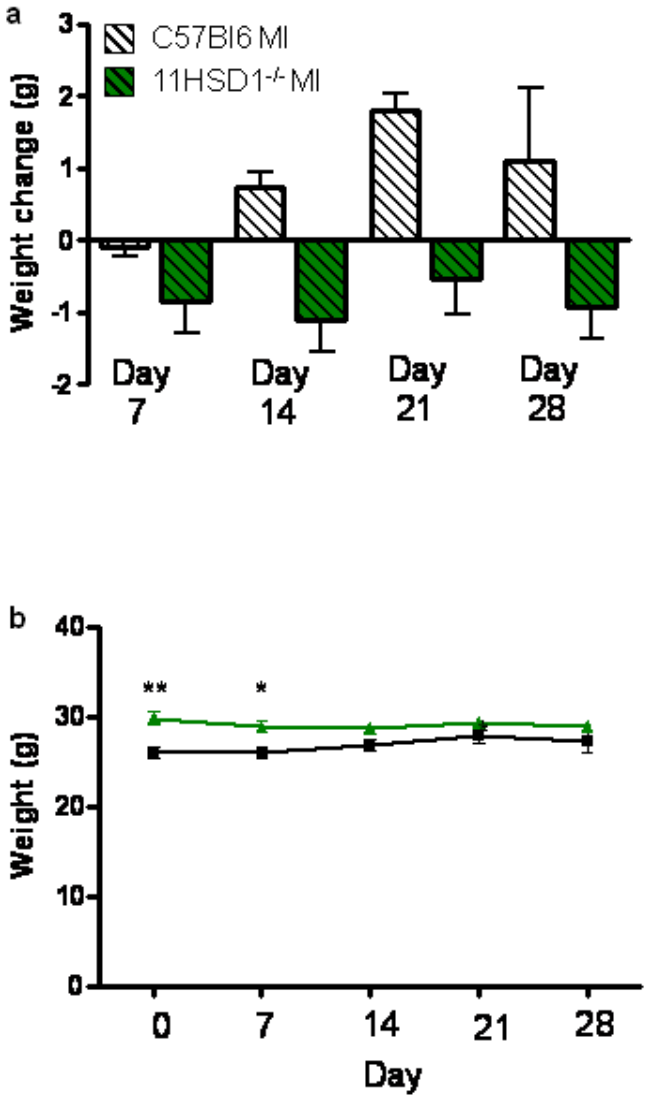

Figure 5-1 Body weight changes after myocardial infarction (MI) or sham surgery

a) 11HSD1$^{-/-}$ mice lost weight after MI and did not regain this over the 28 days post surgery while C57BL6 mice gained weight. Actual mouse body weight over the 28 day period (b). Black line= C57Bl6 mice, green line= 11HSD1$^{-/-}$ mice. n= 10 C57BL6 MI, n=9 11HSD1$^{-/-}$ MI. Data are expressed as mean ± SEM. *P<0.05, **P<0.01 C57Bl6 vs. 11HSD1$^{-/-}$ by 2 way ANOVA.

Circulating corticosterone

Plasma corticosterone decreased dramatically to almost baseline levels within 7 days of the initial increase 1 day after MI ($P<0.001$, Figure 5.2). This decline was similar in C57Bl6 and $11HSD1^{-/-}$ mice and was maintained up to 28 days post infarction.

Maintenance of neovascularisation 28 days post infarction

The density of small CD31 positive vessels seen 7 days post-MI was retained at 28 days, after infarct healing was complete (Figure 5.3 and Figure 5.4). The significant increase in vessel density seen in $11HSD1^{-/-}$ mice relative to C57Bl6 controls was maintained (day 7, 1.82±0.22 vs. 1.33±0.09; day 28, 2.20±0.17 vs. 1.59±0.15 vessels per 400μm^2). Immunohistological staining for αSMA showed that there was also a significant increase in small, smooth muscle-coated vessels in the $11HSD1^{-/-}$ animals compared with controls (Figure 5.3 and Figure 5.4). These CD31 and αSMA positive vessels were found predominantly on the infarct border with a few CD31 positive, αSMA negative vessels remaining (Figure 5.3).

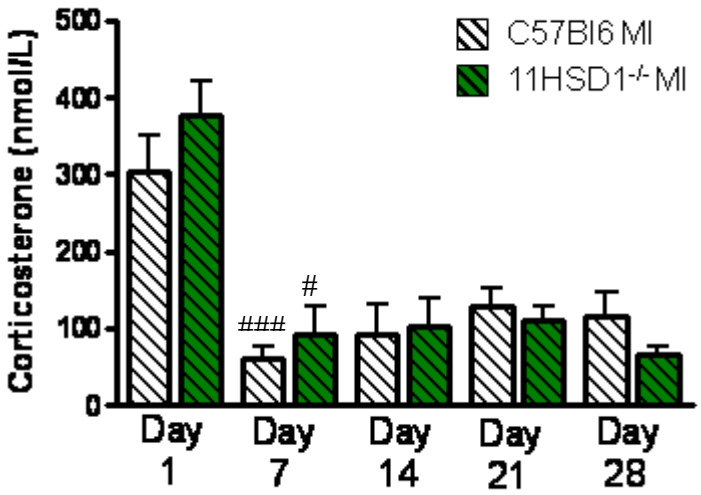

Figure 5-2 Circulating corticosterone after MI surgery

Circulating corticosterone measured by radioimmunoassay up to 28 days post-MI. Plasma corticosterone reduced dramatically by 7 days after the initial increase (that occurred 1 day after MI) and did not change up to 28 days post-MI with genotype having no influence. n= 10 C57BL6 MI, n=9 11HSD1$^{-/-}$ MI except for 1 day MI when n=6. Data are expressed as mean ± SEM. #P<0.05, ###P<0.001 Day 1 vs. Day 7 by 2 way ANOVA.

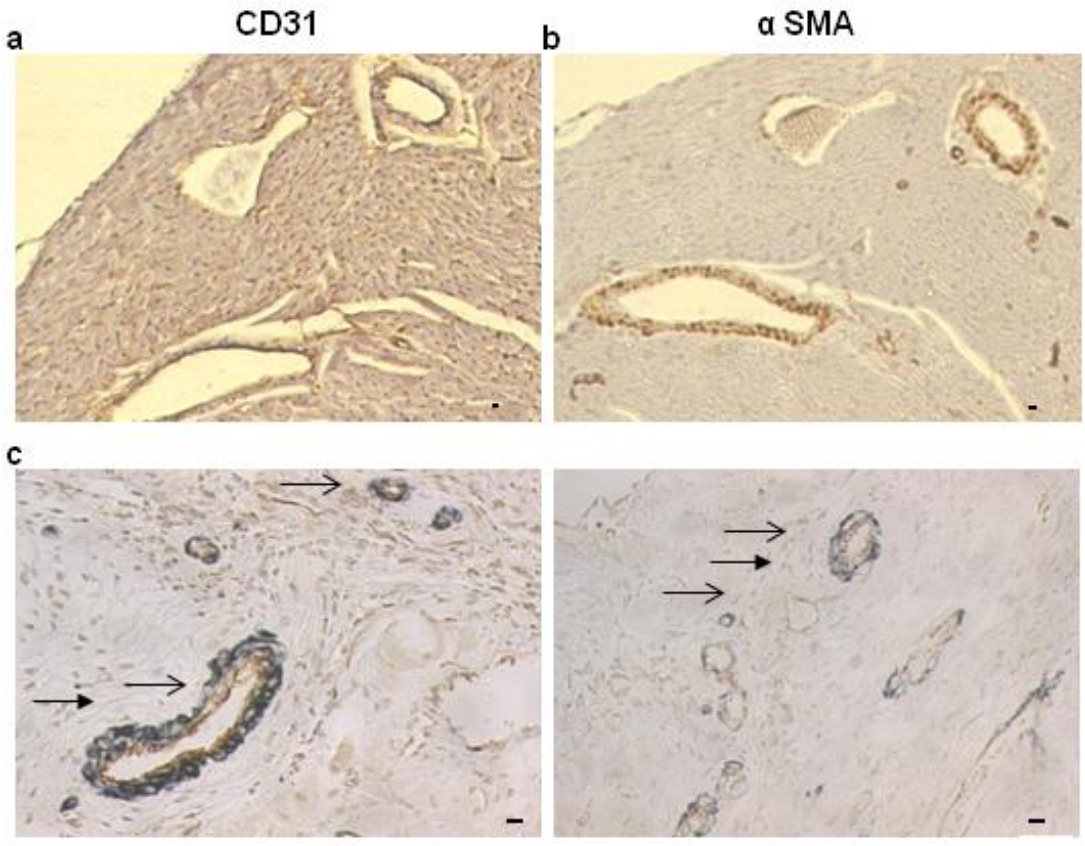

Figure 5-3 Immunohistological analysis of neovascularisation

Vessels stained in brown for (a) CD31 (endothelial cells) and (b) α smooth muscle actin (αSMA, smooth muscle) on the infarct border. c) Double immunolabelling of CD31 (open arrow, brown) and αSMA (closed arrow, blue) on the infarct border. Bar is 10μm.

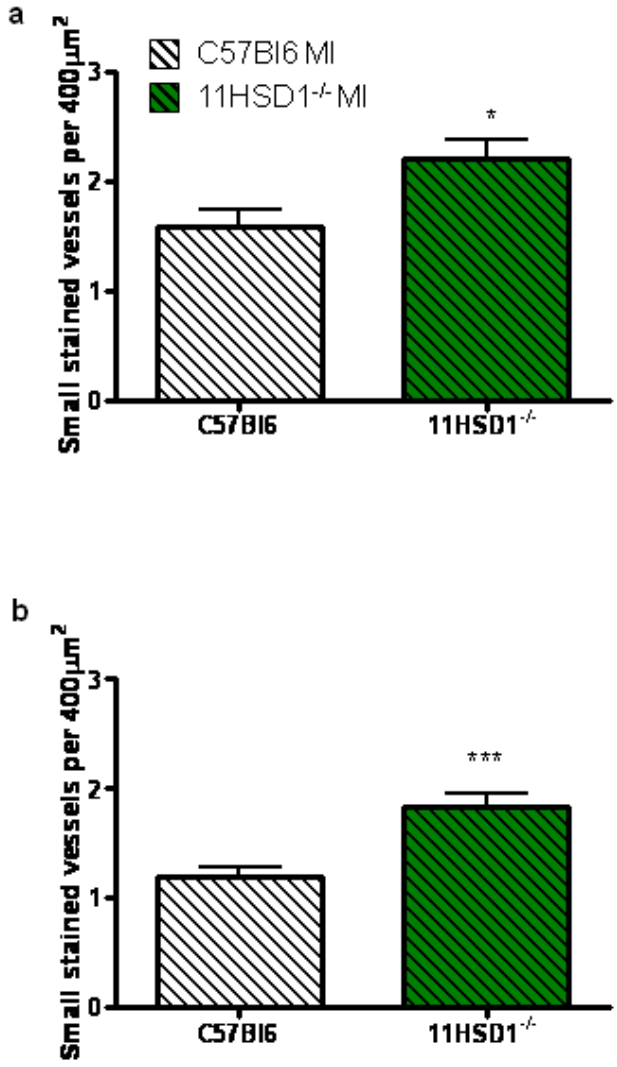

Figure 5-4 Neovascularisation after MI surgery

Vessel density was assessed by counting small (<200µm diameter) vessels in the left ventricle. 11HSD1$^{-/-}$ mice have increased CD31 (a) and αSMA (b) positive vessel density 28 days post-MI relative to C57Bl6 mice. n= 10 C57BL6 MI, n=9 11HSD1$^{-/-}$ MI. Data are expressed as mean ± SEM. *P<0.05, ***P<0.001 by unpaired Student's t-test.

Fibrosis and scar dimensions during infarct healing

Fibrosis evaluated by Picrosirius Red staining as a percent of the left ventricle staining for collagen (Figure 5.5) was comparable between control and $11HSD1^{-/-}$ mice (Figure 5.6). Collagen was seen primarily in the scar tissue and in the infarct border entwined between cells (Figure 5.5). Scar size, assessed by Masson's Trichrome staining was also comparable between the groups (Figure 5.5 and Figure 5.6). $11HSD1^{-/-}$ mice had significantly reduced infarct thinning than C57Bl6 mice ($P<0.001$) and the scars had a tendency to be shorter (Figure 5.5 and Figure 5.7).

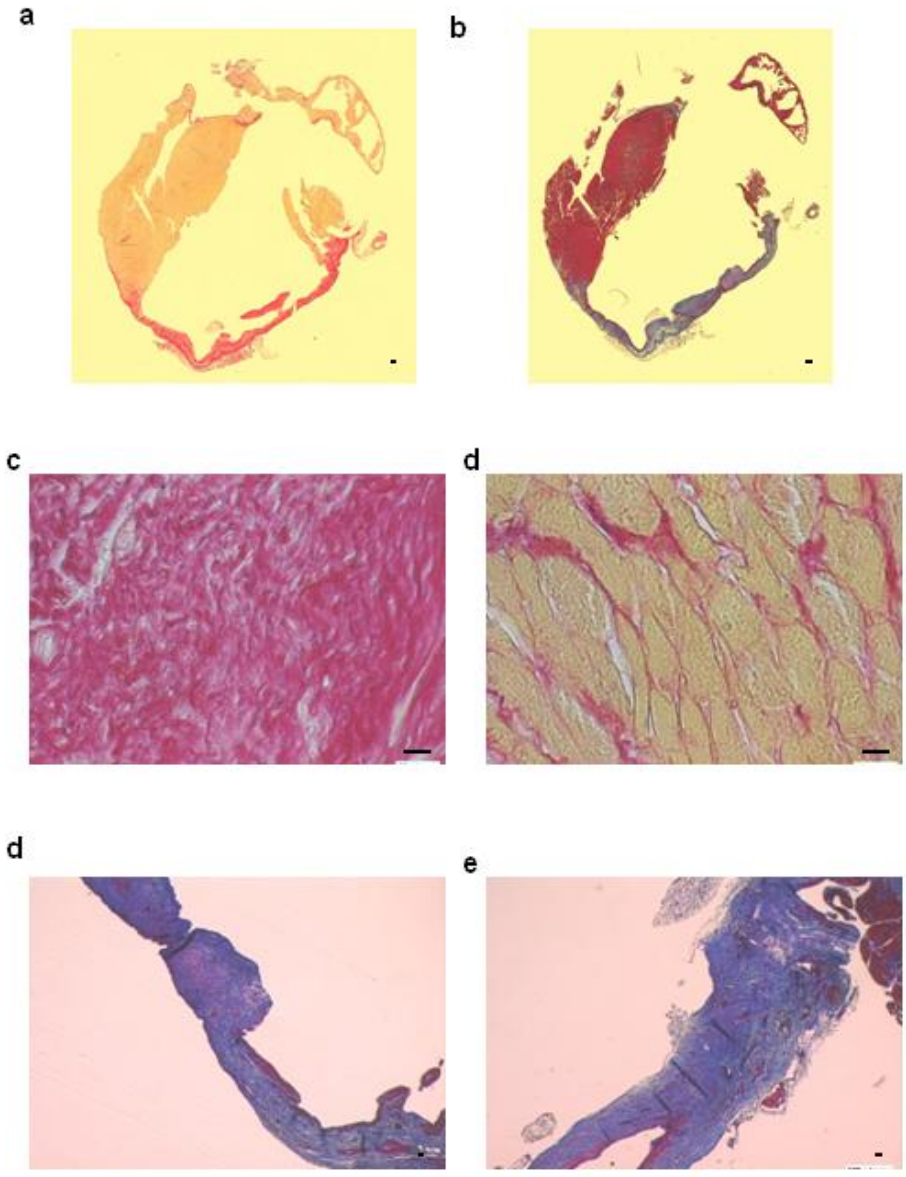

Figure 5-5 Histological analysis of fibrosis and scar formation 28 days post-MI surgery

Tiled images of sections stained with Picrosirius Red (a) to detect collagen deposition in pink and Masson's Trichrome (b) to identify the infarct scar in blue. Dense collagen is found in the infarct scar (c) and border zone (d). Typical examples of Masson's Trichrome stained scars from C57Bl6 (e) and 11HSD1$^{-/-}$ mice (f) which were used to measure infarct thickness. Bar is 10µm.

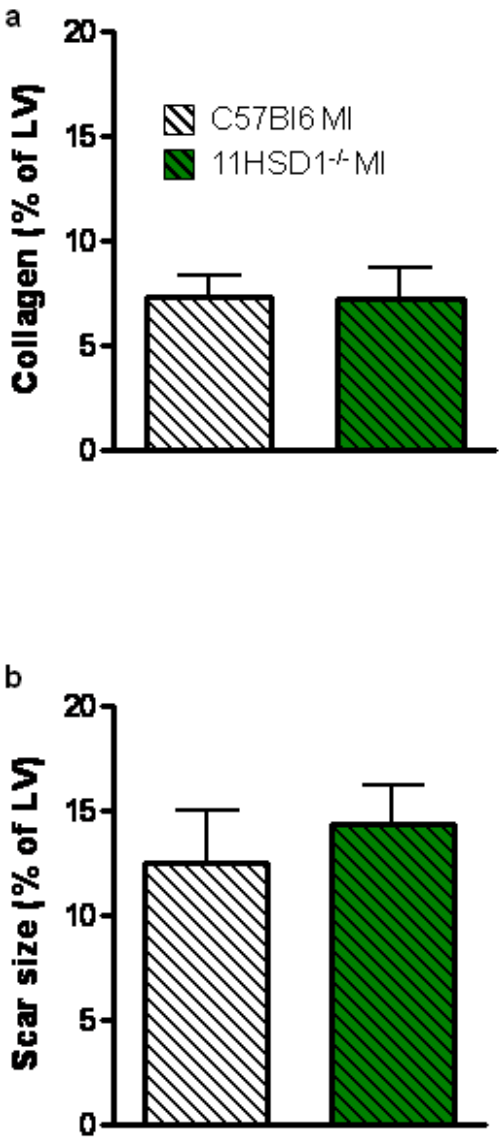

Figure 5-6 Fibrosis and scar formation 28 days after MI surgery

Collagen deposition (a) and scar size (b) as a percent of the left ventricle (%) were assessed from Picrosirius Red and Masson's Trichrome-stained sections respectively and were similar in C57Bl6 and 11HSD1$^{-/-}$ mice. n= 10 C57BL6 MI, n=9 11HSD1$^{-/-}$ MI. Data are expressed as mean ± SEM.

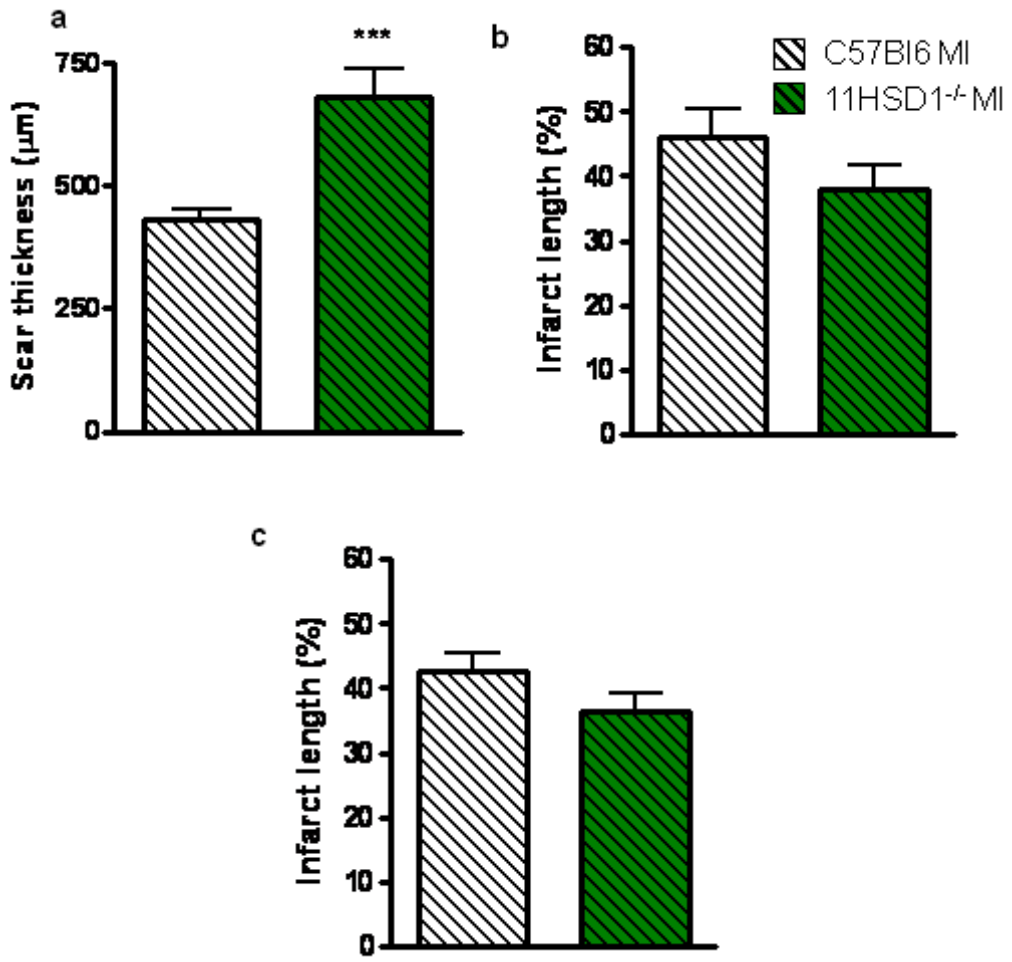

Figure 5-7 Assessment of scar characteristics 28 days after MI surgery

Analysis of scar dimensions was from Masson's Trichrome stained sections. Scar thickness was averaged from 3 points taken across the scar and was significantly greater in 11HSD1$^{-/-}$ mice compared with C57Bl6 controls (a). Epicardial (b) and endocardial (c) infarct lengths were expressed as a percentage of the epicardial and endocardial left ventricle length. There was a tendency for 11HSD1$^{-/-}$ mice to have shorter scars than C57Bl6 mice. n= 10 C57BL6 MI, n=9 11HSD1$^{-/-}$ MI. Data are expressed as mean ± SEM. ***P<0.001 unpaired Student's t test.

Post infarct cardiac function

Left ventricle dimensions, evaluated by echocardiography, were comparable in C57Bl6 and 11HSD1$^{-/-}$ mice at all time points (Table 5.3). There was no progressive increase in LVEDA demonstrating that there was no progressive left ventricle dilation in the C57Bl6 mice and this was comparable to 11HSD1$^{-/-}$ mice (Table 5.3). This suggests that dysfunction was not associated with left ventricular dilation. In both groups of animals ejection fraction was depressed after induction of MI when compared to baseline (Chapter 3) and sham operated animals (Chapter 4). At day 7 after MI ejection fraction was significantly higher in 11HSD1$^{-/-}$ mice relative to C57Bl6 mice as reported in Chapter 4. The improvement in ejection fraction was maintained at 14 and 28 days post-MI (Figure 5.8). This was not accompanied by a significant improvement in fractional shortening.

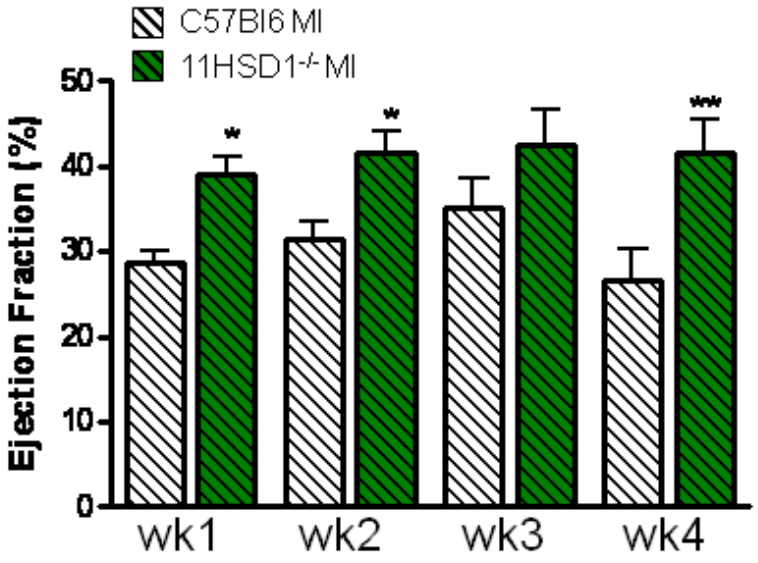

Figure 5-8 Quantified data from echocardiography up to 28 days post-MI

Left ventricle function was expressed as ejection fraction using the equation: (left ventricle end diastolic area- left ventricle end systolic area)/ left ventricle end diastolic area x 100. Ejection fraction was significantly augmented in 11HSD1$^{-/-}$ mice 7, 14 and 28 days post-MI relative to C57Bl6 controls. n= 10 C57BL6 MI, n=9 11HSD1$^{-/-}$ MI. Data are expressed as mean ± SEM. *P<0.05, **P<0.01. C57Bl6 vs. 11HSD1$^{-/-}$ by 2 way ANOVA.

	Day 7		Day 14		Day 21		Day 28	
	C57Bl6	**11HSD1$^{-/-}$**	**C57Bl6**	**11HSD1$^{-/-}$**	**C57Bl6**	**11HSD1$^{-/-}$**	**C57Bl6**	**11HSD1$^{-/-}$**
LVEDA	15.70 ±0.70	16.17 ±1.34	12.17 ±1.09	15.36 ±1.23	15.87 ±1.60	17.23 ±1.16	15.03 ±1.20	16.9 ±1.56
LVESA	11.31 ±0.52	9.88 ±1.08	8.40 ±0.86	8.89 ±0.70	10.05 ±0.88	10.02 ±1.07	11.16 ±1.28	9.69 ±0.87
LVEDD	3.95 ±0.33	3.66 ±0.19	3.42 ±0.12	3.60 ±0.17	3.63 ±0.18	3.69 ±0.12	3.71 ±0.12	3.58 ±0.24
LVESD	3.86 ±0.16	2.65 ±0.16	2.61 ±0.13	2.78 ±0.20	2.88 ±0.16	2.77 ±0.18	2.86 ±0.11	2.46 ±0.23
PWD	0.94 ±0.06	0.97 ±0.06	0.84 ±0.06	1.03 ±0.07	0.95 ±0.07	1.04 ±0.09	0.99 ±0.06	1.03 ±0.07
PWS	1.02 ±0.04	1.08 ±0.05	0.99 ±0.05	1.05 ±0.08	1.07±0.07	0.97 ±0.10	1.08 ±0.04	1.13 ±0.06
EF (%)	28.58 ±1.51	39.03±2.21*	31.48 ±1.98	41.46±2.68*	35.22 ±3.32	42.54 ±4.01	26.65 ±3.75	41.60±3.83**
FS (%)	25.15 ±3.07	27.66 ±1.54	23.74 ±3.10	23.03 ±4.03	20.49 ±2.93	25.95 ±3.37	22.38 ±3.59	32.05 ±3.41

Table 5-3 Left ventricle dimensions after MI surgery

There were no differences in LVEDA (left ventricle end diastolic area), LVESA (left ventricle end systolic area), LVEDD (left ventricle end diastolic diameter), LVESD (left ventricle end systolic diameter), PWD (posterior wall thickness at diastole) or PWS (posterior wall thickness at systole). Whilst fractional shortening was not significantly different at any time point ejection fraction was significantly enhanced in the 11HSD1$^{-/-}$ mice compared with C57Bl6 mice at days 7, 14 and 28 post-MI. n= 10 C57BL6 MI, n=9 11HSD1$^{-/-}$ MI. Data are expressed as mean ± SEM. *P<0.05, **P<0.01 C57Bl6 vs. 11HSD1$^{-/-}$ by 2 way ANOVA.

5.4 Discussion

The aim of the present study was to investigate whether the enhancement in vessel density and the improvement in cardiac function in 11HSD1$^{-/-}$ mice during early infarct healing were retained after infarct healing was complete. Furthermore, the effect of 11HSD1 deficiency on scar formation was assessed. This study showed that the increase in vessel density was maintained in 11HSD1$^{-/-}$ mice 28 days after MI, relative to C57Bl6 mice, and that these vessels matured becoming pericyte coated. These differences were associated with a sustained increase in cardiac contractility. Collagen content and scar size were comparable between the groups but, 11HSD1$^{-/-}$ mice had reduced infarct thinning and infarcts had a tendency to be shorter.

Recovery from surgery and organ weights

Mortality rates and cause were similar between the strains of mice demonstrating that as infarct healing progresses to completion, 11HSD1$^{-/-}$ mice did not develop a grossly abnormal phenotype. While C57Bl6 mice started to gain weight 14 days after surgery 11HSD1$^{-/-}$ mice did not even regain the preoperative weight that was lost and this was not associated with altered food intake. However, at baseline 11HSD1$^{-/-}$ mice were heavier than C57Bl6 mice of the same age and while weight was not regained in these mice there was no significant difference in actual body weights between the strains of mice at day 14 onwards. This is not likely to be due to an altered stress response as circulating corticosterone levels were the same in both groups of mice at all time points.

Heart weights 28 days after MI were similar in C57Bl6 and 11HSD1$^{-/-}$ mice and, likewise, were comparable to heart weights in sham and MI animals when assessed at day 7 (please see Chapter 4). Any loss of heart weight due to infarct thinning seems to have been compensated to a similar degree in both strains. Some groups have reported

an increase in heart weight from 28 days post-MI relative to sham due to progressive cardiomyocyte hypertrophy (Fazel et al., 2006, Tirziu et al., 2007). Although there were no parallel sham-operated mice in the present long term study the data provides no evidence for additional compensatory hypertrophy. It would be interesting to re-examine this at a later time point when the mice develop heart failure and generally changes in hypertrophy are more evident (Shioura et al., 2007, Pfeffer and Braunwald, 1990).

Other organ weights, with the exception of the spleen, did not differ between C57Bl6 and 11HSD1$^{-/-}$ mice. Surprisingly, 11HSD1$^{-/-}$ mice had significantly lighter spleens than those of C57Bl6 controls. There is little in the literature regarding the effect of MI on spleen weight; however, in a mouse model of viral myocarditis increased inflammation was associated with reduced spleen size (Kanda et al., 2004). This would be consistent with the data presented here showing that 11HSD1$^{-/-}$ mice have enhanced inflammation during infarct healing. Furthermore non-selective inhibition of the 11HSD enzymes by glycyrrhetinic acid reduced spleen weight by encouraging splenocyte apoptosis (Horigome et al., 2001). This group hypothesised that increased cell death was a result of elevated circulating corticosterone (Horigome et al., 2001). However no difference in plasma corticosterone was observed in the current study suggesting that the effect of loss of 11HSD1 on spleen weight might be mediated by a different mechanism in our model. A recent publication provides evidence for the spleen being a reservoir for the monocytes that are liberated after MI (Swirski et al., 2009). It is possible that increased monocyte liberation from the spleen may be the source of increased monocyte infiltration into the heart.

Basal corticosterone at the diurnal nadir is about 40nmol/L in C57Bl6 mice (Paterson et al., 2006). There was over an 8 fold increase in plasma corticosterone concentration 1 day after MI, consistent with HPA axis activation after MI. Activation was similar in both strains of mice and in both plasma concentrations declined towards baseline by 7 days and were maintained at this low level over the 28 day period. Plasma levels did not decline to the expected basal concentrations which may reflect that the animals have not returned to full health. Previous work has suggested that 11HSD1$^{-/-}$ mice have a

prolonged stress response to restraint (Harris et al., 2001). However the data presented here shows that the post-infarct stress response is transient and is similar to that in C57Bl6 mice.

Maintenance of neovascularisation

Assembly of a highly organised vasculature requires the interaction of growth factors involved in cell proliferation and migration (VEGF, IL-8) (Kido et al., 2005, Kocher et al., 2006, Li et al., 2003), vessel pruning (Ang-2) (Maisonpierre et al., 1997), pericyte recruitment (PDGF) and vessel stabilisation (PDGF, Ang-1, the Tie-2 receptor and TGF-β1) (Ramsauer et al., 2002, Korpisalo et al., 2008, Greenberg et al., 2008, Thurston et al., 1999, Patan, 2000, Conway et al., 2001). Data presented previously ((Small et al., 2005) and Chapter 4) showed that 11HSD1$^{-/-}$ mice have increased vessel density that is associated with increased cell proliferation and cardiac IL-8 mRNA expression 7 days post-MI. However, for this increase in vessel density to be influential in later left ventricle remodelling it must be retained. Apoptosis of endothelial cells precipitates angiogenic vessel regression occurring 7-21 days post-MI; disposing of excess vasculature (Conway et al., 2001, Grass et al., 2006, Patan, 2000). Over this time vessels are also stabilised by addition of smooth muscle positive pericytes and cell-to-cell junctions are tightened to prevent leakage (Conway et al., 2001). Vessels lose their plasticity and are mature by 28 days post-MI (Ren et al., 2002, Grass et al., 2006, Dewald et al., 2004). Immunohistochemistry data show that 11HSD1$^{-/-}$ mice maintained the enhanced vessel density 28 days post-MI, relative to C57Bl6 controls. There was also evidence that these vessels had become coated with smooth muscle cells, likely to be pericytes and suggesting longevity.

There has been some debate regarding the origin of pericytes. It has been suggested that they may differentiate from mesenchymal stem cells (Bexell et al., 2009), mononuclear cells (Conway et al., 2001), epicardial cells (Dettman et al., 1998) and fibroblasts (Njauw et al., 2008). We have shown previously (Chapter 4) that 11HSD1$^{-/-}$ mice have

enhanced cellular proliferation in the heart 7 days after MI, which may promote formation of both the endothelial cell and the pericyte layer in neovessels. TGF-β initiates differentiation of cells to pericytes (Bergers and Song, 2005) that are subsequently attracted to the vascular endothelial cells by PDGF, which is produced by the endothelial cells themselves (Greenberg et al., 2008). Increased differentiation of cells to pericytes may be the cause of increased pericyte-coated vessel density in 11HSD1$^{-/-}$ mice. The enhanced infiltration of macrophages in 11HSD1$^{-/-}$ mice (Chapter 4) may increase TGF-β, levels thus encouraging pericyte development. Assessment of cardiac TGF-β in these mice warrants investigation.

VEGF has been shown to be a negative regulator of PDGF, preventing pericyte recruitment (Greenberg et al., 2008). The delay in this process prolongs the plasticity window, enabling endothelial cell proliferation and vessel remodelling (Ren et al., 2002, Grass et al., 2006). mRNA expression of VEGF was similar in C57Bl6 and 11HSD1$^{-/-}$ mice up to 7 days after MI (Chapter 4). However, perhaps assessing expression of this growth factor at 2 weeks, when pericytes are being recruited, would demonstrate whether there is altered regulation of pericyte recruitment in the 11HSD1$^{-/-}$ mice. Double labelling has shown co-expression of α SMA and β-catenin, an adhesion molecule present at adheren junctions, suggesting communication occurs between pericyte cells and may aid in vessel maturation (Njauw et al., 2008).

Commonly, pericytes are associated with vessel stability but they have much more diverse functions. Pericytes, like smooth muscle cells, can alter vessel tone in response to vasoactive substances (Kawamura et al., 2004, Kutcher and Herman, 2009). They are found in high density at the blood brain barrier where they form a tight boundary (Ramsauer et al., 2002, Thomas, 1999). Interestingly in this location pericytes can exhibit macrophage like phagocytic behaviour (Thomas, 1999). Some have hypothesised that they could indeed be brain macrophage precursors (Bergers and Song, 2005, Thomas, 1999).

Post infarct resolution of inflammation

It was demonstrated in Chapter 4 that 11HSD1$^{-/-}$ mice have an enhanced inflammatory response in parallel with augmented angiogenesis in the healing phase post-MI. The processes governing the resolution of inflammation are unclear. There is conflicting evidence regarding the effect of deficiency of IL-10, a cytokine reported to inhibit production of inflammatory cytokines (Yang et al., 2000, Zymek et al., 2007). The importance of resolution of inflammation has been shown in studies in which the anti-inflammatory and anti-angiogenic thrombospondin-1 (TSP-1) has been knocked out. Deficiency of TSP-1 elevates and extends inflammation and is associated with scar expansion and adverse remodelling (Frangogiannis et al., 2005). While anti-inflammatory cytokines were not examined in the current study evidence presented here indicates that defective resolution of inflammation was not an issue in the 11HSD1$^{-/-}$ model. The inflammatory cells seen in the infarct area and infarct border up to 7 days post-MI were replaced with a collagenous scar at day 28.

Fibrosis and scar formation

The post-infarct inflammatory response is vital in stimulating the fibrotic process (van Amerongen et al., 2007). Despite an increase in inflammation within 7 days of MI in the 11HSD1$^{-/-}$ mice there was no subsequent increase in collagen deposition. Scar formation and fibrosis are processes that occur over time and are initiated soon after the initial ischaemic event. Increased vascular permeability as a result of MI and disruption of the extracellular matrix by collagenase, matrix metalloprotease and serine protease enzymes enables extravasation of plasma proteins into the infarct during the inflammatory phase of MI healing producing a temporary fibrin-based matrix (Dobaczewski et al., 2006, Dobaczewski et al., 2009). This creates a temporary scaffold for migrating cells. This matrix is gradually lysed and replaced by a more organised matrix of fibronectin and

hyaluronan as the healing response progresses (Dobaczewski et al., 2006). Quiescent fibroblasts undergo a phenotypic change to myofibroblasts, stimulated by TGF-β secreted by macrophages (Cleutjens et al., 1995, Desmouliere et al., 1993, Fadok et al., 1998). Depletion of macrophages reduces collagen deposition demonstrating their importance in the fibrotic response (van Amerongen et al., 2007). Myofibroblasts are characterised by their high capacity for proliferation, secretion of αSMA and collagen (Virag and Murry, 2003, Lutgens et al., 1999, Porter and Turner, 2009, van Amerongen et al., 2008). The transient nature of this activation has been demonstrated by immunohistochemistry for αSMA. In the present study myofibroblast activation increased up to 7 days post-MI (Chapter 4) but by 28 days post-MI all staining was associated with vessel smooth muscle. Deposition of collagen starts from 3 days post MI and increases progressively up to 180 days after infarction (Yang et al., 2002) (Virag and Murry, 2003, Dean et al., 2005) and its cross-linking is vital in providing tensile strength and structural integrity to the weakened myocardium (Dean et al., 2005, Virag and Murry, 2003). The production of collagen may also serve to promote the quiescent phenotype of fibroblasts thus providing a negative feedback mechanism. Dermal fibroblasts stimulated with TGF-β show decreased collagen production in response to a collagen rich environment (Clark et al., 1995). This may prevent excessive fibrosis which may facilitate cardiac arrhythmias (Zannad and Radauceanu, 2005, Li et al., 1999, Kostin et al., 2002).

In the current study collagen deposition and scar area, found in the apical region, were comparable in C57Bl6 and 11HSD1$^{-/-}$ mice. This area is particularly vulnerable as it is a thin part of the heart with the greatest curvature. Damage here leads to a more pronounced decline in heart function (Pfeffer and Braunwald, 1990). Histology showed that 11HSD1$^{-/-}$ mice had reduced infarct thinning and the infarct length had a tendency to be shorter. Improving blood supply may prevent infarct expansion by cardiomyocyte salvage as suggested by the changes in the scar characteristics. Furthermore a thicker scar may be protective against cardiac rupture (Nahrendorf et al., 2006). The modification of the scar characteristics independent of actual scar area is well reported in

the literature (Nahrendorf et al., 2006, Garcia et al., 2007, Hammerman et al., 1983a, Hammerman et al., 1983b, Brown et al., 1983). In humans infarct expansion is greatest in patients with higher blood pressure and greater vascular resistance and these patients are more likely to develop complications (Pfeffer and Braunwald, 1990, Pierard et al., 1987). Unfortunately blood pressure was not measured in the current study. This should be considered in future work. Fibrillar and non-fibrillar collagen is found in the myocardium with fibrillar collagen type I being the most abundant (Shamhart and Meszaros, 2009). In cardiac pathology the abundance of strong, stiff collagen I and elastic collagen III increases (Pauschinger et al., 1999). Furthermore, the proportion of collagen I relative to III increases favouring production of a stiffer scar (Pauschinger et al., 1999). It is possible that the relative abundance of these different types of collagen in the scar may vary between the 11HSD1$^{-/-}$ and C57Bl6 mice having an effect on the contractility of the heart. While it was not possible to differentiate between collagen types from the Picrosirius Red stained sections they can be identified using immunohistochemistry or quantitative RT-PCR and as such this should be considered in future studies.

Cardiac function post-MI

Data presented in Chapter 4 showed that 11HSD1$^{-/-}$ mice have improved ejection fraction 7 days post-MI. It is hypothesised that this was due to the parallel increase in vessel density in the left ventricle. Importantly this improvement in heart function was maintained up to 28 days post-MI in the 11HSD1$^{-/-}$ mice compared to C57Bl6 controls and was associated with increased density of mature blood vessels. The source of the increased post-infarct ejection fraction in 11HSD1$^{-/-}$ mice may be improved perfusion to the infarct border enhancing cardiomyocyte contractility and/or prevention of infarct expansion by salvage of cardiomyocytes, as suggested by reduced infarct thinning and shorter infarct lengths in the 11HSD1$^{-/-}$ mice.

The left ventricle undergoes remodelling to maintain cardiac output and is associated with alterations in cardiac architecture (Pfeffer and Braunwald, 1990). After MI myocytes, particularly those at the infarct border, change to a distorted, irregular shape (Kocher et al., 2001) and become hypertrophic to compensate for the myocytes lost after infarction. This is often inadequate for maintenance of cardiac function. Subsequent left ventricle dilation due to slippage of cardiomyocytes can lead to the development of heart failure (Pfeffer and Braunwald, 1990, Shioura et al., 2007). In Chapter 4 the data demonstrated that the decline in heart function was due to systolic dysfunction; the end systolic volumes assessed in the current study demonstrate that there was no further decline in systolic function. In humans increased end systolic volume is a powerful predictor of death (Pfeffer and Braunwald, 1990, White et al., 1987). The 28 day data are consistent with Shioura et al who found systolic dysfunction up to 28 days post-MI that worsened at 10 weeks as determined by the Millar pressure volume loop (Shioura et al., 2007). In their study the decline in diastolic function was more gradual and showed significance at 10 weeks only (Shioura et al., 2007) fitting with the lack of diastolic dysfunction in this model. LVEDA did not progressively increase over time in either strain suggesting that the improvement in cardiac function in 11HSD1$^{-/-}$ mice was not due to prevention of ventricular dilation. Several other studies have shown that dilation is associated with worsened heart function by this time after MI (Pfeffer and Braunwald, 1990, Yang et al., 2000). It may be that the echocardiography used here was not sufficiently sensitive to detect such changes. MRI could determine whether this is a real issue. Alternatively the results might suggest that the improvement in heart function in 11HSD1$^{-/-}$ compared with C57Bl6 mice may be by a mechanism independent of left ventricle dilation, such as those suggested above; improved infarct border cardiomyocyte contractility due to enhanced perfusion, thicker, shorter scars or altered collagen composition.

Experimental studies that aim to enhance post-infarct angiogenesis often concentrate on the initial angiogenic response and many fail to investigate vessel remodelling and maturation, processes that have a strong influence on vessel longevity. Here we have

shown that the acute enhancement in vessel density in 11HSD1$^{-/-}$ mice during the healing phase post-MI is maintained after healing is complete. Moreover, these vessels have resisted pruning, are mature, are pericyte-coated and are likely to be capable of carrying a blood supply. While actual scar size was not changed it is possible that the alterations in scar dimensions may have greater importance. Certainly, a shorter thicker scar may confer protection from cardiac rupture and may improve heart function. Importantly the acute improvement in heart function at 7 days after MI was maintained at 28 days. It seems logical that this would extend into the longer term as the mice develop heart failure. For such findings to have clinical relevance the effect of pharmacological inhibition of 11HSD1 must be investigated. Pharmacological inhibition of 11HSD1 has proved beneficial in murine models of obesity, diabetes and atherosclerosis (Hermanowski-Vosatka et al., 2005). Whether inhibition of 11HSD1 immediately after MI is sufficient to confer protection is uncertain. It may be possible that there are predetermined effects of the genetic deletion that aids in post-infarct healing. In the next Chapter I investigate whether pharmacological inhibition of 11HSD1 can recapitulate the effect of the knock out on murine infarct healing.

6 The effect of pharmacological inhibition of 11HSD1 on recovery after myocardial infarction

6.1 Introduction

It has previously been demonstrated that mice deficient for the glucocorticoid regenerating enzyme, 11HSD1, have enhanced angiogenesis and cardiac function 7 days after MI that persists for at least 28 days (Chapter 4 and Chapter 5 and (Small et al., 2005)). This is preceded by enhanced infiltration of neutrophils and macrophages (Chapter 4). While this is itself, an interesting observation, its impact would be considerably increased if inhibition of 11HSD1 could be exploited clinically. Manipulation of tissue levels of glucocorticoids using pharmacological inhibitors of 11HSD1 is attractive. Early 11HSD1 inhibitors, including carbenoxolone and glycyrrhetinic acid also had effects that were consistent with 11HSD2 inhibition, such as increasing blood pressure and lowering plasma potassium in humans (Andrews et al., 2003). Selective small molecule inhibitors of 11HSD1 are currently under development and have been successful in rodent models of disease. Inhibition of 11HSD1 has proved beneficial in mouse models of obesity, diabetes and atherosclerosis (Hermanowski-Vosatka et al., 2005, Veniant et al., 2009, Lloyd et al., 2009). There have been very few drugs tested clinically to date however there are 11HSD1 inhibitors that are in clinical trials for the treatment of diabetes (Hawkins, 2008).

The aim of the present study was to investigate the influence of 11HSD1 inhibition using a commercially available 11HSD1 inhibitor known as compound 544 (3-(1-adamantyl)-6,7,8,9-tetrahydro-5H-[1,2,4] triazolo [4,3-α] azepine). This inhibitor was developed by Merck, has previously been used successfully in mice and has oral bioavailability (Hermanowski-Vosatka et al., 2005). We hypothesize that administration of compound 544 in the diet would recapitulate the effect of genetic deletion of 11HSD1. Drug treated mice were predicted to show enhanced inflammation, angiogenesis and improved cardiac function 7 days after MI.

6.2 Methods

6.2.1 Study design

Male C57Bl6 mice (Harlan, UK) were allowed 1 week to acclimatise after their arrival. After this period they were split into pairs and their body weight and food intake were monitored daily for a further week. Subsequently mice were randomised to receive sham or MI operation and vehicle or inhibitor diet. Previous work has shown that administering the 11HSD1 inhibitor, compound 544 (Enamine, Ukraine), in food is an effective method of dosing (Hermanowski-Vosatka et al., 2005). Mice were fed vehicle (0.5% methylcellulose, 5% Tween 80) or compound 544 (30mg/kg/day in the vehicle solution). For details of the diet recipe please refer to Section 2.3.4. After monitoring consumption of vehicle containing diet for one week, and considering previous in-house studies where food intake has been monitored, it was decided that the mice would eat on average 10g food per day. An intraperitoneal injection of vehicle or 10mg/kg inhibitor was given immediately after surgery followed by vehicle or inhibitor diet. Food tubes and body weight were monitored daily to check drug intake.

6.2.2 Coronary artery ligation

Male C57Bl6 mice (Harlan, UK) aged 10-12 weeks were used for all experiments. Mice underwent coronary artery ligation for induction of MI or sham-operation, as described in Section 2.3.1.

6.2.3 Echocardiography

Cardiac function was assessed by echocardiography as described in Section 2.3.2. Mice underwent echocardiography 7 days after surgery in order to obtain measurements of

ventricular dimensions. The observer was blinded to treatment for the purpose of echocardiography measurements and all other subsequent analysis of tissues.

6.2.4 Tissue collection

For analysis of circulating corticosterone levels blood was taken 7 days after surgery, prior to echocardiography, by tail tip at 7:30am (the diurnal nadir), as described in Section 2.3.3. One hour prior to sacrifice mice were injected intra-peritoneally with 2.5mg BrdU dissolved in saline. Mice were killed by cervical dislocation after echocardiography. The hearts were excised, washed in ice cold PBS, weighed and then bisected down the longitudinal axis. They were fixed in 10% neutral buffered formalin for 24 hours for use in immunohistochemistry.

6.2.5 Corticosterone radioimmunoassay

A radioimmunoassay was conducted to determine circulating levels of corticosterone after myocardial infarction, as described in Section 2.5.1.

6.2.6 Immunohistochemistry

Identification of macrophages, vascular endothelial cells and proliferating cells was conducted using: a monoclonal rat anti-mouse mac 2 primary antibody (Cedarlane) diluted 1/6000 in PBS/1%BSA; a monoclonal rat anti-mouse CD31 primary antibody (BD Bioscience) diluted 1/50 in PBS/1% BSA; and a monoclonal mouse anti-mouse BrdU primary antibody (Sigma) diluted 1/1000 in TBS/10% normal goat serum/5%BSA, respectively. For details of the procedure please refer to Section 2.5.1. Quantification of immunohistochemistry was conducted using Image Pro 6.2, Stereologer Anaylser 6 MediaCybernetics. Macrophage infiltration was quantified as the

percent of infarct border stained. Small CD31 positive vessels (<200µm diameter) and BrdU positive nuclei were counted in the left ventricle as described in Section 2.5.2.

6.2.7 Statistics

All values are expressed as mean ±SEM. All comparisons were made using 2-way ANOVA with Bonferroni post-hoc tests.

6.3 Results

The impact of surgery on food intake, body and organ weight

Mouse food intake varied greatly from day to day but there was no difference between the groups on any day (Figure 6.1). There was difficulty in monitoring food intake accurately as mice developed a habit of removing food from the tubes and spreading it around the cage. Ingestion of the diet declined immediately after surgery (at day 7) and remained low for the first 2 days in all groups ($P<0.05$ between day 7 and 8). Body weight was stable prior to sham or MI operations but tended to decline after surgery on day 7, in line with the decrease in food intake, although this failed to reach statistical significance. Mice in all groups returned to pre-operative weight by 7 days post-surgery (Figure 6.1). At the end of the study, 7 days after surgery, heart weights were similar in sham-operated and MI animals regardless of the drug treatment (Table 6.1). Furthermore other organ weights (liver, kidney, spleen, thymus, adrenal gland) did not vary either (Table 6.1).

Circulating corticosterone

Plasma corticosterone levels were comparable 7 days after MI or sham-operations (Figure 6.2) and were unaffected by administration of compound 544.

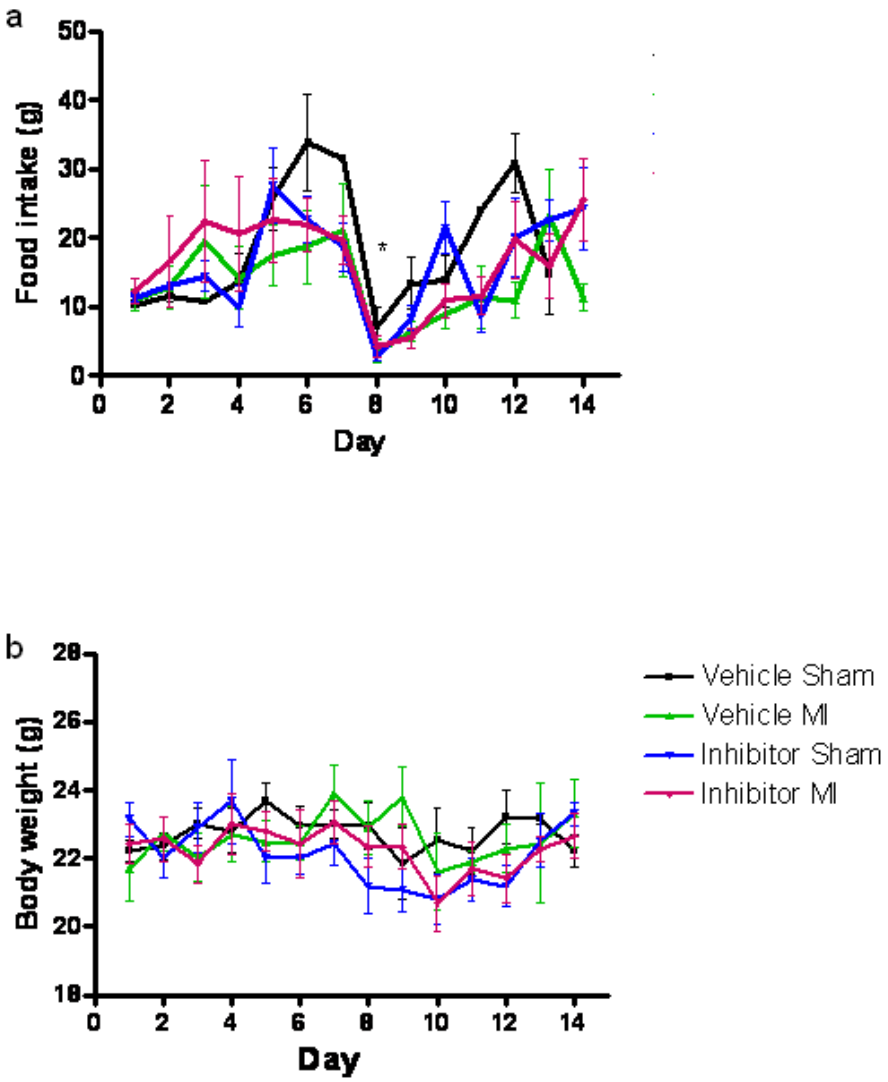

Figure 6-1 Body weight and food intake after myocardial infarction (MI) or sham surgery

a) Food intake and body weight were stable before surgery, after which they declined. Food intake and body weight increased from 2 days after surgery. Arrows denote day of surgery. n=4 vehicle sham, n=4 vehicle MI, n=5 inhibitor sham, n=7 inhibitor MI. Data are expressed as mean ± SEM. *P<0.05 7day vs. 8 day in all groups by 2-way ANOVA.

Organ weights	VEHICLE		INHIBITOR	
	Sham	MI	Sham	MI
Heart (mg)	0.16±0.01	0.18±0.02	0.15±0.01	0.16±0.01
Heart (rel. to body weight)	7.22±0.67	6.07±1.17	6.62±0.15	7.24±0.43
Liver (mg)	1.31±0.05	1.29±0.04	1.35±0.06	1.20±0.02
Liver (rel. to body weight)	57.54±1.61	57.12±1.46	58.41±1.43	54.61±2.31
Kidney (mg)	0.38±0.02	0.38±0.02	0.38±0.01	0.38±0.04
Kidney (rel. to body weight)	16.71±1.11	16.95±1.85	16.46±0.28	16.63±1.68
Spleen (mg)	0.10±0.01	0.13±0.01	0.12±0.02	0.10±0.01
Spleen (rel. to body weight)	4.32±0.41	5.81±0.88	5.28±0.73	4.33±0.59
Thymus (mg)	0.06±0.01	0.05±0.01	0.06±0.01	0.06±0.01
Thymus (rel. to body weight)	2.76±0.34	1.96±0.48	2.44±0.41	2.60±0.23
Adrenal gland (mg)	0.01±0.01	0.01±0.01	0.01±0.01	0.01±0.01
Adrenal gland (rel. to body weight)	0.55±0.11	0.31±0.03	0.63±0.24	0.51±0.11

Table 6-1 Organ weights after MI or sham surgery

Weights of heart, liver, kidney, spleen and adrenal glands and expressed relative to body weight. There were no differences between any of the groups. n=4 vehicle sham, n=4 vehicle MI, n=5 inhibitor sham, n=7 inhibitor MI. Data are expressed as mean ± SEM.

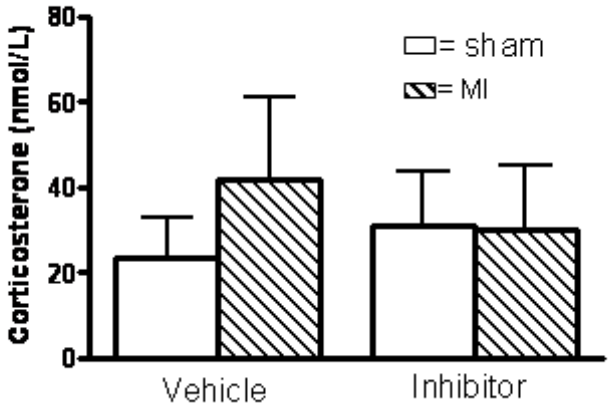

Figure 6-2 Circulating corticosterone after MI or sham surgery

There were no differences in circulating corticosterone levels between the groups 7 days after MI or sham surgery, as assessed by radioimmunoassay. n=4 vehicle sham, n=4 vehicle MI, n=5 inhibitor sham, n=7 inhibitor MI. Data are expressed as mean ±SEM.

Macrophage infiltration

Macrophage infiltration, shown by mac 2 immuno-reactivity, was seen predominantly in the infarct and border zone. Macrophage staining was significantly greater 7 days after MI compared with sham-operated mice (in which staining was negligible; Figure 6.3). Administration of the 11HSD1 inhibitor had no effect on the extent of macrophage infiltration into the infarcted myocardium.

Post infarct neovascularisation

The density of small CD31 positive vessels was increased 7 days post-MI relative to sham-operated controls both in vehicle and in inhibitor treated groups (Figure 6.4). Administration of compound 544 had no effect on the vascularity of the left ventricle. The number of cells proliferating was significantly enhanced after MI, relative to sham-operated mice (Figure 6.4). There was a trend for this to be further enhanced in mice treated with compound 544, but this failed to reach significance (P=0.11).

Left ventricle dimensions and cardiac function

There were no differences in left ventricle end diastolic area (LVEDA) between the groups (Table 6.2). However, left ventricle end systolic area (LVESA) was significantly greater after MI relative to sham-operated mice, suggesting systolic dysfunction. LVESA was similar in vehicle and inhibitor treated mice. Other left ventricle dimensions measured did not vary between the groups. Ejection fraction and fractional shortening were both significantly reduced post-MI relative to sham-operated controls (Figure 6.5 and Table 6.2). Treatment with the 11HSD1 inhibitor had no effect on ejection fraction or fractional shortening in any of the groups.

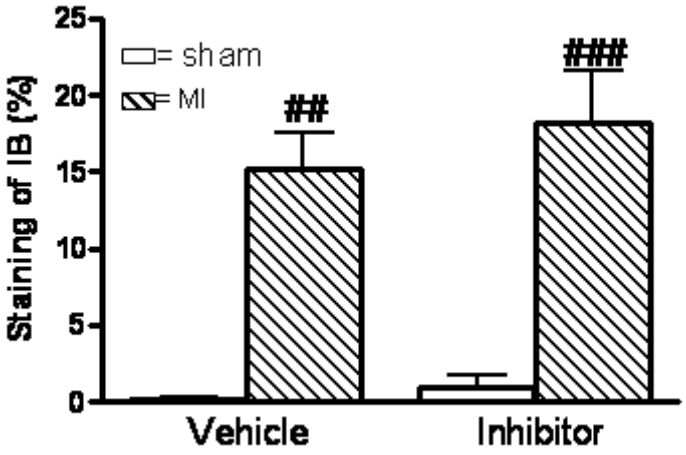

Figure 6-3 Macrophage infiltration after MI or sham surgery

Macrophages identified by mac-2 immuno-reactivity and quantified as a percentage of the infarct border (IB) stained. Mac 2 staining was increased after MI relative to sham-operated mice. Treatment with Compound 544 had no effect. n=4 vehicle sham, n=4 vehicle MI, n=5 inhibitor sham, n=7 inhibitor MI. Data are expressed as mean ±SEM. ## P<0.01, ### P<0.001 Sham vs. MI by 2-way ANOVA.

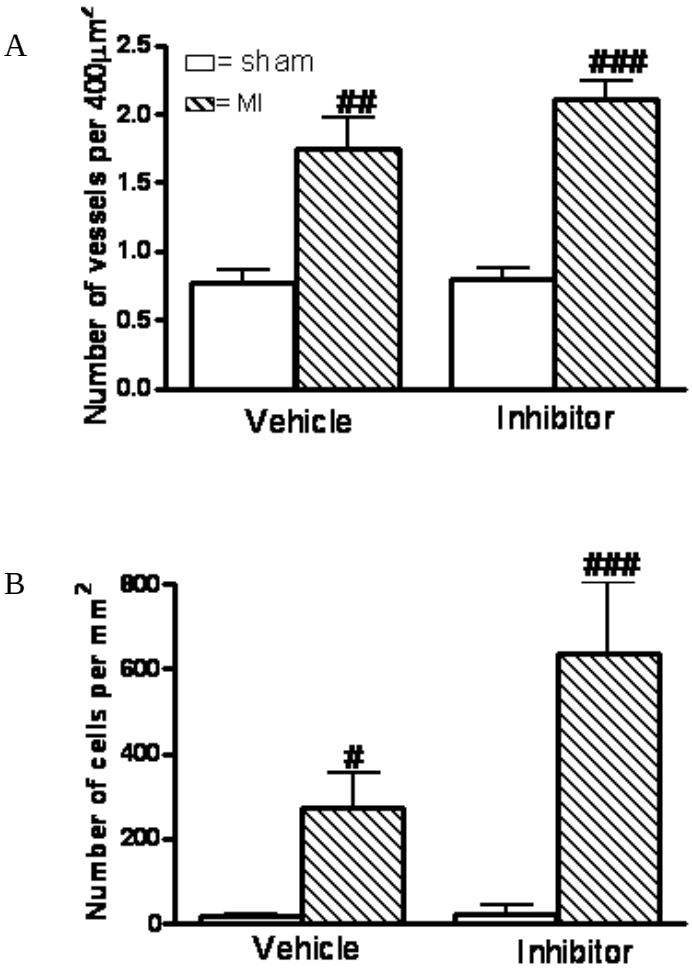

Figure 6-4 Neovascularisation after MI or sham surgery

a) Vessel density was assessed by counting small (<200µm diameter) vessels in the left ventricle. b) Cell proliferation assessed by BrdU incorporation into replicating nuclei, was quantified as number of positive cells per mm^2. Vessel density and cell proliferation were increased after MI compared with sham-operated groups but drug treatment had no effect. n=4 vehicle sham, n=4 vehicle MI, n=5 inhibitor sham, n=7 inhibitor MI. Data are expressed as mean ±SEM. # P<0.05, ## P<0.01, ### P<0.001 Sham vs. MI by 2-way ANOVA.

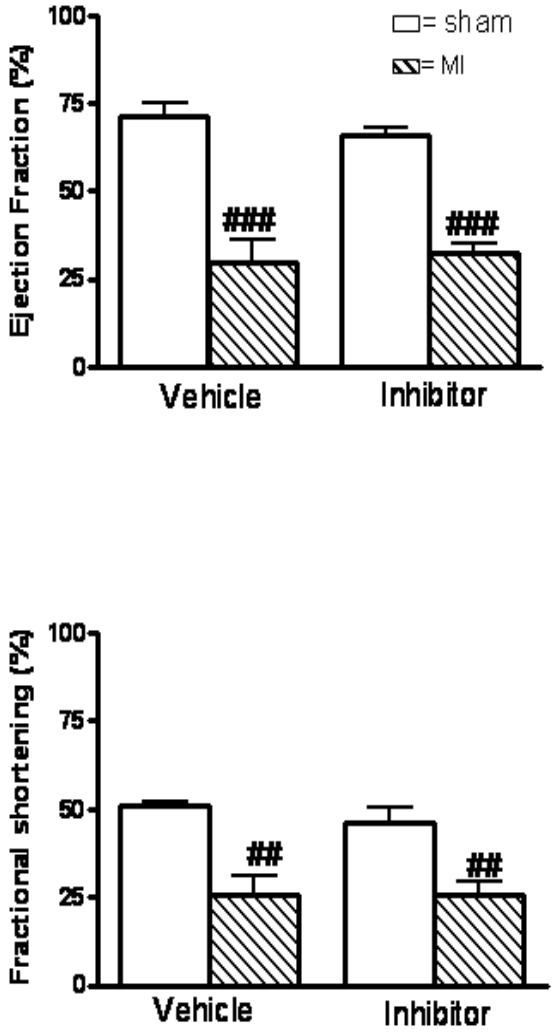

Figure 6-5 Quantified data from echocardiography up to 7 days post-MI or sham-operation.

Left ventricle function was expressed as ejection fraction and fractional shortening using the following equations: Ejection fraction = (left ventricle end diastolic area- left ventricle end systolic area)/ left ventricle end diastolic area x 100. Fractional shortening = (left ventricle end diastolic diameter- left ventricle end systolic diameter)/ left ventricle end diastolic diameter x 100. Ejection fraction and fractional shortening were decreased after MI but drug treatment had no effect. n=4 vehicle sham, n=4 vehicle MI, n=5 inhibitor sham, n=7 inhibitor MI. Data are expressed as mean ±SEM. ## P<0.01, ### P<0.001 sham vs. MI by 2-way ANOVA.

	VEHICLE		INHIBITOR	
	Sham	**MI**	**Sham**	**MI**
LVEDA	16.43±2.04	12.31±0.73	14.74±1.22	13.93±1.26
LVESA	4.55±0.54	8.75±1.20#	5.13±0.67	9.50±1.09#
LVEDD	3.97±0.34	3.59±0.11	3.86±0.15	3.49±0.25
LVESD	1.94±0.14	2.68±0.24	2.05±0.11	2.60±0.25
PWD	0.81±0.11	0.92±0.08	0.77±0.04	1.03±0.12
PWS	1.19±0.11	1.17±0.04	1.38±0.08	1.25±0.10
EF%	71.6±3.32	29.74±6.55 ###	65.72±2.23	32.41±2.89 ###
FS%	50.82±1.42	25.58±5.69 ##	46.60±.4.07	26.00±3.31 ##

Table 6-2 Left ventricle dimensions after MI or sham surgery

LVEDA (left ventricle end diastolic area), LVEDD (left ventricle end diastolic diameter), LVESD (left ventricle end systolic diameter), PWD (posterior wall thickness at diastole) and PWS (posterior wall thickness at systole) did not vary between the groups. LVESA (left ventricle end systolic area) was increased after MI but did not vary between vehicle and inhibitor treated mice. Ejection fraction (EF%) and fractional shortening (FS%) were decreased after MI with drug treatment having no effect. n=4 vehicle sham, n=4 vehicle MI, n=5 inhibitor sham, n=7 inhibitor MI. Data are expressed as mean ± SEM. ## P<0.01, ###P<0.001 Sham vs. MI by 2 way ANOVA.

6.4 Discussion

The aim of the present study was to investigate whether pharmacological inhibition of 11HSD1 after MI would reproduce the beneficial effects of genetically induced 11HSD1 deficiency on murine myocardial infarct healing. It was found, however, that compound 544 treated mice had similar macrophage infiltration, angiogenesis and cardiac function to vehicle treated mice 7 days after MI.

The therapeutic benefit of 11HSD1 inhibition was initially shown with non-selective liquorice derivatives (Monder et al., 1989). Carbenoxolone reduced plasma cholesterol, glucose production and improved insulin sensitivity in humans but also had detrimental effects consistent with inhibition of 11HSD2 (Andrews et al., 2003, Walker et al., 1995). More recently, selective inhibitors of 11HSD1 have been developed including, BVT.14225 (Biovitrum), PF-00915275 (Pfizer) and compound 544 with IC_{50s} of 52, 15 and 97nM respectively, indicating high potency (Barf et al., 2002, Courtney et al., 2008, Hermanowski-Vosatka et al., 2005). Oral administration of compound 544 was shown to produce 60 and 70% inhibition of serum 11HSD1 activity after 1 hour at 10mg/kg and 30mg/kg doses, respectively. This declined rapidly with inhibition being 10 and 30% by 4 hours (Hermanowski-Vosatka et al., 2005). In the same study it was show that administration of the inhibitor in the chow of apoE deficient mice at a dose of approximately 10/mg/kg/day for 8 weeks reduced atherosclerotic plaque progression and improved the lipid profile. Based on these data, a dose of 30mg/kg/day in chow was chosen to achieve effective enzyme inhibition after MI in the current study. Food intake was monitored daily prior to surgery to determine the quantity of drug to be added to the food to attain the required dose of compound 544. Two mice were placed in each cage (my own observations were that mice regain the weight lost after surgery quicker when allowed to recover in groups rather than on their own) thus making it hard to precisely measure the food intake of each mouse. However, data collected in this investigation and in previous studies indicate food intake at approximately 10g per day. Alternatively, other studies have shown that 12 week old male C57Bl6 mice eat on average 4.1g of

standard chow per day (Lewis et al., 2005). In the present study intake varied from 0 to 30g per day. Accurate assessment of food intake proved difficult as food was taken from the tubes by mice and spread across the cage in the bedding. If the estimate intake (4.1g) from Lewis et al is correct it is likely that the dose of 11HSD1 inhibitor received would be closer to 10mg/kg/day rather than 30mg/kg/day (Lewis et al., 2005). Hermanowski-Vosatka et al found that the lower dose of 10mg/kg/day was sufficient to produce physiological effects in a model of atherosclerosis suggesting that this may be enough in post-infarct healing too (Hermanowski-Vosatka et al., 2005). Other work in our laboratory has demonstrated that an oral dose of 30mg/kg compound 544 produces 47% inhibition of hepatic 11HSD1 reductase activity 4 hours after administration (Iqbal, personal communication). This demonstrates that such a dose does not fully inhibit 11HSD1 and may be the reason that that the drug did not reproduce the same effect as the knockout.

After surgery, food intake was consistently reduced so the dose delivered may have been much lower and insufficient to achieve effective enzyme inhibition. Mice received an intra-peritoneal bolus dose of 30mg/kg immediately after surgery which means that 11HSD1 is likely to be inhibited in the first few hours following MI but, after this, and up to at least day 2 when food intake increased; there may have been little enzyme inhibition (Hermanowski-Vosatka et al., 2005). Tissue measurements of 11HSD1 activity were not measured in the current study therefore I cannot rule out the possibility that the 11HSD1 inhibitor was not functional in this model.

Pharmacological inhibitors of 11HSD1 have been reported to have varying effects on body weight. In models of obesity and metabolic syndrome such inhibition has been shown to reduce or have no effect on body weight (Hermanowski-Vosatka et al., 2005, Veniant et al., 2009, Lloyd et al., 2009). In the current study administration of an 11HSD1 inhibitor had no effect on body weight after surgery. Heart weights were similar in both MI and sham-operated groups also in accordance with previous findings (Chapter 4) with drug treatment having no affect either. It has been shown that glucocorticoids can reduce thymus and adrenal gland weight (Brooks et al., 2005).

Administration of an 11HSD1 inhibitor did not have an effect on the thymus or adrenal gland weight in the present study. Additionally, circulating corticosterone levels were similar in vehicle and inhibitor treated animals. This observation is in agreement with other groups that have used 11HSD1 inhibitors for 7 days in a variety of models (Veniant et al., 2009, Hermanowski-Vosatka et al., 2005, Lloyd et al., 2009). Data presented here demonstrates that pharmacological inhibition of 11HSD1 is unlikely to have deleterious effects on activation of the hypothalamic-pituitary-adrenal axis (Hermanowski-Vosatka et al., 2005, Veniant et al., 2009).

Ischaemia associated with MI provokes a powerful inflammatory response that is characterised by neutrophil infiltration early in infarct healing followed by macrophages at 4-7 days after infarction (Chapter 4). Previous work has shown that 11HSD1$^{-/-}$ mice have enhanced neutrophil recruitment at 2 days post-MI relative to C57Bl6 mice (Chapter 4). Alternatively-activated macrophage and general macrophage infiltration was significantly increased in the 11HSD1$^{-/-}$ mice at days 4 and 7 after MI respectively (Chapter 4). In the current study macrophage infiltration was increased 7 days after MI, relative to sham-operated animals, consistent with previous work (Chapter 4) (Dewald et al., 2004, Yang et al., 2002). However, treatment with compound 544 had no effect on macrophage content assessed by mac 2 immuno-reactivity. It was established in Chapter 4 that 11HSD1$^{-/-}$ mice have enhanced angiogenesis (Small et al., 2005, Small, 2005), demonstrated by increased vessel density and cell proliferation, 7 days post-MI. In the current study these parameters were increased 7 days after MI relative to sham as shown previously (Chapter 4) (Lutgens et al., 1999, Small et al., 2005, Virag and Murry, 2003, Ren et al., 2002, Grass et al., 2006). Whilst administration of compound 544 did not influence vessel density, relative to vehicle treatment, there was a trend for increased cell proliferation in the drug treated group. This suggests that administration of an 11HSD1 inhibitor may have direct effects on cell replication.

The results presented in this chapter are preliminary with low n numbers in some of the groups. It is, therefore, difficult to make firm conclusions from the data. However, there are several possible reasons why the inhibitor did not reproduce the outcomes previously

observed in the 11HSD1$^{-/-}$ mice. Firstly, the concentration of the inhibitor achieved in target tissues may not have been sufficient to achieve enzyme inhibition, as discussed above. The ability of the drug to inhibit 11HSD1 *in vivo* was based on work conducted by others in the lab (Iqbal, personal communication) and was not measured in the current study. Assessment of 11HSD1 activity in the heart should be conducted in future studies as there is a small possibility that compound 544 was not functional. Alternatively sufficient inhibition may have been achieved but not until later in the infarct healing process. It was noted that inhibition of the enzyme may have been low in the first few days after surgery due to reduced food intake. The negative outcome of the study may indicate that modification of events occurring in this early phase are critical in determining the later inflammatory and angiogenic responses. These events may include the enhancement in neutrophil infiltration that we have noted previously (Chapter 4). Neutrophil death provides a stimulus for monocyte infiltration (Mosser and Edwards, 2008, Savill et al., 1989a, Savill et al., 1989b). Post-infarct macrophage infiltration is strongly associated with angiogenesis (van Amerongen et al., 2007, Nahrendorf et al., 2007, Fraccarollo et al., 2008) and a reduction in this influx may reduce the stimulus for new blood vessel growth. Neutrophils are an important source of IL-4, a cytokine vital in determining macrophage phenotype (Brandt et al., 2000, Loke et al., 2002) and, as such, a reduction in this cytokine may reduce the abundance of alternatively activated macrophages. In a previous study (Chapter 4), the number of alternatively-activated macrophages was different between 11HSD1$^{-/-}$ and C57Bl6 mice at day 4 but not day 7. For that reason they were not quantified in the current study. Alternatively-activated macrophages secrete IL-8, which was increased in 11HSD1$^{-/-}$ mice 7 days post-MI (Chapter 4), and therefore it would be useful to look at its expression as a surrogate for alternatively-activated macrophage infiltration (Loke et al., 2002, Mosser and Edwards, 2008). Neutrophils have also been more directly linked to angiogenesis. Depletion of neutrophils prior to the 'angiogenic switch' in tumours can prevent blood vessel growth (Nozawa et al., 2006). Further studies are required to assess the impact of pharmacological 11HSD1 inhibition on early infarct healing processes and their role in determining longer term outcome.

Another explanation for the lack of effectiveness of 11HSD1 inhibitor administered after MI is that inhibition of the 11HSD1 is necessary before induction of myocardial injury. It was noted in Chapter 3 that $11HSD1^{-/-}$ mice have significantly lighter hearts that C57Bl6 controls. In addition, 11HSD1 gets upregulated upon differentiation of monocytes to macrophages (Gilmour et al., 2006) and inhibition of the enzyme delays attainment of macrophage phagocytic competence (Gilmour et al., 2006). It is possible that reduced glucocorticoid regeneration prior to onset of MI may have altered the healing response. Programming of monocytes by reduced local glucocorticoids prior to injury may alter their phenotype. Mononuclear cells are liberated from the bone marrow along with progenitor cells post-MI and have been implicated in angiogenesis (Shintani et al., 2001, Orlic et al., 2001, Kastrup et al., 2006). Alterations in the propensity of cells to be mobilised from this location may have an effect on inflammation and angiogenesis and, indeed, 11HSD1 is expressed in the bone marrow (Hardy et al., 2006, Sasaki et al., 2007, Orlic et al., 2001, Kastrup et al., 2006). It is possible that reduced glucocorticoid regeneration in the bone marrow has an effect on the maturation state and liberation potential of inflammatory and progenitor cells. These issues could be tackled by pre-treatment of mice with the 11HSD1 inhibitor prior to MI.

Interestingly, it has previously been shown from this laboratory that the non-selective 11HSD1 inhibitor, carbenoxolone, can prevent the anti-angiogenic effect of 11-dehydrocorticosterone, but not corticosterone, in isolated aortic rings demonstrating that locally regenerated glucocorticoids are anti-angiogenic (Small et al., 2005). One of the mechanisms by which glucocorticoids mediate their angiostatic effect is via reduction of cell proliferation (Banciu et al., 2008b). There was a trend for cell proliferation, assessed by BrdU incorporation into replicating nuclei, to be increased in treated mice, although there was no parallel increase in vessel density. Angiogenesis involves co-ordination of several steps, including proliferation endothelial cells and pericytes, and enhancing one aspect of the process does not necessarily result in robust blood vessel growth (Kido et al., 2005, Greenberg et al., 2008, Korpisalo et al., 2008, Risau, 1997).

While the data presented here suggest that compound 544 has no effect on murine infarct healing it is important to bear in mind several methodological issues. It is likely that inhibition of 11HSD1 was insufficient until day 3. It is probable that this window early in infarct healing is important in coordinating the latter healing response. Increasing the concentration of the drug in the food given just after surgery or altering route of administration may be beneficial. Repeated gavaging and/or intra peritoneal injections may result in extra stress (i.e., greater systemic corticosterone) but use of a mini-pump to deliver the dose of drug throughout the study may be more effective (Balcombe et al., 2004).

Administration of the MR antagonist, epleronone, to rats after MI enhances inflammation and angiogenesis, and improves left ventricular remodelling (Fraccarollo et al., 2008). Whilst epleronone has been used successfully in the clinic it may cause hyperkalaemia and does not prevent the adverse effects of GR activation in infarct healing (Pitt et al., 2005). Inhibition of 11HSD1 is an attractive alternative. Selective small molecule inhibitors of 11HSD1 are still under development and are now entering clinical trials for other diseases (Tu et al., 2008, Su et al., 2009, Hawkins, 2008). An Incyte compound (INCB013739) has entered phase II clinical trials and has been shown to improve insulin sensitivity, plasma LDL cholesterol and plasma total cholesterol in patients with type 2 diabetes (Hawkins, 2008). Furthermore there was a trend for improved fasting glucose, insulin sensitivity and plasma triglycerides in inhibitor treated patients (Hawkins, 2008). Trials to determine the effectiveness of such inhibitors in atherosclerosis and obesity are on the horizon. The preliminary data presented here unfortunately is not conclusive and the use of 11HSD1 inhibitors post-MI certainly warrants further investigation.

7 Discussion

The first aim of this thesis was to investigate whether the previously reported beneficial effects of 11HSD1 deficiency were related to an underlying cardiac phenotype (Chapter 3). Secondly, I aimed to characterise the healing response after MI in 11HSD1$^{-/-}$ mice and to investigate if the enhanced angiogenic response in 11HSD1$^{-/-}$ mice would be preceded by enhanced inflammation (Chapter 4). In Chapter 5 I investigated whether the enhancement in vessel density and cardiac function remained in the long term. The final aim of this thesis was to establish whether the effect of the 11HSD1$^{-/-}$ could be recapitulated using a commercially bought 11HSD1 inhibitor (Chapter 6).

7.1 Basal cardiac phenotype

The metabolic and vascular influence of 11HSD1$^{-/-}$ in mice has been studied extensively in this laboratory (Walker and Seckl, 2003, Hadoke et al., 2001, Kotelevtsev et al., 1997, Morton et al., 2004, Morton et al., 2001, Hadoke et al., 2006, Christy et al., 2003, Paterson et al., 2006), but until now the cardiac phenotype was relatively unknown. The work described in this thesis establishes that 11HSD1$^{-/-}$ mice have significantly lighter hearts compared to C57Bl6 mice and this is not related to reduced body weight. The gross inspection of hearts from 11HSD1$^{-/-}$ mice indicated that the reduction in heart weight may be due to a decrease in cardiomyocyte cross-sectional area, which should be confirmed by morphometric measurements in future studies. Glucocorticoids stimulate expression of genes that promote cellular hypertrophic and I can speculate that a local reduction in corticosterone might reduce cardiomyocyte size via this mechanism (Yoshikawa et al., 2009). These observations may have implications when considering the response of 11HSD1$^{-/-}$ mice to MI. Hypertrophy of the non-infarcted myocardium is part of the healing response after MI, which compensates for cardiomyocyte loss and is apparent by 4 weeks after experimental MI in mice (Mork et al., 2007). It is possible that 11HSD1$^{-/-}$ mice have a modified response to this in infarct healing due to underlying

differences in their cardiomyocytes. However, the studies presented in Chapters 4 and 5 demonstrate that there was no indication of differences in heart weight between 11HSD1$^{-/-}$ and C57Bl6 mice up to 4 weeks after MI, suggesting that this is not the case in this time frame. It may be of interest to culture cardiomyocytes from 11HSD1$^{-/-}$ and C57Bl6 mice and compare their response to hypertrophic stimuli, such as phenylephrine (Gan et al., 2005). Alternatively, the hypertrophic response could be compared *in vivo*, for example, using the aortic constriction model of left ventricular pressure overload. Importantly, despite the decreased heart weight there were no overt structural abnormalities in the 11HSD1$^{-/-}$ hearts relative to controls and cardiac function was similar.

7.2 What mediates the increase in angiogenesis after MI in 11HSD1$^{-/-}$ mice?

Angiogenesis is enhanced in 11HSD1$^{-/-}$ mice, relative to C57Bl6 controls 7 days post-MI and is associated with augmented myocardial IL-8 mRNA expression and increased cell proliferation (Chapter 4). The enhancement of cardiac function occurs in parallel to this neovascularisation and has been demonstrated in several other studies (Engel et al., 2006, Sasaki et al., 2007, Small, 2005, Payne et al., 2007, Orlic et al., 2001, Kastrup et al., 2006, Kido et al., 2005, Fujii et al., 2009, Siragusa et al., 2010, Yang et al., 2010). Several other factors such as SDF-1α, GM-CSF and G-CSF have also been implicated in increasing vessel density post-MI and warrant further investigation in this model (Takahashi et al., 2006, Sasaki et al., 2007, Lakkisto et al., 2010). Most studies examining infarct angiogenesis use standard mature vessel markers such as CD31 and von Willebrand factor and, therefore, do not truly distinguish between new and old vessels. In order to identify new blood vessels immuno-labelling specific markers of angiogenic vasculature such as APN/CD13 and CD105/endoglin could be used (Rangel et al., 2007, Bhagwat et al., 2001, van Laake et al., 2006). An alternative method would be to use fluorophore tagged cNGR, a peptide sequence that homes to CD13 positive cells, and localises to sites of neovascularisation (Buehler et al., 2006).

11HSD1$^{-/-}$ mice have a sustained enhancement in vessel density after infarct healing has completed (Chapter 5). Moreover, the vessels were pericyte coated suggesting maturity and it is likely that they will be maintained in the long term (Grass et al., 2006, Ren et al., 2002). The functionality of these vessels on the infarct border is yet to be elucidated. Assessment of perfusion can be made using micro-angiography (Cheng et al., 2007) but resolution is too low for accurate quantification (Bondke et al., 2007). Laser Doppler is an alternative, but this method also has limitations as penetration depth is low (Scholz et al., 2002, Bondke et al., 2007). Perfusion of fluorescently labelled microspheres, ultrasound contrast microbubbles or microbubbles tagged with endothelial cell specific antibodies are alternatives that could be considered in future studies (Liu et al., 2007, Dickie et al., 2006).

11HSD1$^{-/-}$ mice also have an augmented inflammatory response post-MI, demonstrated by increased neutrophil and macrophage infiltration along with enhanced MCP-1 mRNA expression. Interestingly, 11HSD1$^{-/-}$ mice have significantly lighter spleens 28 days after MI relative to C57Bl6 controls (Chapter 5). A recent publication provides evidence for the spleen being a reservoir for the monocytes that are liberated after MI (Swirski et al., 2009). It is possible that increased monocyte liberation from the spleen in 11HSD1$^{-/-}$ mice may be the source of increased monocyte infiltration into the heart. It is well established that glucocorticoids have immuno-modulatory actions including, inhibiting the production of inflammatory cytokines, upregulating anti-inflammatory mediators and modulating phagocytosis by macrophages (Galon et al., 2002, Cupps and Fauci, 1982, Barnes, 1998, Gilmour et al., 2006, Park et al., 2009). 11HSD1 is upregulated during the maturation of monocytes to macrophages and the local amplification of glucocorticoids by this enzyme may serve to curtail the inflammatory response (Gilmour et al., 2006, Chapman et al., 2009). The enhancement of inflammation in 11HSD1$^{-/-}$ mice has been demonstrated in a variety of models including peritonitis, pleurisy and serum arthritis models, (Gilmour et al., 2006, Chapman et al., 2009, Coutinho 2009).

Interestingly, data presented in Chapter 4 demonstrates an increase in alternatively-activated, pro-resolution, angiogenic macrophages (M2) in the 11HSD1$^{-/-}$ mice, relative

to C57Bl6 controls, 4 days after MI. Maturation of macrophages to this M2 phenotype is stimulated by IL-4 which is reportedly secreted by neutrophils (Mosser and Edwards, 2008, Loke et al., 2002, Brandt et al., 2000). An investigation of IL-4 expression, as the major neutrophil-derived mediator of alternate macrophage programming (Loke et al., 2002, Brandt et al., 2000), would be worthwhile to establish the contribution of neutrophils in 11HSD1$^{-/-}$ mice. There is increasing support for the role of macrophages in stimulating angiogenesis, particularly in cancer models (Sica et al., 2006, Mosser and Edwards, 2008). Macrophage depletion, achieved by administration of liposome-encapsulated clodronate, reduces angiogenesis in aortic ring explants and this effect can be reversed by replenishment with bone marrow-derived macrophages (Gelati et al., 2008). Furthermore, in rodent models of MI, clodronate can reduce angiogenesis and scar formation, and impair cardiac function (Fraccarollo et al., 2008, Nahrendorf et al., 2007, van Amerongen et al., 2007). The work presented in this thesis shows that IL-8, an angiogenic chemokine secreted by M2 macrophages, was increased just after their peak, at day 7 providing a link between macrophages and angiogenesis in this model.

As glucocorticoids can inhibit both inflammation and angiogenesis it is unknown whether the enhancement in angiogenesis in 11HSD1$^{-/-}$ mice is a direct effect of reduced local glucocorticoids or whether it is secondary to the enhancement in inflammation in this model. I cannot rule out direct inhibition of angiogenesis by glucocorticoids but the weight of evidence does support a key contribution of inflammatory cells. Assessment of angiogenesis after macrophage depletion using clodronate (van Amerongen et al., 2007, Nahrendorf et al., 2007, Fraccarollo et al., 2008) or by conditional ablation of CD11b positive cells, mediated by the diphtheria toxin receptor (Duffield et al., 2005), would confirm a role for these cells.

7.3 Post-infarct scar formation

Excessive inflammation is associated with enhanced fibrosis (Liu et al., 2009). Despite an increase in inflammation, the fibrotic response was not enhanced after MI in

11HSD1$^{-/-}$ mice. While actual scar size and collagen content did not differ between the C57Bl6 and 11HSD1$^{-/-}$ mice, the C57Bl6 mice had significantly thinner scars that had a tendency to be longer by 4 weeks post-MI. Scar thinning is correlated with risk of cardiac rupture (Dai et al., 2005, Nahrendorf et al., 2006). Glucocorticoids have been shown to have adverse effects on scar formation in several experimental models (Vivaldi et al., 1987) . Chronic administration of a high dose of methylprednisolone to dogs enhanced scar thinning, increased infarct length and impaired cardiac function with no effect on total collagen or histological appearance (Hammerman et al., 1983a). As expected, the converse is seen in 11HSD1$^{-/-}$ mice. The authors of the previous studies postulate that these adverse effects of glucocorticoids are due to diminished removal of necrotic tissue resulting from inhibition of inflammation. Hammerman et al and Brown et al support this hypothesis by showing that non-steroidal anti-inflammatory drugs, such as ibuprofen and indomethacin, have a similar effect on infarct scar dimensions (Hammerman et al., 1983b, Brown et al., 1983). Perhaps 11HSD1$^{-/-}$ mice have faster replacement of necrotic tissue with granulation tissue. Prolongation of this process may mean that the weakened infarct undergoes expansion prior to deposition of normal collagen (Virag and Murry, 2003). It would be interesting to look at an intermediate time point (week 2) to see whether the area of necrosis is greater in C567Bl6 mice. Infarct expansion can be affected by blood pressure (Pfeffer and Braunwald, 1990, Pierard et al., 1987). Genetic deletion of 11HSD1 has no effect on basal blood pressure, while 11HSD2$^{-/-}$ mice are hypertensive (Kotelevtsev et al., 1999, Kotelevtsev et al., 1997). Blood pressure was not measured in the current study and there have been no published reports of altered blood pressure or alterations in vascular function in 11HSD1$^{-/-}$ mice (Hadoke et al., 2001). However, recent work has demonstrated that carefully measured blood pressure is lower in 11HSD1/ApoE double knockout mice relative to ApoE knockout controls (Iqbal, personal communication). Blood pressure should be measured by tail cuff or carotid artery cannulation in future studies.

Importantly, the improvement in cardiac function observed 7 days post-MI in the 11HSD1$^{-/-}$ mice was maintained at 4 weeks, in parallel with the sustained enhancement

of vessel density in the infarct border. The trend for a reduction in scar length in 11HSD1$^{-/-}$ mice suggests that the increase in vessel density may enhance cardiomyocyte salvage in the infarct border. This could be the source of improved function. Alternatively, the type of collagen making up the scar could be different. A scar with a high proportion of the elastic collagen type III, relative to the stiff type 1, may favour improved cardiac function. This can be investigated using immunohistochemistry. While it is exciting that 11HSD1$^{-/-}$ mice have improved heart function 4 weeks after MI, it is dangerous to over interpret data from a midterm assessment. It has been reported previously that significant improvements in cardiac function 4 weeks after MI were not observed after 3 months (van Laake et al., 2008). A longer term study with the 11HSD1$^{-/-}$ mice to allow development of heart failure is required to determine the true long term potential of 11HSD1 inhibition after MI.

7.4 The potential impact of metabolic changes

One aspect of the 11HSD1$^{-/-}$ mouse phenotype that may have a role in recovery post-MI, but was beyond the scope of this thesis, was the possible effect of the knockout on post-infarct metabolism. After MI, systemic release of glucocorticoids can have effects on the metabolic status of the individual by altering the turnover of free and stored energy (Opie, 1971, Walker, 2007). Glucocorticoids increase hepatic gluconeogenesis, fatty acid and glucose release, along with inhibiting insulin secretion from the pancreas (Walker, 2007a). After MI, glucose utilisation in the heart increases at the expense of fatty acid metabolism, due to the anoxic conditions, and this leads to accumulation of lactate and hydrogen ions which can impair cardiac function (Opie, 1971). In patients, a high level of circulating glucose after admission for MI is positively correlated with development of heart failure and mortality risk (Kosiborod, 2008) and is inversely correlated with ejection fraction after coronary angioplasty or thrombolysis (Ceriello, 2008). The benefits of using insulin to reduce plasma glucose after MI is somewhat contentious; however, there is evidence that such therapy may lower mortality

(Kosiborod, 2008). It has previously been shown that 11HSD1$^{-/-}$ mice resist high fat feeding, have enhanced glucose tolerance, an improved lipid profile and insulin sensitivity (Morton et al., 2004, Morton et al., 2001, Kotelevtsev et al., 1997). It is possible that these changes in 11HSD1$^{-/-}$ mice may translate to alterations on the metabolic disturbances associated with MI. While the post-infarct effect of 11HSD1 deletion on hormonal or metabolic pathways was not investigated the data presented here strongly suggests that the beneficial effects are mediated within the heart. Furthermore, data presented in this thesis demonstrate that there was no difference in circulating corticosterone at any of the time points investigated.

7.5 Therapeutic potential of pharmacological 11HSD1 inhibition

Administration of a small molecule inhibitor of 11HSD1 did not recapitulate the effect of genetic deletion of 11HSD1 on infarct healing in terms of inflammation, angiogenesis and cardiac function. This was a preliminary study and, therefore, it is is hard to make firm conclusions regarding the data. The inhibitor (compound 544) used had already been shown to inhibit 11HSD1 *in vivo* and proved effective in models of diabetes, obesity and atherosclerosis (Hermanowski-Vosatka et al., 2005, Iqbal, personal communication). However, the drug was administered in the food, intake of which was severely compromised immediately after surgery; only a very low dose is likely to have been received in the first 2 days after surgery. This dose may have been insufficient to adequately inhibit 11HSD1 activity during the infarct healing phase. The results of this study may, therefore, point to a key role of events occurring early after MI in determining the eventual outcome. It is likely that the enhanced neutrophil influx observed 2 days after MI in the 11HSD1$^{-/-}$ mice did not occur in the inhibitor treated group, thus, potentially reducing the stimulus for downstream infarct healing events (Savill et al., 1989b, Savill et al., 1989a, Loke et al., 2002, Brandt et al., 2000). To avoid this confounding issue it would be advisable to use an implanted osmotic mini pump to administer the 11HSD1 inhibitor in future studies. Furthermore the inhibition of

11HSD1 in the heart should also be measured in order to be fully confident that the inhibitor is indeed inhibiting the enzyme. The time at which 11HSD1 inhibition commences may be paramount in improving the infarct healing response. As effects of 11HSD1 deficiency on inflammation are observed in the early days after MI pharmacological inhibitors of 11HSD1 should be administered within the first day after MI. It is also possible that the reason compound 544 did not recapitulate the $11HSD1^{-/-}$ mice was because of programmed differences in $11HSD1^{-/-}$ compared with the C57Bl6 mice. 11HSD1 is expressed in the bone marrow and alterations in the propensity of mononuclear and progenitor cells to be mobilised from this location may have an effect on inflammation and angiogenesis (Hardy et al., 2006, Orlic et al., 2001, Sasaki et al., 2007, Kastrup et al., 2006). Inhibition of 11HSD1 before infarction may therefore, be necessary in order to prime the system for a modified inflammatory response. Comparisons of outcomes when an 11HSD1 inhibitor is administered prior to surgery will also be of interest. Flow cytometric analysis in Chapter 4 showed that there was no difference in the number and type of monocytes in the bone marrow, at least at 7 days post-MI, but other cell types and their behaviour warrant further investigation.

7.6 The roles of GR and MR after MI

The majority of evidence from experimental and clinical studies suggests that glucocorticoids are protective when administered initially after MI as they reduce infarct size via stimulation of the GR (Libby et al., 1973, Morrison et al., 1976, Hafezi-Moghadam et al., 2002). In the present study the systemic stress release of corticosterone after MI was comparable in C57Bl6 and $11HSD1^{-/-}$ mice and infarct size was not affected by genotype. Endogenous glucocorticoids can activate both the GR and MR due to their high homology (Funder and Mihailidou, 2009). However, as there are no obvious surrogate markers for their activation it is hard to determine the relative contribution of activation of GR and MR in MI healing. Additionally, receptor specific inhibitors have effects beyond those in the heart. It is, therefore, difficult to know for

certain whether the beneficial effects of the 11HSD1 knockout are due to reduced GR or MR signalling. Evidence certainly suggests that the beneficial role of glucocorticoids on initial infarct size is mediated by the GR (Hafezi-Moghadam et al., 2002) while the detrimental influence of glucocorticoids is likely to be mediated by activation of the MR (Mihailidou et al., 2009). Inhibition of inflammation by GR activation is well established. Less acknowledged is the ability of MR to mediate inhibition of inflammation after MI (Galon et al., 2002, Cupps and Fauci, 1982, Barnes, 1998). Immediate MR blockade, with epleronone, after infarction enhances both inflammation and angiogenesis, reduces infarct expansion and improves cardiac function 7 days post-MI in rats without influencing infarct size (Fraccarollo et al., 2008). Prevention of monocyte infiltration with clodronate abrogated the beneficial effects of MR antagonism, demonstrating the pivotal role of inflammation in MR mediated improvement in myocardial infarct healing (Fraccarollo et al., 2008). MR antagonists can suppress NF-κB activation, thus inhibiting inflammation (Sun et al., 2002). In addition, in a rat model of MI spironolactone treatment, starting immediately after MI and continuing for 14 days, improves cardiac function and decreases interstitial fibrosis and apoptosis, despite no change in infarct area or collagen volume (Takeda et al., 2007). There is limited evidence regarding the direct angiostatic potential of mineralocorticoids whereas glucocorticoids are well established as potent angiostatic agents (Longenecker et al., 1982, Ullian, 1999, Folkman and Ingber, 1987, Hori et al., 1996, Steinbrech et al., 2000, Yano et al., 2006). Mice treated with the GR antagonist, RU38486, exhibited enhanced angiogenesis 7 days post-MI, relative to vehicle treated controls (Small et al., 2005, Small, 2005). This suggests that the reduced glucocorticoid regeneration in $11HSD1^{-/-}$ mice can enhance angiogenesis through reduced GR signalling whilst enhanced inflammation may be mediated by reduced GR and MR signalling. The post-infarct response of the $11HSD1^{-/-}$ mice is similar to that of pharmacological MR blockade in rats which suggests that the beneficial effects of reduced tissue regeneration of corticosterone are mediated by reduced MR activation in the healing phase.

The detrimental effects of glucocorticoids on post-MI scar formation may be mediated by either GR or MR. However, there is overwhelming evidence for the role of MR mediated fibrosis induced by the action of aldosterone in other models. Infusion of aldosterone, or its precursor, to uni-nephrectomised rats drinking 1% NaCl solution leads to cardiac fibrosis and hypertrophy (Young and Funder, 1996, Rickard et al., 2006). These effects were reversed by the co-administration of an MR antagonist demonstrating that this is a MR mediated effect (Young and Funder, 1996, Rickard et al., 2006). In these studies blood pressure was increased, yet several others have shown that the fibrosis is independent of blood pressure. Nagata et al and Kobayashi et al achieved a decrease in fibrosis and hypertrophy using a non-antihypertensive dose of epleronone (Nagata et al., 2006) (Kobayashi et al., 2006). There is some evidence that glucocorticoid action on MR may vary according to tissue and the oxidative conditions. In isolated rabbit cardiomyocytes aldosterone, but not cortisol, activates the Na^+/K^+ ATPase pump under basal conditions (Funder and Mihailidou, 2009). When the cells are under oxidative stress cortisol mimics aldosterone and increases the activity of this pump (Funder and Mihailidou, 2009). As MI creates a state of oxidative stress it follows that, under these conditions, glucocorticoids could act as MR agonists.

Blockade of MR has been shown to be beneficial in patients with heart failure and after MI. In the RALES study (Randomized ALdactone Evaluation Study) patients with severe heart failure and an ejection fraction of 35% or lower were given spironolactone on top of standard therapy (Pitt et al., 1999). Two years later those receiving spironolactone had a 30% reduction in risk of death and this was attributed to a reduction in progression of heart failure and sudden cardiac death (Pitt et al., 1999). In the EPHESUS clinical study (Eplerenone Post-Acute Myocardial Infarction Heart Failure Efficacy and Survival) patients were randomised to receive eplerenone or placebo from 3-14 days after MI (Pitt et al., 2005). At 30 days the risk of death was reduced by 31% in eplerenone treated groups (Pitt et al., 2005). This was associated with a decrease in blood pressure (Pitt et al., 2005). A more recent analysis of this study, after a 16 month follow up, showed that this benefit was only found when eplerenone

treatment was started 3-7 days after MI and was absent when treatment started 7 days after MI (Adamopoulos et al., 2009). These beneficial effects are found in parallel with reduced collagen turnover (Iraqi et al., 2009).

While epleronone is beneficial after MI and in the treatment of heart failure it does have side effects. There has been an increase in the hospitalisation and subsequent death of elderly patients from hyperkalemia as a result of administration of MR antagonists, especially when used in conjunction with other cardiovascular drugs such as beta blockers (McMurray and O'Meara, 2004). These elderly patients are more susceptible to hyperkalemia due to reduced production of aldosterone (McMurray and O'Meara, 2004). Caution must be taken when administering MR blockers to this population and perhaps 11HSD1 inhibition could be a particularly useful alternative therapy in such cases.

7.7 Progenitor and stem cells

There is now plentiful evidence to suggest that enhancement of angiogenesis on the infarct border improves cardiac function after MI (Yamahara and Itoh, 2009, van der Laan et al., 2009). Strategies to enhance angiogenesis include direct injection of growth factors (e.g. VEGF) to stimulate angiogenesis directly, or injection of factors (e.g. SDF-1α and G-CSF) that enhance mobilisation of progenitor cells from the bone marrow. Such techniques have been associated with enhanced angiogenesis and improved cardiac function, however there is also considerable evidence contending this (Ellis et al., 2006, Losordo et al., 1998, Simons, 2005, Ruixing et al., 2007, Pitchford et al., 2009, Sasaki et al., 2007, Orlic et al., 2001). Injection of bone marrow-derived cells (BMDC) directly into the infarcted heart has had more success (Lasala and Minguell, 2009). The BOOST clinical trial demonstrated that an intra-coronary injection of BMDC can improve ejection fraction, but not left ventricle systolic function 18 months after MI (Meyer et al., 2006). This is being followed up by BOOST 2 which aims to give a more comprehensive assessment of the mechanism of improved cardiac function. BMDC have also been shown to enhance cardiac regeneration (Fazel et al., 2006). In more recent

clinical trials BMDCs have shown to improve left ventricle function at 6 months and 2 years (Plewka et al., 2009, Assmus et al., 2010). Furthermore, at 2 years this was associated with a reduction in occurrence of adverse cardiovascular events (Plewka et al., 2009, Assmus et al., 2010). Endothelial progenitor cells (EPC) are one of the BMDC populations that are reported to have a role in post-infarct angiogenesis. Particularly relevant for the work presented here is that monocytes express some of the typical EPC markers and can demonstrate similar behaviour (Apostolakis et al., 2009). It is possible that this is the source of the enhanced angiogenesis in the 11HSD1 deficient model as 11HSD1 is expressed in the bone marrow. The mechanism of BMDC is unclear; however evidence is mounting for a paracrine mechanism (Chien, 2006, Frantz et al., 2008). BMDCs transfected with growth factors have proved particularly impressive in animal models lending support for this (Yau et al., 2005, Payne et al., 2007). Despite a great deal of evidence suggesting that these techniques are beneficial to infarct healing, there is also considerable evidence suggesting there is no benefit (Terrovitis et al., 2004, Maekawa et al., 2004, Jujo et al., 2008). Inconsistency in the purification of cells, cell number and route of administration are some of the confounding variables that make it difficult to directly compare these studies.

7.8 Concluding remarks

Previous work had shown that deficiency of 11HSD1 is associated with increased vessel formation in experimental models of angiogenesis *in vitro* and *in vivo*, including in the healing myocardium of mice that have undergone MI (Small et al., 2005). Data presented in this thesis extends these observations and demonstrates that increased neovascularisation during infarct healing in $11HSD1^{-/-}$ mice follows augmented accumulation of neutrophils and of alternatively activated macrophages, and is in parallel with increased expression of the pro-angiogenic chemokine, IL-8, and enhanced cell proliferation. Simultaneous with increased neovascularisation is an improvement in cardiac function. Enhanced blood vessel density is retained for at least 28 days post-MI

in 11HSD1$^{-/-}$ mice, by which time vessels on the infarct border have matured, and is associated with a reduction in scar thinning and with sustained improvement in cardiac function. Further studies are required to determine whether this benefit of 11HSD1 inhibition continues into the long term as the animals develop heart failure. 11HSD1 inhibitors are currently under development for diseases such as obesity, diabetes and atherosclerosis (Hermanowski-Vosatka et al., 2005). Indeed, orally bio-available, selective inhibitors of 11HSD1 are already in clinical trials for type 2 diabetes. The evidence presented here indicates that small molecule inhibitors of 11HSD1 may also be of benefit in myocardial infarct healing.

8 References

Adamopoulos, C., Ahmed, A., Fay, R., Angioi, M., Filippatos, G., Vincent, J., Pitt, B. & Zannad, F. (2009) Timing of eplerenone initiation and outcomes in patients with heart failure after acute myocardial infarction complicated by left ventricular systolic dysfunction: insights from the EPHESUS trial. *Eur J Heart Fail,* 11**,** 1099-105.

Aguilera, G., Rabadan-Diehl, C. & Nikodemova, M. (2001) Regulation of pituitary corticotropin releasing hormone receptors. *Peptides,* 22**,** 769-74.

Andrews, R. C., Rooyackers, O. & Walker, B. R. (2003) Effects of the 11 beta-hydroxysteroid dehydrogenase inhibitor carbenoxolone on insulin sensitivity in men with type 2 diabetes. *J Clin Endocrinol Metab,* 88**,** 285-91.

Apostolakis, S., Shantsila, E. & Lip, G. Y. (2009) Vascular imaging as a cardiovascular risk stratification tool in systemic lupus erythematosus. *J Rheumatol,* 36**,** 2141-3.

Arras, M., Strasser, R., Mohri, M., Doll, R., Eckert, P., Schaper, W. & Schaper, J. (1998) Tumor necrosis factor-alpha is expressed by monocytes/macrophages following cardiac microembolization and is antagonized by cyclosporine. *Basic Res Cardiol,* 93**,** 97-107.

Assmus, B., Rolf, A., Erbs, S., Elsasser, A., Haberbosch, W., Hambrecht, R., Tillmanns, H., Yu, J., Corti, R., Mathey, D. G., Hamm, C. W., Suselbeck, T., Tonn, T., Dimmeler, S., Dill, T., Zeiher, A. M. & Schachinger, V. (2010) Clinical outcome 2 years after intracoronary administration of bone marrow-derived progenitor cells in acute myocardial infarction. *Circ Heart Fail,* 3**,** 89-96.

Athanasuleas, C. L., Buckberg, G. D., Stanley, A. W., Siler, W., Dor, V., Didonato, M., Menicanti, L., De Oliveira, S. A., Beyersdorf, F., Kron, I. L., Suma, H., Kouchoukos, N.

T., Moore, W., Mccarthy, P. M., Oz, M. C., Fontan, F., Scott, M. L. & Accola, K. A. (2004) Surgical ventricular restoration: the RESTORE Group experience. *Heart Fail Rev,* 9**,** 287-97

Auffray, C., Fogg, D., Garfa, M., Elain, G., Join-Lambert, O., Kayal, S., Sarnacki, S., Cumano, A., Lauvau, G. & Geissmann, F. (2007) Monitoring of blood vessels and tissues by a population of monocytes with patrolling behavior. *Science,* 317**,** 666-70.

Axelrod, J. & Reisine, T. D. (1984) Stress hormones: their interaction and regulation. *Science,* 224**,** 452-9.

Balcombe, J. P., Barnard, N. D. & Sandusky, C. (2004) Laboratory routines cause animal stress. *Contemp Top Lab Anim Sci,* 43**,** 42-51.

Bamberger, C. M. & Chrousos, G. P. (1995) The glucocorticoid receptor and RU 486 in man. *Ann N Y Acad Sci,* 761**,** 296-310.

Banciu, M., Metselaar, J. M., Schiffelers, R. M. & Storm, G. (2008a) Antitumor activity of liposomal prednisolone phosphate depends on the presence of functional tumor-associated macrophages in tumor tissue. *Neoplasia,* 10**,** 108-17.

Banciu, M., Metselaar, J. M., Schiffelers, R. M. & Storm, G. (2008b) Liposomal glucocorticoids as tumor-targeted anti-angiogenic nanomedicine in B16 melanoma-bearing mice. *J Steroid Biochem Mol Biol,* 111**,** 101-10.

Barf, T., Vallgarda, J., Emond, R., Haggstrom, C., Kurz, G., Nygren, A., Larwood, V., Mosialou, E., Axelsson, K., Olsson, R., Engblom, L., Edling, N., Ronquist-Nii, Y., Ohman, B., Alberts, P. & Abrahmsen, L. (2002) Arylsulfonamidothiazoles as a new class of potential antidiabetic drugs. Discovery of potent and selective inhibitors of the 11beta-hydroxysteroid dehydrogenase type 1. *J Med Chem,* 45**,** 3813-5.

Barnes, P. J. (1998) Anti-inflammatory actions of glucocorticoids: molecular mechanisms. *Clin Sci (Lond),* 94**,** 557-72.

Barzilai, D., Plavnick, J., Hazani, A., Einath, R., Kleinhaus, N. & Kanter, Y. (1972) Use of hydrocortisone in the treatment of acute myocardial infarction. Summary of a clinical trial in 446 patients. *Chest,* 61**,** 488-91.

Bates, D. O. & Harper, S. J. (2002) Regulation of vascular permeability by vascular endothelial growth factors. *Vascul Pharmacol,* 39**,** 225-37.

Beggah, A. T., Escoubet, B., Puttini, S., Cailmail, S., Delage, V., Ouvrard-Pascaud, A., Bocchi, B., Peuchmaur, M., Delcayre, C., Farman, N. & Jaisser, F. (2002) Reversible cardiac fibrosis and heart failure induced by conditional expression of an antisense mRNA of the mineralocorticoid receptor in cardiomyocytes. *Proc Natl Acad Sci U S A,* 99**,** 7160-5.

Beltrami, A. P., Barlucchi, L., Torella, D., Baker, M., Limana, F., Chimenti, S., Kasahara, H., Rota, M., Musso, E., Urbanek, K., Leri, A., Kajstura, J., Nadal-Ginard, B. & Anversa, P. (2003) Adult cardiac stem cells are multipotent and support myocardial regeneration. *Cell,* 114**,** 763-76.

Benard, L., Milliez, P., Ambroisine, M. L., Messaoudi, S., Samuel, J. L. & Delcayre, C. (2009) Effects of aldosterone on coronary function. *Pharmacol Rep,* 61**,** 58-66.

Bendeck, M. P. (2000) Mining the myocardium with macrophage drills: A novel mechanism for revascularization. *Circ Res,* 87**,** 341-3.

Bergers, G. & Song, S. (2005) The role of pericytes in blood-vessel formation and maintenance. *Neuro Oncol,* 7**,** 452-64.

Bexell, D., Gunnarsson, S., Tormin, A., Darabi, A., Gisselsson, D., Roybon, L., Scheding, S. & Bengzon, J. (2009) Bone marrow multipotent mesenchymal stroma cells act as pericyte-like migratory vehicles in experimental gliomas. *Mol Ther,* 17**,** 183-90.

Bhagwat, S. V., Lahdenranta, J., Giordano, R., Arap, W., Pasqualini, R. & Shapiro, L. H. (2001) CD13/APN is activated by angiogenic signals and is essential for capillary tube formation. *Blood,* 97**,** 652-9.

Birkedal-Hansen, H., Moore, W. G., Bodden, M. K., Windsor, L. J., Birkedal-Hansen, B., Decarlo, A. & Engler, J. A. (1993) Matrix metalloproteinases: a review. *Crit Rev Oral Biol Med,* 4**,** 197-250.

Bledsoe, R. K., Stewart, E. L. & Pearce, K. H. (2004) Structure and function of the glucocorticoid receptor ligand binding domain. *Vitam Horm,* 68**,** 49-91.

Bondke, A., Hillmeister, P. & Buschmann, I. R. (2007) Exact assessment of perfusion and collateral vessel proliferation in small animal models. *Circ Res,* 100**,** e82-3.

Borish, L. C. & Steinke, J. W. (2003) 2. Cytokines and chemokines. *J Allergy Clin Immunol,* 111**,** S460-75.

Brandt, E., Woerly, G., Younes, A. B., Loiseau, S. & Capron, M. (2000) IL-4 production by human polymorphonuclear neutrophils. *J Leukoc Biol,* 68**,** 125-30.

Brereton, P. S., Van Driel, R. R., Suhaimi, F., Koyama, K., Dilley, R. & Krozowski, Z. (2001) Light and electron microscopy localization of the 11beta-hydroxysteroid dehydrogenase type I enzyme in the rat. *Endocrinology,* 142**,** 1644-51.

Brilla, C. G., Matsubara, L. S. & Weber, K. T. (1993) Antifibrotic effects of spironolactone in preventing myocardial fibrosis in systemic arterial hypertension. *Am J Cardiol,* 71**,** 12A-16A.

British Heart Foundation, O. F. N. S. (2008) Deaths registered by cause, sex and age. England and Wales.

Brooks, K. J., Bunce, K. T., Haase, M. V., White, A., Changani, K. K., Bate, S. T. & Reid, D. G. (2005) MRI quantification in vivo of corticosteroid induced thymus involution in mice: correlation with ex vivo measurements. *Steroids,* 70**,** 267-72.

Brotman, D. J., Girod, J. P., Garcia, M. J., Patel, J. V., Gupta, M., Posch, A., Saunders, S., Lip, G. Y., Worley, S. & Reddy, S. (2005) Effects of short-term glucocorticoids on cardiovascular biomarkers. *J Clin Endocrinol Metab,* 90**,** 3202-8.

Brown, E. J., Jr., Kloner, R. A., Schoen, F. J., Hammerman, H., Hale, S. & Braunwald, E. (1983) Scar thinning due to ibuprofen administration after experimental myocardial infarction. *Am J Cardiol,* 51**,** 877-83.

Brown, R. W., Diaz, R., Robson, A. C., Kotelevtsev, Y. V., Mullins, J. J., Kaufman, M. H. & Seckl, J. R. (1996) The ontogeny of 11 beta-hydroxysteroid dehydrogenase type 2 and mineralocorticoid receptor gene expression reveal intricate control of glucocorticoid action in development. *Endocrinology,* 137**,** 794-7.

Buckingham, J. C. (2006) Glucocorticoids: exemplars of multi-tasking. *Br J Pharmacol,* 147 Suppl 1**,** S258-68.

Buehler, A., Van Zandvoort, M. A., Stelt, B. J., Hackeng, T. M., Schrans-Stassen, B. H., Bennaghmouch, A., Hofstra, L., Cleutjens, J. P., Duijvestijn, A., Smeets, M. B., De Kleijn, D. P., Post, M. J. & De Muinck, E. D. (2006) cNGR: a novel homing sequence for CD13/APN targeted molecular imaging of murine cardiac angiogenesis in vivo. *Arterioscler Thromb Vasc Biol,* 26**,** 2681-7.

Bujak, M. & Frangogiannis, N. G. (2007) The role of TGF-beta signaling in myocardial infarction and cardiac remodeling. *Cardiovasc Res,* 74**,** 184-95.

Burne-Taney, M. J., Yokota-Ikeda, N. & Rabb, H. (2005) Effects of combined T- and B-cell deficiency on murine ischemia reperfusion injury. *Am J Transplant,* 5**,** 1186-93.

Cai, T. Q., Wong, B., Mundt, S. S., Thieringer, R., Wright, S. D. & Hermanowski-Vosatka, A. (2001) Induction of 11beta-hydroxysteroid dehydrogenase type 1 but not -2 in human aortic smooth muscle cells by inflammatory stimuli. *J Steroid Biochem Mol Biol,* 77**,** 117-22.

Camelliti, P., Borg, T. K. & Kohl, P. (2005) Structural and functional characterisation of cardiac fibroblasts. *Cardiovasc Res,* 65**,** 40-51.

Carmeliet, P. (2000) Mechanisms of angiogenesis and arteriogenesis. *Nat Med,* 6**,** 389-95.

Carmeliet, P. & Jain, R. K. (2000) Angiogenesis in cancer and other diseases. *Nature,* 407**,** 249-57.

Cathelin, S., Rebe, C., Haddaoui, L., Simioni, N., Verdier, F., Fontenay, M., Launay, S., Mayeux, P. & Solary, E. (2006) Identification of proteins cleaved downstream of caspase activation in monocytes undergoing macrophage differentiation. *J Biol Chem,* 281**,** 17779-88.

Cavalcanti, D. M., Lotufo, C. M., Borelli, P., Ferreira, Z. S., Markus, R. P. & Farsky, S. H. (2007) Endogenous glucocorticoids control neutrophil mobilization from bone marrow to blood and tissues in non-inflammatory conditions. *Br J Pharmacol,* 152**,** 1291-300.

Ceremuzynski, L. (1981) Hormonal and metabolic reactions evoked by acute myocardial infarction. *Circ Res,* 48**,** 767-76.

Ceriello, A. (2008) Cardiovascular effects of acute hyperglycaemia: pathophysiological underpinnings. *Diab Vasc Dis Res,* 5**,** 260-8.

Chapman, K. E., Coutinho, A. E., Gray, M., Gilmour, J. S., Savill, J. S. & Seckl, J. R. (2009) The role and regulation of 11beta-hydroxysteroid dehydrogenase type 1 in the inflammatory response. *Mol Cell Endocrinol,* 301**,** 123-31.

Chapman, K. E., Gilmour, J. S., Coutinho, A. E., Savill, J. S. & Seckl, J. R. (2006) 11Beta-hydroxysteroid dehydrogenase type 1--a role in inflammation? *Mol Cell Endocrinol,* 248**,** 3-8.

Chen, W., Valamanesh, F., Mirshahi, T., Soria, J., Tang, R., Agarwal, M. K. & Mirshahi, M. (2004) Aldosterone signaling modifies capillary formation by human bone marrow endothelial cells. *Vascul Pharmacol,* 40**,** 269-77.

Chen, C. J., Kono, H., Golenbock, D., Reed, G., Akira, S. & Rock, K. L. (2007) Identification of a key pathway required for the sterile inflammatory response triggered by dying cells. *Nat Med,* 13**,** 851-6.

Cheng, X. W., Kuzuya, M., Nakamura, K., Maeda, K., Tsuzuki, M., Kim, W., Sasaki, T., Liu, Z., Inoue, N., Kondo, T., Jin, H., Numaguchi, Y., Okumura, K., Yokota, M., Iguchi, A. & Murohara, T. (2007) Mechanisms underlying the impairment of ischemia-induced neovascularization in matrix metalloproteinase 2-deficient mice. *Circ Res,* 100**,** 904-13.

Chien, K. R. (2006) Lost and found: cardiac stem cell therapy revisited. *J Clin Invest,* 116**,** 1838-40.

Chiu, K. Y., Loke, S. L. & Ho, F. C. (1994) Immunohistochemical demonstration of c-erbB-2 oncoprotein in gastric adenocarcinoma: comparison of cryostat and paraffin wax sections and effect of fixation. *J Clin Pathol,* 47**,** 117-21.

Christy, C., Hadoke, P. W., Paterson, J. M., Mullins, J. J., Seckl, J. R. & Walker, B. R. (2003) 11beta-hydroxysteroid dehydrogenase type 2 in mouse aorta: localization and influence on response to glucocorticoids. *Hypertension,* 42**,** 580-7.

Clark, R. A., Nielsen, L. D., Welch, M. P. & Mcpherson, J. M. (1995) Collagen matrices attenuate the collagen-synthetic response of cultured fibroblasts to TGF-beta. *J Cell Sci,* 108 (Pt 3)**,** 1251-61.

Cleutjens, J. P., Verluyten, M. J., Smiths, J. F. & Daemen, M. J. (1995) Collagen remodeling after myocardial infarction in the rat heart. *Am J Pathol,* 147**,** 325-38.

Coelho, F. M., Pinho, V., Amaral, F. A., Sachs, D., Costa, V. V., Rodrigues, D. H., Vieira, A. T., Silva, T. A., Souza, D. G., Bertini, R., Teixeira, A. L. & Teixeira, M. M. (2008) The chemokine receptors CXCR1/CXCR2 modulate antigen-induced arthritis by regulating adhesion of neutrophils to the synovial microvasculature. *Arthritis Rheum,* 58**,** 2329-37.

Cohen, B. J., Danon, D. & Roth, G. S. (1987) Wound repair in mice as influenced by age and antimacrophage serum. *J Gerontol,* 42**,** 295-301.

Cole, T. J., Blendy, J. A., Monaghan, A. P., Krieglstein, K., Schmid, W., Aguzzi, A., Fantuzzi, G., Hummler, E., Unsicker, K. & Schutz, G. (1995) Targeted disruption of the glucocorticoid receptor gene blocks adrenergic chromaffin cell development and severely retards lung maturation. *Genes Dev,* 9**,** 1608-21.

Conway, E. M., Collen, D. & Carmeliet, P. (2001) Molecular mechanisms of blood vessel growth. *Cardiovasc Res,* 49**,** 507-21.

Courtney, R., Stewart, P. M., Toh, M., Ndongo, M. N., Calle, R. A. & Hirshberg, B. (2008) Modulation of 11beta-hydroxysteroid dehydrogenase (11betaHSD) activity biomarkers and pharmacokinetics of PF-00915275, a selective 11betaHSD1 inhibitor. *J Clin Endocrinol Metab,* 93**,** 550-6.

Coutinho, A. E. unpublished data.

Cowie, M. R., Wood, D. A., Coats, A. J., Thompson, S. G., Poole-Wilson, P. A., Suresh, V. & Sutton, G. C. (1999) Incidence and aetiology of heart failure; a population-based study. *Eur Heart J,* 20**,** 421-8.

Cupps, T. R. & Fauci, A. S. (1982) Corticosteroid-mediated immunoregulation in man. *Immunol Rev,* 65**,** 133-55.

Cuzzocrea, S., De Sarro, G., Costantino, G., Ciliberto, G., Mazzon, E., De Sarro, A. & Caputi, A. P. (1999) IL-6 knock-out mice exhibit resistance to splanchnic artery occlusion shock. *J Leukoc Biol*, 66**,** 471-80.

Dai, W., Wold, L. E., Dow, J. S. & Kloner, R. A. (2005) Thickening of the infarcted wall by collagen injection improves left ventricular function in rats: a novel approach to preserve cardiac function after myocardial infarction. *J Am Coll Cardiol*, 46**,** 714-9.

De Bosscher, K., Vanden Berghe, W. & Haegeman, G. (2003) The interplay between the glucocorticoid receptor and nuclear factor-kappaB or activator protein-1: molecular mechanisms for gene repression. *Endocr Rev*, 24**,** 488-522.

Dean, R. G., Balding, L. C., Candido, R., Burns, W. C., Cao, Z., Twigg, S. M. & Burrell, L. M. (2005) Connective tissue growth factor and cardiac fibrosis after myocardial infarction. *J Histochem Cytochem*, 53**,** 1245-56.

Deisher, T. A., Garcia, I. & Harlan, J. M. (1993) Cytokine-induced adhesion molecule expression on human umbilical vein endothelial cells is not regulated by cyclic adenosine monophosphate accumulation. *Life Sci*, 53**,** 365-70.

Derbyshire, E. J., Yang, Y. C., Li, S., Comin, G. A., Belloir, J. & Thorpe, P. E. (1996) Heparin-steroid conjugates lacking glucocorticoid or mineralocorticoid activities inhibit the proliferation of vascular endothelial cells. *Biochim Biophys Acta*, 1310**,** 86-96.

Desmouliere, A., Geinoz, A., Gabbiani, F. & Gabbiani, G. (1993) Transforming growth factor-beta 1 induces alpha-smooth muscle actin expression in granulation tissue myofibroblasts and in quiescent and growing cultured fibroblasts. *J Cell Biol*, 122**,** 103-11.

Dettman, R. W., Denetclaw, W., Jr., Ordahl, C. P. & Bristow, J. (1998) Common epicardial origin of coronary vascular smooth muscle, perivascular fibroblasts, and intermyocardial fibroblasts in the avian heart. *Dev Biol*, 193**,** 169-81.

Deuchar, G. A., Hadoke, P.W.F., Armour, D., Brownstein, D.G., Webb, D.J., Mullins, J.J., Seckl, J.R, Kotelevtsev (2009) Glucocorticoid-mediated activation of extra-renal mineralocorticoid receptors exacerbates athersclerosis in mice. *Submitted*.

Dewald, O., Ren, G., Duerr, G. D., Zoerlein, M., Klemm, C., Gersch, C., Tincey, S., Michael, L. H., Entman, M. L. & Frangogiannis, N. G. (2004) Of mice and dogs: species-specific differences in the inflammatory response following myocardial infarction. *Am J Pathol,* 164**,** 665-77.

Dhalla, A. K., Hill, M. F. & Singal, P. K. (1996) Role of oxidative stress in transition of hypertrophy to heart failure. *J Am Coll Cardiol,* 28**,** 506-14.

Dickie, R., Bachoo, R. M., Rupnick, M. A., Dallabrida, S. M., Deloid, G. M., Lai, J., Depinho, R. A. & Rogers, R. A. (2006) Three-dimensional visualization of microvessel architecture of whole-mount tissue by confocal microscopy. *Microvasc Res,* 72**,** 20-6.

Dobaczewski, M., Bujak, M., Zymek, P., Ren, G., Entman, M. L. & Frangogiannis, N. G. (2006) Extracellular matrix remodeling in canine and mouse myocardial infarcts. *Cell Tissue Res,* 324**,** 475-88.

Dobaczewski, M., Gonzalez-Quesada, C. & Frangogiannis, N. G. (2009) The extracellular matrix as a modulator of the inflammatory and reparative response following myocardial infarction. *J Mol Cell Cardiol*.

Donald, R. A., Crozier, I. G., Foy, S. G., Richards, A. M., Livesey, J. H., Ellis, M. J., Mattioli, L. & Ikram, H. (1994) Plasma corticotrophin releasing hormone, vasopressin, ACTH and cortisol responses to acute myocardial infarction. *Clin Endocrinol (Oxf),* 40**,** 499-504.

Douglas, P. S., Morrow, R., Ioli, A. & Reichek, N. (1989) Left ventricular shape, afterload and survival in idiopathic dilated cardiomyopathy. *J Am Coll Cardiol,* 13**,** 311-5.

Draper, N. & Stewart, P. M. (2005) 11beta-hydroxysteroid dehydrogenase and the pre-receptor regulation of corticosteroid hormone action. *J Endocrinol,* 186**,** 251-71.

Du, X. J., Samuel, C. S., Gao, X. M., Zhao, L., Parry, L. J. & Tregear, G. W. (2003) Increased myocardial collagen and ventricular diastolic dysfunction in relaxin deficient mice: a gender-specific phenotype. *Cardiovasc Res,* 57**,** 395-404.

Duffield, J. S., Forbes, S. J., Constandinou, C. M., Clay, S., Partolina, M., Vuthoori, S., Wu, S., Lang, R. & Iredale, J. P. (2005) Selective depletion of macrophages reveals distinct, opposing roles during liver injury and repair. *J Clin Invest,* 115**,** 56-65.

Edwards, C. R., Stewart, P. M., Burt, D., Brett, L., Mcintyre, M. A., Sutanto, W. S., De Kloet, E. R. & Monder, C. (1988) Localisation of 11 beta-hydroxysteroid dehydrogenase--tissue specific protector of the mineralocorticoid receptor. *Lancet,* 2**,** 986-9.

El-Helou, V., Proulx, C., Gosselin, H., Clement, R., Mimee, A., Villeneuve, L. & Calderone, A. (2008) Dexamethasone treatment of post-MI rats attenuates sympathetic innervation of the infarct region. *J Appl Physiol,* 104**,** 150-6.

Elkon, K. B. (2007) IL-1alpha responds to necrotic cell death. *Nat Med,* 13**,** 778-80.

Ellis, S. G., Penn, M. S., Bolwell, B., Garcia, M., Chacko, M., Wang, T., Brezina, K. J., Mcconnell, G. & Topol, E. J. (2006) Granulocyte colony stimulating factor in patients with large acute myocardial infarction: results of a pilot dose-escalation randomized trial. *Am Heart J,* 152**,** 1051 e9-14.

Engel, F. B., Hsieh, P. C., Lee, R. T. & Keating, M. T. (2006) FGF1/p38 MAP kinase inhibitor therapy induces cardiomyocyte mitosis, reduces scarring, and rescues function after myocardial infarction. *Proc Natl Acad Sci U S A,* 103**,** 15546-51.

Esteban, N. V., Loughlin, T., Yergey, A. L., Zawadzki, J. K., Booth, J. D., Winterer, J. C. & Loriaux, D. L. (1991) Daily cortisol production rate in man determined by stable isotope dilution/mass spectrometry. *J Clin Endocrinol Metab,* 72**,** 39-45.

Etoh, T., Joffs, C., Deschamps, A. M., Davis, J., Dowdy, K., Hendrick, J., Baicu, S., Mukherjee, R., Manhaini, M. & Spinale, F. G. (2001) Myocardial and interstitial matrix metalloproteinase activity after acute myocardial infarction in pigs. *Am J Physiol Heart Circ Physiol,* 281**,** H987-94.

Fadok, V. A., Bratton, D. L., Konowal, A., Freed, P. W., Westcott, J. Y. & Henson, P. M. (1998) Macrophages that have ingested apoptotic cells in vitro inhibit proinflammatory cytokine production through autocrine/paracrine mechanisms involving TGF-beta, PGE2, and PAF. *J Clin Invest,* 101**,** 890-8.

Fazel, S., Cimini, M., Chen, L., Li, S., Angoulvant, D., Fedak, P., Verma, S., Weisel, R. D., Keating, A. & Li, R. K. (2006) Cardioprotective c-kit+ cells are from the bone marrow and regulate the myocardial balance of angiogenic cytokines. *J Clin Invest,* 116**,** 1865-77.

Ferdinandy, P., Schulz, R. & Baxter, G. F. (2007) Interaction of cardiovascular risk factors with myocardial ischemia/reperfusion injury, preconditioning, and postconditioning. *Pharmacol Rev,* 59**,** 418-58.

Fernandez, B., Buehler, A., Wolfram, S., Kostin, S., Espanion, G., Franz, W. M., Niemann, H., Doevendans, P. A., Schaper, W. & Zimmermann, R. (2000) Transgenic myocardial overexpression of fibroblast growth factor-1 increases coronary artery density and branching. *Circ Res,* 87**,** 207-13.

Fielding, C. A., Mcloughlin, R. M., Mcleod, L., Colmont, C. S., Najdovska, M., Grail, D., Ernst, M., Jones, S. A., Topley, N. & Jenkins, B. J. (2008) IL-6 regulates neutrophil trafficking during acute inflammation via STAT3. *J Immunol,* 181**,** 2189-95.

Folkman, J. & Ingber, D. E. (1987) Angiostatic steroids. Method of discovery and mechanism of action. *Ann Surg,* 206**,** 374-83.

Folkman, J. & Shing, Y. (1992) Angiogenesis. *J Biol Chem,* 267**,** 10931-4.

Forbes, S. J., Russo, F. P., Rey, V., Burra, P., Rugge, M., Wright, N. A. & Alison, M. R. (2004) A significant proportion of myofibroblasts are of bone marrow origin in human liver fibrosis. *Gastroenterology,* 126**,** 955-63.

Forsythe, J. A., Jiang, B. H., Iyer, N. V., Agani, F., Leung, S. W., Koos, R. D. & Semenza, G. L. (1996) Activation of vascular endothelial growth factor gene transcription by hypoxia-inducible factor 1. *Mol Cell Biol,* 16**,** 4604-13.

Fraccarollo, D., Galuppo, P., Schraut, S., Kneitz, S., Van Rooijen, N., Ertl, G. & Bauersachs, J. (2008) Immediate mineralocorticoid receptor blockade improves myocardial infarct healing by modulation of the inflammatory response. *Hypertension,* 51**,** 905-14.

Frangogiannis, N. G., Youker, K. A., Rossen, R. D., Gwechenberger, M., Lindsey, M. H., Mendoza, L. H., Michael, L. H., Ballantyne, C. M., Smith, C. W. & Entman, M. L. (1998) Cytokines and the microcirculation in ischemia and reperfusion. *J Mol Cell Cardiol,* 30**,** 2567-76.

Frangogiannis, N. G. & Entman, M. L. (2005) Chemokines in myocardial ischemia. *Trends Cardiovasc Med,* 15**,** 163-9.

Frangogiannis, N. G., Mendoza, L. H., Lewallen, M., Michael, L. H., Smith, C. W. & Entman, M. L. (2001) Induction and suppression of interferon-inducible protein 10 in reperfused myocardial infarcts may regulate angiogenesis. *Faseb J,* 15**,** 1428-30.

Frangogiannis, N. G., Ren, G., Dewald, O., Zymek, P., Haudek, S., Koerting, A., Winkelmann, K., Michael, L. H., Lawler, J. & Entman, M. L. (2005) Critical role of

endogenous thrombospondin-1 in preventing expansion of healing myocardial infarcts. *Circulation,* 111**,** 2935-42.

Frangogiannis, N. G., Smith, C. W. & Entman, M. L. (2002) The inflammatory response in myocardial infarction. *Cardiovasc Res,* 53**,** 31-47.

Frantz, S., Tillmanns, J., Kuhlencordt, P. J., Schmidt, I., Adamek, A., Dienesch, C., Thum, T., Gerondakis, S., Ertl, G. & Bauersachs, J. (2007) Tissue-specific effects of the nuclear factor kappaB subunit p50 on myocardial ischemia-reperfusion injury. *Am J Pathol,* 171**,** 507-12.

Frantz, S., Vallabhapurapu, D., Tillmanns, J., Brousos, N., Wagner, H., Henig, K., Ertl, G., Muller, A. M. & Bauersachs, J. (2008) Impact of different bone marrow cell preparations on left ventricular remodelling after experimental myocardial infarction. *Eur J Heart Fail,* 10**,** 119-24.

Fujii, H., Sun, Z., Li, S. H., Wu, J., Fazel, S., Weisel, R. D., Rakowski, H., Lindner, J. & Li, R. K. (2009) Ultrasound-targeted gene delivery induces angiogenesis after a myocardial infarction in mice. *JACC Cardiovasc Imaging,* 2**,** 869-79.

Funder, J. W. (1997) Glucocorticoid and mineralocorticoid receptors: biology and clinical relevance. *Annu Rev Med,* 48**,** 231-40.

Funder, J. W. & Mihailidou, A. S. (2009) Aldosterone and mineralocorticoid receptors: Clinical studies and basic biology. *Mol Cell Endocrinol,* 301**,** 2-6.

Galkina, E. & Ley, K. (2009) Immune and inflammatory mechanisms of atherosclerosis (*). *Annu Rev Immunol,* 27**,** 165-97.

Gallucci, R. M., Simeonova, P. P., Matheson, J. M., Kommineni, C., Guriel, J. L., Sugawara, T. & Luster, M. I. (2000) Impaired cutaneous wound healing in interleukin-6-deficient and immunosuppressed mice. *Faseb J,* 14**,** 2525-31.

Galon, J., Franchimont, D., Hiroi, N., Frey, G., Boettner, A., Ehrhart-Bornstein, M., O'shea, J. J., Chrousos, G. P. & Bornstein, S. R. (2002) Gene profiling reveals unknown enhancing and suppressive actions of glucocorticoids on immune cells. *Faseb J,* 16**,** 61-71.

Gao, H. B., Ge, R. S., Lakshmi, V., Marandici, A. & Hardy, M. P. (1997) Hormonal regulation of oxidative and reductive activities of 11 beta-hydroxysteroid dehydrogenase in rat Leydig cells. *Endocrinology,* 138**,** 156-61.

Garcia, R. A., Go, K. V. & Villarreal, F. J. (2007) Effects of timed administration of doxycycline or methylprednisolone on post-myocardial infarction inflammation and left ventricular remodeling in the rat heart. *Mol Cell Biochem,* 300**,** 159-69.

Gazes, P. C., Richardson, J. A. & Woods, E. F. (1959) Plasma catechol amine concentrations in myocardial infarction and angina pectoris. *Circulation,* 19**,** 657-61.

Gelati, M., Aplin, A. C., Fogel, E., Smith, K. D. & Nicosia, R. F. (2008) The angiogenic response of the aorta to injury and inflammatory cytokines requires macrophages. *J Immunol,* 181**,** 5711-9.

Gilmour, J. S., Coutinho, A. E., Cailhier, J. F., Man, T. Y., Clay, M., Thomas, G., Harris, H. J., Mullins, J. J., Seckl, J. R., Savill, J. S. & Chapman, K. E. (2006) Local amplification of glucocorticoids by 11 beta-hydroxysteroid dehydrogenase type 1 promotes macrophage phagocytosis of apoptotic leukocytes. *J Immunol,* 176**,** 7605-11.

Gomez-Sanchez, E. P., Venkataraman, M. T., Thwaites, D. & Fort, C. (1990) ICV infusion of corticosterone antagonizes ICV-aldosterone hypertension. *Am J Physiol,* 258**,** E649-53.

Gordon, C. B., Li, D. G., Stagg, C. A., Manson, P. & Udelsman, R. (1994) Impaired wound healing in Cushing's syndrome: the role of heat shock proteins. *Surgery,* 116**,** 1082-7.

Grass, T. M., Lurie, D. I. & Coffin, J. D. (2006) Transitional angiogenesis and vascular remodeling during coronary angiogenesis in response to myocardial infarction. *Acta Histochem,* 108**,** 293-302.

Greenberg, J. I., Shields, D. J., Barillas, S. G., Acevedo, L. M., Murphy, E., Huang, J., Scheppke, L., Stockmann, C., Johnson, R. S., Angle, N. & Cheresh, D. A. (2008) A role for VEGF as a negative regulator of pericyte function and vessel maturation. *Nature,* 456**,** 809-13.

Gu, J. W., Brady, A. L., Anand, V., Moore, M. C., Kelly, W. C. & Adair, T. H. (1999) Adenosine upregulates VEGF expression in cultured myocardial vascular smooth muscle cells. *Am J Physiol,* 277**,** H595-602.

Haas, T. L., Milkiewicz, M., Davis, S. J., Zhou, A. L., Egginton, S., Brown, M. D., Madri, J. A. & Hudlicka, O. (2000) Matrix metalloproteinase activity is required for activity-induced angiogenesis in rat skeletal muscle. *Am J Physiol Heart Circ Physiol,* 279**,** H1540-7.

Hadoke, P. W., Christy, C., Kotelevtsev, Y. V., Williams, B. C., Kenyon, C. J., Seckl, J. R., Mullins, J. J. & Walker, B. R. (2001) Endothelial cell dysfunction in mice after transgenic knockout of type 2, but not type 1, 11beta-hydroxysteroid dehydrogenase. *Circulation,* 104**,** 2832-7.

Hadoke, P. W., Iqbal, J. & Walker, B. R. (2009) Therapeutic manipulation of glucocorticoid metabolism in cardiovascular disease. *Br J Pharmacol,* 156**,** 689-712.

Hadoke, P. W., Macdonald, L., Logie, J. J., Small, G. R., Dover, A. R. & Walker, B. R. (2006) Intra-vascular glucocorticoid metabolism as a modulator of vascular structure and function. *Cell Mol Life Sci,* 63**,** 565-78.

Hafezi-Moghadam, A., Simoncini, T., Yang, Z., Limbourg, F. P., Plumier, J. C., Rebsamen, M. C., Hsieh, C. M., Chui, D. S., Thomas, K. L., Prorock, A. J., Laubach, V. E., Moskowitz, M. A., French, B. A., Ley, K. & Liao, J. K. (2002) Acute cardiovascular

protective effects of corticosteroids are mediated by non-transcriptional activation of endothelial nitric oxide synthase. *Nat Med,* 8**,** 473-9.

Hammerman, H., Kloner, R. A., Hale, S., Schoen, F. J. & Braunwald, E. (1983a) Dose-dependent effects of short-term methylprednisolone on myocardial infarct extent, scar formation, and ventricular function. *Circulation,* 68**,** 446-52.

Hammerman, H., Kloner, R. A., Schoen, F. J., Brown, E. J., Jr., Hale, S. & Braunwald, E. (1983b) Indomethacin-induced scar thinning after experimental myocardial infarction. *Circulation,* 67**,** 1290-5.

Hammerman, H., Schoen, F. J., Braunwald, E. & Kloner, R. A. (1984) Drug-induced expansion of infarct: morphologic and functional correlations. *Circulation,* 69**,** 611-7.

Hammond, G. L., Smith, C. L., Paterson, N. A. & Sibbald, W. J. (1990) A role for corticosteroid-binding globulin in delivery of cortisol to activated neutrophils. *J Clin Endocrinol Metab,* 71**,** 34-9.

Hardy, R. (2008) Differential effects of glucocorticoids on fibroblasts: mechanisms underlying the adverse features of Cushing's. *Endocrine Abstracts.* Harrogate.

Hardy, R. S., Filer, A., Cooper, M. S., Parsonage, G., Raza, K., Hardie, D. L., Rabbitt, E. H., Stewart, P. M., Buckley, C. D. & Hewison, M. (2006) Differential expression, function and response to inflammatory stimuli of 11beta-hydroxysteroid dehydrogenase type 1 in human fibroblasts: a mechanism for tissue-specific regulation of inflammation. *Arthritis Res Ther,* 8**,** R108.

Harris, H. J., Kotelevtsev, Y., Mullins, J. J., Seckl, J. R. & Holmes, M. C. (2001) Intracellular regeneration of glucocorticoids by 11beta-hydroxysteroid dehydrogenase (11beta-HSD)-1 plays a key role in regulation of the hypothalamic-pituitary-adrenal axis: analysis of 11beta-HSD-1-deficient mice. *Endocrinology,* 142**,** 114-20.

Hasan, Q., Tan, S. T., Gush, J., Peters, S. G. & Davis, P. F. (2000) Steroid therapy of a proliferating hemangioma: histochemical and molecular changes. *Pediatrics,* 105**,** 117-20.

Hasan, Q., Tan, S. T., Xu, B. & Davis, P. F. (2003) Effects of five commonly used glucocorticoids on haemangioma in vitro. *Clin Exp Pharmacol Physiol,* 30**,** 140-4.

Hawkins, M., Hunter, D., Kishore, P., Scwartz, S., Hompesch, M., Hollis, G., Levy, R., Williams, B., Huber, R. (2008) INCB013739, a selective inhibitor of 11β-hydroxysteroid dehydrogenase type 1 (11βHSD1), improves insulin sensitivity and lowers plasma cholesterol over 28 days in patients with type 2 diabetes mellitus

Proceedings of the New and Novel Treatments for Diabetic Complications, the American Diabetes Association 68th Scientific Sessions

Heasman, S. J., Giles, K. M., Ward, C., Rossi, A. G., Haslett, C. & Dransfield, I. (2003) Glucocorticoid-mediated regulation of granulocyte apoptosis and macrophage phagocytosis of apoptotic cells: implications for the resolution of inflammation. *J Endocrinol,* 178**,** 29-36.

Hench, P. S., Kendall, E. C., Slocumb, C. H. & Polley, H. F. (1950) Cortisone, its effects on rheumatoid arthritis, rheumatic fever, and certain other conditions. *Merck Rep,* 59**,** 9-14.

Henderson, N. C., Mackinnon, A. C., Farnworth, S. L., Kipari, T., Haslett, C., Iredale, J. P., Liu, F. T., Hughes, J. & Sethi, T. (2008) Galectin-3 expression and secretion links macrophages to the promotion of renal fibrosis. *Am J Pathol,* 172**,** 288-98.

Hermanowski-Vosatka, A., Balkovec, J. M., Cheng, K., Chen, H. Y., Hernandez, M., Koo, G. C., Le Grand, C. B., Li, Z., Metzger, J. M., Mundt, S. S., Noonan, H., Nunes, C. N., Olson, S. H., Pikounis, B., Ren, N., Robertson, N., Schaeffer, J. M., Shah, K., Springer, M. S., Strack, A. M., Strowski, M., Wu, K., Wu, T., Xiao, J., Zhang, B. B.,

Wright, S. D. & Thieringer, R. (2005) 11beta-HSD1 inhibition ameliorates metabolic syndrome and prevents progression of atherosclerosis in mice. *J Exp Med,* 202**,** 517-27.

Heymans, S., Luttun, A., Nuyens, D., Theilmeier, G., Creemers, E., Moons, L., Dyspersin, G. D., Cleutjens, J. P., Shipley, M., Angellilo, A., Levi, M., Nube, O., Baker, A., Keshet, E., Lupu, F., Herbert, J. M., Smits, J. F., Shapiro, S. D., Baes, M., Borgers, M., Collen, D., Daemen, M. J. & Carmeliet, P. (1999) Inhibition of plasminogen activators or matrix metalloproteinases prevents cardiac rupture but impairs therapeutic angiogenesis and causes cardiac failure. *Nat Med,* 5**,** 1135-42.

Hochhauser, E., Kivity, S., Offen, D., Maulik, N., Otani, H., Barhum, Y., Pannet, H., Shneyvays, V., Shainberg, A., Goldshtaub, V., Tobar, A. & Vidne, B. A. (2003) Bax ablation protects against myocardial ischemia-reperfusion injury in transgenic mice. *Am J Physiol Heart Circ Physiol,* 284**,** H2351-9.

Holler, N., Zaru, R., Micheau, O., Thome, M., Attinger, A., Valitutti, S., Bodmer, J. L., Schneider, P., Seed, B. & Tschopp, J. (2000) Fas triggers an alternative, caspase-8-independent cell death pathway using the kinase RIP as effector molecule. *Nat Immunol,* 1**,** 489-95.

Hori, Y., Hu, D. E., Yasui, K., Smither, R. L., Gresham, G. A. & Fan, T. P. (1996) Differential effects of angiostatic steroids and dexamethasone on angiogenesis and cytokine levels in rat sponge implants. *Br J Pharmacol,* 118**,** 1584-91.

Horigome, H., Homma, M., Hirano, T. & Oka, K. (2001) Glycyrrhetinic acid induced apoptosis in murine splenocytes. *Biol Pharm Bull,* 24**,** 54-8.

Hynes, R. O. (2002) A reevaluation of integrins as regulators of angiogenesis. *Nat Med,* 8**,** 918-21.

Ishii, H., Amano, T., Matsubara, T. & Murohara, T. (2008) Pharmacological intervention for prevention of left ventricular remodeling and improving prognosis in myocardial infarction. *Circulation,* 118**,** 2710-8.

Ismail, J. A., Poppa, V., Kemper, L. E., Scatena, M., Giachelli, C. M., Coffin, J. D. & Murry, C. E. (2003) Immunohistologic labeling of murine endothelium. *Cardiovasc Pathol,* 12**,** 82-90.

Ivey, C. L., Williams, F. M., Collins, P. D., Jose, P. J. & Williams, T. J. (1995) Neutrophil chemoattractants generated in two phases during reperfusion of ischemic myocardium in the rabbit. Evidence for a role for C5a and interleukin-8. *J Clin Invest,* 95**,** 2720-8.

Jacobson, L. (2005) Hypothalamic-pituitary-adrenocortical axis regulation. *Endocrinol Metab Clin North Am,* 34**,** 271-92, vii.

Jacobson, L. & Sapolsky, R. (1991) The role of the hippocampus in feedback regulation of the hypothalamic-pituitary-adrenocortical axis. *Endocr Rev,* 12**,** 118-34.

Jain, R. K. (2003) Molecular regulation of vessel maturation. *Nat Med,* 9**,** 685-93.

Jaremo, P. & Nilsson, O. (2008) Interleukin-6 and neutrophils are associated with long-term survival after acute myocardial infarction. *Eur J Intern Med,* 19**,** 330-3.

John, M., Lim, S., Seybold, J., Jose, P., Robichaud, A., O'connor, B., Barnes, P. J. & Chung, K. F. (1998) Inhaled corticosteroids increase interleukin-10 but reduce macrophage inflammatory protein-1alpha, granulocyte-macrophage colony-stimulating factor, and interferon-gamma release from alveolar macrophages in asthma. *Am J Respir Crit Care Med,* 157**,** 256-62.

Jonat, C., Rahmsdorf, H. J., Park, K. K., Cato, A. C., Gebel, S., Ponta, H. & Herrlich, P. (1990) Antitumor promotion and antiinflammation: down-modulation of AP-1 (Fos/Jun) activity by glucocorticoid hormone. *Cell,* 62**,** 1189-204.

Jordan, J. E., Zhao, Z. Q. & Vinten-Johansen, J. (1999) The role of neutrophils in myocardial ischemia-reperfusion injury. *Cardiovasc Res,* 43**,** 860-78.

Jujo, K., Ii, M. & Losordo, D. W. (2008) Endothelial progenitor cells in neovascularization of infarcted myocardium. *J Mol Cell Cardiol,* 45**,** 530-44.

Kakio, T., Matsumori, A., Ono, K., Ito, H., Matsushima, K. & Sasayama, S. (2000) Roles and relationship of macrophages and monocyte chemotactic and activating factor/monocyte chemoattractant protein-1 in the ischemic and reperfused rat heart. *Lab Invest,* 80**,** 1127-36.

Kalka, C., Tehrani, H., Laudenberg, B., Vale, P. R., Isner, J. M., Asahara, T. & Symes, J. F. (2000) VEGF gene transfer mobilizes endothelial progenitor cells in patients with inoperable coronary disease. *Ann Thorac Surg,* 70**,** 829-34.

Kanda, T., Takahashi, T., Kudo, S., Takeda, T., Tsugawa, H. & Takekoshi, N. (2004) Leptin deficiency enhances myocardial necrosis and lethality in a murine model of viral myocarditis. *Life Sci,* 75**,** 1435-47.

Kapadia, S. R., Oral, H., Lee, J., Nakano, M., Taffet, G. E. & Mann, D. L. (1997) Hemodynamic regulation of tumor necrosis factor-alpha gene and protein expression in adult feline myocardium. *Circ Res,* 81**,** 187-95.

Kastrup, J., Ripa, R. S., Wang, Y. & Jorgensen, E. (2006) Myocardial regeneration induced by granulocyte-colony-stimulating factor mobilization of stem cells in patients with acute or chronic ischaemic heart disease: a non-invasive alternative for clinical stem cell therapy? *Eur Heart J,* 27**,** 2748-54.

Kawamura, H., Kobayashi, M., Li, Q., Yamanishi, S., Katsumura, K., Minami, M., Wu, D. M. & Puro, D. G. (2004) Effects of angiotensin II on the pericyte-containing microvasculature of the rat retina. *J Physiol,* 561**,** 671-83.

Kayes-Wandover, K. M. & White, P. C. (2000) Steroidogenic enzyme gene expression in the human heart. *J Clin Endocrinol Metab,* 85**,** 2519-25.

Kayisli, U. A., Mahutte, N. G. & Arici, A. (2002) Uterine chemokines in reproductive physiology and pathology. *Am J Reprod Immunol,* 47**,** 213-21.

Kenyon, B. M., Voest, E. E., Chen, C. C., Flynn, E., Folkman, J. & D'amato, R. J. (1996) A model of angiogenesis in the mouse cornea. *Invest Ophthalmol Vis Sci,* 37**,** 1625-32.

Kerrigan, J. R., Veldhuis, J. D., Leyo, S. A., Iranmanesh, A. & Rogol, A. D. (1993) Estimation of daily cortisol production and clearance rates in normal pubertal males by deconvolution analysis. *J Clin Endocrinol Metab,* 76**,** 1505-10.

Kevin, L. G., Novalija, E. & Stowe, D. F. (2005) Reactive oxygen species as mediators of cardiac injury and protection: the relevance to anesthesia practice. *Anesth Analg,* 101**,** 1275-87.

Kido, M., Du, L., Sullivan, C. C., Li, X., Deutsch, R., Jamieson, S. W. & Thistlethwaite, P. A. (2005) Hypoxia-inducible factor 1-alpha reduces infarction and attenuates progression of cardiac dysfunction after myocardial infarction in the mouse. *J Am Coll Cardiol,* 46**,** 2116-24.

Kilgore, K. S., Park, J. L., Tanhehco, E. J., Booth, E. A., Marks, R. M. & Lucchesi, B. R. (1998) Attenuation of interleukin-8 expression in C6-deficient rabbits after myocardial ischemia/reperfusion. *J Mol Cell Cardiol,* 30**,** 75-85.

Kin, H., Wang, N. P., Halkos, M. E., Kerendi, F., Guyton, R. A. & Zhao, Z. Q. (2006) Neutrophil depletion reduces myocardial apoptosis and attenuates NFkappaB activation/TNFalpha release after ischemia and reperfusion. *J Surg Res,* 135**,** 170-8.

Kleiman, A. & Tuckermann, J. P. (2007) Glucocorticoid receptor action in beneficial and side effects of steroid therapy: lessons from conditional knockout mice. *Mol Cell Endocrinol,* 275**,** 98-108.

Klionsky, D. J. & Emr, S. D. (2000) Autophagy as a regulated pathway of cellular degradation. *Science,* 290**,** 1717-21.

Klusonova, P., Rehakova, L., Borchert, G., Vagnerova, K., Neckar, J., Ergang, P., Miksik, I., Kolar, F. & Pacha, J. (2009) Chronic intermittent hypoxia induces 11{beta}-hydroxysteroid dehydrogenase in rat heart. *Endocrinology*.

Koch, A. E., Kunkel, S. L., Harlow, L. A., Johnson, B., Evanoff, H. L., Haines, G. K., Burdick, M. D., Pope, R. M. & Strieter, R. M. (1992) Enhanced production of monocyte chemoattractant protein-1 in rheumatoid arthritis. *J Clin Invest,* 90**,** 772-9.

Kocher, A. A., Schuster, M. D., Bonaros, N., Lietz, K., Xiang, G., Martens, T. P., Kurlansky, P. A., Sondermeijer, H., Witkowski, P., Boyle, A., Homma, S., Wang, S. F. & Itescu, S. (2006) Myocardial homing and neovascularization by human bone marrow angioblasts is regulated by IL-8/Gro CXC chemokines. *J Mol Cell Cardiol,* 40**,** 455-64.

Kocher, A. A., Schuster, M. D., Szabolcs, M. J., Takuma, S., Burkhoff, D., Wang, J., Homma, S., Edwards, N. M. & Itescu, S. (2001) Neovascularization of ischemic myocardium by human bone-marrow-derived angioblasts prevents cardiomyocyte apoptosis, reduces remodeling and improves cardiac function. *Nat Med,* 7**,** 430-6.

Korpisalo, P., Karvinen, H., Rissanen, T. T., Kilpijoki, J., Marjomaki, V., Baluk, P., Mcdonald, D. M., Cao, Y., Eriksson, U., Alitalo, K. & Yla-Herttuala, S. (2008) Vascular endothelial growth factor-A and platelet-derived growth factor-B combination gene therapy prolongs angiogenic effects via recruitment of interstitial mononuclear cells and paracrine effects rather than improved pericyte coverage of angiogenic vessels. *Circ Res,* 103**,** 1092-9.

Kosiborod, M. (2008) Blood glucose and its prognostic implications in patients hospitalised with acute myocardial infarction. *Diab Vasc Dis Res,* 5**,** 269-75.

Kostin, S., Klein, G., Szalay, Z., Hein, S., Bauer, E. P. & Schaper, J. (2002) Structural correlate of atrial fibrillation in human patients. *Cardiovasc Res,* 54**,** 361-79.

Kotelevtsev, Y., Brown, R. W., Fleming, S., Kenyon, C., Edwards, C. R., Seckl, J. R. & Mullins, J. J. (1999) Hypertension in mice lacking 11beta-hydroxysteroid dehydrogenase type 2. *J Clin Invest,* 103**,** 683-9.

Kotelevtsev, Y., Holmes, M. C., Burchell, A., Houston, P. M., Schmoll, D., Jamieson, P., Best, R., Brown, R., Edwards, C. R., Seckl, J. R. & Mullins, J. J. (1997) 11beta-hydroxysteroid dehydrogenase type 1 knockout mice show attenuated glucocorticoid-inducible responses and resist hyperglycemia on obesity or stress. *Proc Natl Acad Sci U S A,* 94**,** 14924-9.

Kreider, T., Anthony, R. M., Urban, J. F., Jr. & Gause, W. C. (2007) Alternatively activated macrophages in helminth infections. *Curr Opin Immunol,* 19**,** 448-53.

Kukielka, G. L., Smith, C. W., Larosa, G. J., Manning, A. M., Mendoza, L. H., Daly, T. J., Hughes, B. J., Youker, K. A., Hawkins, H. K., Michael, L. H. & Et Al. (1995) Interleukin-8 gene induction in the myocardium after ischemia and reperfusion in vivo. *J Clin Invest,* 95**,** 89-103.

Kukielka, G. L., Smith, C. W., Manning, A. M., Youker, K. A., Michael, L. H. & Entman, M. L. (1995) Induction of interleukin-6 synthesis in the myocardium. Potential role in postreperfusion inflammatory injury. *Circulation,* 92**,** 1866-75.

Kutcher, M. E. & Herman, I. M. (2009) The pericyte: cellular regulator of microvascular blood flow. *Microvasc Res,* 77**,** 235-46.

Lakkisto, P., Kyto, V., Forsten, H., Siren, J. M., Segersvard, H., Voipio-Pulkki, L. M., Laine, M., Pulkki, K. & Tikkanen, I. (2010) Heme oxygenase-1 and carbon monoxide promote neovascularization after myocardial infarction by modulating the expression of HIF-1alpha, SDF-1alpha and VEGF-B. *Eur J Pharmacol,* 635**,** 156-64.

Lakshminarayanan, V., Lewallen, M., Frangogiannis, N. G., Evans, A. J., Wedin, K. E., Michael, L. H. & Entman, M. L. (2001) Reactive oxygen intermediates induce monocyte

chemotactic protein-1 in vascular endothelium after brief ischemia. *Am J Pathol,* 159**,** 1301-11.

Lambert, J. M., Lopez, E. F. & Lindsey, M. L. (2008) Macrophage roles following myocardial infarction. *Int J Cardiol,* 130**,** 147-58.

Lan, N. C., Karin, M., Nguyen, T., Weisz, A., Birnbaum, M. J., Eberhardt, N. L. & Baxter, J. D. (1984) Mechanisms of glucocorticoid hormone action. *J Steroid Biochem,* 20**,** 77-88.

Lasala, G. P. & Minguell, J. J. (2009) Bone marrow-derived stem/progenitor cells: their use in clinical studies for the treatment of myocardial infarction. *Heart Lung Circ,* 18**,** 171-80.

Lavery, G. G., Walker, E. A., Draper, N., Jeyasuria, P., Marcos, J., Shackleton, C. H., Parker, K. L., White, P. C. & Stewart, P. M. (2006) Hexose-6-phosphate dehydrogenase knock-out mice lack 11 beta-hydroxysteroid dehydrogenase type 1-mediated glucocorticoid generation. *J Biol Chem,* 281**,** 6546-51.

Law, P. K., Haider, K., Fang, G., Jiang, S., Chua, F., Lim, Y. T. & Sim, E. (2004) Human VEGF165-myoblasts produce concomitant angiogenesis/myogenesis in the regenerative heart. *Mol Cell Biochem,* 263**,** 173-8.

Lefer, A. M. (1968) Influence of corticosdteroids onmechanical performance of isolated rat papillary muscles. *Am J Physiol*, 214, 518-524

Lefer, A. M., Crossley, K., Grigonis, G. & Lefer, D. J. (1980) Mechanism of the beneficial effect of dexamethasone on myocardial cell integrity in acure myocardial ischemia. *Basic Res Cardiol,* 75**,** 328-39.

Lenardo, M. J. & Baltimore, D. (1989) NF-kappa B: a pleiotropic mediator of inducible and tissue-specific gene control. *Cell,* 58**,** 227-9.

Leor, J., Rozen, L., Zuloff-Shani, A., Feinberg, M. S., Amsalem, Y., Barbash, I. M., Kachel, E., Holbova, R., Mardor, Y., Daniels, D., Ocherashvilli, A., Orenstein, A. & Danon, D. (2006) Ex vivo activated human macrophages improve healing, remodeling, and function of the infarcted heart. *Circulation,* 114**,** I94-100.

Levonen, A. L., Vahakangas, E., Koponen, J. K. & Yla-Herttuala, S. (2008) Antioxidant gene therapy for cardiovascular disease: current status and future perspectives. *Circulation,* 117**,** 2142-50.

Lewis, S. R., Ahmed, S., Dym, C., Khaimova, E., Kest, B. & Bodnar, R. J. (2005) Inbred mouse strain survey of sucrose intake. *Physiol Behav,* 85**,** 546-56.

Li, A., Dubey, S., Varney, M. L., Dave, B. J. & Singh, R. K. (2003) IL-8 directly enhanced endothelial cell survival, proliferation, and matrix metalloproteinases production and regulated angiogenesis. *J Immunol,* 170**,** 3369-76.

Li, D., Fareh, S., Leung, T. K. & Nattel, S. (1999) Promotion of atrial fibrillation by heart failure in dogs: atrial remodeling of a different sort. *Circulation,* 100**,** 87-95.

Liao, Y. H. & Cheng, X. (2006) Autoimmunity in myocardial infarction. *Int J Cardiol,* 112**,** 21-6.

Libby, P., Maroko, P. R., Bloor, C. M., Sobel, B. E. & Braunwald, E. (1973) Reduction of experimental myocardial infarct size by corticosteroid administration. *J Clin Invest,* 52**,** 599-607.

Lijnen, P. & Petrov, V. (2000) Induction of cardiac fibrosis by aldosterone. *J Mol Cell Cardiol,* 32**,** 865-79.

Lin, L. & Achermann, J. C. (2004) The adrenal. *Horm Res,* 62 Suppl 3**,** 22-9.

Lindahl, P., Johansson, B. R., Leveen, P. & Betsholtz, C. (1997) Pericyte loss and microaneurysm formation in PDGF-B-deficient mice. *Science,* 277**,** 242-5.

Linde, R., Winn, S., Latta, D. & Hollifield, J. (1981) Graded dose effects of angiotensin II on aldosterone production in man during various levels of potassium intake. *Metabolism,* 30**,** 549-53.

Liu, L., Wang, Y. X., Zhou, J., Long, F., Sun, H. W., Liu, Y., Chen, Y. Z. & Jiang, C. L. (2005) Rapid non-genomic inhibitory effects of glucocorticoids on human neutrophil degranulation. *Inflamm Res,* 54**,** 37-41.

Liu, X., Huang, Y., Pokreisz, P., Vermeersch, P., Marsboom, G., Swinnen, M., Verbeken, E., Santos, J., Pellens, M., Gillijns, H., Van De Werf, F., Bloch, K. D. & Janssens, S. (2007) Nitric oxide inhalation improves microvascular flow and decreases infarction size after myocardial ischemia and reperfusion. *J Am Coll Cardiol,* 50**,** 808-17.

Liu, Y. H., D'ambrosio, M., Liao, T. D., Peng, H., Rhaleb, N. E., Sharma, U., Andre, S., Gabius, H. J. & Carretero, O. A. (2009) N-acetyl-seryl-aspartyl-lysyl-proline prevents cardiac remodeling and dysfunction induced by galectin-3, a mammalian adhesion/growth-regulatory lectin. *Am J Physiol Heart Circ Physiol,* 296**,** H404-12.

Lloyd, D. J., Helmering, J., Cordover, D., Bowsman, M., Chen, M., Hale, C., Fordstrom, P., Zhou, M., Wang, M., Kaufman, S. A. & Veniant, M. M. (2009) Antidiabetic effects of 11beta-HSD1 inhibition in a mouse model of combined diabetes, dyslipidaemia and atherosclerosis. *Diabetes Obes Metab,* 11**,** 688-99.

Loke, P., Nair, M. G., Parkinson, J., Guiliano, D., Blaxter, M. & Allen, J. E. (2002) IL-4 dependent alternatively-activated macrophages have a distinctive in vivo gene expression phenotype. *BMC Immunol,* 3**,** 7.

Lombes, M., Oblin, M. F., Gasc, J. M., Baulieu, F. E., Farman, N. & Bonvalet, J P. (1992) Immunohistochemical and biochemical evidence for a cardiovascular mineralocortioid receptor. *Circ Res,* 71, 503-510

Lombes, M., Alfaidy, N., Eugene, E., Lessana, A., Farman, N. & Bonvalet, J. P. (1995) Prerequisite for cardiac aldosterone action. Mineralocorticoid receptor and 11 beta-hydroxysteroid dehydrogenase in the human heart. *Circulation,* 92**,** 175-82.

Long, F., Wang, Y. X., Liu, L., Zhou, J., Cui, R. Y. & Jiang, C. L. (2005) Rapid nongenomic inhibitory effects of glucocorticoids on phagocytosis and superoxide anion production by macrophages. *Steroids,* 70**,** 55-61.

Longenecker, J. P., Kilty, L. A. & Johnson, L. K. (1982) Glucocorticoid influence on growth of vascular wall cells in culture. *J Cell Physiol,* 113**,** 197-202.

Longenecker, J. P., Kilty, L. A. & Johnson, L. K. (1984) Glucocorticoid inhibition of vascular smooth muscle cell proliferation: influence of homologous extracellular matrix and serum mitogens. *J Cell Biol,* 98**,** 534-40.

Losel, R. & Wehling, M. (2003) Nongenomic actions of steroid hormones. *Nat Rev Mol Cell Biol,* 4**,** 46-56.

Losordo, D. W., Vale, P. R., Symes, J. F., Dunnington, C. H., Esakof, D. D., Maysky, M., Ashare, A. B., Lathi, K. & Isner, J. M. (1998) Gene therapy for myocardial angiogenesis: initial clinical results with direct myocardial injection of phVEGF165 as sole therapy for myocardial ischemia. *Circulation,* 98**,** 2800-4.

Lutgens, E., Daemen, M. J., De Muinck, E. D., Debets, J., Leenders, P. & Smits, J. F. (1999) Chronic myocardial infarction in the mouse: cardiac structural and functional changes. *Cardiovasc Res,* 41**,** 586-93.

Ma, X. L., Tsao, P. S., Viehman, G. E. & Lefer, A. M. (1991) Neutrophil-mediated vasoconstriction and endothelial dysfunction in low-flow perfusion-reperfused cat coronary artery. *Circ Res,* 69**,** 95-106.

Mackinnon, A. C., Farnworth, S. L., Hodkinson, P. S., Henderson, N. C., Atkinson, K. M., Leffler, H., Nilsson, U. J., Haslett, C., Forbes, S. J. & Sethi, T. (2008) Regulation of alternative macrophage activation by galectin-3. *J Immunol,* 180**,** 2650-8.

Maclellan, W. R. & Schneider, M. D. (2000) Genetic dissection of cardiac growth control pathways. *Annu Rev Physiol,* 62**,** 289-319.

Madias, J. E. & Hood, W. B., Jr. (1982) Effects of methylprednisolone on the ischemic damage in patients with acute myocardial infarction. *Circulation,* 65**,** 1106-13.

Maekawa, Y., Anzai, T., Yoshikawa, T., Sugano, Y., Mahara, K., Kohno, T., Takahashi, T. & Ogawa, S. (2004) Effect of granulocyte-macrophage colony-stimulating factor inducer on left ventricular remodeling after acute myocardial infarction. *J Am Coll Cardiol,* 44**,** 1510-20.

Maisonpierre, P. C., Suri, C., Jones, P. F., Bartunkova, S., Wiegand, S. J., Radziejewski, C., Compton, D., Mcclain, J., Aldrich, T. H., Papadopoulos, N., Daly, T. J., Davis, S., Sato, T. N. & Yancopoulos, G. D. (1997) Angiopoietin-2, a natural antagonist for Tie2 that disrupts in vivo angiogenesis. *Science,* 277**,** 55-60.

Mangos, G. J., Walker, B. R., Kelly, J. J., Lawson, J. A., Webb, D. J. & Whitworth, J. A. (2000) Cortisol inhibits cholinergic vasodilation in the human forearm. *Am J Hypertens,* 13**,** 1155-60.

Mani, K. (2008) Programmed cell death in cardiac myocytes: strategies to maximize post-ischemic salvage. *Heart Fail Rev,* 13**,** 193-209.

Maniotis, A. J., Folberg, R., Hess, A., Seftor, E. A., Gardner, L. M., Pe'er, J., Trent, J. M., Meltzer, P. S. & Hendrix, M. J. (1999) Vascular channel formation by human melanoma cells in vivo and in vitro: vasculogenic mimicry. *Am J Pathol,* 155**,** 739-52.

Mann, D. L., Mcmurray, J. J., Packer, M., Swedberg, K., Borer, J. S., Colucci, W. S., Djian, J., Drexler, H., Feldman, A., Kober, L., Krum, H., Liu, P., Nieminen, M.,

Tavazzi, L., Van Veldhuisen, D. J., Waldenstrom, A., Warren, M., Westheim, A., Zannad, F. & Fleming, T. (2004) Targeted anticytokine therapy in patients with chronic heart failure: results of the Randomized Etanercept Worldwide Evaluation (RENEWAL). *Circulation,* 109**,** 1594-602.

Manoonkitiwongsa, P. S., Jackson-Friedman, C., Mcmillan, P. J., Schultz, R. L. & Lyden, P. D. (2001) Angiogenesis after stroke is correlated with increased numbers of macrophages: the clean-up hypothesis. *J Cereb Blood Flow Metab,* 21**,** 1223-31.

Maragoudakis, M. E., Sarmonika, M. & Panoutsacopoulou, M. (1989) Antiangiogenic action of heparin plus cortisone is associated with decreased collagenous protein synthesis in the chick chorioallantoic membrane system. *J Pharmacol Exp Ther,* 251**,** 679-82.

Martin-Fuentes, P., Civeira, F., Recalde, D., Garcia-Otin, A. L., Jarauta, E., Marzo, I. & Cenarro, A. (2007) Individual variation of scavenger receptor expression in human macrophages with oxidized low-density lipoprotein is associated with a differential inflammatory response. *J Immunol,* 179**,** 3242-8.

Masuzaki, H., Paterson, J., Shinyama, H., Morton, N. M., Mullins, J. J., Seckl, J. R. & Flier, J. S. (2001) A transgenic model of visceral obesity and the metabolic syndrome. *Science,* 294**,** 2166-70.

Maulik, N. & Thirunavukkarasu, M. (2008) Growth factors and cell therapy in myocardial regeneration. *J Mol Cell Cardiol,* 44**,** 219-27.

Mcewen, B. S., Biron, C. A., Brunson, K. W., Bulloch, K., Chambers, W. H., Dhabhar, F. S., Goldfarb, R. H., Kitson, R. P., Miller, A. H., Spencer, R. L. & Weiss, J. M. (1997) The role of adrenocorticoids as modulators of immune function in health and disease: neural, endocrine and immune interactions. *Brain Res Brain Res Rev,* 23**,** 79-133.

Mcmurray, J. J. & O'meara, E. (2004) Treatment of heart failure with spironolactone--trial and tribulations. *N Engl J Med,* 351**,** 526-8.

Mcnatt, L. G., Weimer, L., Yanni, J. & Clark, A. F. (1999) Angiostatic activity of steroids in the chick embryo CAM and rabbit cornea models of neovascularization. *J Ocul Pharmacol Ther,* 15**,** 413-23.

Meyer, G. P., Wollert, K. C., Lotz, J., Steffens, J., Lippolt, P., Fichtner, S., Hecker, H., Schaefer, A., Arseniev, L., Hertenstein, B., Ganser, A. & Drexler, H. (2006) Intracoronary bone marrow cell transfer after myocardial infarction: eighteen months' follow-up data from the randomized, controlled BOOST (BOne marrOw transfer to enhance ST-elevation infarct regeneration) trial. *Circulation,* 113**,** 1287-94.

Mihailidou, A. S., Loan Le, T. Y., Mardini, M. & Funder, J. W. (2009) Glucocorticoids Activate Cardiac Mineralocorticoid Receptors During Experimental Myocardial Infarction. *Hypertension*.

Milik, E., Szczepanska-Sadowska, E., Maslinski, W. & Cudnoch-Jedrzejewska, A. (2007) Enhanced expression of mineralocorticoid receptors in the heart after the myocardial infarct in rats. *J Physiol Pharmacol,* 58**,** 745-55.

Monder, C., Stewart, P. M., Lakshmi, V., Valentino, R., Burt, D. & Edwards, C. R. (1989) Licorice inhibits corticosteroid 11 beta-dehydrogenase of rat kidney and liver: in vivo and in vitro studies. *Endocrinology,* 125**,** 1046-53.

Morimoto, H., Takahashi, M., Izawa, A., Ise, H., Hongo, M., Kolattukudy, P. E. & Ikeda, U. (2006) Cardiac overexpression of monocyte chemoattractant protein-1 in transgenic mice prevents cardiac dysfunction and remodeling after myocardial infarction. *Circ Res,* 99**,** 891-9.

Mork, H. K., Sjaastad, I., Sande, J. B., Periasamy, M., Sejersted, O. M. & Louch, W. E. (2007) Increased cardiomyocyte function and Ca2+ transients in mice during early congestive heart failure. *J Mol Cell Cardiol,* 43**,** 177-86.

Mork, H. K., Sjaastad, I., Sejersted, O. M. & Louch, W. E. (2009) Slowing of cardiomyocyte Ca2+ release and contraction during heart failure progression in postinfarction mice. *Am J Physiol Heart Circ Physiol,* 296**,** H1069-79.

Morrison, J., Reduto, L., Pizzarello, R., Geller, K., Maley, T. & Gulotta, S. (1976) Modification of myocardial injury in man by corticosteroid administration. *Circulation,* 53**,** I200-4.

Morton, N. M., Holmes, M. C., Fievet, C., Staels, B., Tailleux, A., Mullins, J. J. & Seckl, J. R. (2001) Improved lipid and lipoprotein profile, hepatic insulin sensitivity, and glucose tolerance in 11beta-hydroxysteroid dehydrogenase type 1 null mice. *J Biol Chem,* 276**,** 41293-300.

Morton, N. M., Paterson, J. M., Masuzaki, H., Holmes, M. C., Staels, B., Fievet, C., Walker, B. R., Flier, J. S., Mullins, J. J. & Seckl, J. R. (2004) Novel adipose tissue-mediated resistance to diet-induced visceral obesity in 11 beta-hydroxysteroid dehydrogenase type 1-deficient mice. *Diabetes,* 53**,** 931-8.

Moskowitz, R. M., Burns, J. J., Dicarlo, E. F., Flaim, S. F., Harrison, T. S., Peuler, J. & Zelis, R. (1979) Cage size and exercise affects infarct size in rat after coronary artery cauterization. *J Appl Physiol,* 47**,** 393-6.

Mosser, D. M. & Edwards, J. P. (2008) Exploring the full spectrum of macrophage activation. *Nat Rev Immunol,* 8**,** 958-69.

Muller, W. A., Weigl, S. A., Deng, X. & Phillips, D. M. (1993) PECAM-1 is required for transendothelial migration of leukocytes. *J Exp Med,* 178**,** 449-60.

Munck, A., Guyre, P. M. & Holbrook, N. J. (1984) Physiological functions of glucocorticoids in stress and their relation to pharmacological actions. *Endocr Rev,* 5**,** 25-44.

Murdoch, C., Muthana, M., Coffelt, S. B. & Lewis, C. E. (2008) The role of myeloid cells in the promotion of tumour angiogenesis. *Nat Rev Cancer,* 8**,** 618-31.

Nahrendorf, M., Hu, K., Frantz, S., Jaffer, F. A., Tung, C. H., Hiller, K. H., Voll, S., Nordbeck, P., Sosnovik, D., Gattenlohner, S., Novikov, M., Dickneite, G., Reed, G. L., Jakob, P., Rosenzweig, A., Bauer, W. R., Weissleder, R. & Ertl, G. (2006) Factor XIII deficiency causes cardiac rupture, impairs wound healing, and aggravates cardiac remodeling in mice with myocardial infarction. *Circulation,* 113**,** 1196-202.

Nahrendorf, M., Swirski, F. K., Aikawa, E., Stangenberg, L., Wurdinger, T., Figueiredo, J. L., Libby, P., Weissleder, R. & Pittet, M. J. (2007) The healing myocardium sequentially mobilizes two monocyte subsets with divergent and complementary functions. *J Exp Med,* 204**,** 3037-47.

Nair, M. G., Gallagher, I. J., Taylor, M. D., Loke, P., Coulson, P. S., Wilson, R. A., Maizels, R. M. & Allen, J. E. (2005) Chitinase and Fizz family members are a generalized feature of nematode infection with selective upregulation of Ym1 and Fizz1 by antigen-presenting cells. *Infect Immun,* 73**,** 385-94.

Nakagawa, Y., Ito, H., Kitakaze, M., Kusuoka, H., Hori, M., Kuzuya, T., Higashino, Y., Fujii, K. & Minamino, T. (1995) Effect of angina pectoris on myocardial protection in patients with reperfused anterior wall myocardial infarction: retrospective clinical evidence of "preconditioning". *J Am Coll Cardiol,* 25**,** 1076-83.

Nauck, M., Karakiulakis, G., Perruchoud, A. P., Papakonstantinou, E. & Roth, M. (1998) Corticosteroids inhibit the expression of the vascular endothelial growth factor gene in human vascular smooth muscle cells. *Eur J Pharmacol,* 341**,** 309-15.

Nelken, N. A., Coughlin, S. R., Gordon, D. & Wilcox, J. N. (1991) Monocyte chemoattractant protein-1 in human atheromatous plaques. *J Clin Invest,* 88**,** 1121-7.

Nian, M., Lee, P., Khaper, N. & Liu, P. (2004) Inflammatory cytokines and postmyocardial infarction remodeling. *Circ Res,* 94**,** 1543-53.

Njauw, C. N., Yuan, H., Zheng, L., Yao, M. & Martins-Green, M. (2008) Origin of periendothelial cells in microvessels derived from human microvascular endothelial cells. *Int J Biochem Cell Biol,* 40**,** 710-20.

Nossuli, T. O., Lakshminarayanan, V., Baumgarten, G., Taffet, G. E., Ballantyne, C. M., Michael, L. H. & Entman, M. L. (2000) A chronic mouse model of myocardial ischemia-reperfusion: essential in cytokine studies. *Am J Physiol Heart Circ Physiol,* 278**,** H1049-55.

Nozawa, H., Chiu, C. & Hanahan, D. (2006) Infiltrating neutrophils mediate the initial angiogenic switch in a mouse model of multistage carcinogenesis. *Proc Natl Acad Sci U S A,* 103**,** 12493-8.

Nyirenda, M. J., Lindsay, R. S., Kenyon, C. J., Burchell, A. & Seckl, J. R. (1998) Glucocorticoid exposure in late gestation permanently programs rat hepatic phosphoenolpyruvate carboxykinase and glucocorticoid receptor expression and causes glucose intolerance in adult offspring. *J Clin Invest,* 101**,** 2174-81.

Oakley, R. H., Sar, M. & Cidlowski, J. A. (1996) The human glucocorticoid receptor beta isoform. Expression, biochemical properties, and putative function. *J Biol Chem,* 271**,** 9550-9.

Olivetti, G., Quaini, F., Sala, R., Lagrasta, C., Corradi, D., Bonacina, E., Gambert, S. R., Cigola, E. & Anversa, P. (1996) Acute myocardial infarction in humans is associated with activation of programmed myocyte cell death in the surviving portion of the heart. *J Mol Cell Cardiol,* 28**,** 2005-16.

Opie, L. H. (1971) Acute metabolic response in myocardial infarction. *Br Heart J,* 33**,** Suppl:129-37.

Orlic, D., Kajstura, J., Chimenti, S., Limana, F., Jakoniuk, I., Quaini, F., Nadal-Ginard, B., Bodine, D. M., Leri, A. & Anversa, P. (2001) Mobilized bone marrow cells repair

the infarcted heart, improving function and survival. *Proc Natl Acad Sci U S A,* 98**,** 10344-9.

Osborn, M., Debus, E. & Weber, K. (1984) Monoclonal antibodies specific for vimentin. *Eur J Cell Biol,* 34**,** 137-43.

Ouvrard-Pascaud, A., Sainte-Marie, Y., Benitah, J. P., Perrier, R., Soukaseum, C., Cat, A. N., Royer, A., Le Quang, K., Charpentier, F., Demolombe, S., Mechta-Grigoriou, F., Beggah, A. T., Maison-Blanche, P., Oblin, M. E., Delcayre, C., Fishman, G. I., Farman, N., Escoubet, B. & Jaisser, F. (2005) Conditional mineralocorticoid receptor expression in the heart leads to life-threatening arrhythmias. *Circulation,* 111**,** 3025-33.

Park, S. K., Jang, W. H. & Yang, Y. I. (2009) Expression of pro-angiogenic cytokines and their inhibition by dexamethasone in an ex vivo model of nasal polyps. *Biochem Biophys Res Commun,* 379**,** 255-60.

Patan, S. (2000) Vasculogenesis and angiogenesis as mechanisms of vascular network formation, growth and remodeling. *J Neurooncol,* 50**,** 1-15.

Paterson, J. M., Holmes, M. C., Kenyon, C. J., Carter, R., Mullins, J. J. & Seckl, J. R. (2006) Liver-selective transgene rescue of hypothalamic-pituitary-adrenal axis dysfunction in 11{beta}-hydroxysteroid dehydrogenase type 1 deficient mice. *Endocrinology*.

Paterson, J. M., Seckl, J. R. & Mullins, J. J. (2005) Genetic manipulation of 11beta-hydroxysteroid dehydrogenases in mice. *Am J Physiol Regul Integr Comp Physiol,* 289**,** R642-52.

Pauschinger, M., Knopf, D., Petschauer, S., Doerner, A., Poller, W., Schwimmbeck, P. L., Kuhl, U. & Schultheiss, H. P. (1999) Dilated cardiomyopathy is associated with significant changes in collagen type I/III ratio. *Circulation,* 99**,** 2750-6.

Payne, T. R., Oshima, H., Okada, M., Momoi, N., Tobita, K., Keller, B. B., Peng, H. & Huard, J. (2007) A relationship between vascular endothelial growth factor, angiogenesis, and cardiac repair after muscle stem cell transplantation into ischemic hearts. *J Am Coll Cardiol,* 50**,** 1677-84.

Penefsky, Z. J. & Kahn, M. (1971) Inotropic effects of dexamethasone in mammalian heart muscle. *Eur J Pharmacol,* 15**,** 259-66.

Pfeffer, M. A. & Braunwald, E. (1990) Ventricular remodeling after myocardial infarction. Experimental observations and clinical implications. *Circulation,* 81**,** 1161-72.

Pierard, L. A., Albert, A., Gilis, F., Sprynger, M., Carlier, J. & Kulbertus, H. E. (1987) Hemodynamic profile of patients with acute myocardial infarction at risk of infarct expansion. *Am J Cardiol,* 60**,** 5-9.

Pitchford, S. C., Furze, R. C., Jones, C. P., Wengner, A. M. & Rankin, S. M. (2009) Differential mobilization of subsets of progenitor cells from the bone marrow. *Cell Stem Cell,* 4**,** 62-72.

Pitt, B., White, H., Nicolau, J., Martinez, F., Gheorghiade, M., Aschermann, M., Van Veldhuisen, D. J., Zannad, F., Krum, H., Mukherjee, R. & Vincent, J. (2005) Eplerenone reduces mortality 30 days after randomization following acute myocardial infarction in patients with left ventricular systolic dysfunction and heart failure. *J Am Coll Cardiol,* 46**,** 425-31.

Plewka, M., Krzeminska-Pakula, M., Lipiec, P., Peruga, J. Z., Jezewski, T., Kidawa, M., Wierzbowska-Drabik, K., Korycka, A., Robak, T. & Kasprzak, J. D. (2009) Effect of intracoronary injection of mononuclear bone marrow stem cells on left ventricular function in patients with acute myocardial infarction. *Am J Cardiol,* 104**,** 1336-42.

Polverini, P. J., Cotran, P. S., Gimbrone, M. A., Jr. & Unanue, E. R. (1977) Activated macrophages induce vascular proliferation. *Nature,* 269**,** 804-6.

Porter, K. E. & Turner, N. A. (2009) Cardiac fibroblasts: at the heart of myocardial remodeling. *Pharmacol Ther,* 123**,** 255-78.

Potts, M. B., Vaughn, A. E., Mcdonough, H., Patterson, C. & Deshmukh, M. (2005) Reduced Apaf-1 levels in cardiomyocytes engage strict regulation of apoptosis by endogenous XIAP. *J Cell Biol,* 171**,** 925-30.

Pratt, W. B. (1978) The mechanism of glucocorticoid effects in fibroblasts. *J Invest Dermatol,* 71**,** 24-35.

Pratt, W. B. (1993) The role of heat shock proteins in regulating the function, folding, and trafficking of the glucocorticoid receptor. *J Biol Chem,* 268**,** 21455-8.

Prech, M., Grajek, S., Marszalek, A., Lesiak, M., Jemielity, M., Araszkiewicz, A., Mularek-Kubzdela, T. & Cieslinski, A. (2006) Chronic infarct-related artery occlusion is associated with a reduction in capillary density. Effects on infarct healing. *Eur J Heart Fail,* 8**,** 373-80.

Pross, C., Farooq, M. M., Lane, J. S., Angle, N., Tomono, C. K., Xavier, A. E., Freischlag, J. A., Collins, A. E., Law, R. E. & Gelabert, H. A. (2002) Rat and human aortic smooth muscle cells display differing migration and matrix metalloproteinase activities in response to dexamethasone. *J Vasc Surg,* 35**,** 1253-9.

Pujols, L., Mullol, J., Roca-Ferrer, J., Torrego, A., Xaubet, A., Cidlowski, J.A., & Picado, C. (2002) Expression of glucocorticoid receptor alpha- and beta- isoforms in human cells and tissues. *Am J Physiol Cell Physiol,* 283, C1324-C1311

Rabbitt, E. H., Gittoes, N. J., Stewart, P. M. & Hewison, M. (2003) 11beta-hydroxysteroid dehydrogenases, cell proliferation and malignancy. *J Steroid Biochem Mol Biol,* 85**,** 415-21.

Rabbitt, E. H., Lavery, G. G., Walker, E. A., Cooper, M. S., Stewart, P. M. & Hewison, M. (2002) Prereceptor regulation of glucocorticoid action by 11beta-hydroxysteroid dehydrogenase: a novel determinant of cell proliferation. *Faseb J,* 16**,** 36-44.

Ramos-Vara, J. A. (2005) Technical aspects of immunohistochemistry. *Vet Pathol,* 42**,** 405-26.

Ramsauer, M., Krause, D. & Dermietzel, R. (2002) Angiogenesis of the blood-brain barrier in vitro and the function of cerebral pericytes. *Faseb J,* 16**,** 1274-6.

Rangel, R., Sun, Y., Guzman-Rojas, L., Ozawa, M. G., Sun, J., Giordano, R. J., Van Pelt, C. S., Tinkey, P. T., Behringer, R. R., Sidman, R. L., Arap, W. & Pasqualini, R. (2007) Impaired angiogenesis in aminopeptidase N-null mice. *Proc Natl Acad Sci U S A,* 104**,** 4588-93.

Rask, E., Olsson, T., Soderberg, S., Andrew, R., Livingstone, D. E., Johnson, O. & Walker, B. R. (2001) Tissue-specific dysregulation of cortisol metabolism in human obesity. *J Clin Endocrinol Metab,* 86**,** 1418-21.

Reckless, J., Tatalick, L. M. & Grainger, D. J. (2001) The pan-chemokine inhibitor NR58-3.14.3 abolishes tumour necrosis factor-alpha accumulation and leucocyte recruitment induced by lipopolysaccharide in vivo. *Immunology,* 103**,** 244-54.

Reckless, J., Tatalick, L., Wilbert, S., Mckilligin, E. & Grainger, D. J. (2005) Broad-spectrum chemokine inhibition reduces vascular macrophage accumulation and collagenolysis consistent with plaque stabilization in mice. *J Vasc Res,* 42**,** 492-502.

Reini, S. A., Dutta, G., Wood, C. E. & Keller-Wood, M. (2008) Cardiac corticosteroid receptors mediate the enlargement of the ovine fetal heart induced by chronic increases in maternal cortisol. *J Endocrinol,* 198**,** 419-27.

Ren, G., Michael, L. H., Entman, M. L. & Frangogiannis, N. G. (2002) Morphological characteristics of the microvasculature in healing myocardial infarcts. *J Histochem Cytochem,* 50**,** 71-9.

Risau, W. (1997) Mechanisms of angiogenesis. *Nature,* 386**,** 671-4.

Roberts, R. D., V. Sobel, B E. (1976) Deleterious effects of methylprednisolone in patients with myocardial infarction. *Circulation,* 53**,** I204-6.

Rogatsky, I., Trowbridge, J. M. & Garabedian, M. J. (1997) Glucocorticoid receptor-mediated cell cycle arrest is achieved through distinct cell-specific transcriptional regulatory mechanisms. *Mol Cell Biol,* 17**,** 3181-93.

Rollins, B. J. (1997) Chemokines. *Blood,* 90**,** 909-28.

Romanic, A. M., Burns-Kurtis, C. L., Gout, B., Berrebi-Bertrand, I. & Ohlstein, E. H. (2001) Matrix metalloproteinase expression in cardiac myocytes following myocardial infarction in the rabbit. *Life Sci,* 68**,** 799-814.

Rossen, R. D., Michael, L. H., Hawkins, H. K., Youker, K., Dreyer, W. J., Baughn, R. E. & Entman, M. L. (1994) Cardiolipin-protein complexes and initiation of complement activation after coronary artery occlusion. *Circ Res,* 75**,** 546-55.

Rossi, F. (1986) The O2- -forming NADPH oxidase of the phagocytes: nature, mechanisms of activation and function. *Biochim Biophys Acta,* 853**,** 65-89.

Ruixing, Y., Dezhai, Y., Hai, W., Kai, H., Xianghong, W. & Yuming, C. (2007) Intramyocardial injection of vascular endothelial growth factor gene improves cardiac performance and inhibits cardiomyocyte apoptosis. *Eur J Heart Fail,* 9**,** 343-51.

Ruiz, L. M., Bedoya, G., Salazar, J., Garcia De, O. D. & Patino, P. J. (2002) Dexamethasone inhibits apoptosis of human neutrophils induced by reactive oxygen species. *Inflammation,* 26**,** 215-22.

Sadoshima, J., Jahn, L., Takahashi, T., Kulik, T. J. & Izumo, S. (1992) Molecular characterization of the stretch-induced adaptation of cultured cardiac cells. An in vitro model of load-induced cardiac hypertrophy. *J Biol Chem,* 267**,** 10551-60.

Sadoshima, J. & Izumo, S. (1993) Molecular characterization of angiotensin II--induced hypertrophy of cardiac myocytes and hyperplasia of cardiac fibroblasts. Critical role of the AT1 receptor subtype. *Circ Res,* 73**,** 413-23.

Sainte-Marie, Y., Cat, A. N., Perrier, R., Mangin, L., Soukaseum, C., Peuchmaur, M., Tronche, F., Farman, N., Escoubet, B., Benitah, J. P. & Jaisser, F. (2007) Conditional glucocorticoid receptor expression in the heart induces atrio-ventricular block. *Faseb J*.

Sakamoto, N., Tanaka, N. G., Tohgo, A., Osada, Y. & Ogawa, H. (1987) Inhibitory effects of heparin plus cortisone acetate on endothelial cell growth both in cultures and in tumor masses. *J Natl Cancer Inst,* 78**,** 581-5.

Sasaki, T., Fukazawa, R., Ogawa, S., Kanno, S., Nitta, T., Ochi, M. & Shimizu, K. (2007) Stromal cell-derived factor-1alpha improves infarcted heart function through angiogenesis in mice. *Pediatr Int,* 49**,** 966-71.

Savill, J. S., Henson, P. M. & Haslett, C. (1989a) Phagocytosis of aged human neutrophils by macrophages is mediated by a novel "charge-sensitive" recognition mechanism. *J Clin Invest,* 84**,** 1518-27.

Savill, J. S., Wyllie, A. H., Henson, J. E., Walport, M. J., Henson, P. M. & Haslett, C. (1989b) Macrophage phagocytosis of aging neutrophils in inflammation. Programmed cell death in the neutrophil leads to its recognition by macrophages. *J Clin Invest,* 83**,** 865-75.

Scarabelli, T., Stephanou, A., Rayment, N., Pasini, E., Comini, L., Curello, S., Ferrari, R., Knight, R. & Latchman, D. (2001) Apoptosis of endothelial cells precedes myocyte cell apoptosis in ischemia/reperfusion injury. *Circulation,* 104**,** 253-6.

Schellings, M. W., Vanhoutte, D., Swinnen, M., Cleutjens, J. P., Debets, J., Van Leeuwen, R. E., D'hooge, J., Van De Werf, F., Carmeliet, P., Pinto, Y. M., Sage, E. H. & Heymans, S. (2009) Absence of SPARC results in increased cardiac rupture and dysfunction after acute myocardial infarction. *J Exp Med,* 206**,** 113-23.

Scheuer, D. A. & Mifflin, S. W. (1997) Chronic corticosterone treatment increases myocardial infarct size in rats with ischemia-reperfusion injury. *Am J Physiol,* 272**,** R2017-24.

Scholz, D., Ziegelhoeffer, T., Helisch, A., Wagner, S., Friedrich, C., Podzuweit, T. & Schaper, W. (2002) Contribution of arteriogenesis and angiogenesis to postocclusive hindlimb perfusion in mice. *J Mol Cell Cardiol,* 34**,** 775-87.

Schweichel, J. U. & Merker, H. J. (1973) The morphology of various types of cell death in prenatal tissues. *Teratology,* 7**,** 253-66.

Seckl, J. R. (2004) 11beta-hydroxysteroid dehydrogenases: changing glucocorticoid action. *Curr Opin Pharmacol,* 4**,** 597-602.

Seckl, J. R. & Walker, B. R. (2001) Minireview: 11beta-hydroxysteroid dehydrogenase type 1- a tissue-specific amplifier of glucocorticoid action. *Endocrinology,* 142**,** 1371-6.

Sekido, N., Mukaida, N., Harada, A., Nakanishi, I., Watanabe, Y. & Matsushima, K. (1993) Prevention of lung reperfusion injury in rabbits by a monoclonal antibody against interleukin-8. *Nature,* 365**,** 654-7.

Sesti, C., Hale, S. L., Lutzko, C. & Kloner, R. A. (2005) Granulocyte colony-stimulating factor and stem cell factor improve contractile reserve of the infarcted left ventricle independent of restoring muscle mass. *J Am Coll Cardiol,* 46**,** 1662-9.

Shamhart, P. E. & Meszaros, J. G. (2009) Non-fibrillar collagens: Key mediators of post-infarction cardiac remodeling? *J Mol Cell Cardiol*.

Sharma, U. C., Pokharel, S., Van Brakel, T. J., Van Berlo, J. H., Cleutjens, J. P., Schroen, B., Andre, S., Crijns, H. J., Gabius, H. J., Maessen, J. & Pinto, Y. M. (2004) Galectin-3 marks activated macrophages in failure-prone hypertrophied hearts and contributes to cardiac dysfunction. *Circulation,* 110**,** 3121-8.

Sheppard, K. E. & Autelitano, D. J. (2002) 11Beta-hydroxysteroid dehydrogenase 1 transforms 11-dehydrocorticosterone into transcriptionally active glucocorticoid in neonatal rat heart. *Endocrinology,* 143**,** 198-204.

Shintani, S., Murohara, T., Ikeda, H., Ueno, T., Honma, T., Katoh, A., Sasaki, K., Shimada, T., Oike, Y. & Imaizumi, T. (2001) Mobilization of endothelial progenitor cells in patients with acute myocardial infarction. *Circulation,* 103**,** 2776-9.

Shioura, K. M., Geenen, D. L. & Goldspink, P. H. (2007) Assessment of cardiac function with the pressure-volume conductance system following myocardial infarction in mice. *Am J Physiol Heart Circ Physiol,* 293**,** H2870-7.

Shishido, T., Nozaki, N., Yamaguchi, S., Shibata, Y., Nitobe, J., Miyamoto, T., Takahashi, H., Arimoto, T., Maeda, K., Yamakawa, M., Takeuchi, O., Akira, S., Takeishi, Y. & Kubota, I. (2003) Toll-like receptor-2 modulates ventricular remodeling after myocardial infarction. *Circulation,* 108**,** 2905-10.

Shohet, R. V. & Garcia, J. A. (2007) Keeping the engine primed: HIF factors as key regulators of cardiac metabolism and angiogenesis during ischemia. *J Mol Med,* 85**,** 1309-15.

Sica, A., Schioppa, T., Mantovani, A. & Allavena, P. (2006) Tumour-associated macrophages are a distinct M2 polarised population promoting tumour progression: potential targets of anti-cancer therapy. *Eur J Cancer,* 42**,** 717-27.

Siragusa, M., Katare, R., Meloni, M., Damilano, F., Hirsch, E., Emanueli, C. & Madeddu, P. (2010) Involvement of phosphoinositide 3-kinase gamma in angiogenesis and healing of experimental myocardial infarction in mice. *Circ Res,* 106**,** 757-68.

Sivakumar, P., Gupta, S., Sarkar, S. & Sen, S. (2008) Upregulation of lysyl oxidase and MMPs during cardiac remodeling in human dilated cardiomyopathy. *Mol Cell Biochem,* 307**,** 159-67.

Silvestre, J. S., Heymes, C., Oubenaissa, A., Robert, V., Aupetit-Faisant, B., Carayon, A., Swynghedauw, B. & Delcayre, C. (1999) Activation of cardiac aldosterone production in rat myocardial infarction: effect of angiotensin II receptor blockade and role in cardiac fibrosis. *Circulation,* 99**,** 2694-701.

Simons, M. (2005) Angiogenesis: where do we stand now? *Circulation,* 111**,** 1556-66.

Slight, S., Ganjam, V. K., Nonneman, D. J. & Weber, K. T. (1993) Glucocorticoid metabolism in the cardiac interstitium: 11 beta-hydroxysteroid dehydrogenase activity in cardiac fibroblasts. *J Lab Clin Med,* 122**,** 180-7.

Slight, S. H., Ganjam, V. K., Gomez-Sanchez, C. E., Zhou, M. Y. & Weber, K. T. (1996) High affinity NAD(+)-dependent 11 beta-hydroxysteroid dehydrogenase in the human heart. *J Mol Cell Cardiol,* 28**,** 781-7.

Small, G. R. (2005) Glucocorticoids and angiogenesis. Edinburgh, University of Edinburgh.

Small, G. R., Hadoke, P. W., Sharif, I., Dover, A. R., Armour, D., Kenyon, C. J., Gray, G. A. & Walker, B. R. (2005) Preventing local regeneration of glucocorticoids by 11beta-hydroxysteroid dehydrogenase type 1 enhances angiogenesis. *Proc Natl Acad Sci U S A,* 102**,** 12165-70.

Solowiej, A., Biswas, P., Graesser, D. & Madri, J. A. (2003) Lack of platelet endothelial cell adhesion molecule-1 attenuates foreign body inflammation because of decreased angiogenesis. *Am J Pathol,* 162**,** 953-62.

Sottile, J. (2004) Regulation of angiogenesis by extracellular matrix. *Biochim Biophys Acta,* 1654**,** 13-22.

Souverein, P. C., Berard, A., Van Staa, T. P., Cooper, C., Egberts, A. C., Leufkens, H. G. & Walker, B. R. (2004) Use of oral glucocorticoids and risk of cardiovascular and cerebrovascular disease in a population based case-control study. *Heart,* 90**,** 859-65.

Spiga, F., Harrison, L. R., Wood, S. A., Atkinson, H. C., Macsweeney, C. P., Thomson, F., Craighead, M., Grassie, M. & Lightman, S. L. (2007) Effect of the glucocorticoid receptor antagonist Org 34850 on basal and stress-induced corticosterone secretion. *J Neuroendocrinol,* 19**,** 891-900.

Staat, P., Rioufol, G., Piot, C., Cottin, Y., Cung, T. T., L'huillier, I., Aupetit, J. F., Bonnefoy, E., Finet, G., Andre-Fouet, X. & Ovize, M. (2005) Postconditioning the human heart. *Circulation,* 112**,** 2143-8.

Stalmans, I., Ng, Y. S., Rohan, R., Fruttiger, M., Bouche, A., Yuce, A., Fujisawa, H., Hermans, B., Shani, M., Jansen, S., Hicklin, D., Anderson, D. J., Gardiner, T., Hammes, H. P., Moons, L., Dewerchin, M., Collen, D., Carmeliet, P. & D'amore, P. A. (2002) Arteriolar and venular patterning in retinas of mice selectively expressing VEGF isoforms. *J Clin Invest,* 109**,** 327-36.

Stancovski, I. & Baltimore, D. (1997) NF-kappaB activation: the I kappaB kinase revealed? *Cell,* 91**,** 299-302.

Stanley, A. W., Jr., Athanasuleas, C. L. & Buckberg, G. D. (2004) Heart failure following anterior myocardial infarction: an indication for ventricular restoration, a surgical method to reverse post-infarction remodeling. *Heart Fail Rev,* 9**,** 241-54.

Sternberg, E. M. (2006) Neural regulation of innate immunity: a coordinated nonspecific host response to pathogens. *Nat Rev Immunol,* 6**,** 318-28.

Steinbrech, D. S., Mehrara, B. J., Saadeh, P. B., Greenwald, J. A., Spector, J. A., Gittes, G. K. & Longaker, M. T. (2000) VEGF expression in an osteoblast-like cell line is regulated by a hypoxia response mechanism. *Am J Physiol Cell Physiol,* 278**,** C853-60.

Stewart, P. M. & Krozowski, Z. S. (1999) 11 beta-Hydroxysteroid dehydrogenase. *Vitam Horm,* 57**,** 249-324.

Su, X., Vicker, N., Trusselle, M., Halem, H., Culler, M. D. & Potter, B. V. (2009) Discovery of novel inhibitors of human 11beta-hydroxysteroid dehydrogenase type 1. *Mol Cell Endocrinol,* 301**,** 169-73.

Sudhir, K., Jennings, G. L., Esler, M. D., Korner, P. I., Blombery, P. A., Lambert, G. W., Scoggins, B. & Whitworth, J. A. (1989) Hydrocortisone-induced hypertension in humans: pressor responsiveness and sympathetic function. *Hypertension,* 13**,** 416-21.

Sumitra, M., Manikandan, P., Nayeem, M., Manohar, B. M., Lokanadam, B., Vairamuthu, S., Subramaniam, S. & Puvanakrishnan, R. (2005) Time course studies on the initiation of complement activation in acute myocardial infarction induced by coronary artery ligation in rats. *Mol Cell Biochem,* 268**,** 149-58.

Sun, Y. & Weber, K. T. (2000) Infarct scar: a dynamic tissue. *Cardiovasc Res,* 46**,** 250-6.

Sun, Y., Zhang, J. Q., Zhang, J. & Lamparter, S. (2000) Cardiac remodeling by fibrous tissue after infarction in rats. *J Lab Clin Med,* 135**,** 316-23.

Sunderkotter, C., Steinbrink, K., Goebeler, M., Bhardwaj, R. & Sorg, C. (1994) Macrophages and angiogenesis. *J Leukoc Biol,* 55**,** 410-22.

Svendsen, J. H. & Bjerrum, P. J. (1992) Effects of exogenous oxygen derived free radicals on myocardial capillary permeability, vascular tone, and incidence of ventricular arrhythmias in the canine heart. *Cardiovasc Res,* 26**,** 1181-8.

Swirski, F. K., Nahrendorf, M., Etzrodt, M., Wildgruber, M., Cortez-Retamozo, V., Panizzi, P., Figueiredo, J. L., Kohler, R. H., Chudnovskiy, A., Waterman, P., Aikawa, E., Mempel, T. R., Libby, P., Weissleder, R. & Pittet, M. J. (2009) Identification of

splenic reservoir monocytes and their deployment to inflammatory sites. *Science,* 325**,** 612-6.

Syntichaki, P., Xu, K., Driscoll, M. & Tavernarakis, N. (2002) Specific aspartyl and calpain proteases are required for neurodegeneration in C. elegans. *Nature,* 419**,** 939-44.

Takahashi, T., Kalka, C., Masuda, H., Chen, D., Silver, M., Kearney, M., Magner, M., Isner, J. M. & Asahara, T. (1999) Ischemia- and cytokine-induced mobilization of bone marrow-derived endothelial progenitor cells for neovascularization. *Nat Med,* 5**,** 434-8.

Takahashi, M., Li, T. S., Suzuki, R., Kobayashi, T., Ito, H., Ikeda, Y., Matsuzaki, M. & Hamano, K. (2006) Cytokines produced by bone marrow cells can contribute to functional improvement of the infarcted heart by protecting cardiomyocytes from ischemic injury. *Am J Physiol Heart Circ Physiol,* 291**,** H886-93.

Takeda, M., Tatsumi, T., Matsunaga, S., Hayashi, H., Kimata, M., Honsho, S., Nishikawa, S., Mano, A., Shiraishi, J., Yamada, H., Takahashi, T., Matoba, S., Kobara, M. & Matsubara, H. (2007) Spironolactone modulates expressions of cardiac mineralocorticoid receptor and 11beta-hydroxysteroid dehydrogenase 2 and prevents ventricular remodeling in post-infarct rat hearts. *Hypertens Res,* 30**,** 427-37.

Takeda, Y., Miyamori, I., Yoneda, T., Iki, K., Hatakeyama, H., Blair, I. A., Hsieh, F. Y. & Takeda, R. (1994) Synthesis of corticosterone in the vascular wall. *Endocrinology,* 135**,** 2283-6.

Tao, Z. Y., Cavasin, M. A., Yang, F., Liu, Y. H. & Yang, X. P. (2004) Temporal changes in matrix metalloproteinase expression and inflammatory response associated with cardiac rupture after myocardial infarction in mice. *Life Sci,* 74**,** 1561-72.

Taylor, K. R., Trowbridge, J. M., Rudisill, J. A., Termeer, C. C., Simon, J. C. & Gallo, R. L. (2004) Hyaluronan fragments stimulate endothelial recognition of injury through TLR4. *J Biol Chem,* 279**,** 17079-84.

Terrovitis, J., Charitos, C., Dolou, P., Papalois, A., Eleftheriou, A., Tsolakis, E., Charitos, E., Mponios, M., Karanastasis, G., Koudoumas, D., Agapitos, E. & Nanas, J. N. (2004) No effect of stem cell mobilization with GM-CSF on infarct size and left ventricular function in experimental acute myocardial infarction. *Basic Res Cardiol,* 99**,** 241-6.

Thelen, M., Peveri, P., Kernen, P., Von Tscharner, V., Walz, A. & Baggiolini, M. (1988) Mechanism of neutrophil activation by NAF, a novel monocyte-derived peptide agonist. *Faseb J,* 2**,** 2702-6.

Thiemermann, C. (2002) Corticosteroids and cardioprotection. *Nat Med,* 8**,** 453-5.

Thieringer, R., Le Grand, C. B., Carbin, L., Cai, T. Q., Wong, B., Wright, S. D. & Hermanowski-Vosatka, A. (2001) 11 Beta-hydroxysteroid dehydrogenase type 1 is induced in human monocytes upon differentiation to macrophages. *J Immunol,* 167**,** 30-5.

Thomas, W. E. (1999) Brain macrophages: on the role of pericytes and perivascular cells. *Brain Res Brain Res Rev,* 31**,** 42-57.

Thompson, R. D., Noble, K. E., Larbi, K. Y., Dewar, A., Duncan, G. S., Mak, T. W. & Nourshargh, S. (2001) Platelet-endothelial cell adhesion molecule-1 (PECAM-1)-deficient mice demonstrate a transient and cytokine-specific role for PECAM-1 in leukocyte migration through the perivascular basement membrane. *Blood,* 97**,** 1854-60.

Thornberry, N. A. & Lazebnik, Y. (1998) Caspases: enemies within. *Science,* 281**,** 1312-6.

Thurston, G., Suri, C., Smith, K., Mcclain, J., Sato, T. N., Yancopoulos, G. D. & Mcdonald, D. M. (1999) Leakage-resistant blood vessels in mice transgenically overexpressing angiopoietin-1. *Science,* 286**,** 2511-4.

Tirziu, D., Chorianopoulos, E., Moodie, K. L., Palac, R. T., Zhuang, Z. W., Tjwa, M., Roncal, C., Eriksson, U., Fu, Q., Elfenbein, A., Hall, A. E., Carmeliet, P., Moons, L. & Simons, M. (2007) Myocardial hypertrophy in the absence of external stimuli is induced by angiogenesis in mice. *J Clin Invest,* 117**,** 3188-97.

Tomlinson, J. W. & Stewart, P. M. (2005) Mechanisms of disease: Selective inhibition of 11beta-hydroxysteroid dehydrogenase type 1 as a novel treatment for the metabolic syndrome. *Nat Clin Pract Endocrinol Metab,* 1**,** 92-9.

Tu, H., Powers, J. P., Liu, J., Ursu, S., Sudom, A., Yan, X., Xu, H., Meininger, D., Degraffenreid, M., He, X., Jaen, J. C., Sun, D., Labelle, M., Yamamoto, H., Shan, B., Walker, N. P. & Wang, Z. (2008) Distinctive molecular inhibition mechanisms for selective inhibitors of human 11beta-hydroxysteroid dehydrogenase type 1. *Bioorg Med Chem,* 16**,** 8922-31.

Ullian, M. E. (1999) The role of corticosteriods in the regulation of vascular tone. *Cardiovasc Res,* 41**,** 55-64.

Van Amerongen, M. J., Bou-Gharios, G., Popa, E., Van Ark, J., Petersen, A. H., Van Dam, G. M., Van Luyn, M. J. & Harmsen, M. C. (2008) Bone marrow-derived myofibroblasts contribute functionally to scar formation after myocardial infarction. *J Pathol,* 214**,** 377-86.

Van Amerongen, M. J., Harmsen, M. C., Van Rooijen, N., Petersen, A. H. & Van Luyn, M. J. (2007) Macrophage depletion impairs wound healing and increases left ventricular remodeling after myocardial injury in mice. *Am J Pathol,* 170**,** 818-29.

Van Den Bos, E. J., Mees, B. M., De Waard, M. C., De Crom, R. & Duncker, D. J. (2005) A novel model of cryoinjury-induced myocardial infarction in the mouse: a comparison with coronary artery ligation. *Am J Physiol Heart Circ Physiol,* 289**,** H1291-300.

Van Der Horst, I. C., Voors, A. A. & Van Veldhuisen, D. J. (2007) Treatment of heart failure with ACE inhibitors and beta-blockers: what is next? Aldosterone receptor antagonists? *Clin Res Cardiol,* 96**,** 193-5.

Van Der Laan, A. M., Piek, J. J. & Van Royen, N. (2009) Targeting angiogenesis to restore the microcirculation after reperfused MI. *Nat Rev Cardiol,* 6**,** 515-23.

Van Es, S. & Devreotes, P. N. (1999) Molecular basis of localized responses during chemotaxis in amoebae and leukocytes. *Cell Mol Life Sci,* 55**,** 1341-51.

Van Heerebeek, L., Hamdani, N., Handoko, M. L., Falcao-Pires, I., Musters, R. J., Kupreishvili, K., Ijsselmuiden, A. J., Schalkwijk, C. G., Bronzwaer, J. G., Diamant, M., Borbely, A., Van Der Velden, J., Stienen, G. J., Laarman, G. J., Niessen, H. W. & Paulus, W. J. (2008) Diastolic stiffness of the failing diabetic heart: importance of fibrosis, advanced glycation end products, and myocyte resting tension. *Circulation,* 117**,** 43-51.

Van Laake, L. W., Passier, R., Monshouwer-Kloots, J., Nederhoff, M.G., Ward-Van Oostwaard, D., Field, L.J., Van Echteld, C.J., Doevendans, P.A., Mummery, C.L. (2007) Monitoring of cell therapy and assesment of cardiac function using magnetic resonance imaging in a mouse model of myocardial infarction. *Nature protocols,* 2**,** 2551-2567.

Van Laake, L. W., Van Den Driesche, S., Post, S., Feijen, A., Jansen, M. A., Driessens, M. H., Mager, J. J., Snijder, R. J., Westermann, C. J., Doevendans, P. A., Van Echteld, C. J., Ten Dijke, P., Arthur, H. M., Goumans, M. J., Lebrin, F. & Mummery, C. L. (2006) Endoglin has a crucial role in blood cell-mediated vascular repair. *Circulation,* 114**,** 2288-97.

Vandervelde, S., Van Amerongen, M. J., Tio, R. A., Petersen, A. H., Van Luyn, M. J. & Harmsen, M. C. (2006) Increased inflammatory response and neovascularization in reperfused vs. non-reperfused murine myocardial infarction. *Cardiovasc Pathol,* 15**,** 83-90.

Vandervelde, S., Van Luyn, M. J., Rozenbaum, M. H., Petersen, A. H., Tio, R. A. & Harmsen, M. C. (2007) Stem cell-related cardiac gene expression early after murine myocardial infarction. *Cardiovasc Res,* 73**,** 783-93.

Vanhoutte, D., Schellings, M., Pinto, Y. & Heymans, S. (2006) Relevance of matrix metalloproteinases and their inhibitors after myocardial infarction: a temporal and spatial window. *Cardiovasc Res,* 69**,** 604-13.

Velagaleti, R. S., Pencina, M. J., Murabito, J. M., Wang, T. J., Parikh, N. I., D'agostino, R. B., Levy, D., Kannel, W. B. & Vasan, R. S. (2008) Long-term trends in the incidence of heart failure after myocardial infarction. *Circulation,* 118**,** 2057-62.

Veniant, M. M., Hale, C., Komorowski, R., Chen, M. M., St Jean, D. J., Fotsch, C. & Wang, M. (2009) Time of the day for 11beta-HSD1 inhibition plays a role in improving glucose homeostasis in DIO mice. *Diabetes Obes Metab,* 11**,** 109-17.

Virag, J. I. & Murry, C. E. (2003) Myofibroblast and endothelial cell proliferation during murine myocardial infarct repair. *Am J Pathol,* 163**,** 2433-40.

Vivaldi, M. T., Eyre, D. R., Kloner, R. A. & Schoen, F. J. (1987) Effects of methylprednisolone on collagen biosynthesis in healing acute myocardial infarction. *Am J Cardiol,* 60**,** 424-5.

Vliegen, H. W., Van Der Laarse, A., Cornelisse, C. J. & Eulderink, F. (1991) Myocardial changes in pressure overload-induced left ventricular hypertrophy. A study on tissue composition, polyploidization and multinucleation. *Eur Heart J,* 12**,** 488-94.

Wagner, E. M., Sanchez, J., Mcclintock, J. Y., Jenkins, J. & Moldobaeva, A. (2008) Inflammation and ischemia-induced lung angiogenesis. *Am J Physiol Lung Cell Mol Physiol,* 294**,** L351-7.

Walker, B. R. (2007a) Extra-adrenal regeneration of glucocorticoids by 11beta-hydroxysteroid dehydrogenase type 1: physiological regulator and pharmacological target for energy partitioning. *Proc Nutr Soc,* 66**,** 1-8.

Walker, B. R. (2007b) Glucocorticoids and cardiovascular disease. *Eur J Endocrinol,* 157**,** 545-59.

Walker, B. R., Connacher, A. A., Lindsay, R. M., Webb, D. J. & Edwards, C. R. (1995) Carbenoxolone increases hepatic insulin sensitivity in man: a novel role for 11-oxosteroid reductase in enhancing glucocorticoid receptor activation. *J Clin Endocrinol Metab,* 80**,** 3155-9.

Walker, B. R., Connacher, A. A., Webb, D. J. & Edwards, C. R. (1992) Glucocorticoids and blood pressure: a role for the cortisol/cortisone shuttle in the control of vascular tone in man. *Clin Sci (Lond),* 83**,** 171-8.

Walker, B. R. & Seckl, J. R. (2003) 11beta-hydroxysteroid dehydrogenase type 1 as a novel therapeutic target in metabolic and neurodegenerative disease. *Expert Opin Ther Targets,* 7**,** 771-83.

Walker, B. R., Yau, J. L., Brett, L. P., Seckl, J. R., Monder, C., Williams, B. C. & Edwards, C. R. (1991) 11 beta-hydroxysteroid dehydrogenase in vascular smooth muscle and heart: implications for cardiovascular responses to glucocorticoids. *Endocrinology,* 129**,** 3305-12.

Weathington, N. M., Van Houwelingen, A. H., Noerager, B. D., Jackson, P. L., Kraneveld, A. D., Galin, F. S., Folkerts, G., Nijkamp, F. P. & Blalock, J. E. (2006) A novel peptide CXCR ligand derived from extracellular matrix degradation during airway inflammation. *Nat Med,* 12**,** 317-23.

Weber, K. T. (1989) Cardiac interstitium in health and disease: the fibrillar collagen network. *J Am Coll Cardiol,* 13**,** 1637-52.

Wei, L., Macdonald, T. M. & Walker, B. R. (2004) Taking glucocorticoids by prescription is associated with subsequent cardiovascular disease. *Ann Intern Med,* 141**,** 764-70.

White, H. D., Norris, R. M., Brown, M. A., Brandt, P. W., Whitlock, R. M. & Wild, C. J. (1987) Left ventricular end-systolic volume as the major determinant of survival after recovery from myocardial infarction. *Circulation,* 76**,** 44-51.

Whitehurst, R. M., Jr., Zhang, M., Bhattacharjee, A. & Li, M. (1999) Dexamethasone-induced hypertrophy in rat neonatal cardiac myocytes involves an elevated L-type Ca(2+)current. *J Mol Cell Cardiol,* 31**,** 1551-8.

Whitworth, J. A. (1994) Studies on the mechanisms of glucocorticoid hypertension in humans. *Blood Press,* 3**,** 24-32.

Whitworth, J. A., Schyvens, C. G., Zhang, Y., Andrews, M. C., Mangos, G. J. & Kelly, J. J. (2002) The nitric oxide system in glucocorticoid-induced hypertension. *J Hypertens,* 20**,** 1035-43.

Xu, M., Uemura, R., Dai, Y., Wang, Y., Pasha, Z. & Ashraf, M. (2007) In vitro and in vivo effects of bone marrow stem cells on cardiac structure and function. *J Mol Cell Cardiol,* 42**,** 441-8.

Yamahara, K. & Itoh, H. (2009) Potential use of endothelial progenitor cells for regeneration of the vasculature. *Ther Adv Cardiovasc Dis,* 3**,** 17-27.

Yang, F., Liu, Y. H., Yang, X. P., Xu, J., Kapke, A. & Carretero, O. A. (2002) Myocardial infarction and cardiac remodelling in mice. *Exp Physiol,* 87**,** 547-55.

Yang, S. & Zhang, L. (2004) Glucocorticoids and vascular reactivity. *Curr Vasc Pharmacol,* 2**,** 1-12.

Yang, Z., Zingarelli, B. & Szabo, C. (2000) Crucial role of endogenous interleukin-10 production in myocardial ischemia/reperfusion injury. *Circulation,* 101**,** 1019-26.

Yang, Z. J., Chen, B., Sheng, Z., Zhang, D. G., Jia, E. Z., Wang, W., Ma, D. C., Zhu, T. B., Wang, L. S., Li, C. J., Wang, H., Cao, K. J. & Ma, W. Z. (2010) Improvement of heart function in postinfarct heart failure swine models after hepatocyte growth factor gene transfer: comparison of low-, medium- and high-dose groups. *Mol Biol Rep,* 37**,** 2075-81.

Yano, A., Fujii, Y., Iwai, A., Kageyama, Y. & Kihara, K. (2006) Glucocorticoids suppress tumor angiogenesis and in vivo growth of prostate cancer cells. *Clin Cancer Res,* 12**,** 3003-9.

Yano, T., Miura, T., Whittaker, P., Miki, T., Sakamoto, J., Nakamura, Y., Ichikawa, Y., Ikeda, Y., Kobayashi, H., Ohori, K. & Shimamoto, K. (2006) Macrophage colony-stimulating factor treatment after myocardial infarction attenuates left ventricular dysfunction by accelerating infarct repair. *J Am Coll Cardiol,* 47**,** 626-34.

Yaoita, H., Ogawa, K., Maehara, K. & Maruyama, Y. (1998) Attenuation of ischemia/reperfusion injury in rats by a caspase inhibitor. *Circulation,* 97**,** 276-81.

Yau, T. M., Kim, C., Li, G., Zhang, Y., Weisel, R. D. & Li, R. K. (2005) Maximizing ventricular function with multimodal cell-based gene therapy. *Circulation,* 112**,** I123-8.

Yau, J. L., Noble, J., Kenyon, C. J., Hibberd, C., Kotelevtsev, Y., Mullins, J. J. & Seckl, J. R. (2001) Lack of tissue glucocorticoid reactivation in 11beta -hydroxysteroid dehydrogenase type 1 knockout mice ameliorates age-related learning impairments. *Proc Natl Acad Sci U S A,* 98**,** 4716-21.

Yoshikawa, N., Nagasaki, M., Sano, M., Tokudome, S., Ueno, K., Shimizu, N., Imoto, S., Miyano, S., Suematsu, M., Fukuda, K., Morimoto, C. & Tanaka, H. (2009) Ligand-based gene expression profiling reveals novel roles of glucocorticoid receptor in cardiac metabolism. *Am J Physiol Endocrinol Metab,* 296**,** E1363-73.

Ytrehus, K., Liu, Y., Tsuchida, A., Miura, T., Liu, G. S., Yang, X. M., Herbert, D., Cohen, M. V. & Downey, J. M. (1994) Rat and rabbit heart infarction: effects of

anesthesia, perfusate, risk zone, and method of infarct sizing. *Am J Physiol,* 267**,** H2383-90.

Zannad, F. & Radauceanu, A. (2005) Effect of MR blockade on collagen formation and cardiovascular disease with a specific emphasis on heart failure. *Heart Fail Rev,* 10**,** 71-8.

Zhang, T. Y., Ding, X. & Daynes, R. A. (2005) The expression of 11 beta-hydroxysteroid dehydrogenase type I by lymphocytes provides a novel means for intracrine regulation of glucocorticoid activities. *J Immunol,* 174**,** 879-89.

Zhao, W., Zhao, D., Yan, R. & Sun, Y. (2009) Cardiac oxidative stress and remodeling following infarction: role of NADPH oxidase. *Cardiovasc Pathol,* 18**,** 156-66.

Zhou, L., Azfer, A., Niu, J., Graham, S., Choudhury, M., Adamski, F. M., Younce, C., Binkley, P. F. & Kolattukudy, P. E. (2006) Monocyte chemoattractant protein-1 induces a novel transcription factor that causes cardiac myocyte apoptosis and ventricular dysfunction. *Circ Res,* 98**,** 1177-85.

Zymek, P., Nah, D. Y., Bujak, M., Ren, G., Koerting, A., Leucker, T., Huebener, P., Taffet, G., Entman, M. & Frangogiannis, N. G. (2007) Interleukin-10 is not a critical regulator of infarct healing and left ventricular remodeling. *Cardiovasc Res,* 74**,** 313-22.

Appendix 1: Solutions

Acid alcohol

300ml 74 OP + 3ml concentrated HCl.

ACK red blood cell lysis buffer

8.29g NH_4Cl (0.15M), 1g $KHCO_3$ (1mM), 37.2mg NA_2EDTA (0.1mM). Add 800ml water; adjust to pH 7.2-7.4 with 2N HCl. Add water up to 1 litre. Filter sterilize through 0.2µM filter.

Alkaline tap water

400ml tap water + 2-3 drops of ammonia

Anaesthetic

To make a 5ml solution add 0.5ml medetomidine, 0.38ml ketamine and 0.5ml atropine to 3.62ml sterile saline or water for injections.

Aniline blue

2.5g Aniline blue +2ml acetic acid, glacial + 100ml distilled water

Borate buffer (130mM Boric acid, 67.5mM Na OH)

4.125g boric acid + 1.75 concentrated HCl + 500ml distilled water. pH to 7.6 then add 2.5g BSA fraction V. Store at -20°C.

BrdU

Dissolve 2.5mg BrdU in 0.5ml warm sterile saline

Collagenase

Dissolve 50mg collagenase type IA-S in 99ml PBS then add 11ml fetal calf serum.

Citrate buffer

1.92g citrate buffer in 1000ml distilled water, pH to 6.0 then add 1ml Tween 20

DEPC treated water

100µl diethyl pyrocarbonate (DEPC) in 100ml distilled water. Left overnight before autoclaving.

DAB (3, 3'-diaminobenzidine) Substrate

To 5ml distilled water add 2 drop buffer solution, mix well, 4 drops DAB stock solution, mix well and 2 drops hydrogen peroxide, mix well. All reagents are provided in the kit.

2N HCl

20ml 10N HCl to 80ml distilled water

Mouse on Mouse (MOM) blocking solution

To 2.5ml PBS or TBS add 2 drops MOM blocking solution.

Picrosirius Red

0.5g Direct Red in 500ml saturated picric acid

Phosphomolybdic-phosphotungstic acid

25 ml 5% phosphomolybdic acid + 25 ml 5% phosphotungstic acid

Phosphate buffered saline

1 tablet per 200ml distilled water

SG Substrate kit

To 5ml PBS (pH7.5) add 3 drops of chromagen, mix well, 3 drops hydrogen peroxide and mix well. Reagents are provided in the kit

Tail buffer

0.05M Tris HCl, 0.1M EDTA, 0.1M NaCl, 1% SDS

TE buffer

50mM Tris Base, 1MM EDTA, pH8.0

Triphenyltetrazolium

Tetrasodiumchloride 1%: 1g in 100ml phos buffer at pH7.4

Tris buffered saline (TBS)-Tween

30.5g Tris base, 45g NaCl, 2.5ml Tween 20 in 500ml distilled water for 20x stock. Diluted 1 in 10 for working stock. For TBS make omit the Tween

Tris-EDTA buffer

1.21g Tris base, 0.37g EDTA in 100ml distilled water. pH to 9.0. Diluted 1 in 10 for working stock and add 0.5ml Tween 20.

Trypsin

1g Trypsin, 1g CaCl in 800ml distilled water, pH to 7.4, make up to 1000ml.

Weigert's iron haematoxylin

Solution A 1g haematoxylin + 100ml 95% ethanol

Solution B 4ml 29% ferric chloride in water + 95ml distilled water + 1ml HCl

To make working stock solutions A and B were added in equal volumes and mixed thoroughly

Appendix 2: Published paper

OXFORD UNIVERSITY PRESS LICENSE TERMS AND CONDITIONS

Aug 13, 2010

This is a License Agreement between Sara J McSweeney ("You") and Oxford University Press ("Oxford University Press") provided by Copyright Clearance Center ("CCC"). The license consists of your order details, the terms and conditions provided by Oxford University Press, and the payment terms and conditions.

All payments must be made in full to CCC. For payment instructions, please see information listed at the bottom of this form.

License Number	2473611385377
License date	Jul 21, 2010
Licensed content publisher	Oxford University Press
Licensed content publication	Cardiovascular Research
Licensed content title	Improved heart function follows enhanced inflammatory cell recruitment and angiogenesis in 11βHSD1-deficient mice post-MI:
Licensed content author	Sara J. McSweeney, Patrick W.F. Hadoke, Agnieszka M. Kozak, Gary R. Small, Hiba Khaled, Brian R. Walker, Gillian A. Gray
Licensed content date	05/21/2010
Type of Use	Thesis/Dissertation
Institution name	
Title of your work	11 beta hydroxysteroid deydrogenase type 1: A new therapeutic target post-myocardial infarction?
Publisher of your work	n/a
Expected publication date	Jul 2010
Permissions cost	0.00 GBP
Value added tax	0.00 GBP
Total	0.00 GBP
Total	0.00 GBP
Terms and Conditions	

STANDARD TERMS AND CONDITIONS FOR REPRODUCTION OF MATERIAL

FROM AN OXFORD UNIVERSITY PRESS JOURNAL

1. Use of the material is restricted to the type of use specified in your order details.

2. This permission covers the use of the material in the English language in the following territory: world. If you have requested additional permission to translate this material, the terms and conditions of this reuse will be set out in clause 12.

3. This permission is limited to the particular use authorized in (1) above and does not allow you to sanction its use elsewhere in any other format other than specified above, nor does it apply to quotations, images, artistic works etc that have been reproduced from other sources which may be part of the material to be used.

4. No alteration, omission or addition is made to the material without our written consent. Permission must be re-cleared with Oxford University Press if/when you decide to reprint.

5. The following credit line appears wherever the material is used: author, title, journal, year, volume, issue number, pagination, by permission of Oxford University Press or the sponsoring society if the journal is a society journal. Where a journal is being published on behalf of a learned society, the details of that society must be included in the credit line.

6. For the reproduction of a full article from an Oxford University Press journal for whatever purpose, the corresponding author of the material concerned should be informed of the proposed use. Contact details for the corresponding authors of all Oxford University Press journal contact can be found alongside either the abstract or full text of the article concerned, accessible from www.oxfordjournals.org Should there be a problem clearing these rights, please contact journals.permissions@oxfordjournals.org

7. If the credit line or acknowledgement in our publication indicates that any of the figures, images or photos was reproduced, drawn or modified from an earlier source it will be necessary for you to clear this permission with the original publisher as well. If this permission has not been obtained, please note that this material cannot be included in your publication/photocopies.

8. While you may exercise the rights licensed immediately upon issuance of the license at the end of the licensing process for the transaction, provided that you have disclosed complete and accurate details of your proposed use, no license is finally effective unless and until full payment is received from you (either by Oxford University Press or by Copyright Clearance Center (CCC)) as provided in CCC's Billing and Payment terms and conditions. If full payment is not received on a timely basis, then any license preliminarily granted shall be deemed automatically revoked and shall be void as if never granted. Further, in the event that you breach any of these terms and conditions or any of CCC's Billing and Payment terms and conditions, the license is automatically revoked and shall be void as if never granted. Use of materials as described in a revoked license, as well as any use of the

materials beyond the scope of an unrevoked license, may constitute copyright infringement and Oxford University Press reserves the right to take any and all action to protect its copyright in the materials.

9. This license is personal to you and may not be sublicensed, assigned or transferred by you to any other person without Oxford University Press's written permission.

10. Oxford University Press reserves all rights not specifically granted in the combination of (i) the license details provided by you and accepted in the course of this licensing transaction, (ii) these terms and conditions and (iii) CCC's Billing and Payment terms and conditions.

11. You hereby indemnify and agree to hold harmless Oxford University Press and CCC, and their respective officers, directors, employs and agents, from and against any and all claims arising out of your use of the licensed material other than as specifically authorized pursuant to this license.

12. Other Terms and Conditions:

v1.4